

ADSORPTION AND LUBRICATION OF STEEL  
WITH OILINESS ADDITIVES

by

KAZUTO DATE

A Thesis Submitted for the Degree of  
DOCTOR OF PHILOSOPHY  
of the University of London  
and also for the  
DIPLOMA OF MEMBERSHIP OF IMPERIAL COLLEGE

September 1981

Lubrication Laboratory  
Department of Mechanical Engineering  
Imperial College of Science and Technology  
London SW7 2AZ

ABSTRACT

This thesis investigates the mechanism of interaction between oiliness reagents and extreme pressure films produced by sulphur-type extreme pressure additives. The effect of the interaction on friction and wear in boundary lubrication has been studied.

A Flow Microcalorimeter is used to measure heats of adsorption of oiliness reagents, such as stearic acid, stearyl alcohol and methyl stearate, onto iron (II) sulphide and iron oxides such as  $\alpha\text{-Fe}_2\text{O}_3$ ,  $\gamma\text{-Fe}_2\text{O}_3$  and  $\text{Fe}_3\text{O}_4$ . Heat of adsorption of oiliness reagents onto iron (II) sulphide is significantly affected by the oxidation condition of the surface. Production of sulphates on the surface by oxidation results in high heat of adsorption, but the heat of adsorption on iron (II) sulphide is found to be small.

A combination of degree of adsorption and heat of adsorption results indicates that the chemical adsorption of stearic acid occurs on  $\text{Fe}^{3+}$  at an octahedral position in iron oxide.  $\text{Fe}_3\text{O}_4$  and  $\gamma\text{-Fe}_2\text{O}_3$ , which have  $\text{Fe}^{3+}$  at an octahedral position, are suitable for lubrication by an oil containing stearic acid but  $\alpha\text{-Fe}_2\text{O}_3$  is not. On the other hand, stearyl alcohol adsorbs on the anion site ( $\text{O}^{2-}$ ) and forms a physically adsorbed film.

Low speed friction tests at room temperature demonstrate that the extreme pressure film produced with dibenzyl disulphide can reduce the coefficient of friction but the addition of oiliness reagents does not give any further drop in the coefficient of friction.

Wear during running-in is shown to have the same trends as coefficient of friction.

ACKNOWLEDGEMENTS

I am most grateful to Professor A Cameron for his kind help and advice, and also to all the members of the Lubrication Laboratory for providing such comfortable circumstances in which to work.

I should also like to thank Mr R Dobson, Mr T Whymark and Mr P Garden for instructing and aiding me in many technical problems and Dr H Spikes, Miss P Cann and Mr G Wan for kind discussions and help in writing my thesis.

I should also like to express my gratitude to Professor T Sakurai and Dr Groszek for their helpful discussions and suggestions for this work.

I also owe much to the Nippon Mining Company and all members of the Company for their financial support and helpful co-operation in this work.

Finally, I would like to pay my gratitude to Mrs J Buss for her typing of this thesis.

CONTENTS

|   |    |
|---|----|
| ABSTRACT                                | 1  |
| ACKNOWLEDGEMENTS                        | 3  |
| CONTENTS                                | 4  |
| LIST OF TABLES, PHOTOGRAPHS AND FIGURES | 9  |
| NOMENCLATURE                            | 15 |

|                    |  |    |
|--------------------|--|----|
| <u>CHAPTER ONE</u> | <u>GENERAL INTRODUCTION</u>  |    |
| 1.10               | Introduction to the Project  | 17 |
| 1.20               | Boundary Lubrication   | 20 |
| 1.21               | Friction Coefficient of Mixed or<br>Boundary Lubrication           | 21 |
| 1.22               | Wear under Boundary Lubrication                                    | 25 |
| 1.23               | Effect of Oiliness Reagent   | 27 |
| 1.24               | EP Additives   | 28 |
| 1.25               | Effective EP Film Produced by<br>Sulphur-Type EP Additive          | 31 |
| 1.26               | Mechanism of Reaction Between<br>Sulphur-Type EP Additive and Iron | 33 |
| 1.27               | Effectiveness of Sulphur-Type<br>EP Additive                       | 36 |
| 1.30               | Adsorption and Heat of Adsorption                                  | 38 |
| 1.31               | Surface Free Energy and Adsorption                                 | 38 |
| 1.32               | Adsorption at the Liquid-Solid<br>Interface                        | 39 |
| 1.33               | Physical and Chemical Adsorption                                   | 41 |
| 1.34               | Rate of Adsorption and Equilibrium<br>of Adsorption                | 43 |

|      |  |    |
|------|--|----|
| 1.35 | Adsorption on Metal                                    | 47 |
| 1.36 | Heat of Adsorption                                     | 50 |
| 1.37 | Heat of Adsorption and Friction<br>Coefficient         | 55 |
| 1.38 | Heat of Adsorption and Wear                            | 57 |
| 1.40 | Analysis of Lubricated Surface                         | 59 |
| 1.41 | Recent Development of Surface<br>Analytical Techniques | 60 |
| 1.42 | Analyses of EP Films                                   | 63 |
| 1.50 | Scope of Research                                      | 65 |

CHAPTER TWO      HEAT OF ADSORPTION

|      |   |     |
|------|---|-----|
| 2.10 | Introduction  | 66  |
| 2.20 | Experimental  | 67  |
| 2.21 | Materials   | 67  |
| 2.22 | Apparatus   | 75  |
| 2.23 | Procedure   | 80  |
|      | . Saturation Method                                   | 80  |
|      | . Other Methods                                       | 81  |
|      | . Calibration   | 83  |
|      | . Effective Amount of Powder                          | 87  |
|      | . Heat of Dilution                                    | 89  |
| 2.30 | Results   | 91  |
| 2.31 | Heat of Adsorption at Room Temperature                | 91  |
| 2.32 | The Influence of Temperature on Heat<br>of Adsorption | 97  |
| 2.33 | The Influence of Solvent on Heat of<br>Adsorption     | 107 |

|      |  |     |
|------|--|-----|
| 2.40 | Discussions  | 113 |
| 2.41 | Heat of Adsorption by a Flow Micro-calorimeter                       | 113 |
| 2.42 | Comparison of Heat of Adsorption Results with Those of Other Authors | 116 |
| 2.43 | Reversibility of Adsorption  | 125 |
| 2.44 | Heat of Adsorption onto Iron Oxide                                   | 131 |
| 2.45 | Heat of Adsorption of DBDS   | 133 |
| 2.50 | Conclusions  | 135 |

CHAPTER THREE     ADSORPTION

|      |                                    |     |
|------|------------------------------------|-----|
| 3.10 | Introduction                       | 138 |
| 3.20 | Experimental                       | 139 |
| 3.21 | Materials                          | 139 |
| 3.22 | Procedure                          | 140 |
| 3.23 | Measurement of Concentration       | 141 |
| 3.24 | Calculation of Adsorption Value    | 141 |
| 3.30 | Results                            | 143 |
| 3.31 | Rate of Adsorption                 | 143 |
| 3.32 | Adsorption Isotherm                | 146 |
| 3.40 | Discussions                        | 149 |
| 3.41 | Heat of Adsorption per Molecule    | 149 |
| 3.42 | Thermodynamic Aspect of Adsorption | 158 |
| 3.43 | Structure of Adsorbed Film         | 167 |
| 3.50 | Conclusions                        | 170 |

| <u>CHAPTER FOUR</u> | <u>FRICITION AND WEAR</u>                                |     |
|---------------------|--|-----|
| 4.10                | Introduction   | 172 |
| 4.20                | Experimental   | 173 |
| 4.21                | Materials  | 173 |
| 4.22                | Apparatus  | 173 |
| 4.23                | Preparation of Test Piece                                | 176 |
| 4.24                | Preparation of Test Lubricant                            | 178 |
| 4.25                | Procedure  | 181 |
|                     | (i) Cleaning of test piece                               | 181 |
|                     | (ii) Operation of Bowden Leben<br>machine                | 182 |
|                     | (iii) Calibration of friction<br>coefficient             | 183 |
|                     | (iv) Measurement of wear                                 | 183 |
| 4.30                | Results  | 183 |
| 4.31                | Effect of EP Film on Friction<br>Coefficient             | 185 |
| 4.32                | Friction Coefficient at First Traverse                   | 191 |
| 4.33                | Friction Coefficient at Tenth Traverse                   | 199 |
| 4.34                | Effect of EP Film and Oiliness Reagent<br>on Wear        | 205 |
| 4.40                | Discussions  | 211 |
| 4.41                | Friction Coefficient                                     | 211 |
|                     | (i) Interaction between base oil and<br>oiliness reagent | 212 |
|                     | (ii) Interaction between adsorption<br>film and EP film  | 213 |
| 4.42                | Wear   | 214 |
| 4.50                | Conclusions  | 216 |



|                       |   |     |
|-----------------------|---|-----|
| <u>CHAPTER FIVE</u>   | <u>CONCLUSIONS AND SUGGESTIONS FOR FURTHER WORK</u>                 |     |
| 5.10                  | General Conclusions   | 219 |
| 5.20                  | Suggestions for Further Work  | 223 |
| <br><u>APPENDICES</u> |   |     |
| Appendix A            | Heat of Adsorption on a Different<br>$\alpha\text{-Fe}_2\text{O}_3$ | 226 |
| Appendix B            | Change of Friction Coefficient with<br>Traverses                    | 231 |
| <u>REFERENCES</u>     |   | 256 |

LIST OF TABLES, PHOTOGRAPHS AND FIGURES

|           |   |         |
|-----------|---|---------|
| Table 2.1 | Specific surface area of powders  | 74      |
| Table 2.2 | Chemical component of powder  | 74      |
| Table 2.3 | Thermal sensitivity of the thermistor<br>in a Flow Microcalorimeter                               | 87      |
| Table 2.4 | Effective amount of powder and the<br>amount of powder packed in the cell                         | 89      |
| Table 2.5 | Comparison of heat of adsorption with<br>results in the literature (reference 99)                 | 118     |
| Table 2.6 | Analytical results of FeS powder by ESCA  | 121     |
| Table 3.1 | Heat of adsorption per mole   | 150/151 |
|           |   |         |
| Photo 2.1 | Secondary images of scanning electron<br>micrograph of $\alpha\text{-Fe}_2\text{O}_3$             | 69      |
| Photo 2.2 | Secondary images of scanning electron<br>micrograph of $\gamma\text{-Fe}_2\text{O}_3$             | 70      |
| Photo 2.3 | Secondary images of scanning electron<br>micrograph of $\text{Fe}_3\text{O}_4$                    | 71      |
| Photo 2.4 | Secondary images of scanning electron<br>micrograph of FeS  | 72      |
| Photo 2.5 | View of a Flow Microcalorimeter   | 76      |
| Photo 4.1 | View of a Bowden Leben Machine  | 174     |
| Photo 4.2 | X-ray microanalysis of test pieces<br>treated with DBDS reaction at 216°C                         | 179     |
| Photo A.1 | Secondary images of scanning electron<br>micrograph of a different $\alpha\text{-Fe}_2\text{O}_3$ | 228     |

|            |  |    |
|------------|--|----|
| Figure 1.1 | Schematic diagram of friction behaviour<br>in boundary lubrication             | 18 |
| Figure 1.2 | Schematic diagram of wear behaviour<br>in boundary lubrication                 | 18 |
| Figure 1.3 | Schematic diagram of wear process  | 25 |
| Figure 1.4 | Typical shapes of isotherms for adsorp-<br>tion of solid from solution         | 46 |
| Figure 1.5 | Information by incidence of electro-<br>magnetic wave into surface             | 61 |
| Figure 1.6 | Information by incidence of change<br>particle into surface                    | 61 |
| Figure 2.1 | Schematic diagram of a Flow Micro-<br>calorimeter                              | 76 |
| Figure 2.2 | Schematic drawing of the cell in a<br>Flow Microcalorimeter                    | 78 |
| Figure 2.3 | Circuit diagram of the Flow Micro-<br>calorimeter Mark II V model              | 79 |
| Figure 2.4 | Typical peaks of heat of adsorption<br>and desorption                          | 82 |
| Figure 2.5 | Microheater for calibration  | 84 |
| Figure 2.6 | Thermal sensitivity of thermistor in<br>FeS powder                             | 86 |
| Figure 2.7 | Cumulative heat evolved vs amount of<br>FeS powder                             | 86 |
| Figure 2.8 | Heat change of stearic acid solution<br>(12.0mMol/l) in Fe powder              | 90 |
| Figure 2.9 | Cumulative heat of adsorption onto<br>$\alpha\text{-Fe}_2\text{O}_3$ at 26.5°C | 92 |

|             |  |     |
|-------------|--|-----|
| Figure 2.10 | Cumulative heat of adsorption onto $\gamma\text{-Fe}_2\text{O}_3$ at 26.5°C  | 93  |
| Figure 2.11 | Cumulative heat of adsorption onto $\text{Fe}_3\text{O}_4$ at 26.5°C   | 94  |
| Figure 2.12 | Cumulative heat of adsorption onto FeS at 26.5°C   | 95  |
| Figure 2.13 | Cumulative heat of adsorption of stearyl alcohol onto $\alpha\text{-Fe}_2\text{O}_3$ at several different temperatures | 99  |
| Figure 2.14 | Cumulative heat of adsorption of stearic acid onto $\gamma\text{-Fe}_2\text{O}_3$ at several different temperatures    | 100 |
| Figure 2.15 | Cumulative heat of adsorption of stearyl alcohol onto $\gamma\text{-Fe}_2\text{O}_3$ at several different temperatures | 101 |
| Figure 2.16 | Cumulative heat of adsorption of stearic acid onto $\text{Fe}_3\text{O}_4$ at several different temperatures           | 102 |
| Figure 2.17 | Cumulative heat of adsorption of stearyl alcohol onto $\text{Fe}_3\text{O}_4$ at several different temperatures        | 103 |
| Figure 2.18 | Cumulative heat of adsorption of stearic acid onto FeS at several different temperatures                               | 104 |
| Figure 2.19 | Cumulative heat of adsorption of stearyl alcohol onto FeS at several different temperatures                            | 105 |

|              |  |     |
|--------------|--|-----|
| Figure 2.20  | Influence of solvent on cumulative heat of adsorption of stearic acid onto $\gamma\text{-Fe}_2\text{O}_3$    | 108 |
| Figure 2.21  | Influence of solvent on cumulative heat of adsorption of stearyl alcohol onto $\gamma\text{-Fe}_2\text{O}_3$ | 109 |
| Figure 2.22  | Influence of solvent on cumulative heat of adsorption of stearic acid onto $\text{Fe}_3\text{O}_4$           | 111 |
| Figure 2.23  | Influence of solvent on cumulative heat of adsorption of stearyl alcohol onto $\text{Fe}_3\text{O}_4$        | 112 |
| Figure 2.24a | Calibration curve for Graphon  | 115 |
| Figure 2.24b | Cumulative heat of adsorption of n-dotriacontane onto Graphon  | 115 |
| Figure 2.25  | Comparison of heat of adsorption between the results in this study and the results in reference (11)         | 120 |
| Figure 2.26  | Influence of oxidation of FeS on heat of adsorption  | 123 |
| Figure 2.27  | Heat of adsorption and desorption onto $\alpha\text{-Fe}_2\text{O}_3$ at $26.5^\circ\text{C}$                | 127 |
| Figure 2.28  | Heat of adsorption and desorption onto $\gamma\text{-Fe}_2\text{O}_3$ at $26.5^\circ\text{C}$                | 128 |
| Figure 2.29  | Heat of adsorption and desorption onto $\text{Fe}_3\text{O}_4$ at $26.5^\circ\text{C}$                       | 129 |
| Figure 2.30  | Mechanism of adsorption on iron oxide  | 134 |
| Figure 2.31  | Cumulative heat of adsorption of DBDS onto $\gamma\text{-Fe}_2\text{O}_3$ at $26.5^\circ\text{C}$            | 136 |

|            |  |     |
|------------|--|-----|
| Figure 3.1 | Absorbance of carbonyl absorption in IR vs concentration of adsorbate  | 142 |
| Figure 3.2 | Adsorption rate at 26.5°C  | 144 |
| Figure 3.3 | Adsorption isotherm at 26.5°C  | 147 |
| Figure 3.4 | Enthalpy change of adsorption per mole for stearic acid  | 152 |
| Figure 3.5 | Enthalpy change of adsorption per mole for methyl stearate   | 153 |
| Figure 3.6 | Differential enthalpy change of adsorption vs coverage of stearic acid   | 157 |
| Figure 3.7 | Concentration/adsorption plotted against concentration   | 165 |
| Figure 4.1 | Analytical results of sulphur content on surface of test piece by EDXRF  | 180 |
| Figure 4.2 | Calibration curve for friction force   | 184 |
| Figure 4.3 | Typical change of friction coefficient with traverse   | 186 |
| Figure 4.4 | Influence of EP film formed by the reaction with DBDS on coefficient of friction during running-in                     | 187 |
| Figure 4.5 | Influence of the film formed by the reaction with DBDS and acid immersion on coefficient of friction during running-in | 189 |
| Figure 4.6 | Influence of oiliness reagents on coefficient of friction at first traverse (I)  | 192 |

|             |   |     |
|-------------|---|-----|
| Figure 4.7  | Influence of oiliness reagents on coefficient of friction at first traverse (II)  | 193 |
| Figure 4.8  | Influence of oiliness reagents on coefficient of friction at first traverse (III) | 194 |
| Figure 4.9  | Influence of oiliness reagents on coefficient of friction at first traverse (IV)  | 195 |
| Figure 4.10 | Influence of oiliness reagents on coefficient of friction at tenth traverse (I)   | 200 |
| Figure 4.11 | Influence of oiliness reagents on coefficient of friction at tenth traverse (II)  | 202 |
| Figure 4.12 | Influence of oiliness reagents on coefficient of friction at tenth traverse (III) | 203 |
| Figure 4.13 | Influence of oiliness reagents on coefficient of friction at tenth traverse (IV)  | 204 |
| Figure 4.14 | Influence of oiliness reagents on wear during running-in (I)                      | 206 |
| Figure 4.15 | Influence of oiliness reagents on wear during running-in (II)                     | 208 |
| Figure 4.16 | Influence of oiliness reagents on wear during running-in (III)                    | 209 |
| Figure 4.17 | Influence of oiliness reagents on wear during running-in (IV)                     | 210 |

NOMENCLATURE

Symbols used infrequently are defined in the text.

|            |   |  |
|------------|---|--|
| A          | : | contact area   |
| $\alpha$   | : | fraction of area   |
| c          | : | concentration  |
| $\Gamma$   | : | surface excess   |
| $\gamma$   | : | interfacial tension                                      |
| DBDS       | : | dibenzyl-disulphide                                      |
| EP         | : | extreme pressure   |
| F          | : | friction force   |
| f          | : | coefficient of friction                                  |
| $\Delta G$ | : | free energy change                                       |
| H          | : | heat or enthalpy   |
| h          | : | film thickness   |
| $\theta$   | : | fraction of surface covered by the adsorbed<br>molecules |
| K          | : | equilibrium constant                                     |
| K*         | : | probability to produce a worn particle                   |
| l          | : | sliding distance, litre                                  |
| n          | : | moles  |
| p          | : | pressure   |
| p*         | : | plastic yield pressure                                   |
| $\bar{p}$  | : | average pressure   |
| R          | : | gas constant   |
| S          | : | shear strength or entropy                                |
| T          | : | temperature  |
| $\bar{V}$  | : | total volume worn  |



|             |   |   |
|-------------|---|---|
| $\bar{V}^*$ | : | sliding velocity                              |
| v           | : | amount of adsorbate in the adsorbed molecules |
| W           | : | load  |
| X           | : | mole fraction                                 |

Subscripts

|          |   |                       |
|----------|---|-----------------------|
| ads      | : | adsorption            |
| BL       | : | boundary lubrication  |
| crit.    | : | critical              |
| D        | : | deformation           |
| dil      | : | dilution              |
| EP       | : | extreme pressure film |
| F        | : | formation             |
| hydro    | : | hydrodynamic          |
| I        | : | immersion             |
| i        | : | pieces                |
| l or liq | : | liquid                |
| m        | : | monolayer             |
| plough   | : | ploughing             |
| s        | : | surface               |
| sol.     | : | solid                 |
| W        | : | load                  |
| wet      | : | wetting               |

## CHAPTER 1

### GENERAL INTRODUCTION

#### 1.10 Introduction to the Project

Boundary lubrication occurs when there is an insufficiently thick film of lubricant separating two solid surfaces in relative motion, with the result that there is considerable direct contact between the solids. The role of the lubricant is then to modify the solid surfaces chemically, so as to reduce adhesion, friction and plastic deformation as the sliding takes place (1).

Boundary lubrication is commonly improved by adding small amounts of one or more of three types of chemical additive to an oil. These are known as "oiliness", "anti-wear" and "extreme pressure (EP)" additives.

The influence of these additives on the coefficient of friction is shown in a stylized diagram (Figure 1.1). Curve (I) is a system lubricated by a base oil free of friction reducing additive. Curve (II) contains an oiliness additive, such as stearic acid, which results in a low coefficient of friction at low temperature, but is ineffective at high temperature. Oiliness agents are surfactants and are believed to work by forming an adsorbed film on rubbing solids. At high temperature desorption or disorientation of such film makes them ineffective. Curve (III) shows an oil with an EP additive. The additive reacts chemically with metal at high temperature and forms a thick EP film on the lubricated surface, which can decrease

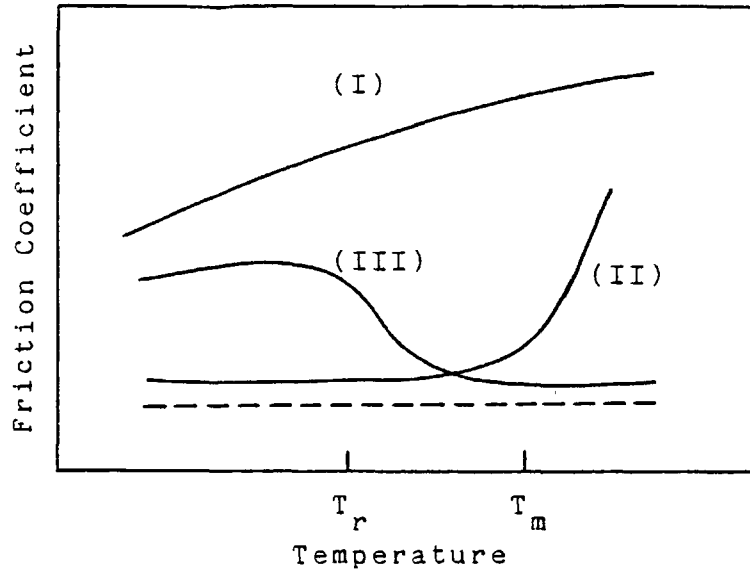


Fig.1-1, Schematic diagram of friction behaviour in boundary lubrication

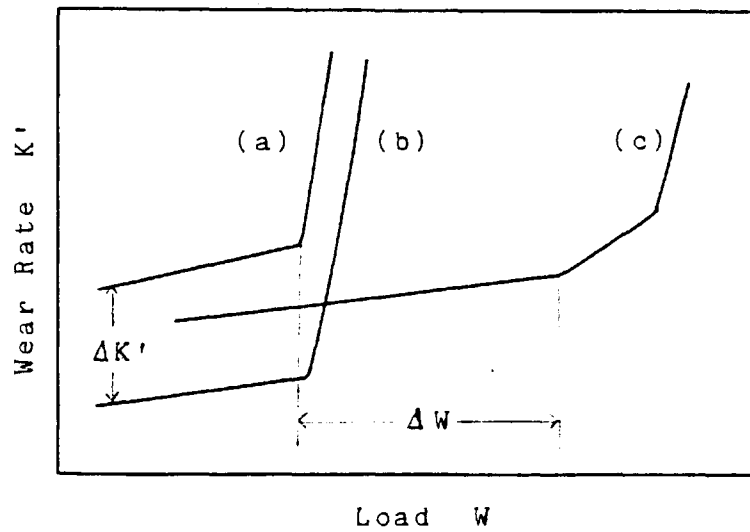


Fig.1-2, Schematic diagram of wear behaviour in boundary lubrication

friction, as shown by the Curve (III). It is possible to maintain a low coefficient of friction throughout a wide range of temperature by a careful combination of oiliness reagent and EP additive.

Wear behaviour of different boundary lubrication systems is shown in Figure 1.2, in which the mean coefficient  $K$  [(wear volume)  $\times$  (load)<sup>-1</sup>  $\times$  (sliding distance)<sup>-1</sup>] on a log scale is plotted versus the load  $W$  (3). Curve (a) represents the wear behaviour of base oil. There are two distinct effects of lubricant additives in a base oil, i.e. (i) a reduction of the wear rate  $K'$  by a certain amount  $\Delta K'$ , (ii) an increase of the load-carrying capacity  $W_{crit.}$  by a certain amount  $\Delta W$ . The additives used for the former effect are called anti-wear additives [curve (b)] and the additives having load-carrying capacity are EP additives [curve (c)].

As described above, a good deal is known about the performance of oiliness reagents, anti-wear additives and EP additives. However less is understood of their mechanism. In view of the great commercial importance of friction and wear, very little work has been done on the fundamental processes that occur (4) (5).

One possibly important insight into the mechanism of friction and wear reducing additives has been proposed by Cameron (6) (7) (8) and Sakurai (9) (10) (11) (12). They suggest that the adsorption of polar compounds onto EP films may be very effective in reducing friction and wear. Although some preliminary heat of adsorption measurement by Sakurai supports this hypothesis, there is insufficient data

to prove the general principle. Quantitative data are required at various adsorption conditions.

The acquisition of such data and the testing of Cameron and Sakurai's hypothesis form an important part of this study, which looks at the interaction between oiliness reagents, (stearic acid, stearyl alcohol and methyl stearate) and the main components of an EP film (iron oxides and iron (II) sulphide).

This project is divided into five parts. The rest of this Chapter 1 forms a brief review of the pertinent literature on adsorption and boundary lubrication. Chapters 2, 3, and 4 describe and analyse the main experimental work carried out on heat of adsorption, degree of adsorption, and friction respectively. Finally Chapter 5 lists the general conclusion for the study as a whole.

## 1.20 Boundary Lubrication

It is convenient to classify lubrication by the film thickness  $h$ . The following classification of three regimes is usually described in many text books and papers (2) (3) (5) (13).

(1) Hydrodynamic Lubrication  $h > 10^{-4}$  mm

(2) Elastohydrodynamic Lubrication  $h \approx 10^{-3} \sim 10^{-5}$  mm

(3) Boundary Lubrication  $h =$  a few molecular length

The term mixed lubrication is used occasionally, and is a combination of hydrodynamic and solid contact between moving surfaces. This regime of lubrication is very important in industry. Blok (14) has further classified

the boundary lubrication regime as follows:

- (a) low-pressure and temperature boundary lubrication (mild boundary lubrication),
- (b) high-temperature boundary lubrication,
- (c) high-pressure boundary lubrication,
- (d) high-pressure and temperature boundary lubrication (extreme-pressure lubrication).

In this reference, practical industrial examples are also shown. As many lubricant additives are used to reduce friction and wear in boundary lubrication, this type of classification is useful for selection of appropriate additives.

### 1.21 Friction Coefficient of Mixed or Boundary Lubrication

As mixed lubrication is a combination of a hydrodynamic film and solid contact between moving surfaces, the total frictional force  $F$  is expressed as the sum of solid friction at asperity peaks, liquid friction in the void and the ploughing contribution  $F_{\text{plough}}$  (13) (15).

$$F = A[\alpha_w \cdot S_{\text{sol}} + (1 - \alpha_w) S_{\text{liq}}] + F_{\text{plough}} \quad (1.1)$$

where

$\alpha_w$  : the fraction of area  $A$  at which solid contact occurs

$S_{\text{sol}}, S_{\text{liq}}$  : the shear strengths of solid surface layer and of liquid respectively

$W$  : the load

Since the load  $W$  is supported both by solid contact at asperity peaks and by hydrodynamic pressure generation in the voids,  $W$  is expressed as follows:

$$W = A[\alpha_w p^* + (1 - \alpha_w) p_{\text{hydro}}] \quad (1.2)$$

where

$p^*$  : the plastic yield pressure of the softer metal

$p_{\text{hydro}}$  : the hydrodynamic pressure generated between asperity

whereas  $S_{\text{liq}} \ll S_{\text{sol}}$ ,  $p_{\text{hydro}}$  is only slightly less than  $p^*$ .

It is therefore convenient to define an average pressure  $\bar{p}$

such that  $p^* > \bar{p} > p_{\text{hydro}}$  and equation (1.2) can then be

approximately represented in the form:

$$W = A\bar{p} \quad (1.3)$$

Then, the coefficient of mixed lubrication  $f_{\text{BL}}$ :

$$f_{\text{BL}} = \frac{F}{W} = \alpha_w \left( \frac{S_{\text{sol}}}{\bar{p}} \right) + (1 - \alpha_w) \frac{S_{\text{liq}}}{\bar{p}} + f_{\text{plough}} \quad (1.4)$$

Excluding a special case such as running-in condition, the

ploughing contribution ( $f_{\text{plough}} = F_{\text{plough}}/A\bar{p}$ ) may be

neglected. Therefore

$$f_{\text{BL}} = \alpha_w \frac{S_{\text{sol}}}{\bar{p}} + (1 - \alpha_w) \frac{S_{\text{liq}}}{\bar{p}} \quad (1.5)$$

or

$$f_{BL} = \alpha_w f_{sol} + (1 - \alpha_w) f_{liq} \quad (1.6)$$

As in most cases,  $S_{liq}$  is smaller than  $S_{sol}$ , it is therefore possible to reduce  $f_{BL}$  by decreasing  $\alpha_w$ .

As shown by many authors, under the boundary lubrication, other type of films, such as adsorbed layers of surfactants and EP films produced on the lubricated surface by EP additives, can be effective for lubrication. Therefore, equation (1.5) is re-written,

$$f_{BL} = (1 - \Sigma\alpha_i) \frac{S_{sol}}{\bar{p}} + \Sigma\alpha_i \frac{S_i}{\bar{p}} \quad (1.7)$$

where

$\alpha_i$  : the fraction of area of each films other than solid contacts

$S_i$  : the shear strength of each films other than solid contacts.

Depending on the severity of the lubrication condition, the fraction of metal contact  $(1 - \Sigma\alpha_i)$  changes. When the values  $(1 - \Sigma\alpha_i)$  reach a critical limit, seizure occurs due to temperature increase by the intense shear strength of solid contacts. The major role of oiliness reagents and EP additives is to depress the increase of this value, giving good lubrication without catastrophic seizure.



## 1.22 Wear Under Boundary Lubrication

Metallic wear is a complex process and includes such complicating factors as work hardening, oxidation of exposed metal, metal transfer and metallurgical phase changes. At the moment, the mechanism of wear is still not understood and cannot be used to explain observed wear results. Nevertheless, wear is one of the most important features of lubrication.

According to the classification of wear by Barwell (16) the following four different main physical mechanisms has been distinguished:

- (1) Adhesive wear
- (2) Abrasive wear
- (3) Corrosive wear
- (4) Surface fatigue wear.

The characteristics of each process have been described in the references (17) (18) (19) (20). One problem in understanding these mechanisms is that wear may start in one mode but often moves into another (5). Peterson (21) has explained the transfer of wear mechanism as shown in Figure 1.3. The curve (a) is for adhesive wear which occurs with lubrication by a poor lubricant oil. If hydrodynamic lubrication is achieved by the increase of contact area, the wear does not increase [curve (b)]. Assuming the rate of formation of solid films  $U_F$  and the rate of deformation of the films  $U_D$ , the small rate of wear is observed at the condition  $U_F \gg U_D$  [curve (c)]. On the other hand, if  $U_D$  is larger than  $U_F$  severe wear occurs [curve (d)]. The

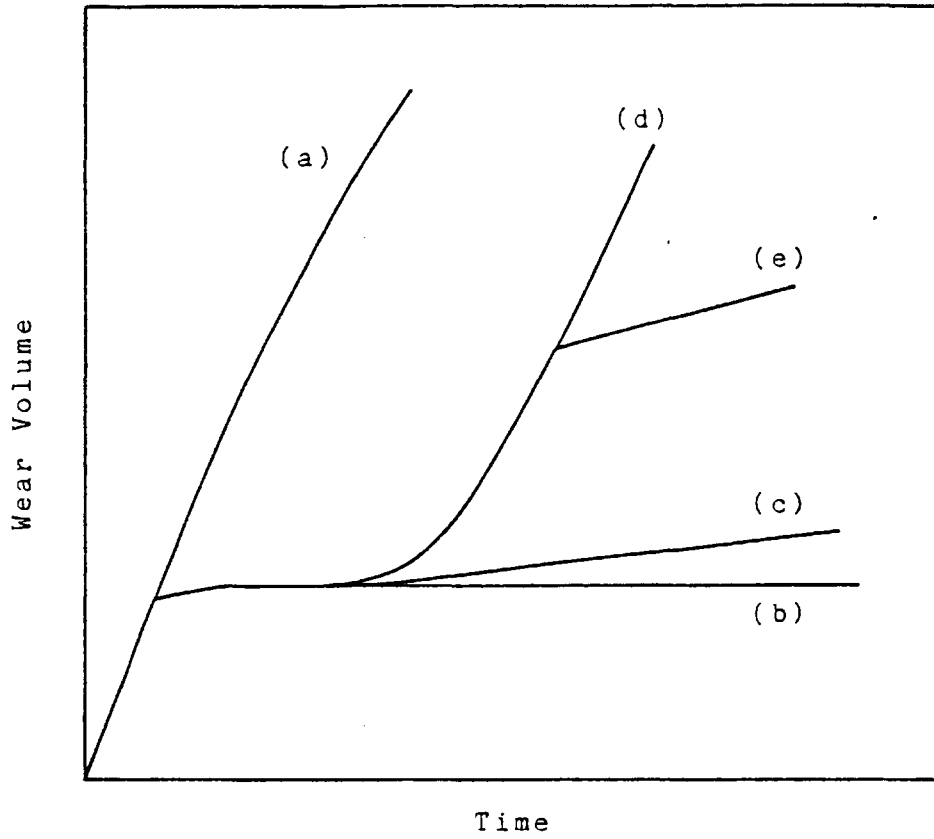


Fig.1-3, Schematic diagram of wear process

- (a) Metal contact wear
- (b) Fluid film lubrication
- (c) Film wear
- (d) Film wear transition
- (e) Recovery

phenomenon of the slowing down of the wear rate shown by curve (e) is sometimes seen, it is due to the increase of contact area by wear or solid film formation by additives under severe wear condition. As stated above, it is necessary in understanding wear processes not only to classify them systematically but also to understand the transfer of mode. Several authors have described the transitions of mode in wear behaviour (22) (23).

There have been several attempts to derive formula expressing the microscopic observed wear (24). The essential concept has been summarized by Archard (3) (5). The equation for adhesive wear has been suggested as follows:

$$\frac{V}{\ell} = \frac{K*W}{3p*} \quad (1.8)$$

where

V : the total volume worn

$\ell$  : the sliding distance

K\* : the probability that any given event will  
produce a worn particle

W : the load

p\* : the yield pressure (used in equation 1.2)

A major difficulty of this equation is an estimation of K\* (5).

Quinn (18) has explained the K\* factor by using the oxidative wear theory for severe wear. For example, the expression for severe wear is given by:

$$\frac{K*}{3} = \frac{B_1 h_1}{d_{c_1}} + \frac{B_2 h_2}{d_{c_2}} \quad (1.9)$$

where

- $h_1, h_2$  : the removed layer thickness from one surface  
 $d_{c_1}, d_{c_2}$  : the critical plastic displacements for each surface  
 $B_1, B_2$  : factors depending mainly on topography and are not well defined

Quinn (18) has emphasized that the equation cannot be used to predict wear rates without making further assumptions about the surface model. At the moment, there is no satisfactory theoretical model of wear processes, or a theoretical model to show the effect of adsorption of polar compounds on wear in boundary condition. The development of such models is a study for the future.

### 1.23 Effect of Oiliness Reagent

Oiliness reagents affect friction and wear in lubrication under low load conditions, an influence due to the adsorption of the additive onto the lubricated surface. The strength of the adsorbed layer is therefore important.

As metal or metal oxide has polar sites on the surface, oiliness reagents need a polar terminal group to have an interaction with the surface. Moreover, in order for the adsorbed film to have reasonable load carrying capacity, the additive must be a long molecule (15) (25). For oiliness reagents, fatty acid with long chain, such as stearic acid and oleic acid, long chain alcohol, fatty acid ester and long chain amine are used in practice.

As described in Section 1.21, the fraction of solid

contact area  $\alpha_w$  in equation (1.5) is a major factor for the coefficient of friction under boundary lubrication conditions. As the adsorbed layer of oiliness reagents can depress the  $\alpha_w$  value under mild boundary conditions, the coefficient of friction is decreased by oiliness reagents. However, it is impossible to expect such effects under severe boundary lubrication, because the adsorbed film cannot exist on the surface at high temperature. Concerning wear, the fraction of solid contact area is included in  $(1 - \Sigma\alpha_i)$  in equation (1.7). Therefore a similar effect to an oiliness reagent can be expected in lubrication under mild boundary conditions.

The effect of oiliness reagents on friction and wear is related to adsorption. The details of the adsorption will be described later.

#### 1.24 EP Additives

Although oiliness reagents have an effect in lubrication under mild boundary conditions, EP additives are used for lubrication under severe boundary conditions. The mechanism of the reaction of EP additives is not fully understood. An EP additive is considered to react on the lubricated surface due to frictional heat and to produce solid films called EP films. Therefore, EP additives must have the following properties:

- (1) The additive must have a suitable reactivity with metal at the high temperatures achieved by friction. This reaction must be rapid enough

to produce EP films which avoid metal contacts. It is, however, impossible to use a too reactive additive owing to the corrosive wear by the additive (26).

- (2) The EP films produced by the reaction of EP additives must have a high melting point, low shear strength and chemical stability. As only a solid film is effective for severe boundary lubrication, the EP films of low melting point cannot have a good performance. However, the EP films of melting point higher than that of the metal is also meaningless.

There are chlorine-type, sulphur-type, phosphorus-type and organo-metallic additives used as EP additives for steel/steel lubrication. As these additives have different properties, a suitable combination of the additives is necessary for any particular purpose. As the characteristics of the EP film produced by sulphur-type EP additives is important for this study, the details will be described in the next section. In this section, the characteristics of EP films produced by EP additives other than sulphur-type are described briefly.

#### (i) Chlorine-type

The film of iron chloride decreases coefficient of friction markedly. This is due to the low shear strength of the material which has a layered structure like graphite. As the melting point of iron chloride is low (iron (II) chloride is about 600°C, iron (III) chloride is about 300°C), the breakdown of the films occurs at a relatively low

temperature. The presence of water induces hydrolysis of the films, and produces HCl, a cause of corrosion. Analytical results of the films has shown the existence of hydrolysed iron oxide and iron oxide as well as iron chloride and hydrated iron chloride (27). Two reaction schemes for the production of the film have been proposed, i.e. (a) the reaction of metal with HCl produced as an intermediate (28), (b) the direct reaction of metal with the additive (29).

(ii) Phosphorus Type

Iron phosphide produced by the reaction of phosphorus-type EP additives does not have the properties required by a lubricant material. However, iron and iron phosphide produce a eutectic mixture of low melting point (30), which makes the lubricated surface smooth (31) (32). This smoothed surface is considered to decrease frictional heat which is the cause of adhesion of metal. There is however no report of detection of iron phosphide on the lubricated surface. Only iron phosphate has been detected (32).

(iii) Organo Metallic Additives

The salts of Zn, Sb and Pb with naphthenic acid, di-alkyl-dithiophosphate and di-alkyl-dithiocarbonic acids are used as organo metallic EP additives. Of these additives, Zn-dithiophosphate (ZDTP) is well known, and is used in many kinds of oils. Two mechanisms of action of the additive have been proposed, i.e. (a) the reactions of reactive atoms such as S and P, which are included in the additive, (b) the formation of EP film by the reaction of the additive only or with other additives in a lubricant

oil (33). The reaction scheme of (a) is essentially the same as sulphur-type of phosphorus-type EP additives.

#### 1.25 Effective EP Film Produced by Sulphur-Type EP Additive

It is stated the EP additives react with the lubricated surface and produce EP films which have anti-wear properties and load carrying capacity. However, the mechanism is not easy to understand owing to the complexity of the parameters of frictional heat, contact pressure, reactivity of new surface by wear and mechanochemical reaction on the surface (34) (35) (36).

Concerning sulphur-type EP additives, the details of the mechanism of the additive in boundary lubrication have still not been explained. However, the results of many studies of this problem have been published. In this section, the mechanism of friction and wear by EP films produced by sulphur-type EP additives are summarized. The analytical methods and analytical results of the EP films will be described in Section 1.41 and 1.42.

The effect of EP additives in boundary lubrication is divided into two categories, i.e. (1) the anti-wear performance in mild boundary lubrication (anti-wear region) and (2) the load carrying capacity in severe boundary lubrication (EP region) (37) (38) (39) (40). The adsorbed film of the additives has an effect of anti-wear performance, but the solid EP film is required for the load carrying capacity. The performance of additives is not always the same in these two regions.



In the EP region, (a) the formation of oxide film and (b) the formation of sulphide film has been proposed as a mechanism of sulphur-type EP additives. Godfrey (41) has analysed the lubricated surface after a SAE friction test using an oil containing elementary sulphur. The results of analysis show that the film of 0.5-1.0 $\mu$  includes  $Fe_3O_4$  as a main component and FeS as a minor component. In the experiment, the load carrying capacity of each film is measured. The films of  $Fe_3O_4$  and FeS do not increase the load carrying capacity. The presence of both, in the surface layers of the metal, is the condition for high load carrying capacity. From these results, Godfrey has proposed a mechanism that the load carrying capacity of sulphur-type EP additives depends on the oxidation of iron, promoted by the iron sulphide as a product of the additives. The production of iron sulphide in the lattice of iron oxide crystal makes the oxide film porous. As a result, the oxide grows to about 1 $\mu$  thick, owing to easy diffusion of oxygen in the film. Moreover, as this type of film of iron oxide tends to occlude oil, a high load carrying capacity is obtained. There are some studies which support this mechanism of iron oxide (7) (30) (42) (43) (44).

On the other hand, Allum (37) has analysed the wear scar of a four ball test using oils containing disulphides and show that the disulphides of high load carrying capacity forms iron sulphide films of thickness up to 1-2 $\mu$ . The amount of iron sulphide film is in proportion to the load carrying capacity, but the amount of iron oxide film decreases with the capacity. From these results Allum has

proposed a mechanism of iron sulphide films. Many authors have supported the same mechanism (39) (45). Bancroft (46) has found the film of  $\text{FeSO}_4$  as a main component on the surface of gear run with an oil containing elementary sulphur and has reported that this film grows to 0.3-0.5 $\mu$ . The difference of the films produced by sulphur-type EP additives may be due to the difference of the condition of friction, though the mechanisms described above are derived from the results of experiments in EP region.

In the anti-wear region, a different kind of mechanism must be considered. In this region, although some EP film is considered to be produced by the collision of asperities, the adsorption of EP additives and other polar materials in oil onto the lubricated surface is an important factor for the anti-wear performance of the additive (6) (7) (39) (47). The similar effect of the adsorption has been recognised in a friction test using copper. The friction coefficient decreased linearly depending on the increase of copper sulphide, which is the reaction product between a copper surface and DBDS (48).

#### 1.26 Mechanism of Reaction Between Sulphur-Type EP

##### Additive and Iron

The mechanism of reaction between sulphur-type EP additives and iron has been investigated by the radio-tracer method (9) (48) (49) (50) (51), hot wire method (43) (52) (53) and concentration analysis by many authors. The reaction mechanism is dependent on reaction temperature

and pressure, atmosphere and type of EP additives.

Many authors have proposed the following mechanism for the reaction of disulphides (38) (45) (54).

(1) Adsorption onto iron surface



(2) Production of mercaptide



(3) Production of iron sulphide



In this mechanism, monosulphide is produced as a result of the reaction (3). This monosulphide can react with iron at high temperature and produce iron sulphide and radicals which form alkane, olefin, etc, by radical reactions. At low temperature, below 150°C, the reaction occurs slowly through (1), (2) and (3). In this case, the same mole of monosulphide is produced by the consumption of disulphide. However, at high temperature, 370°C-400°C, the following process occurs:



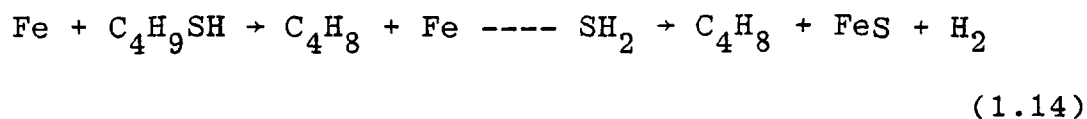
In this case, there is no formation of monosulphide, therefore, at low temperatures, the reactivity of disulphide is different

from that of monosulphide, but at high temperature there is no such difference.

According to Forbes and co-workers (54) (55), the production of mercaptide occurs by cleavage of sulphur-sulphur bond of disulphide in the anti-wear region, and the production of iron sulphide occurs by cleavage of the sulphur-carbon bond of the additives at high temperature in the EP region (38) (47) (54). Therefore, the ease of cleavage of the sulphur-carbon bond governs the load carrying capacity of a sulphur-type EP additive, and the anti-wear performance depends on the ease of cleavage of the sulphur-sulphur bond. The cleavage of the sulphur-sulphur bond and the sulphur-carbon bond is very important for the mechanism of a sulphur-type EP additives (56). At the moment, however, it is not certain whether the cleavages occur as a simple thermal decomposition or a catalytic reaction by the iron surface or materials in oil. The existence of oxygen affects the sulphuration reaction in a complicated manner (27) (28) (57) (58). Two separate effects can have (a) to change the sequence of reactions leading to the formation of intermediate products which actually intervene in the surface reaction, and (b) the blocking of the surface by oxygen present at the interface (43) (59).

The effect of chemical structure of sulphur-type EP additives on the mechanism of reaction has been discussed by Llopis and co-workers (59). The mechanisms of mono and disulphide are explained as those described above. The reaction mechanism proposed by these authors to explain the action of butyl mercaptan on iron can be represented

by the scheme:



In the case of trisulphide, as the central sulphur atom is labile, the reaction of this labile sulphur occurs first as follows (59):



This reaction is considered to occur at a lower temperature than the reaction temperature of mono- and disulphide. The more labile central sulphur atom in polysulphide, other than tetra, can make the sulphuration reaction easily (7). It is also confirmed that the lubrication reaction of sulphur-type EP additives is very temperature-dependent (51) (58).

### 1.27 Effectiveness of Sulphur-Type EP Additive

In the previous section, the reaction mechanism of sulphur-type EP additives with iron is described. In this section, the relationship between the chemical structure or reactivity of a sulphur-type EP additive and the anti-wear performance in the anti-wear region and the load carrying capacity in the EP region are discussed.

According to Forbes (38), the load carrying capacity of disulphide in the EP region is:

diphenyl<di-n-butyl<di-sec-butyl<di-tert-butyl<dibenzyl  
(1.16)

The same order for monosulphides is obtained. This order follows absolutely that of bond energies of sulphur-carbon bond formed in the literature. From these results, it has been suggested that the observed order of load carrying capacity can be accounted for in terms of variations of the strength of the sulphur-carbon bond, i.e. the weaker the sulphur bond, the less is the wear caused under extreme pressure conditions (EP region).

In the case of the anti-wear properties in the anti-wear region, Forbes and co-workers (55) have found the following order of effectiveness in a series of experiments using disulphides:

di-n-butyl<dialkyl<dibenzyl<diphenyl (1.17)

For the anti-wear property, the amount of mercaptide produced by the reaction of the additives and the formation of the solid film by mercaptide is important (54) (55). It is difficult to discuss both the effects of the additives owing to the lack of detailed information. However, concerning diphenyl disulphide, as phenyl mercaptyl radical produced by the cleavage of sulphur-sulphur bond can have a resonance structure, the dissociation energy of the bond is considered to be small. This estimation explains the good anti-wear performance of diphenyl disulphide qualitatively.

There are other reports that investigate the effectiveness of mono-, di- and polysulphide additives. Most of the

authors have stated that the reactivity of additives with iron or thermal stability are a good measure of anti-wear property and load carrying capacity. In the practical usage of these additives, however, too reactive additives induce chemical corrosion of the surface. In such a case, a specific inhibitor must be considered (7).

### 1.30 Adsorption and Heat of Adsorption

As described in the previous sections, the phenomenon of adsorption of polar compounds in a lubricant oil governs the coefficient of friction and anti-wear effectiveness in boundary lubrication under relatively mild conditions. In this section, the fundamental aspects of adsorption and the applications of study of adsorption and heat of adsorption to lubrication are briefly reviewed.

### 1.31 Surface Free Energy and Adsorption

Adsorption is defined as a phenomenon that results in the concentration at interface of two phases being different from that of the bulk phase. In principle Gibbs adsorption equation can be used as the basis of adsorption theory. The surface excess of component 2 ( $\Gamma_2$ ) adsorbed onto a solid from a binary solution is given by (60):

$$\Gamma_2 = - \frac{1}{RT} \frac{d \gamma}{d \ln C_2} \quad (1.18)$$

where

$C_2$  : the concentration of component 2 in the liquid phase (the activity should be used at high concentration)

$\gamma$  : the interfacial tension (= the interfacial free energy)

$R$  : gas constant

$T$  : temperature

It is impossible to measure  $\gamma$  at the liquid-solid interface. It is apparent from this equation that the surface excess decreases with the interfacial tension. Therefore, as the interfacial tension increases with temperature, the adsorption decreases.

### 1.32 Adsorption at the Liquid-Solid Interface

The most important adsorption for lubrication takes place at the liquid-solid interface. In this section, the characteristics of this type of adsorption are described.

It is easy to measure adsorption on a solid directly by the change in concentration of the bulk liquid. Assuming the immersion of a sample solid into a binary solution of component 1 (solvent) and component 2 (solute), the amount of adsorption of solute onto solid is calculated by the change in concentration  $\Delta X_2$  as follows:

$$n_2^S = \frac{n_0 \Delta X_2}{W^*} \quad (1.19)$$



where

$n_2^S$  : the mole fraction of component 2 in the adsorbed layer

$n_0$  : the total moles of component 1 and component 2

$X_2$  : the mole fraction of component 2

$W^*$  : the weight of solid sample

Thermodynamically, adsorption is given by the surface excess  $\Gamma_2$  as follows (60):

$$\Gamma_2 = \frac{n}{\sigma} (X_2^S - X_2) \quad (1.20)$$

where

$n^S$  : the total moles in the adsorbed layer,  $n^S = n_1^S + n_2^S$

$X_2^S$  : the mole fraction in the adsorbed layer,

$$X_1^S + X_2^S = 1, X_1 + X_2 = 1$$

$\sigma$  : the surface area of solid per unit weight

therefore

$$\Gamma_2 = \frac{1}{\sigma} (n_2^S X_1 - n_1^S X_2) \quad (1.21)$$

Assuming a dilute solution, i.e.  $X \approx 0$ ,  $X \approx 1$ ,

$$n_2^S = \sigma \Gamma_2 \quad (1.22)$$

Therefore, in the dilute solution,  $n_2^S$  calculated by the change in concentration and equation (1.22) gives the surface excess.

In the past, as the measurement of surface area of solids has not been easy, most of the results of adsorption

relating to lubrication are expressed in terms of unit weight. This difficulty has been a barrier to quantitative discussion about adsorption. The quantitative aspect of adsorption is a major feature of this work.

### 1.33 Physical and Chemical Adsorption

In adsorption from a solution by a solid, there is an interaction between the solid surface and the adsorbed molecule. When the forces of this interaction are weak, e.g. the Van de Waals forces, the adsorption is called physical adsorption. Generally, physical adsorption has a relatively rapid rate of adsorption. It is a reversible process and the adsorption energies are of the order of  $8 \sim 40\text{KJ/mole}$ .

On the other hand, when the adsorbed molecule is bound to a surface of a solid through a chemical bond, the phenomenon is called chemical adsorption. In chemical adsorption, the energy of adsorption is usually in the order of  $40 \sim 400\text{KJ/mole}$ . Most chemical adsorptions occur slowly due to an activation energy for this process, and desorption of chemically adsorbed molecule is difficult as compared with physically adsorbed molecules (61) (62) (63).

In the boundary lubrication system, the same polar additives in a lubricant oil are physically adsorbed. The polar additives condense on the surface to form a solid film (64). Many molecules pack in as closely as possible and strengthen the film with lateral cohesive forces (63) (65). This solid film has the ability to resist penetration

of asperities and thus prevents metal-to-metal contact. As described in Section 1.31, the interfacial tension increases with temperature, so that the coverage of adsorbed film decreases at high temperature. In addition, the large motion of molecules in solution at high temperatures breaks the solid film formed by physical adsorption. Therefore, at a high temperature, as the change of the film from solid state to liquid state occurs by desorption, disorientation and melting of the film, the film loses its capacity for anti-wear and low friction. Thus, boundary lubrication dependent upon physical adsorption is limited to low temperatures and conditions of low frictional heat generation, i.e. low loads and low sliding velocities.

A well known example of chemical adsorption in boundary lubrication is the reaction of stearic acid and reactive metals. The film of metal soap produced by the reaction acts as a boundary lubricant. The metal soap formed has a higher melting point than the acid itself and breakdown of the film occurs at the higher soap melting point. In the case of zinc, for example, stearic acid reacts with the metal and forms films of metal soap on the surface, so that the temperature of disorientation is enhanced to 90-95°C which is the melting point of the zinc stearate. With unreactive metals such as platinum, stearic acid can form only a physically adsorbed film on this metal. In this case, a large increase of friction coefficient occurs at about 70°C, which is the melting point of stearic acid, and disorientation of adsorbed molecule has been observed at this temperature by electron diffraction analysis. As

an example of chemical adsorption other than fatty acid in boundary lubrication, the adsorption of 1-cetene ( $C_{14}H_{29}CH=CH_2$ ) on aluminium has been reported. In this case, the transfer of  $\pi$ -electron from double bond to metal causes chemical adsorption. Therefore, 1-cetene is a better lubricant than cetane on aluminium (66).

Schulman (67) has suggested that there are adsorption other than physical and chemical adsorption as follows:

(i) Precipitation adsorption

Fatty acid adsorbs chemically on the surface of reactive metal. When the desorption of the metal soap occurs, this material precipitates on the surface owing to the low solubility in the lubricant (25). This precipitation adsorption makes multilayers, so that the further chemical adsorption is obstructed by these layers. It is stated that the adsorption of fatty acid onto copper, lead and zinc becomes precipitation adsorption of multilayers (68) (117).

(ii) Sensitized adsorption

This is a combine physical adsorption and chemical adsorption, i.e. physical adsorption on a layer of chemical adsorption. For example, if alkyl sodium sulphate and cholesterol exist in an oil, the latter adsorbed physically on the surface of chemically adsorbed monolayer by the former.

1.34 Rate of Adsorption and Equilibrium of Adsorption

In the description of adsorption, it is necessary to divide the problem into equilibrium and rate. Both of them

are very important in boundary lubrication.

Well known equilibrium adsorption isotherms are as follows (60):

(i) Freundlich equation: empirical equation for adsorption of gases and dilute solutions.

$$X = a.C^{\frac{1}{b}} \quad (1.23)$$

where

X : the weight of adsorbate in the adsorbed layer

C : the concentration of the solution at equilibrium

a,b : constant

(ii) Langmuir equation: monolayer adsorption model.

$$\theta = \frac{AP}{1 + BP} \quad (1.24)$$

where

$\theta$  : the fraction of surface covered by the adsorbed molecules

P : the partial pressure of adsorbate

A,B : constants

(iii) BET equation: multilayer adsorption model

$$v = \frac{v_m C x}{(1 - x)[1 + (C - 1)x]} \quad (1.25)$$

where

v : the amount of adsorbate in the adsorbed layer

$v_m$  : the amount of adsorbate in the monolayer (constant)

C : constant

$x$  :  $x = P/P_0$  ( $P$ ,  $P_0$  are partial and saturation pressure of adsorbate)

$v_m$  is usually used to calculate specific surface area of adsorbents. However, these models are too simple to apply to adsorption in boundary lubrication. In practice, several other shapes of adsorption curves are often observed.

A convenient classification of shapes of isotherms for adsorption of solids from solution has been described by Giles according to the scheme shown in Figure 1.4 (60):

The S Curve is obtained if (i) the solvent is strongly adsorbed, (ii) there is strong inter-molecular attraction within the adsorbed layer, (iii) the adsorbate is mono-functional. The second condition can be seen frequently in the adsorption of oiliness reagents, owing to the additive having a long chain. The inter-molecular attractions within the adsorbed layer are called cohesive forces, which are important in forming useful solid films for boundary lubrication.

The L Curve is of the so-called Langmuir type. It can be found when there is no strong competition from the solvent for sites on the surface.

The H Curve occurs when there is high affinity between the adsorbate and adsorbent which is shown even in very dilute solutions. This type of isotherm has been shown in the study of lubrication by many authors (68) (69) (70) (71) (72), in which the adsorption of fatty acid onto metals or metal oxides has been investigated.

The C Curve indicates constant partition of the adsorbate between the solution and adsorbent. This type

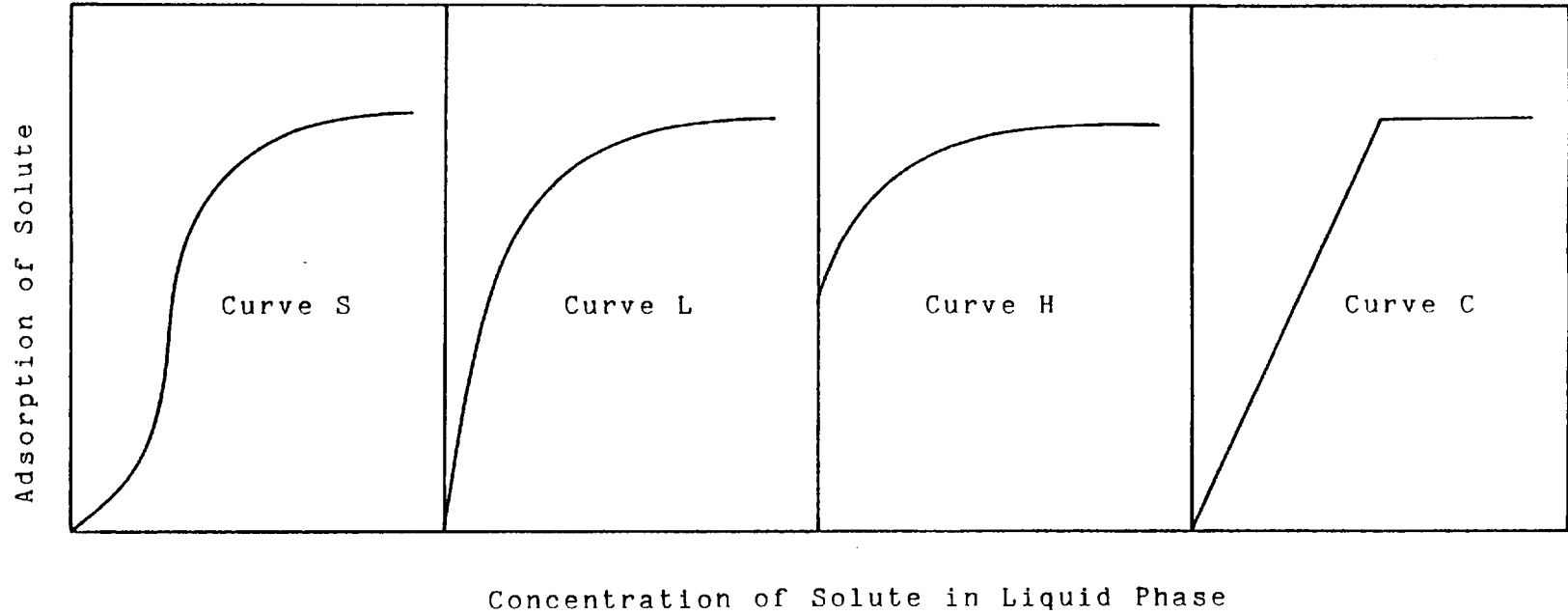


Fig.1-4, Typical shapes of isotherms for adsorption of solid from solution

of isotherm is not familiar in the adsorption of oiliness reagents onto metals or metal oxides.

As described above, much useful information of adsorption can be obtained from a classification of isotherms. In this study, the results heat of adsorptions having shapes of S-curve and the L-curve were obtained.

Dynamic analysis of adsorption is also important in boundary lubrication. In the case of physical adsorption, the adsorbed molecule cannot stay in the same site for a long time. Repetition of the adsorption and desorption process occurs continuously. In order to investigate collisions of small asperities, which is a fundamental process for friction and wear in boundary lubrication, a treatment of the residence time of adsorbed molecules is necessary. To date, this has been studied only theoretically.

### 1.35 Adsorption on Metal

The adsorption of oiliness reagents onto metals and metal oxides has been investigated by many authors. In boundary lubrication, such study is mainly confined to physical or chemical adsorption.

Bowden and co-workers (15) (70) have investigated the adsorption of stearic acid, stearyl alcohol and ethyl stearate onto many metals, such as platinum, gold, zinc, cadmium and copper, by the radio tracer technique. On non-reactive metals, such as platinum and gold, all kinds of oiliness reagents adsorb physically. However, on



reactive metals such as zinc, cadmium and copper, physical adsorption occurs with stearyl alcohol, whilst with stearic acid, chemical reaction occurs. In the case of ethyl stearate, the results of chemical adsorption have been obtained with reactive metals, but there is some possibility that the chemical adsorption actually occurred with stearic acid as an impurity or a product of hydrolysis.

The authors (70) have also investigated the lubrication breakdown temperature, shown in Figure 1.1, of the adsorption films. The lubrication breakdown of physical adsorption occurs at around the melting point of the oiliness reagent (stearic acid 70°C, stearyl alcohol 58°C, ethyl stearate 34°C). Whilst the lubrication breakdown temperature of chemical adsorption films is 90-120°C, which is the melting point of the metal soap. Tabor has published a similar study of adsorption films using an electron diffraction technique (73) (74), and several other researchers have recognised the formation of metal soap (62) (75) (76) (77) (78).

As most practical lubrication is carried out in normal atmosphere, the surface of metals (except a few special ones), are covered by the oxide films formed by oxygen in the lubricant oil. In boundary lubrication, the film of oxide is not only effective on friction and anti-wear (44) (79) (80) (81) (82), but also the film has an influence on adsorption of polar compounds onto the surface (69) (72) (79) (83). According to a study by Allen (72), iron covered with oxides adsorbs more stearic acid than iron without an oxide film. In the case of copper, the

influence of oxide films is not observed. Generally the existence of oxygen and an oxide film is necessary for the adsorption of fatty acid onto metal (69) (78) (79). However, there are some reports which describe the same adsorption onto metals with and without oxide films, though the reasons for this observation have not been explained (71) (84) (85). In the case of adsorption of olefin onto aluminium, the existence of the oxide film obstructs the adsorption by blocking the film.

On lubricated surfaces, water frequently exists as hydrates, chemically adsorbed water, physically adsorbed water, etc. This water has an influence on adsorption of lubricant additives. According to Hirst (86), for the unreactive powders,  $TiO_2$ ,  $SiO$ ,  $TiC$ ,  $SiC$ , the presence of water merely reduces the amount of acid adsorbed. On the reactive powders,  $Cu$ ,  $Cu_2O$ ,  $CuO$  and  $Zn$ , it appears that under dry conditions, the acid is physically adsorbed: the influence of water is to initiate chemical reaction. In addition, the influence of water depends very markedly on the nature of the surface layer of oxide. As a consequence, the formation of metal soap is markedly affected by water and oxide.

As described in Sections 1.25-1.27, the adsorption of EP additives is very important in the anti-wear region of boundary lubrication. However, the study of this phenomenon is difficult, due to the reaction occurring at high temperature, and the sulphuration reaction occurring successively.

### 1.36 Heat of Adsorption

As heat of adsorption is a good measure for expressing the strength of adsorbed layer, the problem of stability of an adsorbed film in boundary lubrication is frequently discussed in terms of heat of adsorption. It is, however, not easy to obtain exact heats of adsorption owing to the complexity of adsorption phenomena. The adsorption at a solid/solution interface needs careful treatment due to the existence of solvent.

When a dried solid is immersed in a liquid, some heat is released without dissolution of any chemical reactions. This heat is called heat of immersion,  $\Delta H_I$ . The solid comes into contact with the adsorbed layer, and a heat of wetting,  $\Delta H_{\text{wet}}$ , is involved. Also, a heat of dilution,  $\Delta H_{\text{dil}}$ , should be considered owing to the change of composition in the adsorbed layer by adsorption. Thus,

$$\Delta H_I = \Delta H_{\text{wet}} + \Delta H_{\text{dil}} \quad (1.26)$$

In an experimental measurement,  $\Delta H_{\text{dil}}$  can be neglected when the amount of solution is much greater than the solid. As  $\Delta H_{\text{wet}}$  of solvent can be measured directly, the heat of adsorption of solute  $\Delta H_{\text{ads}}$  is obtained as follows:

$$\Delta H_{\text{ads}} = \Delta H_{\text{wet:solution}} - \Delta H_{\text{wet:solvent}} \quad (1.27)$$

If the measurement of  $\Delta H_{\text{wet}}$  is carried out in the atmosphere,  $\Delta H_{\text{ads}}$  is the enthalpy change of adsorption.

Frewing (87) has calculated enthalpy change of adsorption indirectly from the transition temperature in friction test. Assuming a Langmuir type adsorption isotherm, the equilibrium constant K is:

$$\frac{\theta}{C(1-\theta)} = K \quad (1.28)$$

where

K : the equilibrium constant

$\theta$  : the fraction of surface covered with the adsorbed film

C : the concentration of adsorbate

The variation of K with temperature is given by the Van't Hoff isochore

$$\frac{d \log_e K}{dT} = - \frac{\Delta H_{ads}}{RT^2} \quad (1.29)$$

As  $\Delta H_{ads}$  is independent of temperature, the equation (1.29) can be integrated by temperature,

$$\log_e K = \frac{\Delta H_{ads}}{RT} + \text{integration constant} \quad (1.30)$$

Assuming that the transition from smooth sliding to stick-slip occurs when the surface concentration of the adsorbed and oriented film decreases to a definite value, i.e. at  $\theta = \theta_0$

$$\frac{\theta_0}{C(1-\theta_0)} = \frac{\Delta H_{ads}}{RT_t} + \text{integration constant} \quad (1.31)$$

whence

$$2.3 \log_{10} C = \frac{\Delta H_{\text{ads}}}{RT_t} + \text{constant} \quad (1.32)$$

where

$T_t$  : the transition temperature

From the slope of a straight line plotting  $\log_{10} C$  against  $1/T_t$ ,  $\Delta H_{\text{ads}}$  can be estimated. In this method, the following assumptions are included:

(i) As the adsorption of the Langmuir type is assumed, the lubricated surface is homogeneous and the inter molecule cohesive force, which is a necessary factor in forming a solid adsorbed film, is neglected.

(ii) The equilibrium of equation (1.24) can be applied to physical adsorption, which is reversible.

In principle, therefore, it is impossible to apply this method to chemical adsorptions such as the metal soap formation of fatty acid.

Frewing (87) has estimated the enthalpy change of adsorption  $\Delta H_{\text{ads}}$  of stearic acid and methyl stearate onto steel as follows:

|                 | $\Delta H_{\text{ads}}$ |
|-----------------|-------------------------|
| stearic acid    | 54.5/mole               |
| methyl stearate | 36.0/mole               |

Zisman (88) has obtained the following values of enthalpy change from the measurement of oleophobic monolayer breakdown temperature on platinum surface, and Sakurai

calculated the value from the temperature of rectification disappearance as follows:

|         |                 | $\Delta H_{ads}$ |
|---------|-----------------|------------------|
| Zisman  | stearyl alcohol | 41.9KJ/mole      |
| Zisman  | stearic acid    | 41.9KJ/mole      |
| Sakurai | stearic acid    | 44.4KJ/mole      |

Spikes and Cameron (89) (90) have measured the adsorption isotherm of n-octadecylamine onto stainless steel at several different temperatures and estimated the enthalpy change of adsorption  $\Delta H_{ads}$  from the slope of a straight line plotting  $\log_{10} C$  against  $1/T$ , in which C is equilibrium concentration at the fixed fraction of coverage in equation (1.24). They have reported the interesting result that the enthalpy change of adsorption is different with temperature and the fraction of coverage.

Further advanced thermodynamical treating of adsorption has been carried out by Cameron and co-workers (91) (92) (93) (94) (95). Although the Frewing assumption i.e., Langmuir type adsorption and the transition temperature of stick-slip, are used, the following fundamental thermodynamic equation has been introduced.

$$\Delta G = - RT \ln K \quad (1.33)$$

where

$\Delta G$  : the free energy change of adsorption

From equation (1.28) and the definition of free energy change

$$-\frac{\Delta H}{T} + \Delta S = R \left( \ln \frac{\alpha_i}{(1 - \alpha_i)} - \ln C \right) \quad (1.34)$$

where

$\Delta H$  : the enthalpy change of adsorption

$\Delta S$  : the entropy change of adsorption

$\alpha_i$  : the fraction of coverage when the transition  
from smooth sliding to stick-slip occurs

As the authors have assumed that the value of  $\alpha_i$  is near  $\frac{1}{2}$ ,  
 $\ln \alpha_i / (1 - \alpha_i)$  can be neglected. Therefore,

$$\frac{\Delta H}{T} - \Delta S = R \ln C \quad (1.35)$$

From this equation and the results of friction test,  
the following values of enthalpy and entropy changes are  
reported. The adsorption of cetylamine onto stainless  
steel (93),

$$\Delta H = 54-101 \text{KJ/mole}$$

$$\Delta S = 105-230 \text{J/mole } ^\circ\text{C}$$

The adsorption of stearic acid onto stainless steel (93),

$$\Delta H = 54-67 \text{KJ/mole}$$

$$\Delta S = 96-134 \text{J/mole } ^\circ\text{C}$$

The adsorption of the naturally occurring surfactant in oil  
onto stainless steel (95),

$$\Delta H = 114 \text{KJ/mole}$$

The adsorption of stearic acid onto stainless steel (91)  
(determined by medium speed friction test)

$$\Delta H = 168\text{KJ/mole}$$

This last large value has been explained as a result of chain matching. The estimation of enthalpy and entropy change of adsorption makes the discussion of interesting problems such as the chain matching phenomenon possible. However, as the theoretical analysis derived by Frewing and Cameron includes many assumptions, the range of application should be limited.

Groszek (96)(105), Sakurai (10) (11) and others (47) (55) (106) have measured heats of adsorption onto several powders by a Flow Microcalorimeter. Although these values are heats of adsorption measured directly, the values are expressed by heat release per unit weight or unit surface area of powders. It is therefore impossible to compare the values with the heats of adsorption obtained by the results of friction tests. Nevertheless, these values are useful, as it is possible to compare the relative strength of the adsorption film of added materials in lubrication, such as oiliness reagent.

### 1.37 Heat of Adsorption and Friction Coefficient

The relationship between heat of adsorption and the phenomenon of stick-slip has been discussed in the previous section. In this section, the influence of heat of



adsorption on friction coefficient at normal lubrication condition is discussed.

Kingsbury (107) has assumed a relationship between  $\alpha$ , the fractional film defect, and the ratio of the time for the asperity to travel a distance equivalent to the diameter of the adsorbed molecule ( $t_z$ ) and the average residence time that a molecule remains at a given surface site ( $t_r$ ) as follows,

$$(1 - \alpha) = \exp(- t_z/t_r). \quad (1.36)$$

$\alpha$  is defined in equation (1.1) and  $t_z$  is given by

$$t_z = \frac{Z}{V^*} \quad (1.37)$$

where

Z : the diameter of the adsorbed molecule

V\* : the sliding velocity

In addition, the average residence time of adsorbed molecule given by the following expression,

$$t_r = t_o \exp \left( \frac{E}{RT} \right) \quad (1.38)$$

where

$t_o$  : the fundamental time of vibration of adsorbed molecule

E : the heat of adsorption

From equations (1.36), (1.37), (1.38) and the fundamental equation in boundary equation [equation (1.6)], the friction coefficient is given by,

$$f = f_{\text{sol}} \{1 - \exp[(-z/vt_0) \exp(-E/RT)]\} + f_{\text{liq}} [(-z/vt_0) \exp(-E/RT)] \quad (1.39)$$

Therefore,  $f$  is a single exponential function of sliding velocity, and a double exponential function of temperature of heat of adsorption. However, none has ever clarified this relationship experimentally. Further investigation is clearly needed to justify Kingsbury's model.

### 1.38 Heat of Adsorption and Wear

A model of adhesive wear has been proposed by Rowe (108) (109). The equation derived by him is shown as follows:

$$\frac{V}{\ell} = k_m (1 + 3f^2)^{\frac{1}{2}} \alpha \frac{W}{P_m} \quad (1.40)$$

where

- $V$  : the total wear volume
- $\ell$  : the sliding surface
- $k_m$  : the wear coefficient for metal-metal contact area
- $f$  : the coefficient of friction
- $\alpha$  : the fractional film defect

W : the load

P<sub>m</sub> : the flow pressure under static loading

As  $\alpha$  has apparent values of 0.01 or less at poor lubrication, a good approximation of  $\ln(1 - \alpha)$  is  $(-\alpha)$ . Therefore, the approximation form of Kingsbury's equation (1.36), is given by:

$$\alpha = \frac{Z}{V^* t_o} \cdot e^{-E/RT} \quad (1.41)$$

combining equations (1.40) and (1.41),

$$\frac{V}{L} = \frac{k_m \gamma Z}{t_o P_m} \cdot \frac{W}{V^*} \cdot e^{-E/RT} \quad (1.42)$$

where V\* : the sliding velocity

$$\gamma = (1 + 3f^2)^{\frac{1}{2}}$$

Equation (1.42) states that if the values of  $k_m$  were known, wear rates could be calculated for partially lubricated systems, i.e. the rate of adhesive wear is an exponential of heat of adsorption. This model has been confirmed by the experiment of a copper pin sliding against a steel disk with n-hexadecane as lubricant the heat of adsorption for n-hexadecane by this model is 48.2KJ/mole.

On the other hand, several authors have discussed the relationship between wear and heat adsorption as measured experimentally. Sakurai and co-workers (10) (11) (106) have investigated heats of adsorption of oiliness reagents onto  $\alpha$ -Fe<sub>2</sub>O<sub>3</sub>, Fe<sub>3</sub>O<sub>4</sub> and FeS by a Flow Microcalorimeter. As the heats of adsorption of oiliness reagents onto FeS are large, the authors have stated that the interaction

of polar compounds in oil with EP films produced by sulphur-type EP additive plays an important part on anti-wear. In a similar way, a good correlation between the heats of adsorption and the wear-reducing ability has been reported by Groszek (97).

The two types of study, i.e. the theoretical approach and the experimental approach, have been described. At the moment, however, there are too many problems to combine both together.

#### 1.40 Analysis of Lubricated Surface

Recently, there has been much progress in surface analytical tools in boundary lubrication. The use of analyses are to get information on both qualitative and quantitative aspects, such as composition, film thickness, energy bond and so on. If it were possible to obtain this information in situ, it would be most valuable. However, in most cases, it is impossible to expect such analytical data, because most surface analytical apparatus must be used under high vacuum conditions. Therefore, in general, it is only possible to obtain analytical information of surface before and after lubrication.

In this study, electron spectroscopy for chemical analysis (ESCA), scanning electron microscopy (SEM), X-ray diffraction (XRD) and energy dispersive X-ray fluorescence (EDXRF) were used for analysis of sample and test piece. Godfrey (110) published an excellent review on the usefulness of new surface analysis instruments. Alternative methods

which have recently been applied to boundary lubrication problems are also described.

#### 1.41 Recent Development of Surface Analysis Techniques

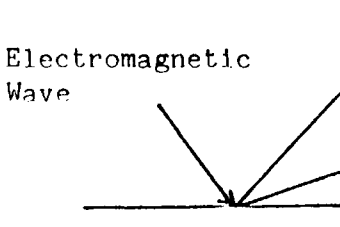
It is possible to classify analytical techniques of solid surfaces into two categories, i.e. methods which use (i) electromagnetic radiation, and (ii) charged particle such as ions and electrons. Schematic diagrams of these methods are shown in Figure 1.5 and 1.6.

From a different point of view, it is possible to classify methods into (i) diffraction method to investigate periodicity of atomic arrangement and the properties of a small mass of atoms, i.e. techniques which reveal structure and techniques which reveal topography and shape.

(ii) spectrometry method to analyse atomic surface qualitatively and quantitatively and bond energy, i.e. chemical analysis of surface.

(i) Techniques which reveal structure, topography and shape.

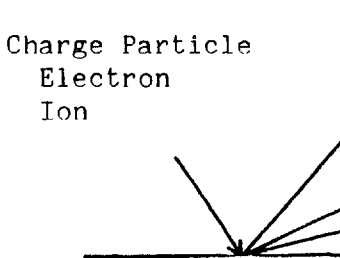
X-Ray Diffraction (XRD), Electron Diffraction (ED) give structure of crystalline material from which compounds can be identified. XRD gives information of the depth over than  $\mu\text{m}$  (52). For ED, the shorter wave length of electrons compared to X-rays allows analysis of small crystallites and thinner films (41). In this study, XRD was used for analysis of powders which were used in the heat of adsorption and adsorption measurements.



| Method                                     | Information* |        |   |      |   |
|--|--------------|--------|---|------|---|
|  | Qual.        | Quant. | E | Str. | H |
| Electron-Photoelectron Spectroscopy [ESCA] | ○            | △      | ○ | X    | △ |
| [UPS]                                      | X            | X      | ○ | X    | △ |
| Electromagnetic Wave { Ellipsometry        | X            | X      | △ | X    | ○ |
| { IR,Raman Spectroscopy                    | △            | X      | ○ | X    | △ |
| { X-ray Spectroscopy                       | ○            | △      | △ | X    | △ |
| { X-ray Diffraction                        | △            | △      | △ | ○    | △ |
| { Mössbauer Spectrometry                   | X            | X      | ○ | X    | △ |

Fig.1-5, Informations by incidence of electromagnetic wave into surface

\* Qual. : Qualitative Analysis, Quant. : Quantitative Analysis,  
 E : Bonding Energy, Str. : Structure of Atom, H : Film Thickness  
 ○ : Suitable, △ : Applicable, X : Inapplicable



| Method   | Information* |        |   |      |   |
|--|--------------|--------|---|------|---|
|  | Qual.        | Quant. | E | Str. | H |
| Electron { Auger Electron Spectroscopy             | ○            | △      | △ | X    | △ |
| { Low Energy Electron Diffraction                  | X            | X      | △ | ○    | △ |
| { High Energy Electron Diffraction                 | △            | △      | △ | ○    | △ |
| { Reflection "                                     | △            | X      | △ | ○    | △ |
| { Exo Electron                                     | X            | X      | △ | X    | △ |
| Ion { Secondary Ion Mass Spectrometry              | ○            | △      | X | X    | △ |
| Electromagnetic Wave { Electron X-ray Spectrometry | ○            | ○      | △ | X    | △ |
| { Ion X-ray Spectrometry                           | ○            | △      | ○ | X    | △ |

Fig.1-6, Informations by incidence of charge particle into surface

\* Qual. : Qualitative Analysis, Quant. : Quantitative Analysis,  
 E : Bonding Energy, Str. : Structure of Atom, H : Film Thickness,  
 ○ : Suitable, △ : Applicable, X : Inapplicable

Low Energy Electron Diffraction (LEED) utilizes a low energy electron beam which is diffracted by molecules regularly arranged on a surface. LEED reveals the location of atoms and the structure of surface of less than half a monolayer. Buckley (111) first used this method for investigation of lubricated surfaces.

Scanning Electron Microscopy (SEM) provides photographs of three-dimensional quality of surfaces at a wide range of magnification. This is an important method for the investigation of wear and the topography of surfaces. In this study SEM observed the powders which were used in experiments of heat of adsorption and adsorption.

(ii) Methods which provide chemical analysis of surfaces

Electron Probe Microanalysis (EPMA) provides information on the location and concentration of the elements on and in surface layers by X-rays emitted from an element which is bombarded with an electron beam. EPMA does not give direct information on the compounds in a film. In boundary lubrication, EPMA was used for investigation of reaction of EP additives (37) (38) (47).

Electron Spectroscopy for Chemical Analysis (ESCA) determines the elements on a surface to a depth about  $20\text{\AA}$  by measuring their binding energies. From electrons emitted from the atoms in the surface irradiated with X-ray, the binding energy is deduced to identify the element (112). In this study, ESCA was used to investigate the extent of oxidation of the surface of FeS powder which was used in the experiment of heat of adsorption and adsorption.

Auger Electron Spectroscopy (AES) is a method which permits analysis of the surface layers for very small areas of a surface. This method analyses all elements heavier than helium (33). AES can be combined with LEED and SEM.

Energy Dispersive X-ray Fluorescence (EDXRF) detects elements heavier than sodium by exciting the specimen with X-rays and detecting the elements characteristic X-ray. It is rapid, non-destructive, and capable of simultaneous multi-element analysis in the ppm range. EDXRF is very useful in BL for detecting elements in metals, in films on metals and in oils. In this study, EDXRF was used to measure sulphur content on the surface of test pieces prepared for friction and wear tests, which is described in Chapter Four.

#### 1.42 Analysis of EP Film

As described in Section 1.24, there are three types of EP additive, sulphur, chlorine and phosphorus. These additives react with metal under boundary condition and produce an EP film which has load carrying and anti-wear capacity. There are many publications which have reported the results of analyses of these EP films. As the main object of this project is to investigate interaction between oiliness reagents and EP films produced by sulphur-type EP additives. The results of analyses of the film and the technique used for that analysis are described here.

Allum and Forbes (38) (47) (55) (113) first used SEM and EPMA for analyses of sulphur and oxygen on wear scars



from a four-ball wear test and reported that the sulphur content increased with an increase in applied load up to a maximum observed sulphur content of approximately 30%. On the other hand, the oxygen content of the wear scar decreased with an increase in sulphur content. Coy and Quinn (39) also measured sulphur content on the scars formed with disulphides by EPMA and reported almost the same results as that by Allum and Forbes.

The analysis of surface films formed by sulphur compounds by XRD have been reported by Coy and Quinn (39), Godfrey (41), Sakurai and co-workers (22). Coy and Quinn suggested that in the EP region, iron sulphide, FeS, was found to be a major constituent along with increased amounts of Fe<sub>3</sub>C in scars formed with DBDS additives. They also reported that these scars had very small amounts of iron oxides,  $\alpha$ -Fe<sub>2</sub>O<sub>3</sub> and Fe<sub>3</sub>O<sub>4</sub>, were observed.

On the other hand, Godfrey (41) described that surface films formed by sulphur compounds in the presence of air were composed of a mixture of iron sulphide and iron oxide, and also suggested that Fe<sub>3</sub>O<sub>4</sub> was an important material for load carrying capacity. This kind of a mixture of Fe<sub>3</sub>O<sub>4</sub> and FeS was detected with ED by Hamaguchi and co-workers (35) (36). Buckley (29) (33) was the first user of AES for sliding surfaces analysis and demonstrated that sulphide films on iron surfaces were displaced by oxygen, the reverse process hardly occurred.

ESCA was used by Baldwin and Wheeler (114) to characterise the first few atomic layers of surfaces after wear-testing in oil formulations which contained organo-

sulphur additives produce the same metal sulphide and the sulphide concentration shows a correlation with wear. By means of ESCA, Tamai (115) found evidence of mechanochemical activity in the reaction between steel and organic sulphur compound after mild cutting.

### 1.50 Scope of Research

The purpose of this thesis is to clarify the mechanism of interaction between oiliness compounds and EP films produced with sulphur-type EP additive, and to investigate the effect of this interaction on friction and wear in boundary lubrication. The following three experiments have been carried out for this purpose.

#### (1) Heat of Adsorption (Chapter 2)

The measurement of heats of adsorption of stearic acid, stearyl alcohol and methyl stearate onto  $\alpha$ -Fe<sub>2</sub>O<sub>3</sub>,  $\gamma$ -Fe<sub>2</sub>O<sub>3</sub>, Fe<sub>3</sub>O<sub>4</sub> and FeS by a Flow Micro-calorimeter.

#### (2) Adsorption (Chapter 3)

The measurement of adsorptions of stearic acid and methyl stearate onto  $\alpha$ -Fe<sub>2</sub>O<sub>3</sub>,  $\gamma$ -Fe<sub>2</sub>O<sub>3</sub>, Fe<sub>3</sub>O<sub>4</sub> and FeS.

#### (3) Friction and Wear (Chapter 4)

The measurement of friction and wear during running-in by a Bowden Leben machine.

CHAPTER TWO  
HEAT OF ADSORPTION

2.10 Introduction

The heat of adsorption is a valuable parameter for measuring the stability of adsorbed films. Frewing (89) has proposed a relationship between the heat of adsorption and the transition from smooth sliding to stick-slip phenomenon in boundary lubrication. Cameron and co-workers (89)~(95) have advanced this concept and have obtained many useful thermodynamic values such as enthalpy change of adsorption ( $\Delta H_{ads}$ ) and entropy change of adsorption ( $\Delta S_{ads}$ ). In their studies, the interesting phenomenon of chain matching between oiliness reagent and base oil has been partially explained (94) (95). However, as the values obtained are calculated ones using the theoretical equation, there are some difficulties in applying the results to complicated phenomenon such as the influence of chemical nature of the lubricated surface on adsorption.

As most of the theoretical study described above assume a simple Langmuir-type adsorption, several authors have tried to measure enthalpy change of adsorption of oiliness reagents in solution directly by a Flow Micro-calorimeter and have discussed the relationship to boundary lubrication (10) (11) (47) (55) (96)~(106). By this kind of study, it is possible to investigate the stabilities of adsorbed films on the surface with differing chemical natures. If EP additives exist in lubricant oil, then EP films as

described in Section 1.24 are produced in boundary lubrication. In the case of sulphur-type EP additives, EP films composed of FeS and iron oxides such as  $\text{Fe}_3\text{O}_4$  are formed. Sakurai and co-workers (9)~(12) have suggested that the interaction of oiliness reagents with FeS play an important role in reducing wear in boundary lubrication. Cameron (6) (7) (8) and Yagi (12) have also supported this suggestion.

This study has been designed in order to help to make this interaction clear. For this purpose, the heats of adsorption (the enthalpy change of adsorption) of oiliness reagents such as stearic acid, stearyl alcohol and methyl stearate, onto  $\alpha\text{-Fe}_2\text{O}_3$ ,  $\gamma\text{-Fe}_2\text{O}_3$ ,  $\text{Fe}_3\text{O}_4$  and FeS were measured by a Flow Microcalorimeter. The influence of solvent and temperature on the heat of adsorption was investigated as well as the heats of adsorption at room temperature. Combining these results with the data of adsorption measurement, which are shown in the next chapter, the heats of adsorption per mole are calculated. It is possible to compare the results obtained in this study with the theoretical values obtained by other authors.

## 2.20 Experimental

### 2.21 Materials

Adsorbates: three kinds of oiliness reagents were used as adsorbates for this work; stearic acid, stearyl alcohol and methyl stearate. All three reagents were supplied by BDH as a puriss grade. They were then purified by

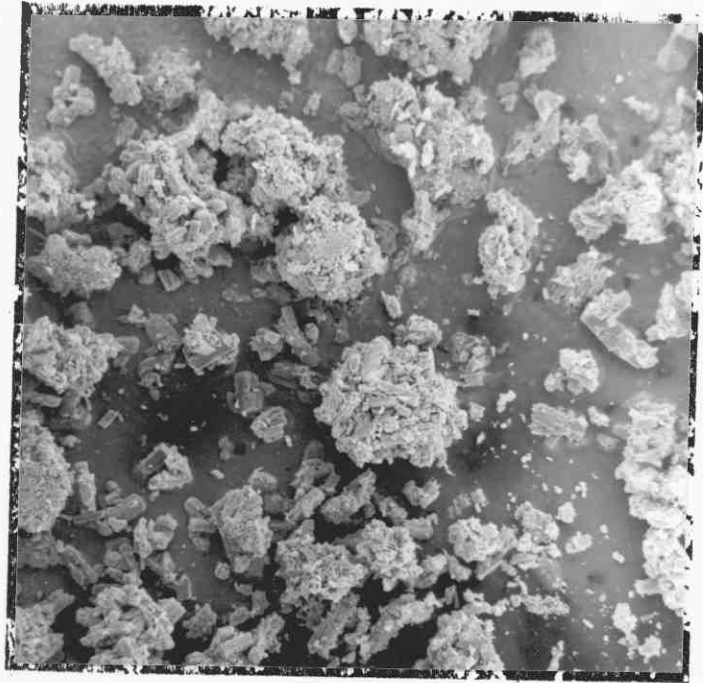
recrystallization from methanol. After two recrystallizations stearic acid, stearyl alcohol and methyl stearate showed melting points of 71.5-72.0°C, 60.0-60.5°C and 39.5-40.0°C, respectively. The purities determined by GLC and elemental analysis are listed below:

|                 | GLC   | Experimental Analysis |
|-----------------|-------|-----------------------|
| Stearic acid    | 99.5% | -                     |
| Stearyl alcohol | 99.7% | -                     |
| Methyl stearate | 99.5% | -                     |
| DBDS            | 99.9% | 99.9%                 |

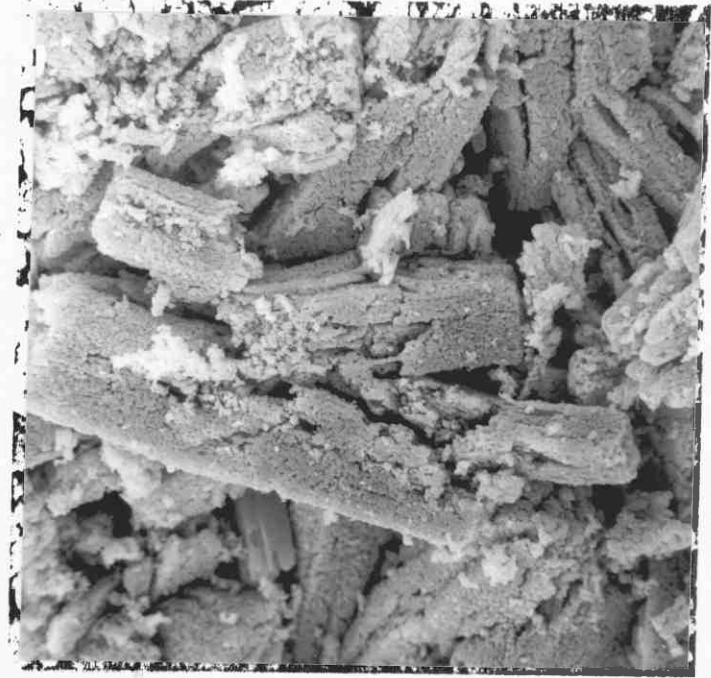
Solvents: n-Heptane, n-Decane and n-hexadecane were used as solvents. They were purified by percolation through a silica gel-alumina column, followed by continuous contact with silica gel and alumina for a week. The solvents were further dried by a molecular sieve (5Å) for at least two days before use in adsorption experiments to ensure that the water contents were the same for each experiment.

Adsorbent Powders:  $\alpha$ -Fe<sub>2</sub>O<sub>3</sub>,  $\gamma$ -Fe<sub>2</sub>O<sub>3</sub>, Fe<sub>3</sub>O<sub>4</sub> and FeS powders were used for the measurement of heat of adsorptions.  $\alpha$ -Fe<sub>2</sub>O<sub>3</sub> (>100 mesh) was purchased from Johnson & Massey Co Ltd,  $\gamma$ -Fe<sub>2</sub>O<sub>3</sub>, Fe<sub>3</sub>O<sub>4</sub> and FeS were purchased from High Purity Chemicals Co Ltd, Japan.  $\gamma$ -Fe<sub>2</sub>O<sub>3</sub> and Fe<sub>3</sub>O<sub>4</sub> powders were finer than 100 mesh and FeS was finer than 200 mesh. The exact distribution of particle sizes is shown in Photographs 2.1 to 2.4, which show secondary images of scanning electron micrographs.

The following results are summarized from the observation of these photographs.



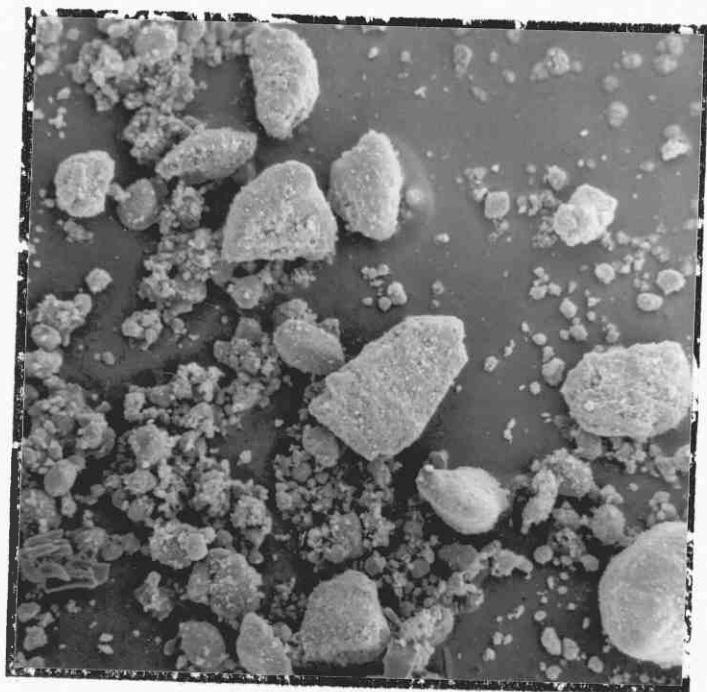
— 50 u



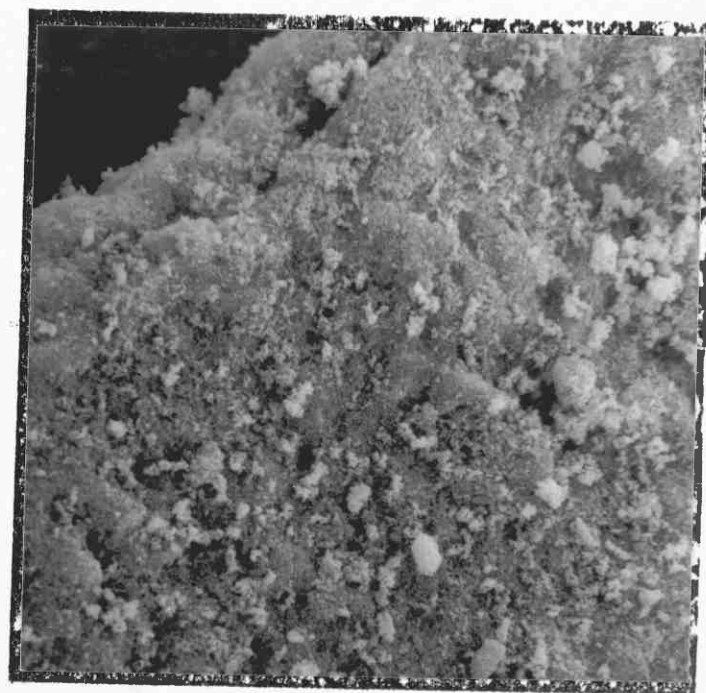
— 5 u

Photo.2-1, The secondary images of scanning electron micrograph of  $\alpha\text{-Fe}_2\text{O}_3$

-70-



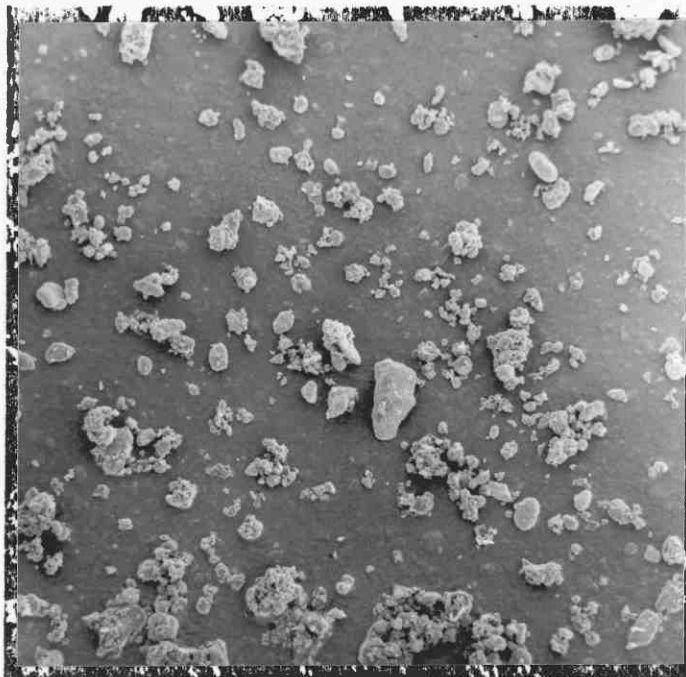
— 50u



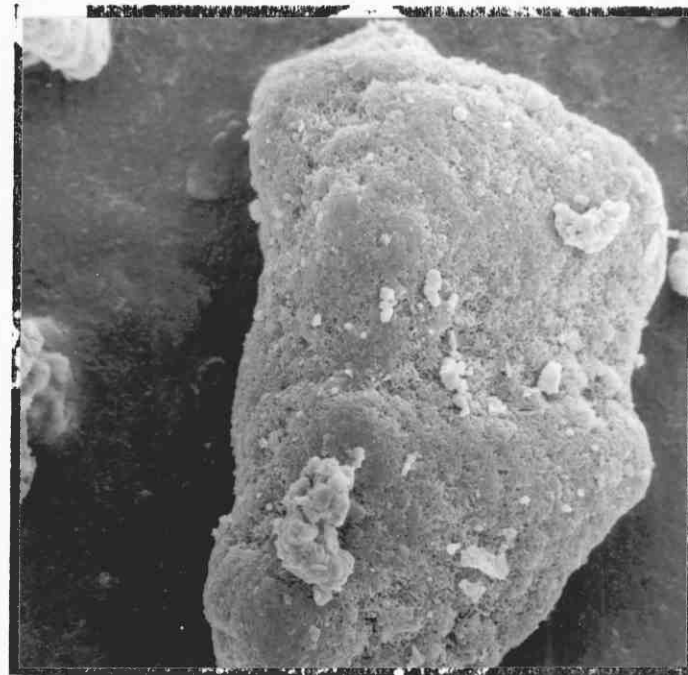
— 5u

Photo.2-2, The secondary images of scanning electron micrograph of  $\gamma\text{-Fe}_2\text{O}_3$

-71-



— 50u

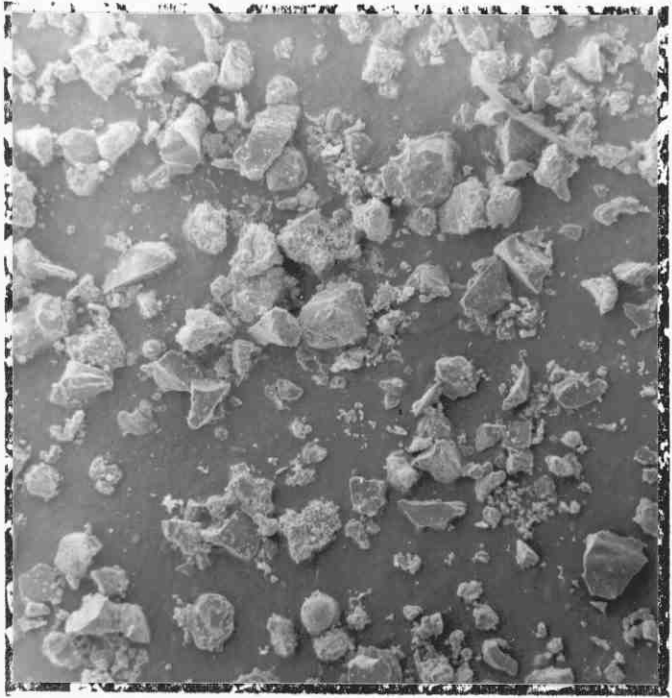


— 5u

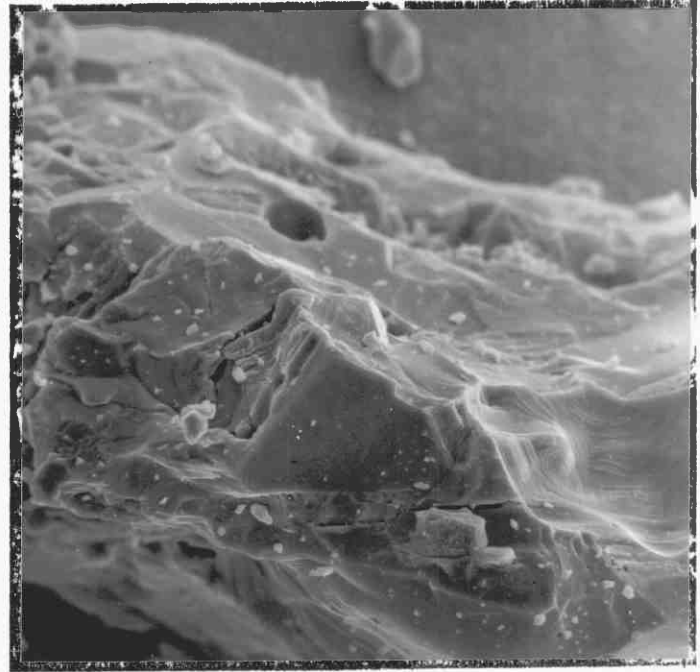
Photo.2-3, The secondary images of scanning electron micrograph of  $\text{Fe}_3\text{O}_4$



-72-



— 50u



— 5u

Photo.2-4, The secondary images of scanning electron micrograph of FeS

- $\alpha\text{-Fe}_2\text{O}_3$  : pillared particles of about  $50 \times 100\mu$  occurring as clusters, with the surfaces of each particle covered with very fine particles.
- $\gamma\text{-Fe}_2\text{O}_3$  : very fine particles below  $0.5\mu$  attached to the surface of larger particles.
- $\text{Fe}_3\text{O}_4$  : small particles ( $2\text{-}3\mu$ ) occurring in clusters of size  $10\text{-}100\mu$ .
- FeS : the surfaces of the particles were smooth, sometimes hollow, below  $2\mu$ , can be seen on the surfaces.

An estimate of specific surface area was made by the Brunauer-Emmett-Teller (BET) method with nitrogen and krypton. The results are listed in Table 2.1. Large differences were noted between the results obtained from the different methods. As the results from the nitrogen method were found to be inconsistent at the low values, data from the krypton method was used to calculate the cumulative heat of adsorption per unit surface area of powder.

The elemental compositions of the powders were determined by chemical analysis and are listed in Table 2.2. The iron content was determined by oxidation/reduction titration using  $\text{K}_2\text{Cr}_2\text{O}_7$ . To measure the sulphur content, a sample of the powder was burned in air and the gaseous products were absorbed in hydrogen peroxide solution. The resulting sulphuric acid was titrated by a standard alkaline solution. A large difference was found between the experimental data and the calculated values for iron oxides. The results for FeS however were close to the calculated values.

TABLE 2.1

Specific Surface Area of Powders  
BET Method (m<sup>2</sup>/g)

| Powder                           | N <sub>2</sub> |        | Kr    |
|----------------------------------|----------------|--------|-------|
|                                  | First          | Second |       |
| α-Fe <sub>2</sub> O <sub>3</sub> | 3.75           | 3.44   | 3.63  |
| γ-Fe <sub>2</sub> O <sub>3</sub> | 17.99          | 18.85  | 17.00 |
| Fe <sub>3</sub> O <sub>4</sub>   | 6.18           | 6.28   | 8.04  |
| FeS                              | 1.44           | 1.38   | 1.70  |

α-Fe<sub>2</sub>O<sub>3</sub> was supplied by Johson and Massey Co Ltd, and the other samples were purchased from High Purity Chemicals Co Ltd, Japan.

TABLE 2.2

Chemical Component of Powder

| Powder                           | Fe %        | S %         |
|----------------------------------|-------------|-------------|
| α-Fe <sub>2</sub> O <sub>3</sub> | 68.6 (69.9) |             |
| γ-Fe <sub>2</sub> O <sub>3</sub> | 63.5 (69.9) |             |
| Fe <sub>3</sub> O <sub>4</sub>   | 65.0 (78.5) |             |
| FeS                              | 62.3 (63.5) | 35.6 (36.5) |

Figures in parentheses indicate calculated values.

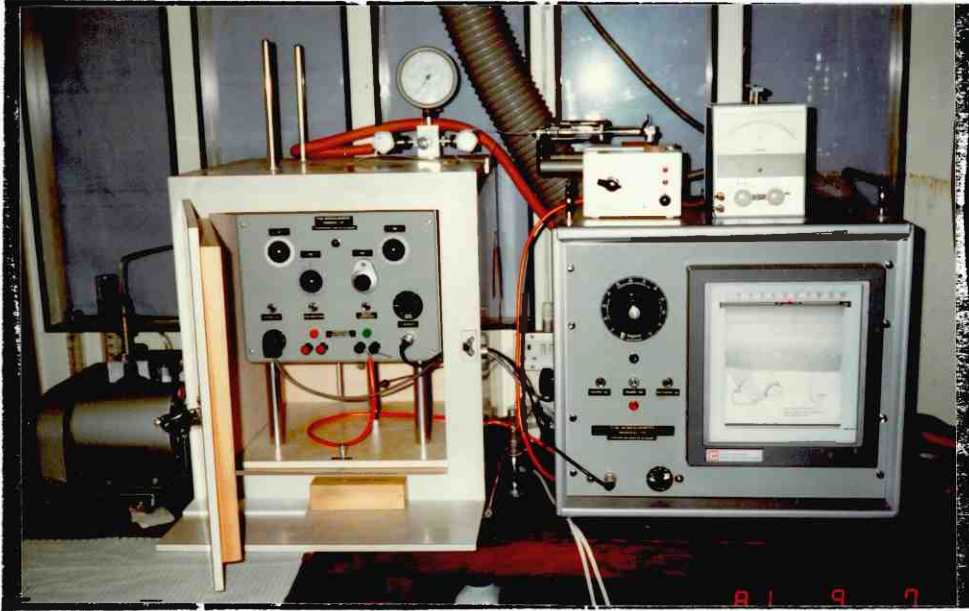
X-ray diffraction analysis was performed in order to characterise the structure of the samples. The main results are given by:

- $\alpha\text{-Fe}_2\text{O}_3$  : the strong peaks for hematite ( $\alpha\text{-Fe}_2\text{O}_3$ ) were confirmed, and no other peaks were detectable.
- $\gamma\text{-Fe}_2\text{O}_3$  : the strong peaks for maghemite ( $\gamma\text{-Fe}_2\text{O}_3$ ) were confirmed, and no impurity peaks were recognised.
- $\text{Fe}_3\text{O}_4$  : the strong peaks for magnetite ( $\text{Fe}_3\text{O}_4$ ) were confirmed. This sample includes a small amount of wustite (FeO) and fayalite [ $(\text{Fe}_X\text{Mg}_Y)_2\text{O}\cdot\text{SiO}_2$ ] as impurities.
- FeS : the strong peaks for troilite (FeS) and pyrrhotite ( $\text{Fe}_{1-x}\text{S}$ ) were recognised.

Prior to measurement in a Flow Microcalorimeter experiment, the powders of  $\alpha\text{-Fe}_2\text{O}_3$ ,  $\text{Fe}_3\text{O}_4$  and FeS were degassed at 300°C for four hours under vacuum (< 1mm Hg). For  $\gamma\text{-Fe}_2\text{O}_3$ , 270°C was adopted for the degassing, to avoid transition from  $\gamma\text{-Fe}_2\text{O}_3$  to  $\alpha\text{-Fe}_2\text{O}_3$ .

## 2.22 Apparatus

All of the heat of adsorption data in this work were measured by a Flow Microcalorimeter type Mark II V produced by Microscal Ltd. The Flow Microcalorimeter was designed for the detection of heats of solute/solid or gas/solid interaction, which are usually physical or chemical adsorptions. This apparatus is made up to four units; the calorimeter, the recorder, the vacuum system and a flow control pump (see Photograph 2.5 and Figure 2.1).



Photograph 2-5, View of a Flow Microcalorimeter

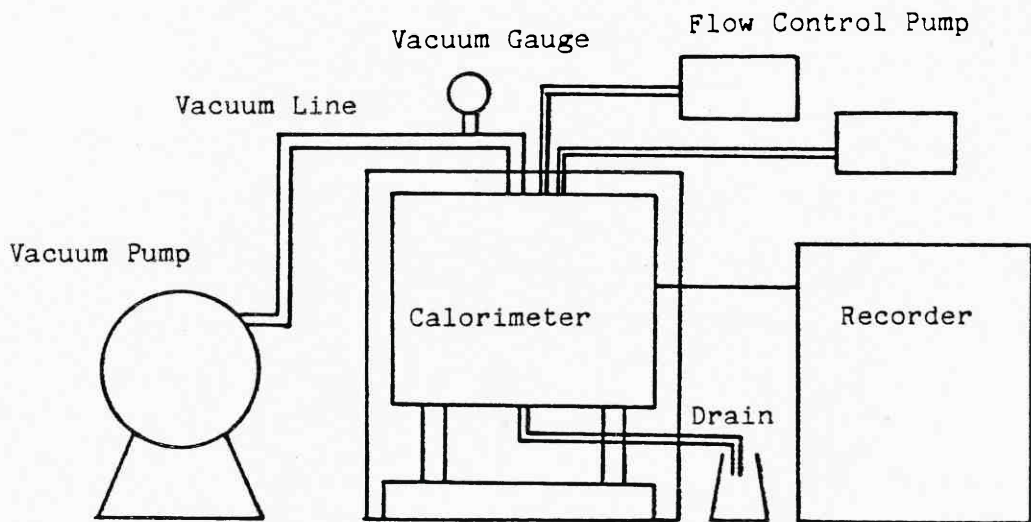


Fig.2-1, Schematic diagram of Flow Microcalorimeter

The calorimeter was enclosed by a draught proof enclosure to avoid outside thermal effects. The vacuum system of this apparatus was not used, since these experiments were confined to the investigation of solute/solid interaction in solution.

A schematic drawing of the reaction cell in the calorimeter is shown in Figure 2.2. The reaction cell is surrounded by a PTFE wall. Both the inlet and the outlet to the reaction cell are made of stainless steel. The outlet was 500 mesh gauze to hold adsorbent powder in the reaction cell. The total volume of the reaction cell is about 0.17ml. The volume of adsorbent used was 0.10-0.13ml, thus forming a bed in the reaction cell of the calorimeter, approximately 3.2-4.2mm high, and filling the cell to a level of 0.8-1.8mm above that of the thermistors. A pair of thermistors ( $T_m$ ) are placed in direct contact with the adsorbent and a pair of identical reference thermistors ( $T_{rf}$ ) are embedded in the PTFE above the reaction cell. Two fine stainless steel tubes for solvent and solute are fixed in the inlet tube supporter.

Any changes in the temperature of the cell contents, which accompany the adsorption process, are measured by the thermistors arranged in Wheatstone Bridge circuit as shown in Figure 2.3. The output from the bridge is fed into a variable range potentiometer recorder of 100 $\mu$ V to 5000 $\mu$ V full scale deflection. Thus the departure and subsequent return to equilibrium in the reaction cell can be monitored and recorded.

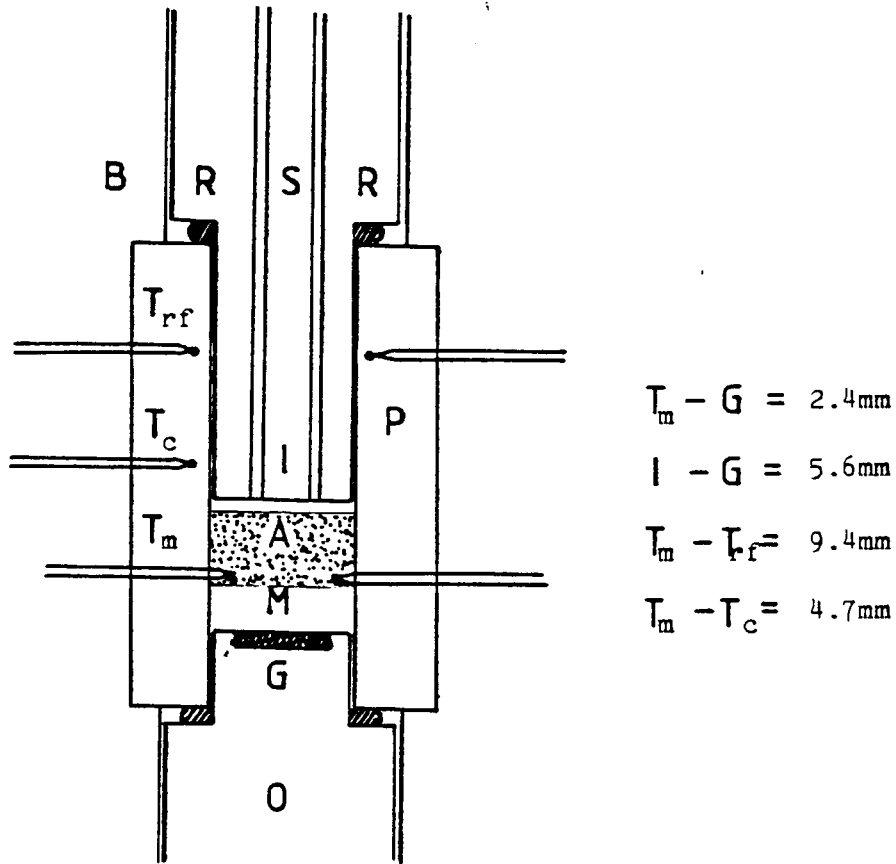


Fig.2-2, Schematic drawing of the cell in a Flow Microcalorimeter

- S : Inlet tube supporter
- B : Metal block
- I : Inlet tube
- P : PTEF cell
- A : Adsorbent
- M : Inert metal powder
- G : Gauze forming the bottom of the cell
- O : Outlet tube
- $T_m$  : Thermistors to measure heat release
- $T_{rf}$  : Reference thermistors
- $T_c$  : Thermocouple to measure cell temperature
- R : O ring

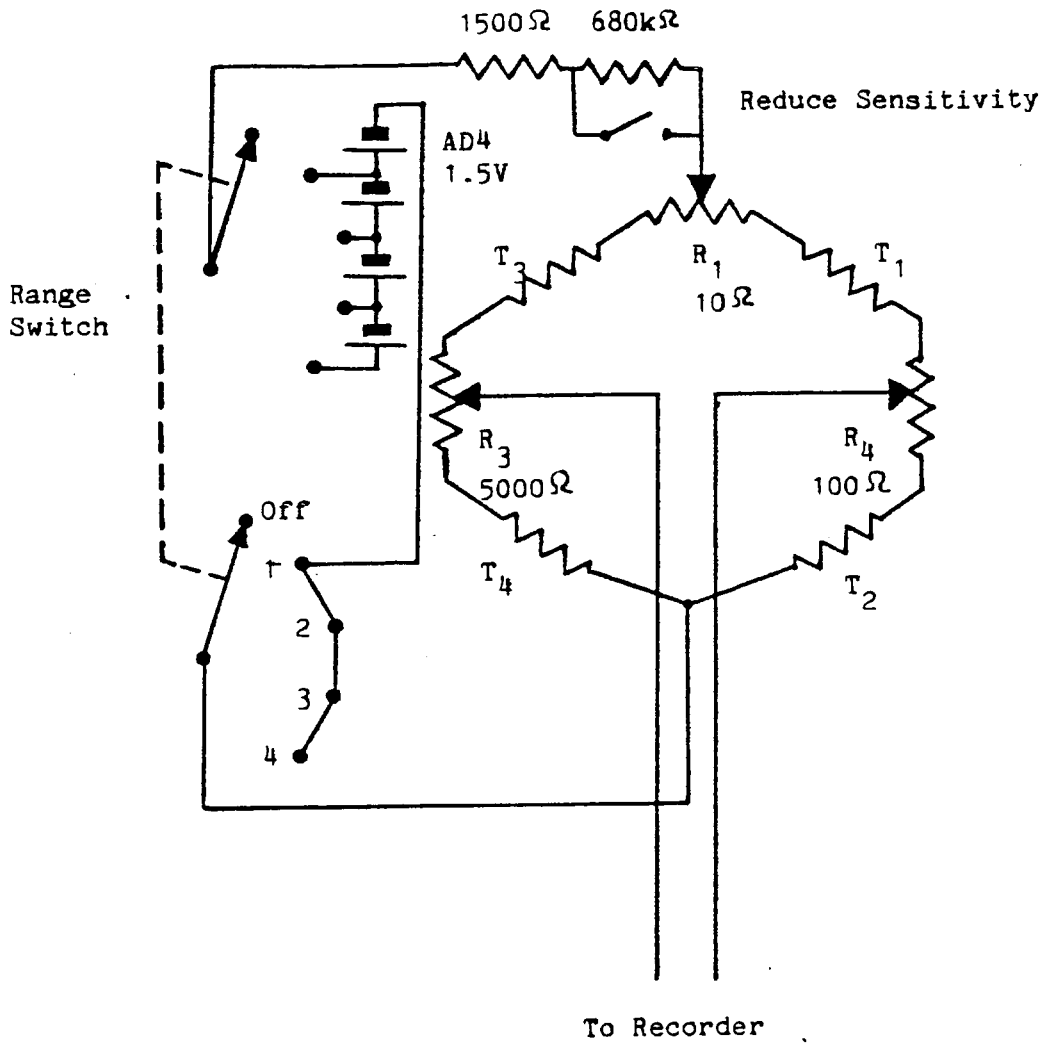


Fig.2-3, Circuit diagram of the Flow Microcalorimeter  
Mark II V Model

$T_1 \sim T_4$  : Nominal 100kΩ Thermistors



### 2.23 Procedure

One of the adsorbent powders of volume 0.10-0.13ml (the precise volume is dependent on the powder), is weighed to the nearest milligramme and poured slowly through a funnel into the cell which has already been filled with n-heptane. Air surrounding the adsorbent particles is released as soon as these are wetted with the solvent. In order to obtain the best results it is necessary to have an even packing of adsorbent bed and a smooth, steady flow of fluid through it.

Then, the inlet tube is fixed in the calorimeter to start percolation of solvent. Thermal equilibrium at room temperature is reached in about 30 minutes and a steady base line is established on the recorder chart. Longer stabilization is necessary for a measurement at high temperature. Preheating up to a few degrees higher than the setting temperature can save a lot of time in stabilizing for measurements at high temperature. Once the thermal stabilization is established, the flow of solvent is replaced by the flow of the sample solution. Depending on the method of sample injection, three types of measurement can be carried out: the saturation method, the injection method and the percolation method.

Saturation method: this method gives information about the cumulative heats of adsorption of the samples (96). The flow of the solvent is stopped and the flow of solution is continued until adsorption is completed. When adsorption is completed, and the equilibrium between solution and powder

is reached, heat ceases to be evolved and thermal equilibrium is established again. A single peak is obtained on the recorder by this procedure. By measuring the area under the peak and multiplying this by the calibration factor of the thermistor ( $k^*$ ), one can obtain the cumulative heat of adsorption. All the heats of adsorption in this work were obtained by this method. In the same manner, if the flow of solution is replaced by a flow of solvent after the saturation of adsorption has been reached, the cumulative heat of desorption can be measured. Charts showing typical peaks caused by the cumulative heats of adsorption and desorption on applying this method are shown in Figure 2.4.

Other methods: Some authors use the injection method (97) (99) and the percolation method (10) (11) (106) to investigate adsorption and desorption. Although these methods were not used in this work, a brief explanation of them is given here.

The injection method is suitable for measuring the concentration of adsorbate. A few microlitres of dilute solution of adsorbate is introduced into the stream of solvent. The peak of adsorption and desorption resulting from the adsorbate's passage through the cell is recorded subsequently. A relationship between the amount of adsorbate injected and the peak height can be obtained if the proper type and quantity of adsorbent is selected. It is possible to measure the concentration of adsorbate by using this relationship.

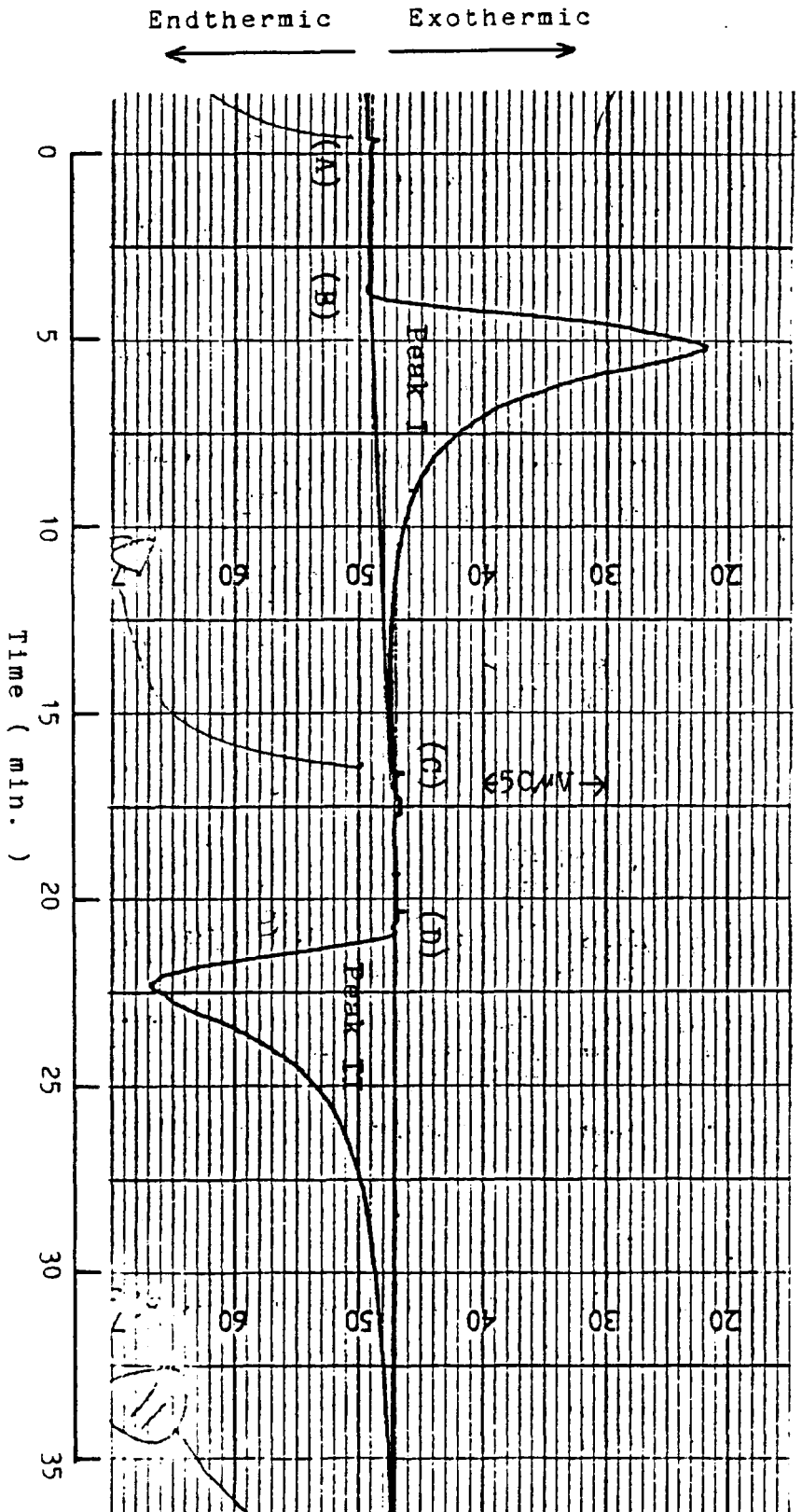
The percolation method has been used to determine the

FIG.2-4, Typical peaks of heat of adsorption and desorption

Peak I : Adsorption of methyl stearate (24.05 m Mol/l)  
Peak II : Desorption of methyl stearate (24.05 m Mol/l)

Conditions

Adsorbent :  $Fe_3O_4$  Solvent : n-Heptane  
Temperature : 26.5°C Flow rate : 3.30 ml/hour



amount of adsorption. If it is possible to make a precolumn containing an inert solid having the same interstitial volume as the adsorbent, the amount of adsorption can be calculated from the following equation by comparing the retention time of precolumns containing the adsorbent and inert solid described above.

$$x = t \text{ cf}/W \quad (2.1)$$

where

t : the retention time difference

c : the concentration of solute in mg/ml

f : the flow rate of solution in ml/min

W : the weight of adsorbent in the precolumns

The difficulty of this method is that a selection of an inert solid can have the same interstitial volume as the adsorbent.

Calibration: Calibration of the calorimeter is effected by introducing heat electrically into the adsorption bed.

This is achieved by using the calibration unit, which has a small heating coil, in place of the standard outlet. The reaction cell filled with adsorbent and the calorimeter may then be used in the normal way. By supplying electric current to the coil, various amounts of energy can be introduced into the adsorbent so as to obtain a series of peaks of different shape and size. From these procedures the calibration curve between the heat release in the adsorbent bed and the peak area on the chart recorder is obtained.

The layout of the calibration heater is given in Figure 2.5. The resistance of the calibration unit including

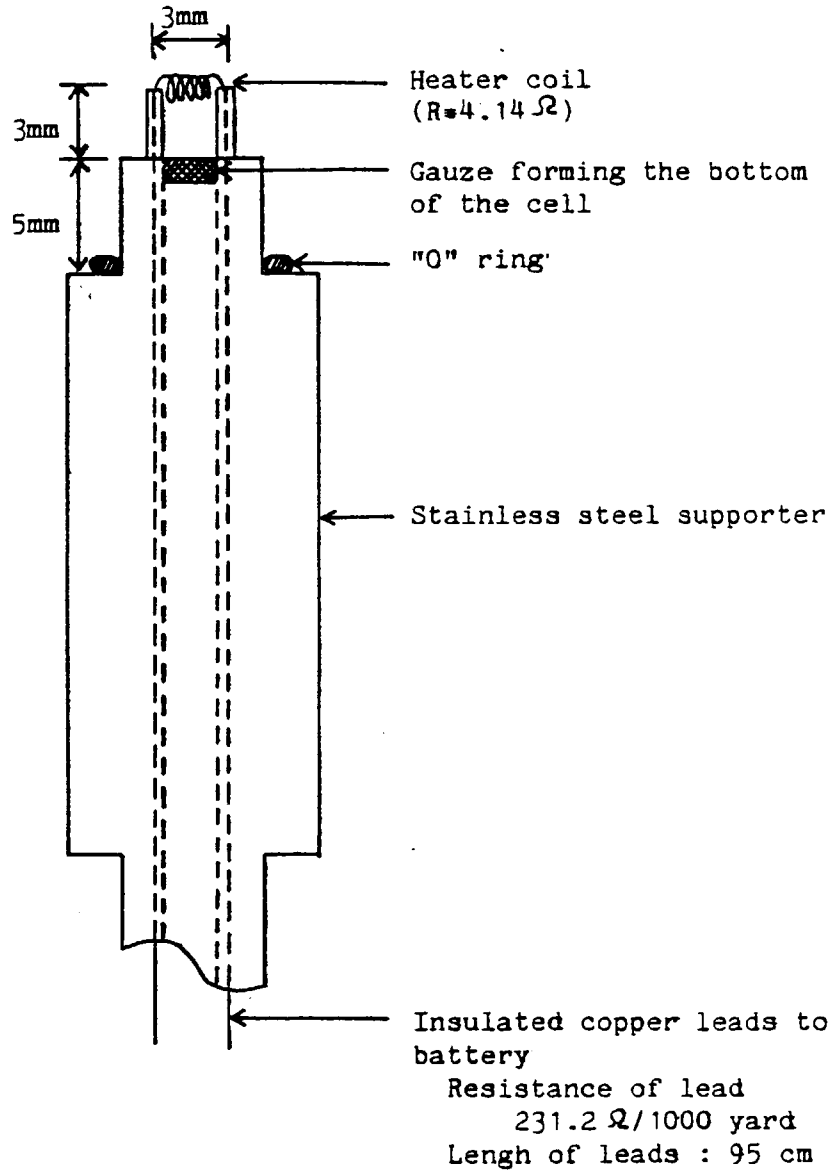


Fig.2-5, Microheater for calibration

the lead was 4.38ohms and calculated value of resistance of the lead was 0.24ohms (symbol r). Therefore the resistance of the coil (symbol R) was 4.14ohms. The energy dissipated by the calibration coil was calculated from the following equation:

$$W = \frac{V^2 Rt}{(R + r)^2} \times 1000(\text{mil J}) \quad (2.2)$$

where

$$r/(R + r) = 0.216$$

V : power input (volts)

t : time (seconds)

Typical calibration curves derived from this procedure are shown in Figure 2.6. As the curves were straight lines, the thermal sensitivity of the thermistor (symbol k\*) can be given.

$$\Delta H = k^* A \quad (2.3)$$

where

$\Delta H$  : heat release (mil J)

k\* : thermal sensitivity of the thermistor

A : peak area on chart recorder ( $\mu\bar{V}$  x min)

The thermal sensitivity k\* was not influenced by small changes of slow speed of solution and rate of energy dissipation from the heater. However, temperature of adsorbent and the type of powder have much influence on the sensitivity. So, a range of values of k\* were measured (Table 2.3).

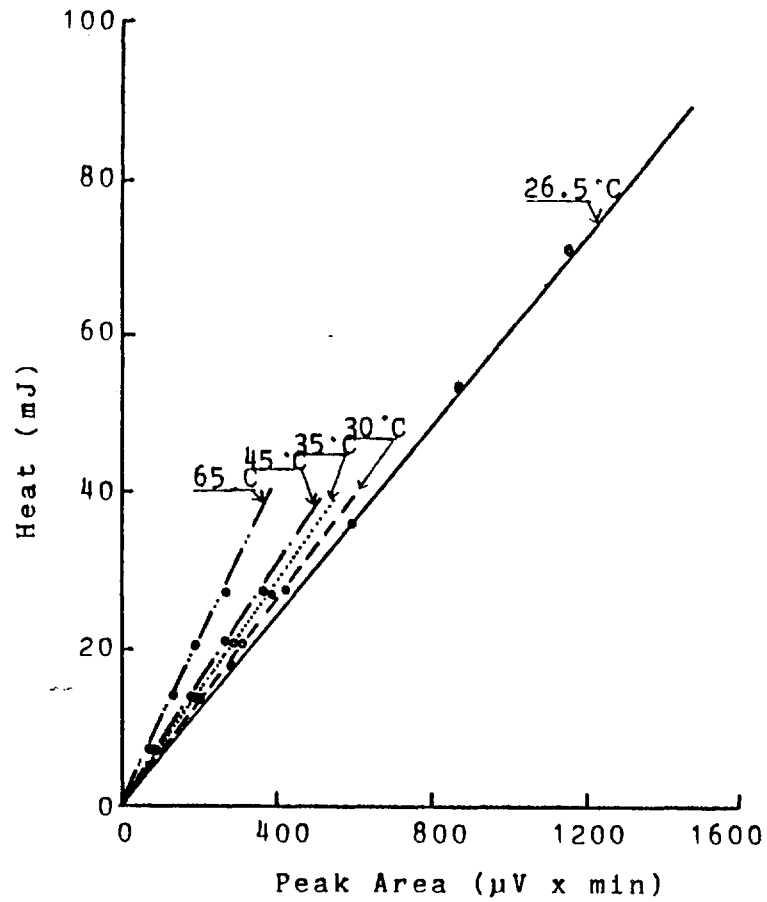


Fig.2-6, Thermal sensitivity of thermistor in FeS powder

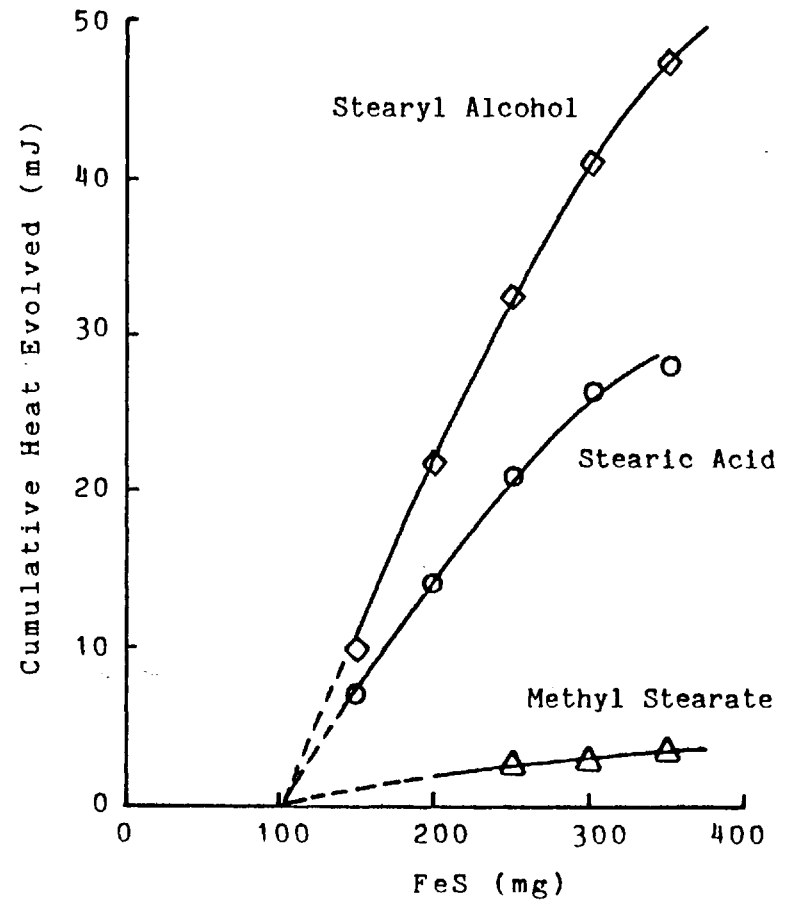


Fig.2-7, Cumulative heat evolved vs. amount of FeS powder

TABLE 2.3

Thermal Sensitivity of the Thermistor  
in a Flow Microcalorimeter

| Sensitivity (k*) = $\Delta H(\text{mJ})/\text{Peak Area} (\mu\text{v} \times \text{min})$ |                                |                                |                         |        |
|---|--------------------------------|--------------------------------|-------------------------|--------|
| Powder Temp (°C)  | $\alpha\text{-Fe}_2\text{O}_3$ | $\gamma\text{-Fe}_2\text{O}_3$ | $\text{Fe}_3\text{O}_4$ | FeS    |
| 26.5  | 0.0500                         | 0.0594                         | 0.0608                  | 0.0610 |
| 30  | 0.0518                         | 0.0491                         | 0.0612                  | 0.0660 |
| 35  | 0.0550                         | 0.0518                         | 0.0648                  | 0.0697 |
| 45  | 0.0591                         | 0.0599                         | 0.0715                  | 0.0760 |
| 55  |                                |                                | 0.0815                  |        |
| 65  | 0.0860                         | 0.0867                         | 0.0983                  | 0.1030 |

Effective amount of powder: It is necessary to confirm the linearity between the amount of powder packed in the cell and heat release, in order to obtain the quantitative heat of adsorption from the Flow Microcalorimeter. As no-one other than Groszek (96) has ever discussed this problem, the influence of the amount of powder on heat release was investigated before the series of experiments was started.

As shown clearly in Figure 2.7, the heat release is not directly proportional to the amount of powder. This figure indicates that the thermistors cannot detect the heat release from the powder situated lower than a certain level in the cell, and that the thermistors cannot detect all



of heat release from powders which overflow the cell. However, it is possible to assume the concept of a dead volume of powder, i.e. that amount which has no effect on the heat recorded on a chart recorder. From this concept, the effective amount of powder, which is the difference between the total amount of powder packed in the cell and the powder in the dead volume described above, was introduced in this work to calculate the cumulative heat of adsorption and desorption per unit surface area of powder.

In order to obtain linearity between the heat of adsorption and the amount of powder, it is important to estimate the exact dead volume of powder. Table 2.4 shows that the dead volume is dependent on type of powder used. Experiment has shown that it is independent of type of solution and release of different heats of adsorption. Figure 2.7 shows that an identical dead volume is observed for three different solutions. From these results, the postulation of constant dead volume in measurements at different temperatures and with solutions of different concentrations is adopted to avoid excessive preliminary experiments. To obtain results in the linear part of the curve, it is necessary to keep the volume of powder below a certain level depending on the type of powder used. It was usually found desirable to use the maximum volume up to this level, as small volumes of powder gave poorly reproducible results. Therefore the amount of powder packed in the cell was selected carefully in this work. The effective amount of powder and the amount of powder packed in the cell for each sample are listed in Table 2.4.

TABLE 2.4

Effective Amount of Powder and the Amount  
of Powder Packed in the Cell

| Powder                         | Effective    | Packed       |
|--------------------------------|--------------|--------------|
| $\alpha\text{-Fe}_2\text{O}_3$ | 36mg         | 70mg         |
| $\gamma\text{-Fe}_2\text{O}_3$ | 49mg         | 60mg         |
| $\text{Fe}_3\text{O}_4$        | 148mg        | 250mg        |
| FeS                            | 195 or 145mg | 300 or 250mg |

Heat of dilution: Heat of dilution is inevitable in the measurement of heat of adsorption with a Flow Microcalorimeter (96), but it is possible to estimate the magnitude of it by using solids having negligible adsorptive capacity. One of the results of a heat of dilution determined, is shown in Figure 2.8. In this experiment, steel particles having a surface area of  $0.21\text{m}^2/\text{g}$  were used as an adsorption bed in the cell of a Flow Microcalorimeter, and the stearic acid solution ( $20\text{mMol}/\ell$ ) was used as an adsorbate. The heat release in this experiment was so small that it was difficult to obtain reproducible results. The peak area for the heat release on the chart recorder was less than  $20\mu\text{V} \times \text{min}$ . This means that the heat of dilution of  $20\text{mMol}/\ell$  stearic acid solution by n-heptane is less than about  $1\text{mJ}$ . Compared with the heat of adsorption measured in this study, this value is small enough to neglect.

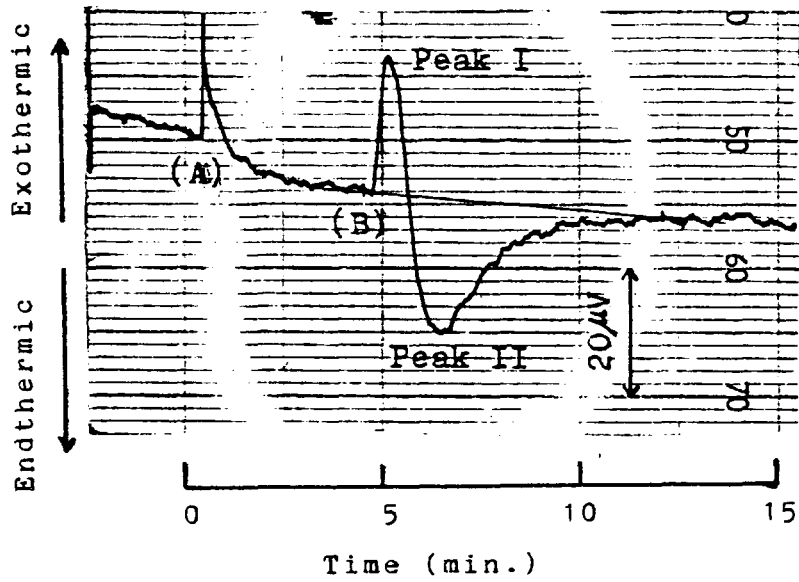


Fig.2-8, Heat change of stearic acid solution (12.0 m Mol/l) in Fe powder

Conditions

Adsorbent : Fe powder  
Solvent : n-Heptane  
Temperature : 26.5 C  
Flow rate : 3.30 ml/hour

## 2.30 Results

### 2.31 Heats of Adsorption at Room Temperature

The results of cumulative heats of adsorption at room temperature (26.5°C) are presented in Figures 2.9 to 2.12 and relate to adsorption on  $\alpha$ -Fe<sub>2</sub>O<sub>3</sub>,  $\gamma$ -Fe<sub>2</sub>O<sub>3</sub>, Fe<sub>3</sub>O<sub>4</sub> and FeS respectively, where the cumulative heat evolved is reported as mil Joule (mJ) per m<sup>2</sup> of adsorbent surface area. All of these results were obtained by the saturation method using n-heptane as a solvent.

The cumulative heats of adsorption on  $\alpha$ -Fe<sub>2</sub>O<sub>3</sub> at 26.5°C are shown in Figure 2.9. In this figure, the results of three oiliness reagents, stearic acid, stearyl alcohol and methyl stearate, were compared at various concentrations. The order of the heats of adsorption for the oiliness reagent with different functional groups is:

Alcohol >> Acid > Ester

The heat of adsorption of stearyl alcohol has not only a large value, but also has a two step heat release (at about 15mMol/l). As explained by many authors, this secondary enhancement of heat depends on change of angle of the adsorbed molecule (71) (99). For methyl stearate, the heat of adsorption is so small that it is difficult to find the same trend of secondary enhancement such as in stearyl alcohol.

The cumulative heat of adsorption of stearic acid on

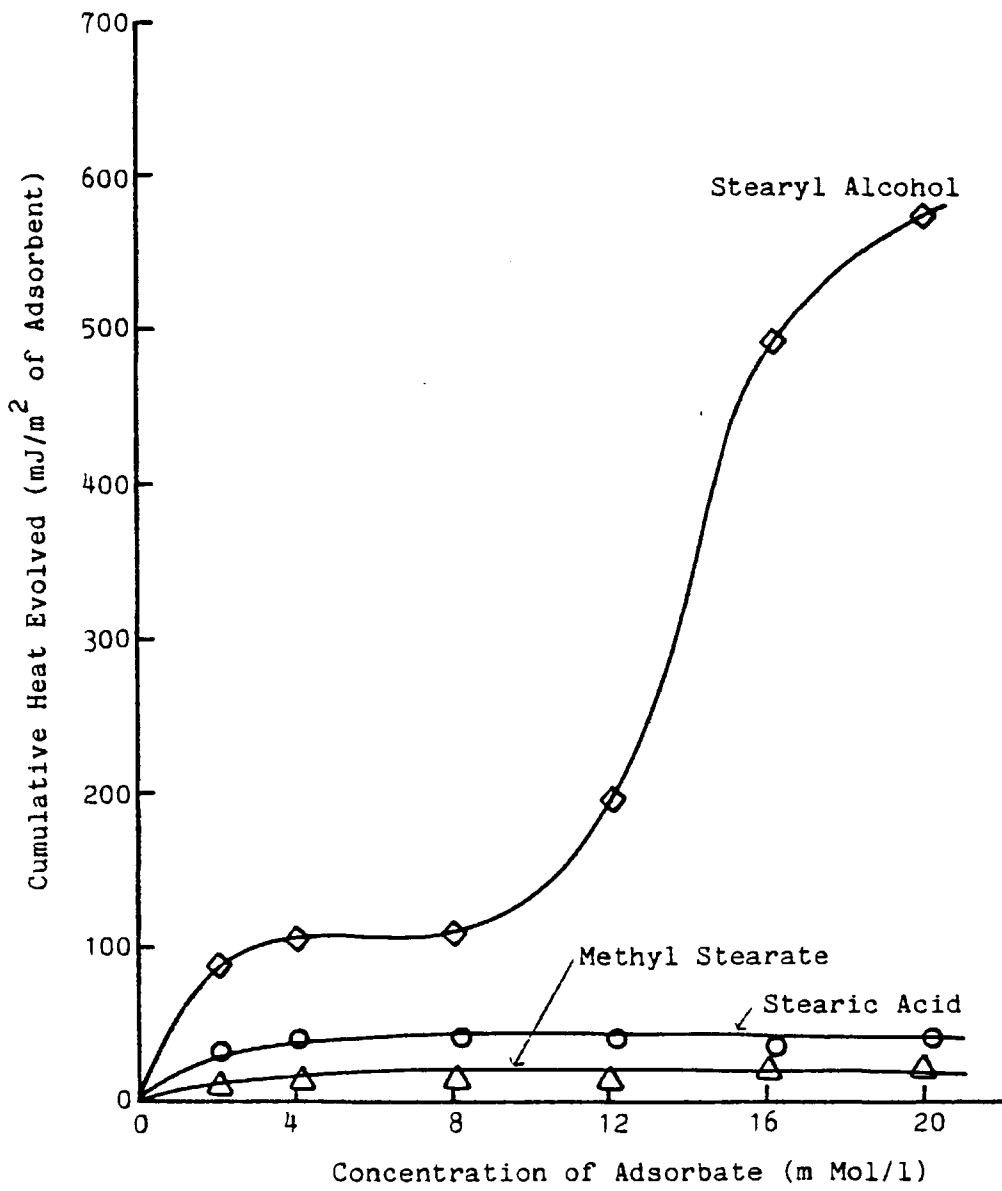


Fig.2-9, Cumulative heat of adsorption onto  $\alpha$ -Fe<sub>2</sub>O<sub>3</sub> at 26.5 °C

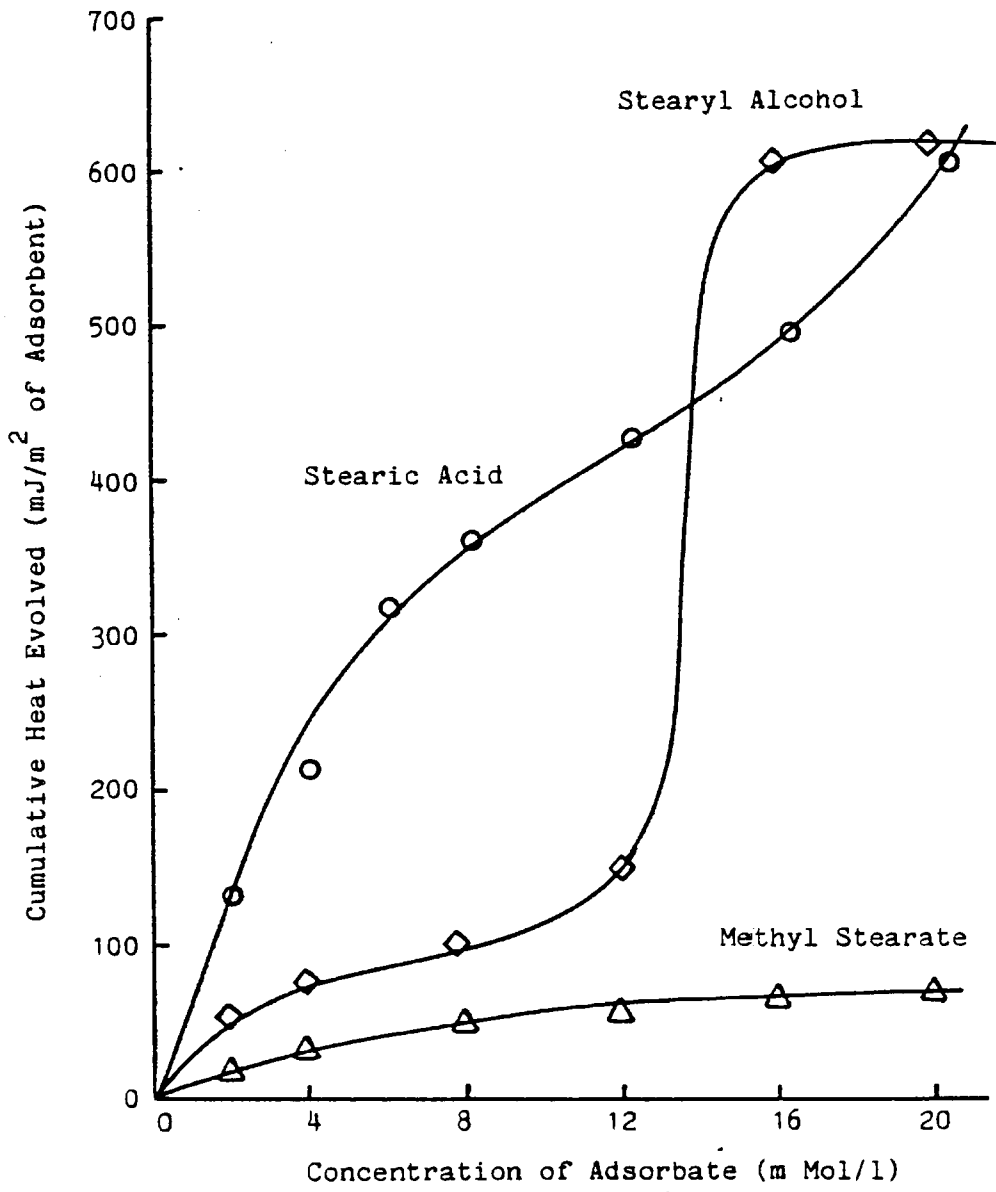


Fig.2-10, Cumulative heat of adsorption onto  $\gamma$ -Fe<sub>2</sub>O<sub>3</sub> at 26.5 °C

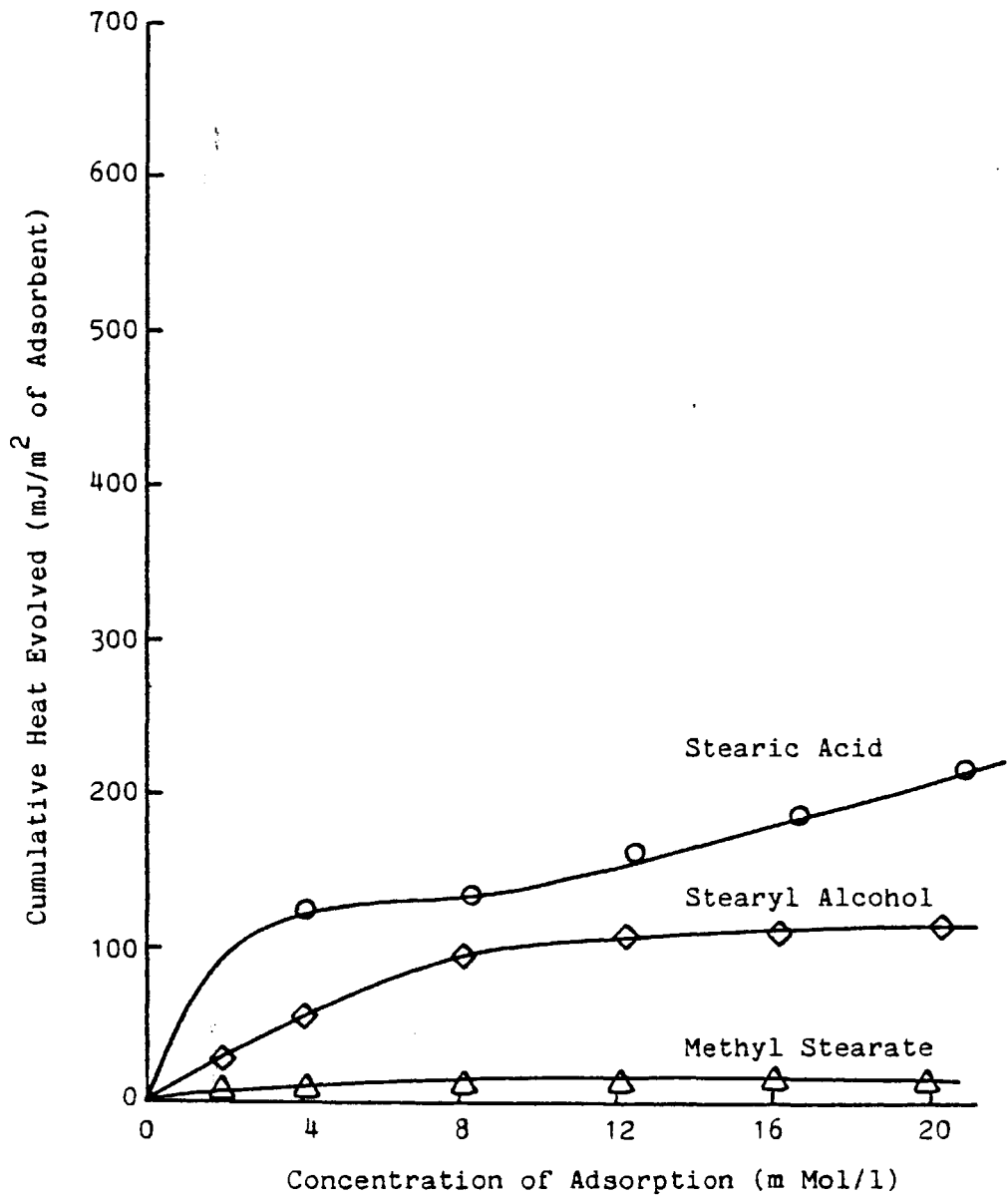


Fig.2-11, Cumulative heat of adsorption onto Fe<sub>3</sub>O<sub>4</sub> at 26.5°C

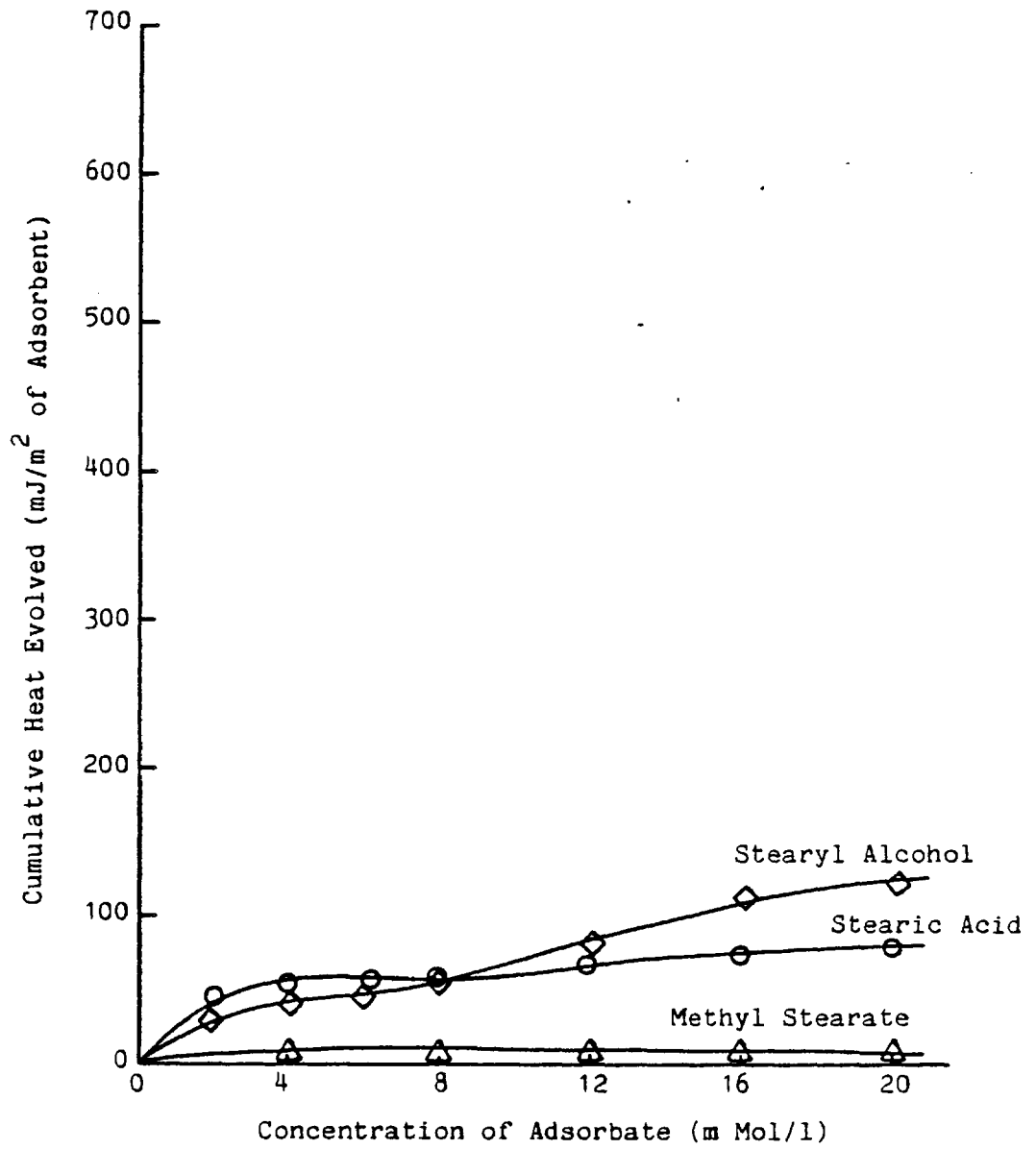


Fig.2-12, Cumulative heat of adsorption onto FeS at 26.5°C



$\gamma\text{-Fe}_2\text{O}_3$  was completely different from that on  $\alpha\text{-Fe}_2\text{O}_3$ .

In this case, the heat of adsorption was quite high and the saturation step was not achieved right up to the solubility limit. The heat of adsorption of stearyl alcohol was similar to that on  $\alpha\text{-Fe}_2\text{O}_3$  however, the secondary increase of heat with concentration of solution became more vivid. For methyl stearate, the value of heat of adsorption became higher and reached saturation at higher concentration compared to  $\alpha\text{-Fe}_2\text{O}_3$ .

Figure 2.11 shows the heat of adsorption on  $\text{Fe}_3\text{O}_4$ . The curve of heat of adsorption for stearic acid revealed that the saturation of the heat occurred at a concentration of 4 to 8mMol/l and then the heat increased slowly at high concentration. The heat of adsorption of stearic acid onto  $\text{Fe}_3\text{O}_4$  was not large, compared to that on  $\gamma\text{-Fe}_2\text{O}_3$ . The heat of adsorption onto  $\alpha\text{-Fe}_2\text{O}_3$  and  $\gamma\text{-Fe}_2\text{O}_3$  showed a secondary increase at high concentration, however, no such trend was seen in the case of  $\text{Fe}_3\text{O}_4$ . The heat of adsorption of stearyl alcohol onto  $\text{Fe}_3\text{O}_4$  at concentrations higher than 10mMol/l was almost same as that of the primary saturation with  $\alpha\text{-Fe}_2\text{O}_3$  and  $\gamma\text{-Fe}_2\text{O}_3$ , which was about 100mJ/m<sup>2</sup>. The heat of adsorption of methyl stearate onto  $\text{Fe}_3\text{O}_4$  was very small compared with stearic acid and stearyl alcohol.

The heats of adsorption onto FeS were small in comparison with  $\alpha\text{-Fe}_2\text{O}_3$ ,  $\gamma\text{-Fe}_2\text{O}_3$  and  $\text{Fe}_3\text{O}_4$ , as shown in Figure 2.12. The curve of heat of adsorption of stearic acid onto FeS was similar to that onto  $\text{Fe}_3\text{O}_4$ , however, the amount of heat was not the same as, but close to, that onto  $\alpha\text{-Fe}_2\text{O}_3$ . The heat of adsorption of stearyl alcohol was not large, but

showed the phenomenon of secondary increase of heat. The heat evolved after the secondary was not as high as that onto iron oxide powder. The heat of adsorption of methyl stearate was very small ( $< 10\text{mJ/m}^2$ ).

Comparing the heats of adsorption of each oiliness reagent, the following order was obtained:

|                 |                                |        |                                |       |                         |        |                                |
|-----------------|--------------------------------|--------|--------------------------------|-------|-------------------------|--------|--------------------------------|
| Stearic acid    | $\gamma\text{-Fe}_2\text{O}_3$ | $\gg$  | $\text{Fe}_3\text{O}_4$        | $>$   | $\text{FeS}$            | $\sim$ | $\alpha\text{-Fe}_2\text{O}_3$ |
| Stearyl alcohol | $\alpha\text{-Fe}_2\text{O}_3$ | $\sim$ | $\gamma\text{-Fe}_2\text{O}_3$ | $\gg$ | $\text{Fe}_3\text{O}_4$ | $>$    | $\text{FeS}$                   |
| Methyl stearate | $\gamma\text{-Fe}_2\text{O}_3$ | $>$    | $\alpha\text{-Fe}_2\text{O}_3$ | $>$   | $\text{Fe}_3\text{O}_4$ | $>$    | $\text{FeS}$                   |

### 2.32 The Influence of Temperature on Heat of Adsorption

The heats of adsorption of oiliness reagents onto iron oxide and iron sulphide were measured at several different temperatures to investigate the influence of temperature. The powders and the oiliness reagents measured in this section were limited to those which showed especially interesting adsorption phenomena at room temperature.

As far as lubrication is concerned, it is desirable to measure the heat of adsorption at fairly high temperatures. However, it is very difficult to operate a Flow Microcalorimeter at high temperature for the following three reasons; firstly, the sensitivity of thermistors decreases at high temperature; secondly, the thermal effect from outside at high temperature is so large that it is not easy to obtain a thermally stable condition; and thirdly, the heat of adsorption detected by the Flow Microcalorimeter became small at high temperature. Moreover, as the volatility

of n-Heptane used in this work as a solvent limited the upper temperature, the maximum temperature adopted in the experiment described in this section was 65°C.

The results for the temperature effect on heat of adsorption are shown in Figures 2.13 to 2.19. The heats of adsorption of stearyl alcohol onto  $\alpha$ -Fe<sub>2</sub>O<sub>3</sub> at several different temperatures are shown in Figure 2.13. In Section 2.21, the phenomenon of two steps increase of heat of adsorption was seen at room temperature. The secondary increase of this phenomenon was shifted to high concentration of stearyl alcohol at high temperature. As described in Section 1.34, the secondary increase depends on attractive interactions between adsorbed molecules. This attractive interaction became weak at high temperature and the secondary increase of heat was not seen at 45°C in the range below 20m Mol/l.

Figure 2.14 revealed the heats of adsorption of stearic acid onto  $\gamma$ -Fe<sub>2</sub>O<sub>3</sub> at several different temperatures. The reduction of heat with temperature was seen at all concentrations up to 20m Mol/l. The effect of temperature on heat release changed remarkably at low temperatures. The heat of adsorption decreased by about one third when the temperature was increased from 26.5°C to 30°C.

The effect of temperature on heat of adsorption of stearyl alcohol onto  $\gamma$ -Fe<sub>2</sub>O<sub>3</sub> was shown in Figure 2.15. As seen in the case of  $\alpha$ -Fe<sub>2</sub>O<sub>3</sub>, the secondary increase of heat release was shifted to higher concentration with temperature and disappeared at temperature higher than 35°C. Comparing the results of  $\gamma$ -Fe<sub>2</sub>O<sub>3</sub> with that of  $\alpha$ -Fe<sub>2</sub>O<sub>3</sub>, most of the

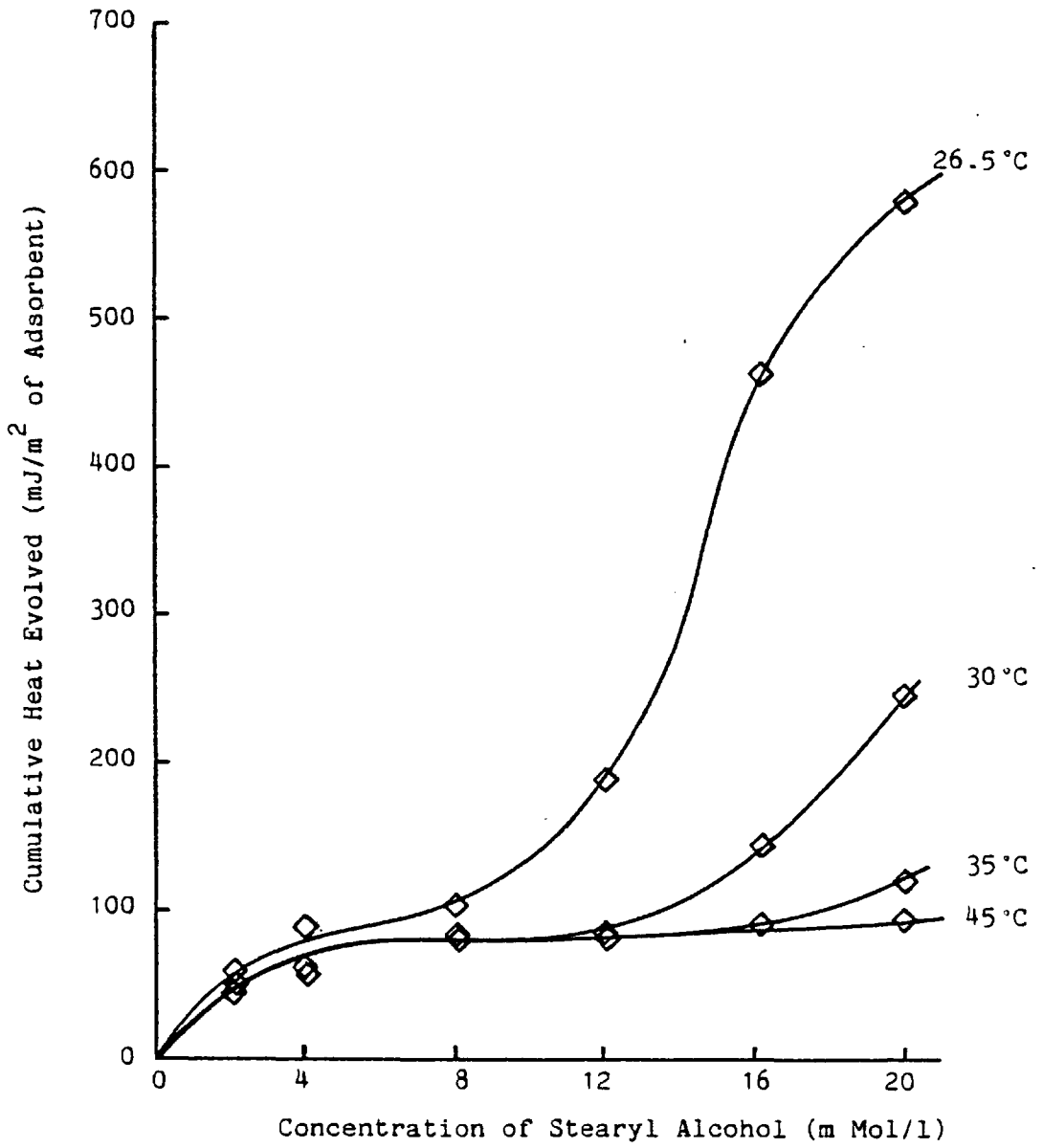


Fig.2-13, Cumulative heat of adsorption of stearyl alcohol onto  $\alpha$ -Fe<sub>2</sub>O<sub>3</sub> at several different temperature

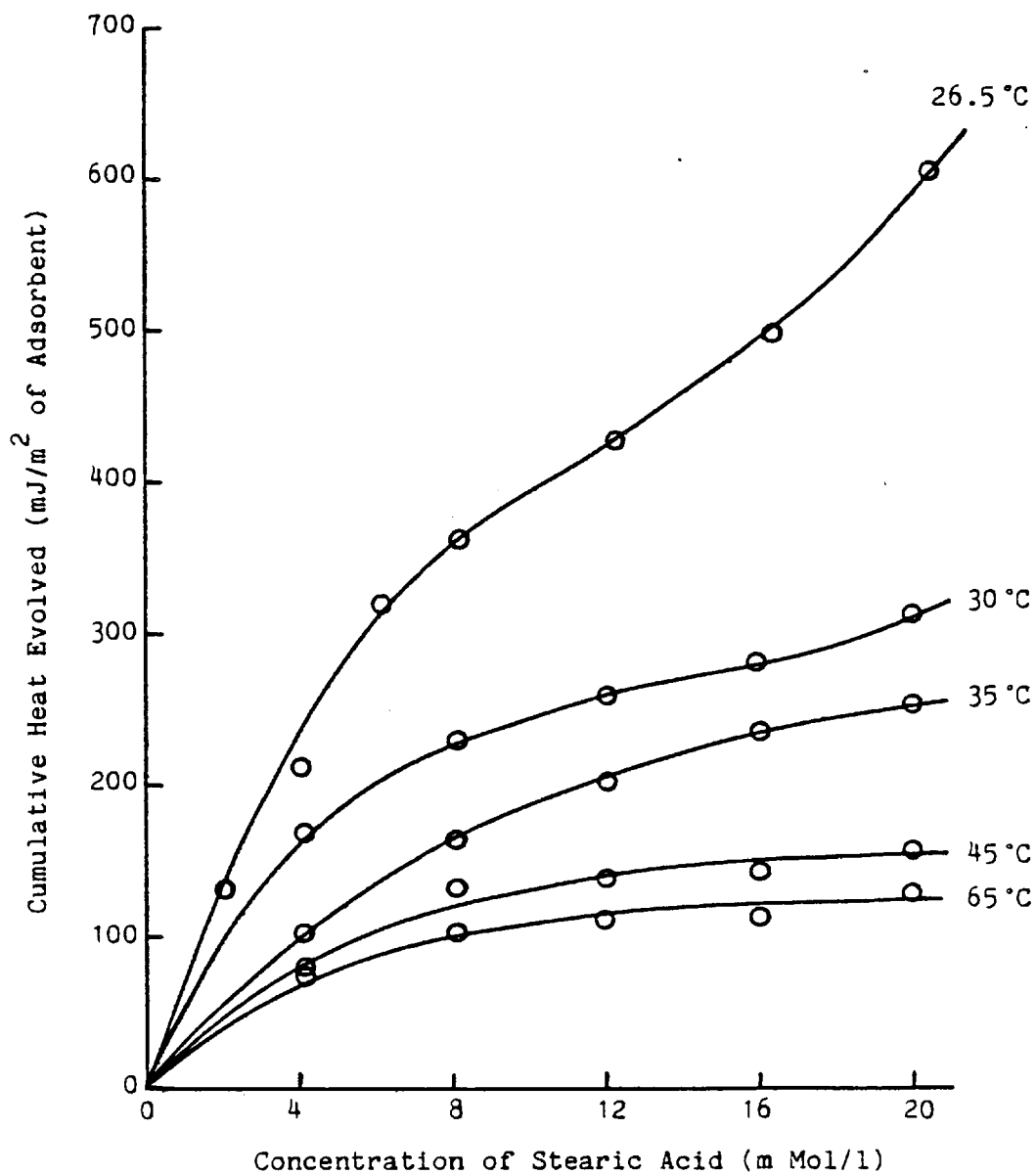


Fig.2-14, Cumulative heat of adsorption of stearic acid onto  $\gamma$ -Fe<sub>2</sub>O<sub>3</sub> at several different temperature

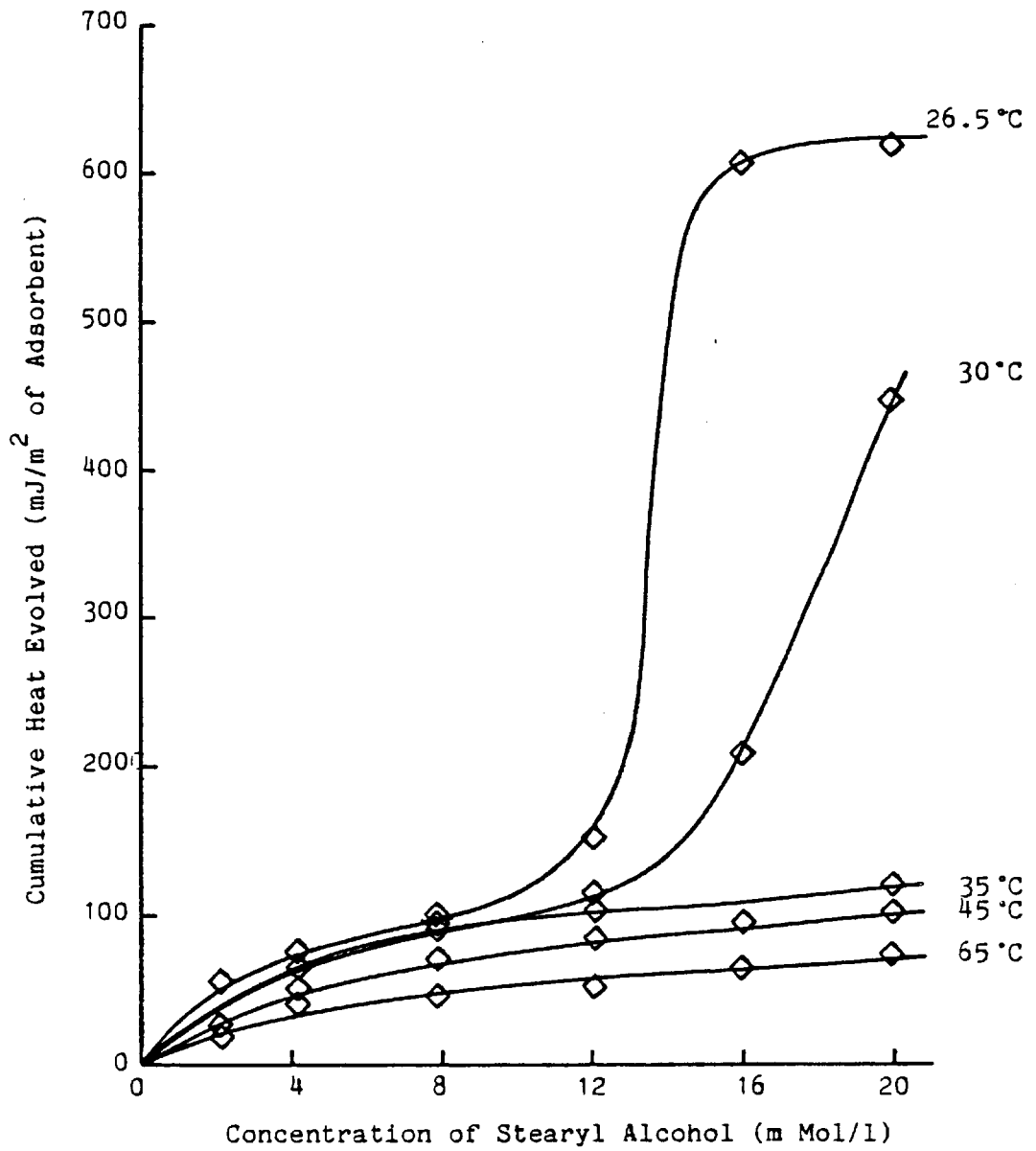


Fig.2-15, Cumulative heat of adsorption of stearyl alcohol onto  $\gamma$ -Fe<sub>2</sub>O<sub>3</sub> at several different temperature

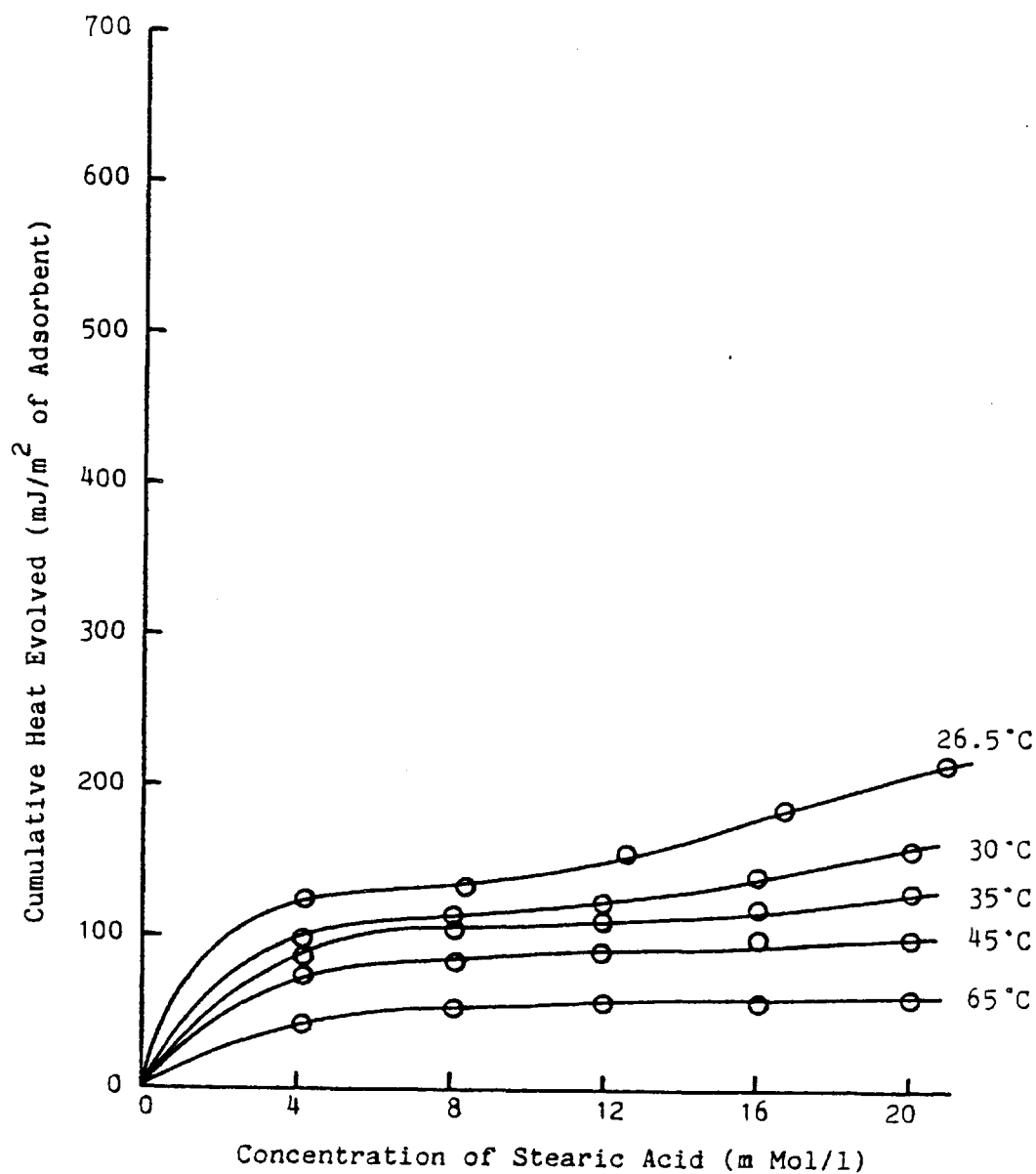


Fig.2-16, Cumulative heat of adsorption of stearic acid onto  $Fe_3O_4$  at several different temperature

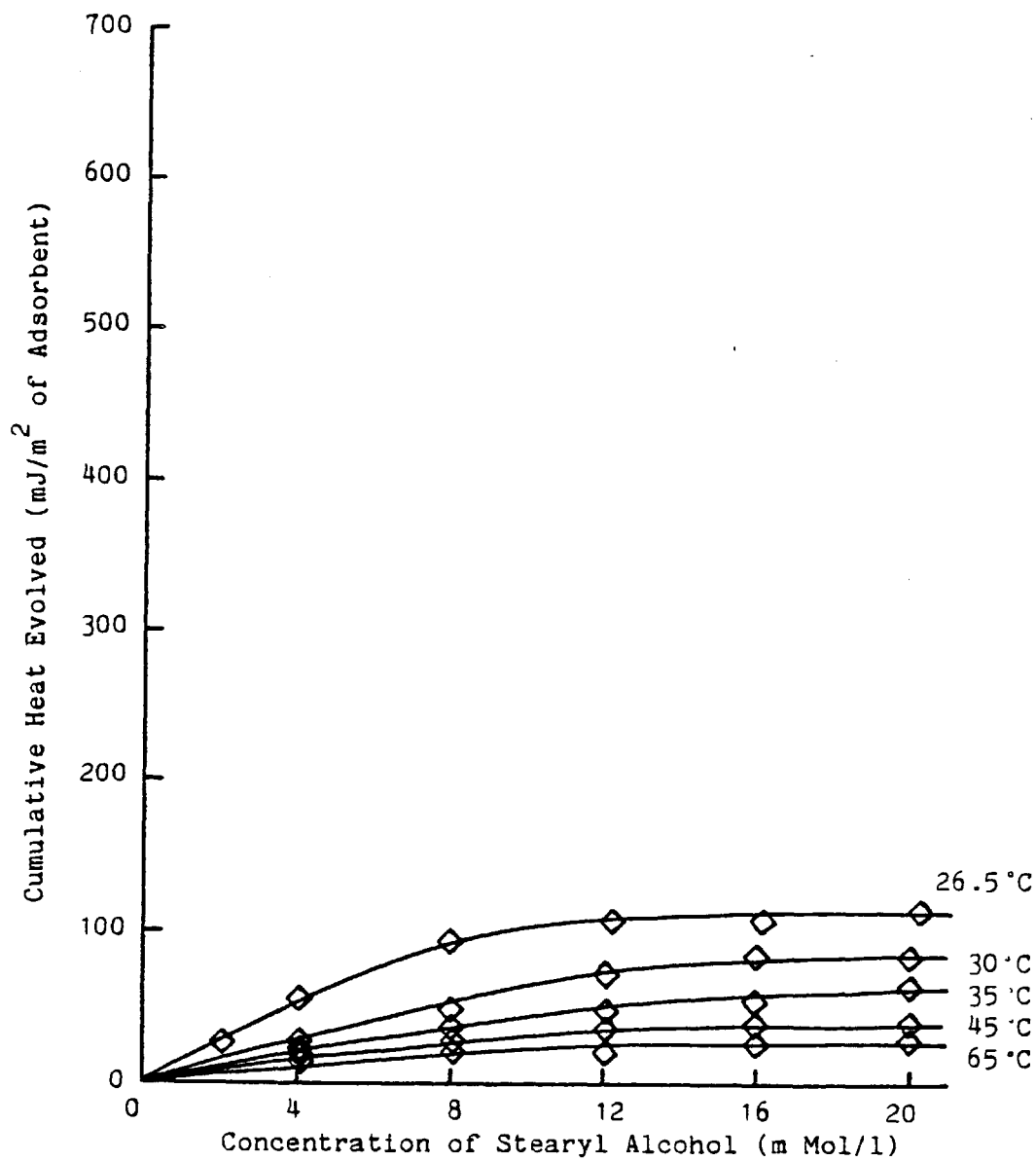


Fig.2-17, Cumulative heat of adsorption of stearyl alcohol onto  $Fe_3O_4$  at several different temperature



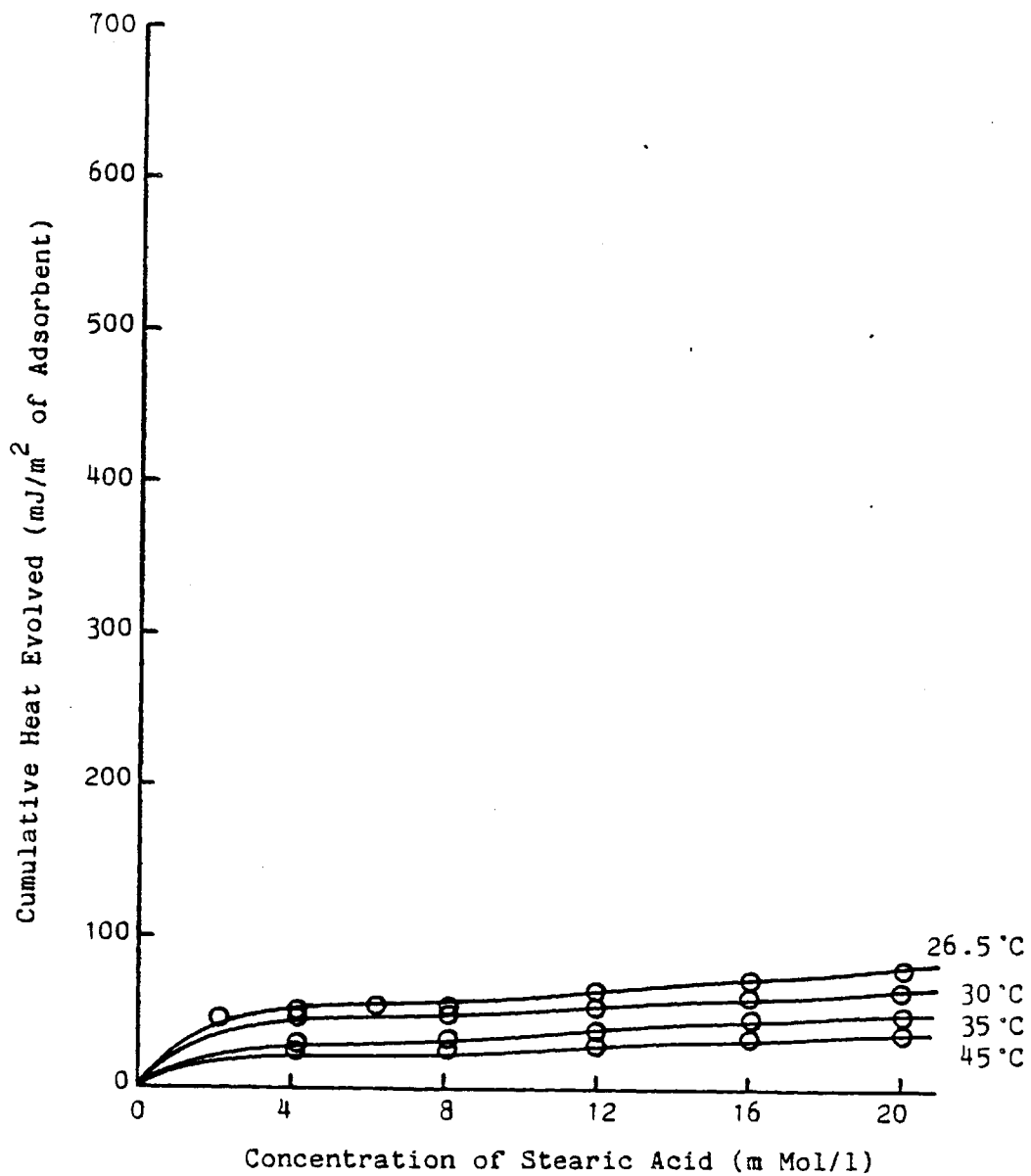


Fig.2-18, Cumulative heat of adsorption of stearic acid onto FeS at several different temperature

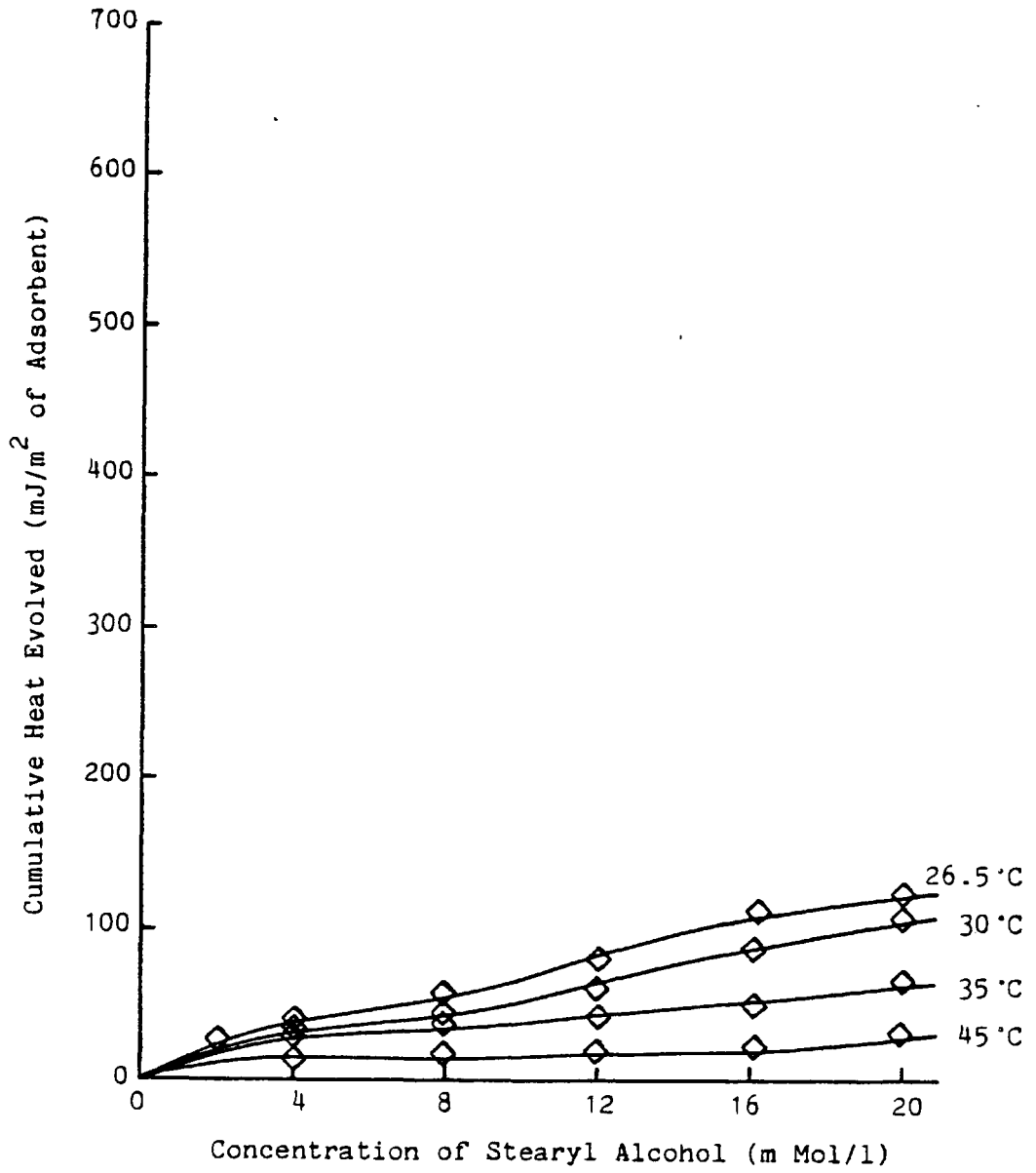


Fig.2-19, Cumulative heat of adsorption of stearyl alcohol onto FeS at several different temperature

trends of results of were similar. Only the secondary increase of heat of adsorption was influenced at temperature lower than 35°C. In the region higher than this temperature, the heat of adsorption at all concentrations was reduced with temperature.

The temperature effect on heats of adsorption of stearic acid and stearyl alcohol onto  $\text{Fe}_3\text{O}_4$  were shown in Figures 2.16 and 2.19 respectively. The influence of temperature on these heat of adsorption were the same as the cases of  $\alpha\text{-Fe}_2\text{O}_3$  and  $\gamma\text{-Fe}_2\text{O}_3$ . The heats of adsorption decreased with temperature. Although the heat of adsorption of stearic acid at 26.5°C had a slight secondary increase at high concentration, this increase also disappeared at higher temperature.

The results of heats of adsorption of stearic acid and stearyl alcohol onto FeS were shown in Figures 2.18 and 2.19 respectively. The temperature effects observed with FeS were similar to those with  $\text{Fe}_3\text{O}_4$ .

Comparing the amount of heat of adsorption onto each powder at 45°C, the following order was obtained.

Stearic acid       $\gamma\text{-Fe}_2\text{O}_3 > \text{Fe}_3\text{O}_4 > \text{FeS}$

Stearyl alcohol    $\alpha\text{-Fe}_2\text{O}_3 \sim \gamma\text{-Fe}_2\text{O}_3 \sim \text{Fe}_3\text{O}_4 > \text{FeS}$

In the case of stearic acid, the same order as that at 26.5°C was obtained, however, the order of heat of adsorption of stearyl alcohol was different from that at 26.5°C shown in Section 2.31. No difference was found in the heat of adsorption of stearyl alcohol onto iron oxide powders.

### 2.33 The Influence of Solvent on Heat of Adsorption

The results described in Section 2.31 and 2.32 were obtained by using n-heptane as a solvent. In this section, the influence of solvent on heat of adsorption was investigated using n-heptane, n-decane and n-hexadecane. As described in Section 2.32, it is so difficult to measure heat of adsorption at high temperature that the investigation was confined to  $\gamma\text{-Fe}_2\text{O}_3$  and  $\text{Fe}_3\text{O}_4$ , which had large specific surface areas, to obtain large heat of adsorption. In the Flow Microcalorimeter measurement, the peak area for heat of adsorption on chart recorder is in proportion to the surface area of powder packed in the cell.

All of the results obtained in this section are shown in Figures 2.20 to 2.23. Figure 2.20 shows the effect of solvent on heat of adsorption at different temperatures. In the case of n-decane and n-hexadecane, the results at 85°C were obtained because these solvents had high boiling points. As shown clearly in Figure 2.20, the effect of solvent extends from low to high temperature. The large n-paraffin solvent molecules result in higher heats of adsorption.

The effect of solvent on heat of adsorption of stearyl alcohol onto  $\gamma\text{-Fe}_2\text{O}_3$  is seen in Figure 2.21. As the stearyl alcohol solution of 8.0m Mol/l was used in this experiment, the heat of adsorption from n-heptane had a value on the plateau between the primary and the secondary increase, which are shown in Figures 2.10 and 2.15. At low temperature, there were many differences between heats of adsorption

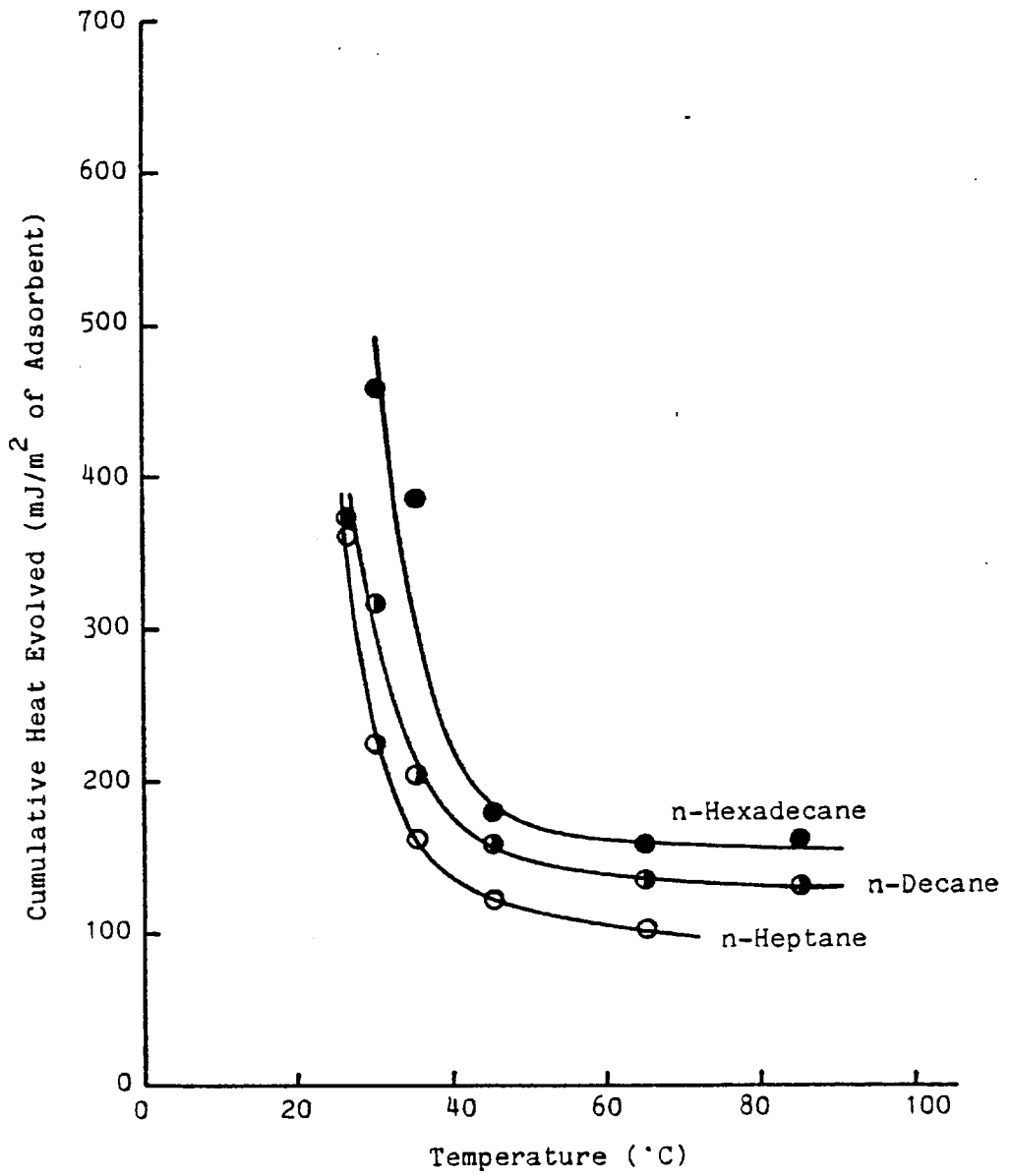


Fig.2-20, Influence of solvent on cumulative heat of adsorption of stearic acid onto  $\gamma$ -Fe<sub>2</sub>O<sub>3</sub>

Stearic Acid 8.0 m Mol/l

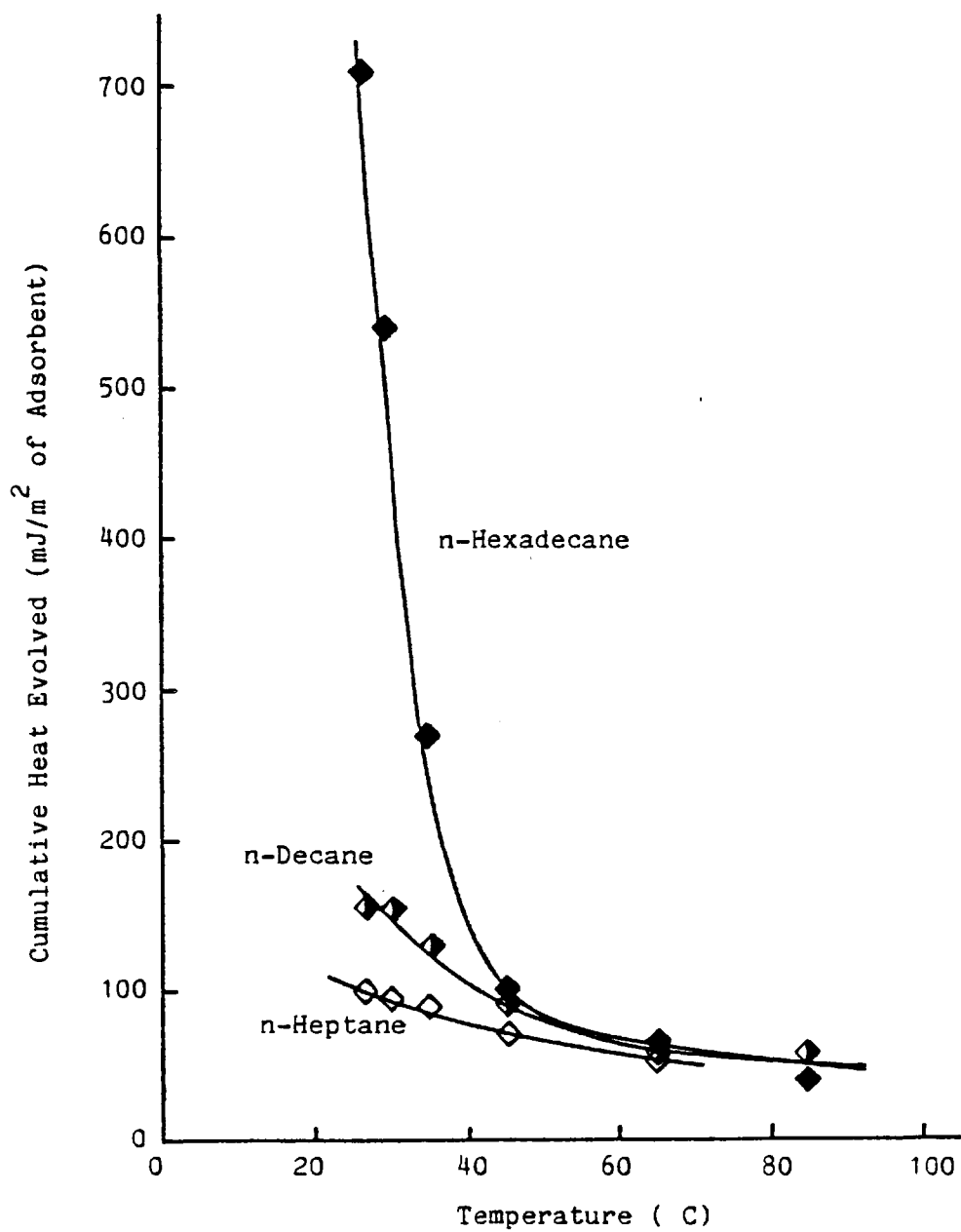


Fig.2-21, Influence of solvent on cumulative heat of adsorption of stearyl alcohol onto  $\gamma$ -Fe<sub>2</sub>O<sub>3</sub>

Stearyl Alcohol 8.0 m Mol/l

from each solvent, however, these differences became small with temperature and approached the same value at the temperature over 60°C. The results from n-hexadecane showed a large increase of heat release at low temperature. This phenomenon is considered to be related to the secondary increase of heat of adsorption. In the adsorption from n-hexadecane, the secondary increase occurs at lower concentration.

The influence of solvent on heat of adsorption of stearic acid and stearyl alcohol onto  $\text{Fe}_3\text{O}_4$  are shown in Figures 2.22 and 2.23. In this case, there is little effect of solvent on heat release in contrast to  $\gamma\text{-Fe}_2\text{O}_3$ .

In Section 2.31 and 2.32, the amount of heat of adsorption for each powder was compared at 25.5°C and 45°C respectively. In the similar way, the comparison of the heat release of 8.0m Mol/l solutions at 85°C is shown as follows:

Stearic acid       $\gamma\text{-Fe}_2\text{O}_3 > \text{Fe}_3\text{O}_4$

Stearyl alcohol    $\gamma\text{-Fe}_2\text{O}_3 > \text{Fe}_3\text{O}_4$

The vivid difference was seen in the heat of adsorption of stearyl alcohol, though such difference was not seen in the heats of adsorption of the solution 8.0m Mol/l at 26.5°C and 45°C.

The effect of temperature on heat of adsorption at high temperature also illustrated from Figures 2.20 to 2.23. Concerning stearic acid, the heats of adsorption onto  $\gamma\text{-Fe}_2\text{O}_3$  and  $\text{Fe}_3\text{O}_4$  became constant in the region above 65°C. On the other hand, the heat of adsorption of stearyl alcohol decreased slowly with temperature. These results can be

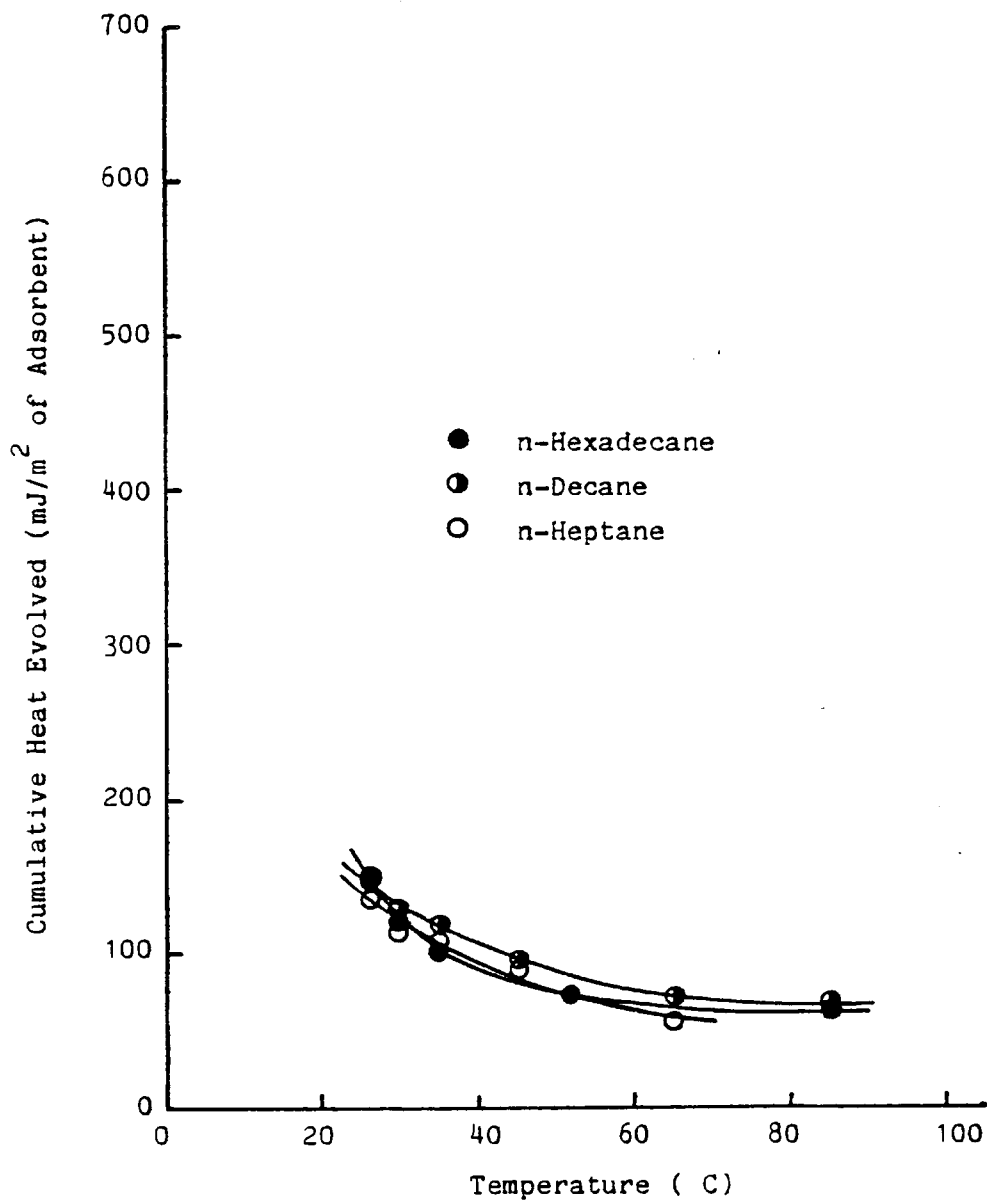


Fig.2-22, Influence of solvent on cumulative heat of adsorption of stearic acid onto  $Fe_3O_4$

Stearic Acid 8.0 m Mol/l



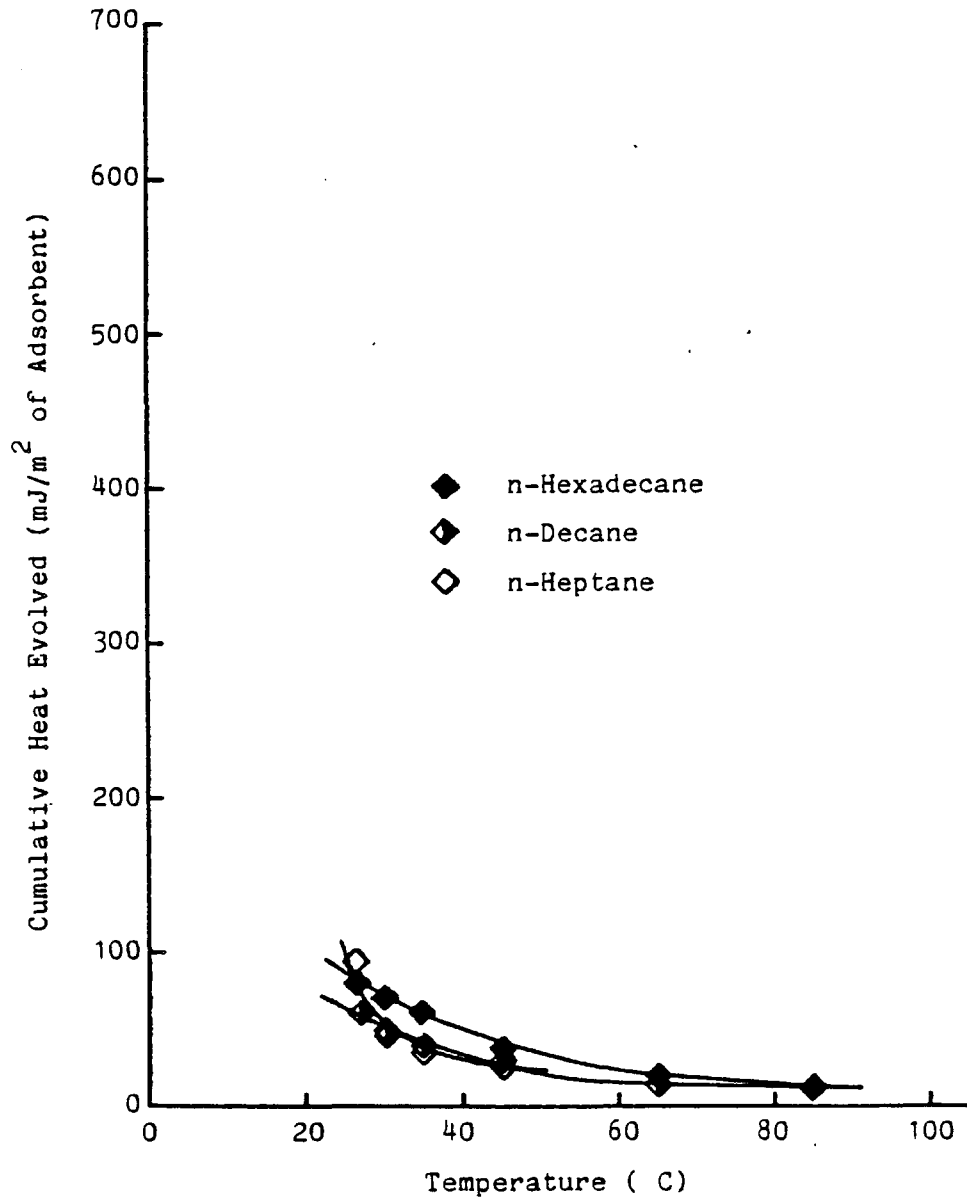


Fig.2-23, Influence of solvent on cumulative heat of adsorption of stearyl alcohol onto  $Fe_3O_4$

Stearyl Alcohol 8.0 m Mol/l

explained by the classification of physical and chemical adsorption. Although the details are described in Section 2.43 and 2.44, the adsorption of stearyl alcohol is dominated by physical adsorption and the adsorption of stearic acid onto  $\gamma\text{-Fe}_2\text{O}_3$  and  $\text{Fe}_3\text{O}_4$  includes some chemical adsorption. As chemical adsorption is accelerated with temperature and physical adsorption decreases with temperature, it is possible for these two processes to cancel each other at high temperature.

## 2.40 Discussion

### 2.41 Heat of Adsorption by a Flow Microcalorimeter

Groszek (96)<sup>(105)</sup> has used a Flow Microcalorimeter to measure heat of adsorption and published many papers about adsorption related to lubrication. However, the values of heat of adsorption reported by different authors have not always been the same, as will be described in the next section. Therefore, in this section the problems of a Flow Microcalorimeter are investigated.

In this study, heat of adsorption was calculated using the concept of an effective amount of powder which was described in Section 2.21. No other authors have ever used this method. Groszek (96) (99) used the method of adjustment of the bottom height of the cell in a Flow Microcalorimeter by inert powder to reduce the dead volume to zero. If the complete adjustment were achieved, the linear relation between heat release and amount of powder poured into the

cell could be obtained. However, as the Flow Microcalorimeter used in this study has been produced recently, the cell shown in Figure 2.2 has been modified to have a small dead volume for various powders (116). It is therefore possible to use the method of correction with an effective amount of powder, which is explained in Section 2.23.

In order to compare the results by Groszek with the results in this study, Groszek kindly provided a standard sample of Graphon, which had cumulative heat of adsorption by n-dotriacontane 4.53J/g as shown in reference (96). The results of this sample by the Flow Microcalorimeter used in this study are shown in Figure 2.24 (a) and (b). Figure 2.24(a) shows the calibration curve obtained by the heater, which is shown in Figure 2.25, bedded in 60mg Graphon. Figure 2.24(b) shows the relation between the cumulative heat of adsorption of n-dotriacontane and the amount of Graphon. This relation is almost linear in the lower range and the dead volume in this experiment is the volume which is equivalent to 11mg of Graphon. Assuming that the effective amount of Graphon is 49mg in the experiment 60mg Graphon, the value of the cumulative heat of adsorption is 6.89J/g.

This value is 63% higher than that given by Groszek. There are many possible reasons for this difference, but most significant is the concept of dead volume of powder, which was adopted in this study, but which Groszek did not employ. If zero dead volume were assumed in this study, the difference between this and Groszek's results

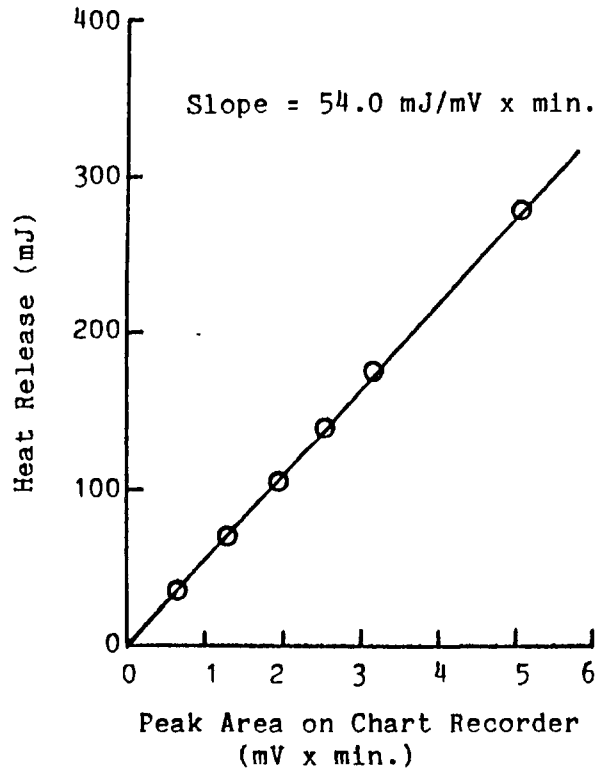


Fig.2-24(a), Calibration curve for Graphon  
Graphon 60 mg

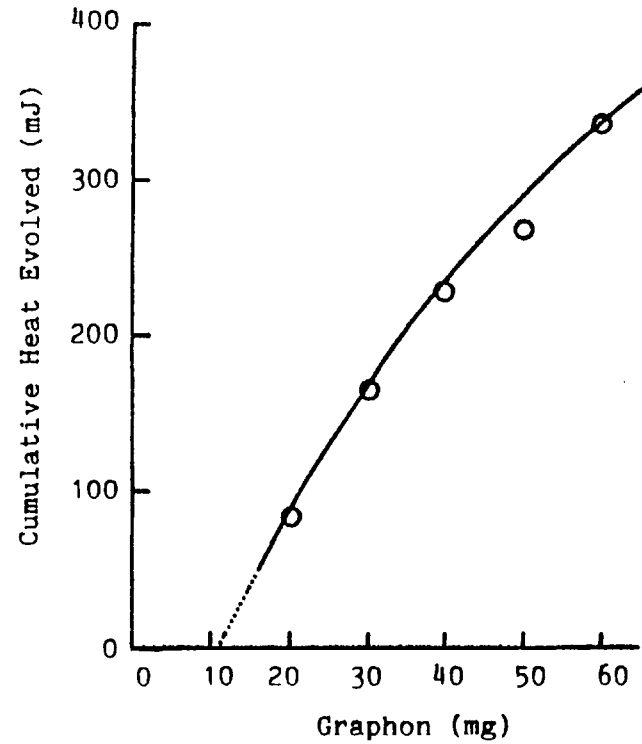


Fig.2-24(b), Cumulative heat of adsorption of  
n-dotriacontane

n-dotriacontane solution 2 g/l

decreases to 24%. Another important cause is the change of nature of the Graphon surface. As the Graphon provided by Groszek had been kept in a bottle for several years, the sample was degassed as described in Section 2.21. The results of heat of adsorption in reference (96) were obtained using the Graphon without any pretreatment such as degassing. Consequently, there might be some difference in the nature of the Graphon surface between the two samples. Generally degassing would be expected to increase adsorption.

No further investigation were carried out to clarify the causes of this difference. It is, however, necessary to use the 63% correction when the results in this study are compared with results by Groszek.

#### 2.42 Comparison of Heat of Adsorption Results with Those of Other Authors

Groszek (99) and Sakurai (10) (11) have reported heat of adsorption of oiliness compounds on iron oxide by a Flow Microcalorimeter. A comparison of results in this study with results obtained by them was carried out, and reported in this section.

Groszek (99) has measured heats of adsorption of stearic acid and stearyl alcohol onto  $\alpha$ -Fe<sub>2</sub>O<sub>3</sub>,  $\gamma$ -Fe<sub>2</sub>O<sub>3</sub> and Fe<sub>3</sub>O<sub>4</sub>. These results are listed in Table 2.5, in which chemical analysis of the powders were also shown. He used the same solvent, n-heptane, as in this study, but he did not describe the temperature. For reference, the results obtained in this study at the same condition (except

temperature) are also listed in the table. There is considerable difference in heats of adsorption of stearyl alcohol onto  $\alpha\text{-Fe}_2\text{O}_3$  between the results by Groszek and those obtained here, in spite of the use of similar  $\alpha\text{-Fe}_2\text{O}_3$  which both had very high purity about  $3\text{m}^2/\text{g}$  surface area.

As shown in Figures 2.9 and 2.13, the heat of adsorption of stearyl alcohol has a secondary increase with concentration. Moreover this secondary increase is influenced critically by temperature and bed condition of powder (the shift of the secondary increase to high concentration by use of inert powder to adjust the dead volume of powder was observed in preliminary experiments). The value after secondary increase is shown in Table 2.5. However, the value obtained by Groszek may be on the plateau between primary and secondary increase. This is possibly the main reason for the discrepancy, and also the difference in sensitivity of the instrument, which was described in the previous section.

There is also much difference in heat of adsorption of stearic acid onto  $\alpha\text{-Fe}_2\text{O}_3$ . In this study, all powders were degassed under vacuum condition at high temperature ( $300^\circ\text{C}$ ). Concerning  $\alpha\text{-Fe}_2\text{O}_3$ , it was noticed that this degassing process reduced heat of adsorption. This degassing process may be one of the reasons that small value is obtained in this study.

Although there are many differences in the results of heat of adsorption onto  $\gamma\text{-Fe}_2\text{O}_3$  and  $\text{Fe}_3\text{O}_4$ , it is impossible to compare it directly, owing to the difference

TABLE 2.5

Comparison of Heat of Adsorption with  
Results in the Literature (Reference 99)

| Sample                                   | Heat of Adsorption (mJ/m <sup>2</sup> ) |                            |
|--|---|----------------------------|
|  | Stearyl Alcohol<br>18.5m Mol/l          | Stearic Acid<br>3.5m Mol/l |
| $\alpha$ -Fe <sub>2</sub> O <sub>3</sub> | 155 (150)                               | 113 ( 40)                  |
| $\gamma$ -Fe <sub>2</sub> O <sub>3</sub> | 402 (620)                               | 42 (210)                   |
| Fe <sub>3</sub> O <sub>4</sub>           | 251 (110)                               | - ( - )                    |

Figures in parentheses indicate results obtained in this study.

Specific surface area and analytical results of the samples in reference (99) are given by,

$\alpha$ -Fe<sub>2</sub>O<sub>3</sub> : Sample used as spectroscopic standard.

Total impurity content: 5ppm

Specific surface area by BET method: 3m<sup>2</sup>/g

$\gamma$ -Fe<sub>2</sub>O<sub>3</sub> : Principally  $\gamma$ -Fe<sub>2</sub>O<sub>3</sub> containing 0.1 to 1.0wt% quantities of Al, Cu, Si and Ni.

Specific surface area by BET method: 19m<sup>2</sup>/g

Fe<sub>3</sub>O<sub>4</sub> : Fe<sub>3</sub>O<sub>4</sub> containing 10wt% Mn, traces of Al, Cu, Si.

Specific surface area by BET method: 9m<sup>2</sup>/g

of powders used in both experiments. Some impurities in powder sometimes result in large heat of adsorption.

Sakurai and co-workers (10) (11) recently reported heats of adsorption of stearic acid, stearyl alcohol and methyl stearate onto  $\alpha\text{-Fe}_2\text{O}_3$ ,  $\text{Fe}_3\text{O}_4$  and FeS using a Flow Microcalorimeter. They measured heat of adsorption at the similar condition to this study. The comparison of results both in this study and by Sakurai are shown in Figure 2.25. The main characteristic of Sakurai's results is that heats of adsorption onto  $\text{Fe}_3\text{O}_4$  and FeS are much greater than that onto  $\alpha\text{-Fe}_2\text{O}_3$ . However, same results were not obtained in this study as shown in Figure 2.25. In this study, there was little difference between heats of adsorption onto  $\alpha\text{-Fe}_2\text{O}_3$  and that onto  $\text{Fe}_3\text{O}_4$  and the heat of adsorption onto FeS was small in contrast to that by Sakurai. From the results obtained here, it is impossible to expect a strong interaction between oiliness compounds and FeS film on a surface, as described by Sakurai.

It is well known that FeS is easily oxidised by air. The difference of results onto FeS may be due to the oxidation condition on the surface of FeS powder. To make clear this problem, the following investigation was carried out. In order to investigate the effect of degree of oxidation on heat of adsorption, FeS powder used was oxidised in water for 24 hours and dried by the same method as the original FeS powder.

The analytical results of both non-oxidised (the original FeS) and oxidised FeS by ESCA are shown in Table 2.6, in which the following summary of results are included:



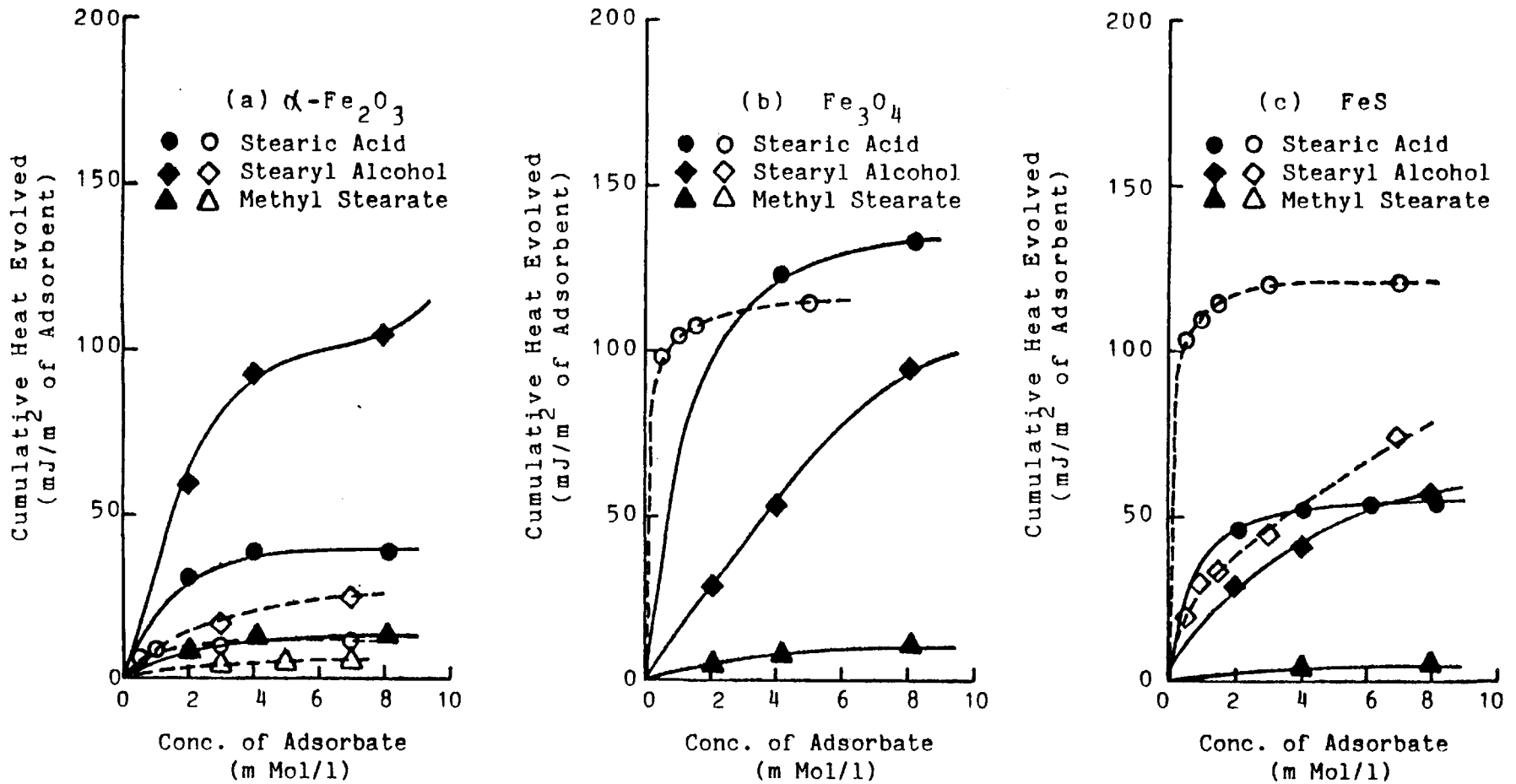


Fig.2-25, Comparison of heat of adsorption between the result in this study and the result in reference (11)

————— Results in this study  
----- Results in reference(11)

TABLE 2.6

Analytical Results of FeS Powder by ESCA

| Element Signal | Original Sample   |                    | Oxidised Sample   |                    |
|----------------|-------------------|--------------------|-------------------|--------------------|
|                | Binding Energy eV | Relative Intensity | Binding Energy eV | Relative Intensity |
| C(1s)          | 285               | 1.27               | 285               | 0.75               |
| O(1s) 1.       | 530.0             | 0.62               | 530.0             | 0.66               |
| 2.             | 531.6             | 0.40               | 531.7             | 0.43               |
| 3.             | 533.3             | 0.08               | 533.3             | 0.08               |
| Fe(2p 3/2)     | 710.5             | 1.0                | 710.5             | 1.0                |
| S(2p)          |                   |                    |                   |                    |
| 1. Sulphide    | 161.9             | 0.033              | ND                |                    |
| 2. Sulphate    | 169.1             | 0.016              | 169.3             | 0.053              |

Notes

1. Binding energies are reference to carbon (1s) = 285 eV
2. Intensities are ratioed to that of Fe(2p) = 1
3. ND = not detected

- (1) The surfaces of both the original and oxidised FeS are almost oxidised.
- (2) The oxygen peak can be deconvoluted into three binding states which are typical of an air-formed  $\text{Fe}_2\text{O}_3/\text{FeOOH}$  film on metallic iron.
- (3) The ferrous sulphide is recognisable on the surface of non-oxidised FeS (the original FeS) but on the oxidised FeS the sulphide is apparently all converted to sulphate.

From these analytical results, it becomes apparent that the results of heat of adsorption supposedly onto FeS, which are shown in Sections 2.31 to 2.33, actually relate not only to the interaction between oiliness compounds and FeS but also that between oiliness compounds and a film including iron oxide, sulphide and sulphate.

The results of heat of adsorption measurement with both original and oxidised FeS are illustrated in Figure 2.26. The large increase of heat of adsorption of stearic acid and stearyl alcohol by oxidation of FeS was recognised. This change is large enough to expect some change of interaction between powder and oiliness compound, even allowing for the possibility of changes in the surface area of powder by oxidation. This large increase of heat of adsorption may be due to the strong interaction between oiliness reagent and sulphate.

Careful inspection of Figure 2.26 shows that the curve of heat of adsorption of both oiliness reagents onto three kinds of FeS are similar, i.e. the heat of adsorption of stearic acid saturates at low concentration and that of

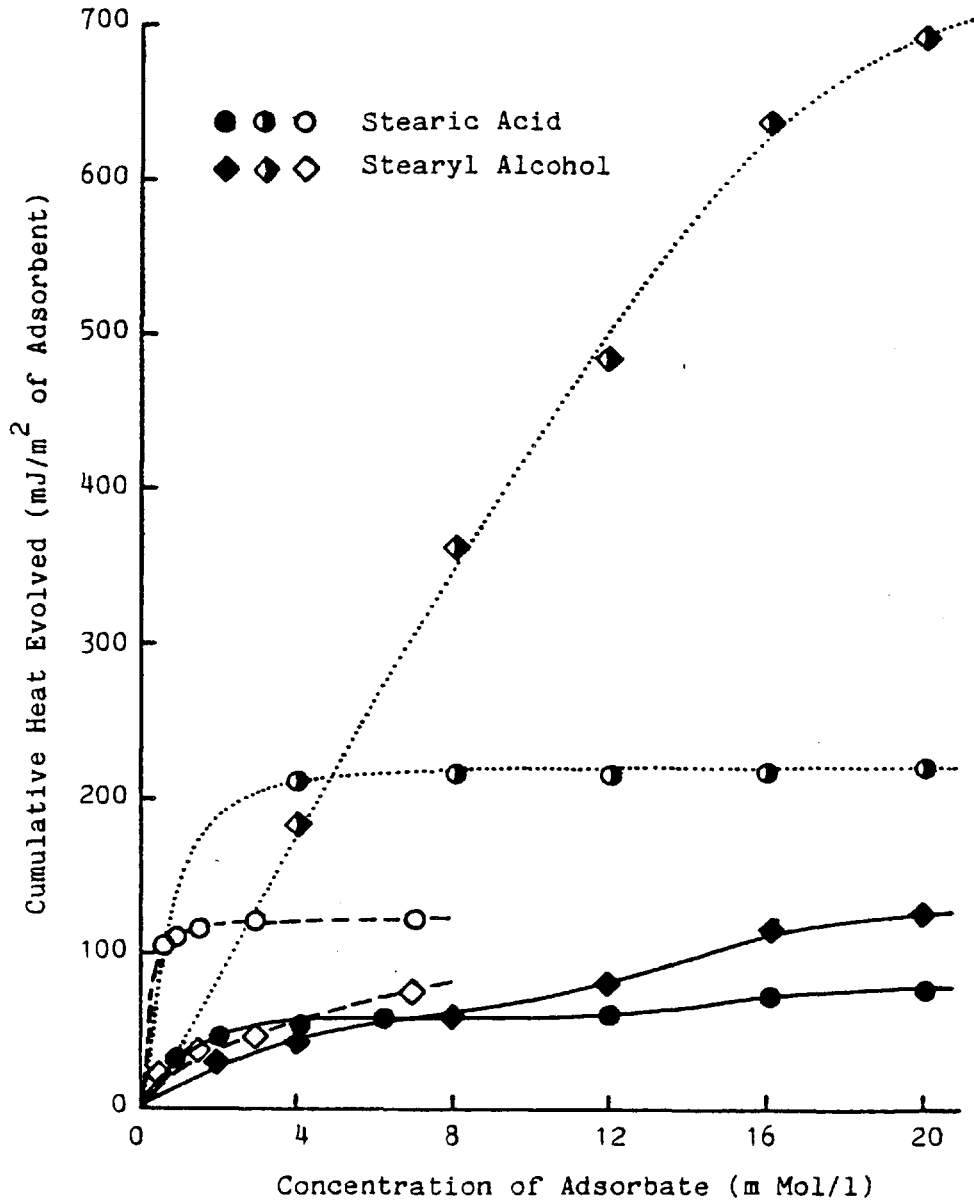


Fig.2-26, Influence of oxidation of FeS on heat of adsorption

— results from the original FeS sample  
..... results from the oxidized FeS sample  
- - - results in reference (11)

stearyl alcohol increases with concentration.

It is impossible to avoid any oxidation on a surface of FeS unless this material is treated under high vacuum conditions or in an inert atmosphere. In experiments done by Sakurai, the weighing and filling up of powder were carried out in normal atmosphere. Therefore, it is natural to consider that the surface of FeS used by Sakurai has been oxidised to some extent. Judging from the results in Figure 2.26, the surface of FeS used by Sakurai should be more oxidised than the original FeS used here. Consequently, the heat of adsorption reported by Sakurai is quite high.

There are many differences in heats of adsorption on  $\alpha\text{-Fe}_2\text{O}_3$  between results in this study and that in reference (10) (11). As described in Section 2.41, the heat of adsorption on  $\alpha\text{-Fe}_2\text{O}_3$  had a tendency to decrease by a degassing process at high temperature. This difference may be due to difference of temperature for degassing before use (Sakurai's 350°C, in this study 300°C).

In order to investigate the causes of this difference,  $\alpha\text{-Fe}_2\text{O}_3$  powder, which had the same specification, was purchased from the company which supplied the  $\alpha\text{-Fe}_2\text{O}_3$  powder used in reference (10) (11) (106). Although particle size (100-200 mesh) and purity (99.9%) were the same, there was much difference in the surface area of the powder. The surface area of this powder was so small that it was impossible to obtain reliable data by the BET method ( $0.27\text{m}^2/\text{g}$ ). Therefore, as it is meaningless to compare these results directly, the results of heat of adsorption onto this powder are given in Appendix A for the purpose of reference.

### 2.43 Reversibility of Adsorption

A comparison of adsorption with desorption gives useful information about the classification into physical and chemical adsorption. Generally speaking, a compound which has weak polar radical like alcohol, usually adsorbs physically on metal or metal oxide and this process is reversible. On the other hand, a compound which has strong polarity like fatty acid, sometimes adsorbs chemically on metal or metal oxide and makes a metal soap. Most chemical adsorption is an irreversible process (15) (70).

In lubrication it is stated that oiliness reagents, fatty acid, alcohol, ester, adsorb physically or chemically on lubricated surface and affect on friction and wear in boundary lubrication. It is interesting to investigate which kind of adsorption is effective on friction and wear in boundary lubrication.

As cumulative heats of desorption were measured by a Flow Microcalorimeter, heats of desorption of the same system were easily obtained by the change of flow from solution to solvent. The cumulative heat of adsorption is the heat change when the replacement of solvent molecules by adsorbate molecules occurs. The cumulative heat of desorption means the heat change by the replacement of adsorbate molecules by solvent molecules. Cumulative heats of desorption from  $\alpha\text{-Fe}_2\text{O}_3$ ,  $\gamma\text{-Fe}_2\text{O}_3$  and  $\text{Fe}_3\text{O}_4$  were measured by change of flow of solution to solvent after completion of adsorption (completion means that no further detectable heat was evolved). In experiment on a Flow Microcalorimeter, it is possible to

repeat this process of adsorption and desorption indefinitely.

The results were shown in Figures 2.27 to 2.29. The values of cumulative heat of adsorption in these figures are not always identical to those shown in Sections 2.31 to 2.33. The reason for this is that the values in Sections 2.31 to 2.33 are average of 2-4 experiments but the results in Figures 2.27 to 2.29 are values from a single experiment.

The results can be classified into two groups. The first group has the trend that there is no change of value between the first run and the following run. On the other hand, in another group there was some decrease of value after the first run. The adsorption of the first group is considered to be entirely reversible but the second group clearly includes some irreversible effects. Assuming that the difference of heat change between the first run and the following run depends on an irreversible process and that the ratio of the reversible process is proportional to the ratio of the value at first run and the average value of the following run, then the following results are obtained:

Percentage of Reversible Process

| <u>Adsorbent</u>               | <u>Adsorbate</u> | <u>% of reversible process</u> |
|--------------------------------|------------------|--------------------------------|
| $\alpha\text{-Fe}_2\text{O}_3$ | Stearic acid     | 100%                           |
|                                | Stearyl alcohol  | 100%                           |
| $\gamma\text{-Fe}_2\text{O}_3$ | Stearic acid     | 75%                            |
|                                | Stearyl alcohol  | 100%                           |
| $\text{Fe}_3\text{O}_4$        | Stearic acid     | 12%                            |
|                                | Stearyl alcohol  | 77%                            |

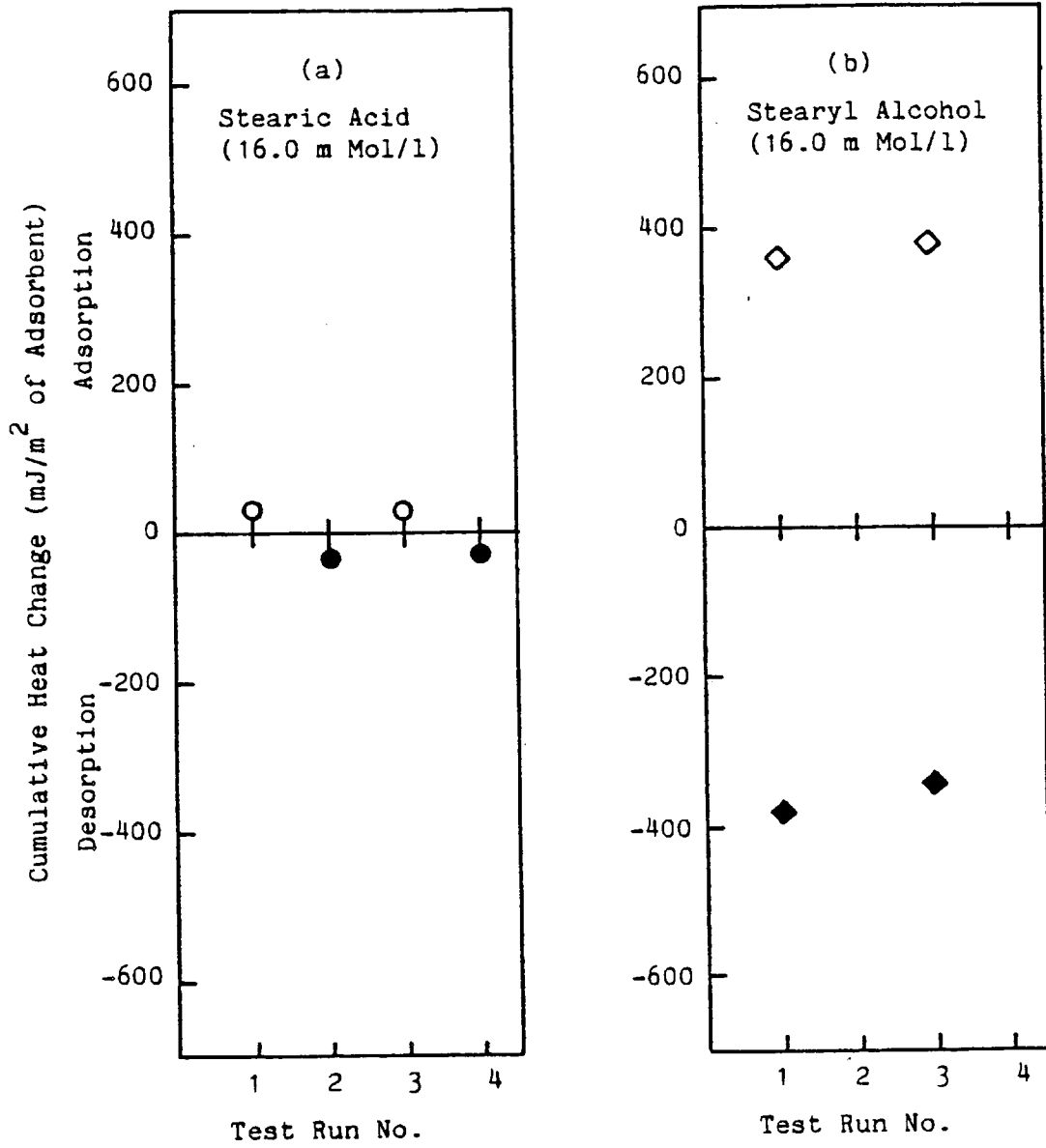


Fig.2-27, Heat of adsorption and desorption onto  $\alpha$ -Fe<sub>2</sub>O<sub>3</sub> at 26.5°C

Solvent n-Heptane



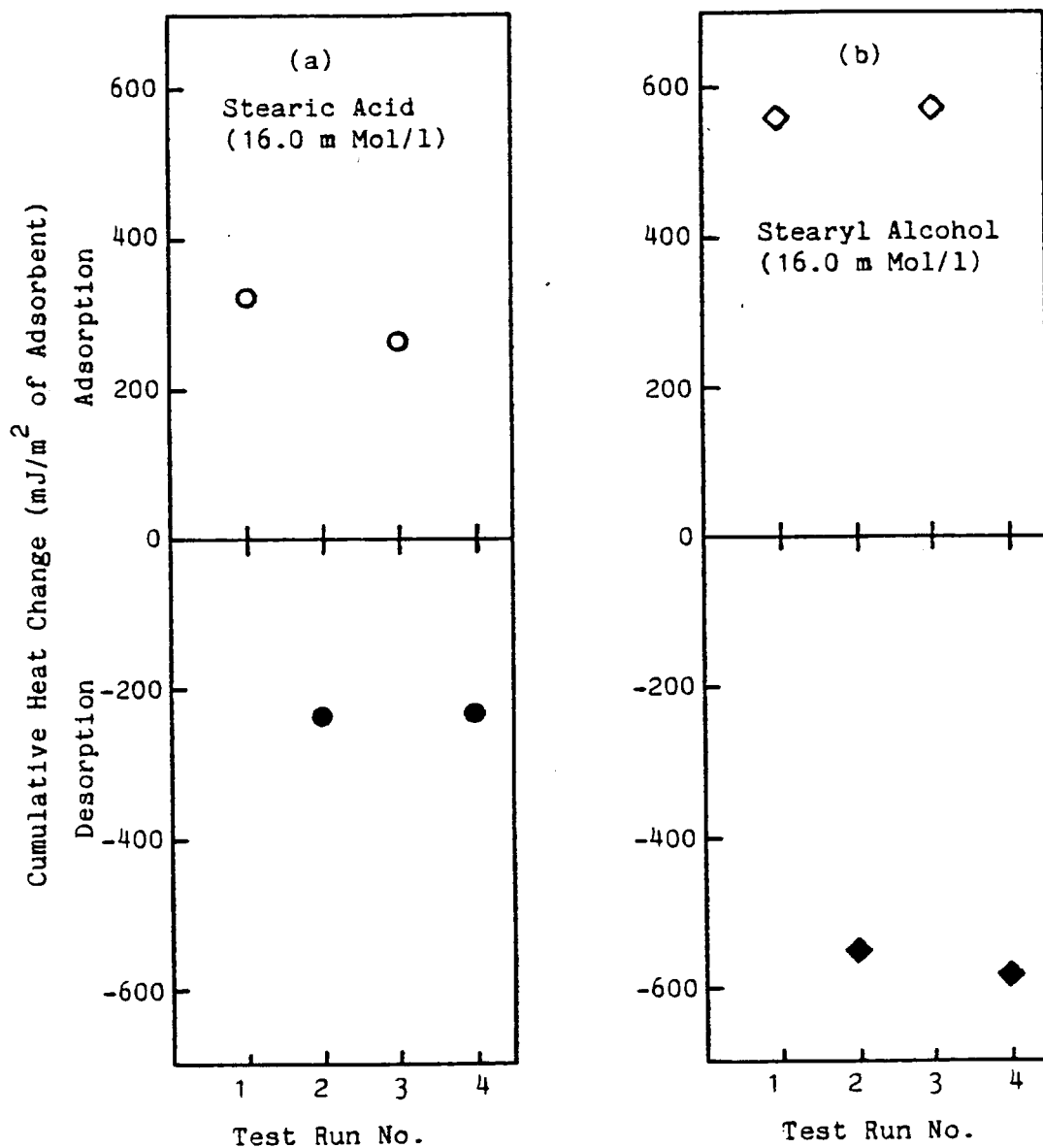


Fig.2-28, Heat of adsorption and desorption onto  $\gamma$ -Fe<sub>2</sub>O<sub>3</sub> at 26.5°C

Solvent n-Heptane

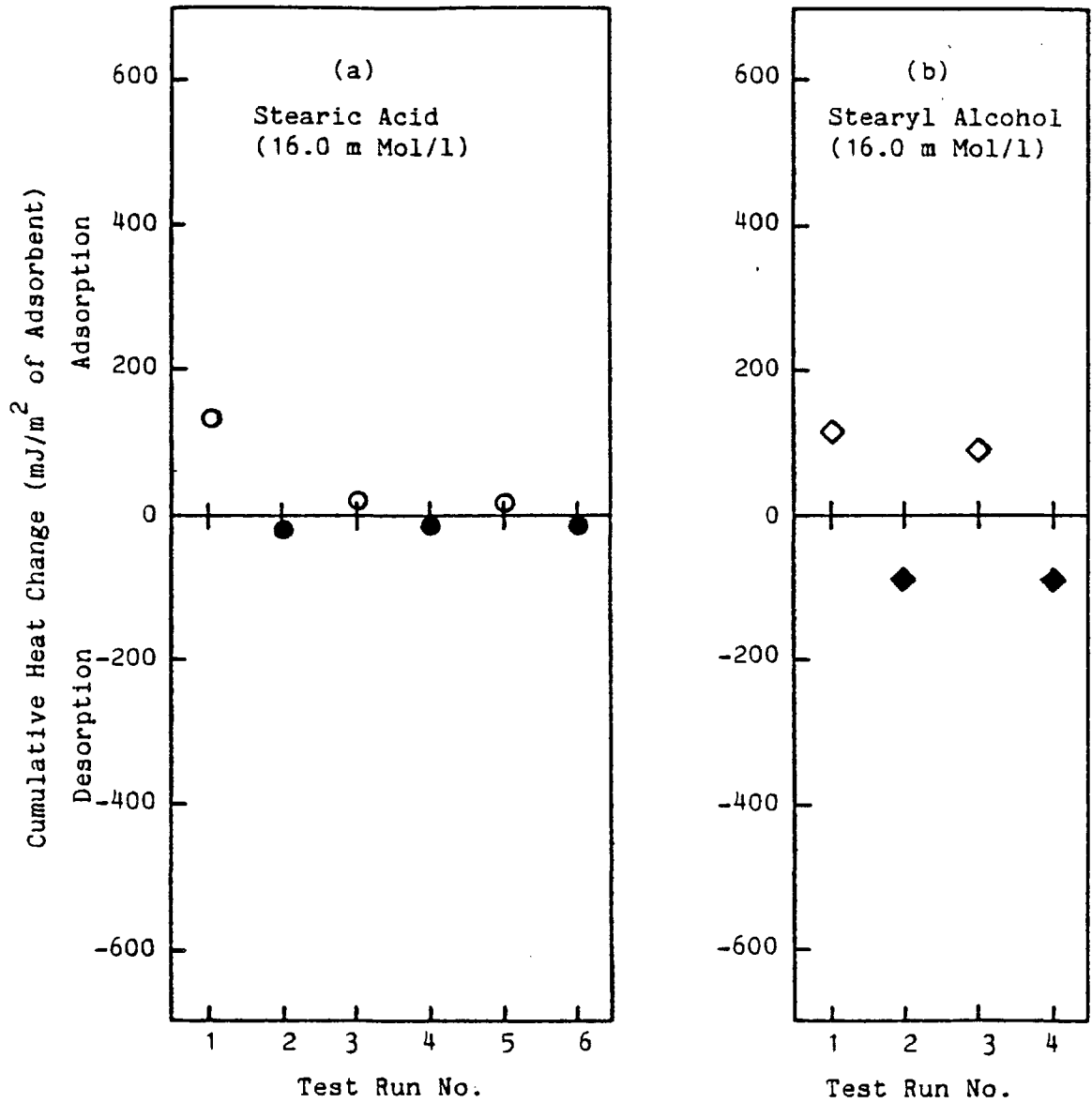


Fig.2-29, Heat of adsorption and desorption onto Fe<sub>3</sub>O<sub>4</sub> at 26.5°C

The three kinds of iron oxide have different characteristics. Adsorption of stearic acid and stearyl alcohol onto  $\alpha\text{-Fe}_2\text{O}_3$  are 100% reversible. Adsorption of stearyl alcohol onto  $\gamma\text{-Fe}_2\text{O}_3$  is also 100% reversible but that of stearic acid includes 25% irreversible process. In the case of  $\text{Fe}_3\text{O}_4$ , stearic acid is only 12% reversible and stearyl alcohol is 77% reversible. There are two reasons for irreversibility, i.e. one is porosity of surface and another is chemical adsorption on the surface. It is reasonable to consider that irreversibility of stearyl alcohol is related to porosity and that of stearic acid depends on both porosity and chemical adsorption. Therefore  $\gamma\text{-Fe}_2\text{O}_3$  has not porosity but has high activity for chemical adsorption of stearic acid. As shown in Section 2.31, there was much difference in the heat of adsorption of stearic acid between  $\alpha\text{-Fe}_2\text{O}_3$  and  $\gamma\text{-Fe}_2\text{O}_3$ , despite that the heats of adsorption of stearyl alcohol onto both  $\alpha\text{-Fe}_2\text{O}_3$  and  $\gamma\text{-Fe}_2\text{O}_3$  were similar. This difference may be due to chemical adsorption onto  $\gamma\text{-Fe}_2\text{O}_3$ .

$\text{Fe}_3\text{O}_4$  has both aspects of porosity and chemical adsorption. The literature suggests that sulphur type EP additives form  $\text{Fe}_3\text{O}_4$  on a lubricated surface as well as FeS, and  $\text{Fe}_3\text{O}_4$  produces a porous surface which can store oil to reduce friction and wear (41). The results obtained here support this suggestion, even if there are many assumptions on the way to this conclusion.

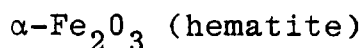
Many authors have reported chemical adsorption onto metal or metal oxide. In those experiments, the equilibrium condition of chemical adsorption is achieved after a long

reaction time (68) (90) (91) (92) (99). However the heat change detected by a Flow Microcalorimeter was complete in an hour. Therefore, the adsorption process in this study should be considered to be limited to initial rapid processes. It is necessary to consider that the chemical adsorption described above occurs rapidly and this process is not the same as those described in the literature.

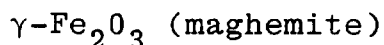
#### 2.44 Heat of Adsorption onto Iron Oxide

In this study, many results concerning heat of adsorption of oiliness reagents onto iron oxide, i.e. cumulative heat of adsorption, effect of temperature, effect of solvent, reversibility or adsorption, were obtained. From them it is possible to tentatively discuss the relationship between adsorption phenomena and the crystallographic characteristics of each iron oxide.

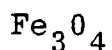
Each iron oxide used in this study has characteristics as shown below (118):



The most stable sesquioxide of iron which has a very narrow range of homogeneity. All  $\text{Fe}^{3+}$  ions are in the octagonal position of the rhombohedral structure.



$\text{Fe}^{3+}$  ions are dispersed at randomly tetragonal and octagonal positions of an inverse spinal structure.



8  $\text{Fe}^{2+}$  ions and 16  $\text{Fe}^{3+}$  ions occupy the following positions of an inverse spinal structure:

8 Fe<sup>3+</sup> ions - tetragonal

8 Fe<sup>2+</sup> ions - octagonal

8 Fe<sup>3+</sup> ions - octagonal

As adsorption of stearic acid onto  $\alpha$ -Fe<sub>2</sub>O<sub>3</sub> is 100% reversible and the heat of adsorption is not great,  $\alpha$ -Fe<sub>2</sub>O<sub>3</sub> should be considered to be relatively inactive for adsorption of stearic acid. Therefore Fe<sup>3+</sup> ions in an octagonal position are not favoured sites for adsorption of stearic acid. The fact that stearic acid can absorb chemically onto both  $\gamma$ -Fe<sub>2</sub>O<sub>3</sub> and Fe<sub>3</sub>O<sub>4</sub> indicates that Fe<sup>3+</sup> ions in tetragonal positions may be active sites for that adsorption. Although there was much difference between the heat of adsorption of stearic acid onto  $\gamma$ -Fe<sub>2</sub>O<sub>3</sub> and onto Fe<sub>3</sub>O<sub>4</sub> as shown in Figures 2.10 and 2.11, the heats of adsorption per mole of stearic acid onto both  $\gamma$ -Fe<sub>2</sub>O<sub>3</sub> and Fe<sub>3</sub>O<sub>4</sub> are almost the same as shown in the next chapter. This fact supports the mechanism of adsorption of stearic acid, described above.

As the adsorption of methyl stearate released only a small amount of heat, it is not necessary to consider chemical interaction like stearic acid.

The adsorption of stearyl alcohol onto  $\alpha$ -Fe<sub>2</sub>O<sub>3</sub>,  $\gamma$ -Fe<sub>2</sub>O<sub>3</sub> and Fe<sub>3</sub>O<sub>4</sub> releases the same level of heat in the region where there is no secondary increasing. This suggests that these adsorptions occur in the same mechanism. Therefore the author proposes that adsorption of stearyl alcohol occurs on the position of the anion (O<sup>2-</sup>). The secondary increase of heat of adsorption, which was observed in adsorption of stearyl alcohol onto  $\alpha$ -Fe<sub>2</sub>O<sub>3</sub> and  $\gamma$ -Fe<sub>2</sub>O<sub>3</sub>, must be influenced by crystallographic characteristics. For

further discussions about this problem, however, information of geographical surface structure of a crystal of each iron oxide is necessary.

From these limited results, a mechanism of adsorption is proposed, which is shown in Figure 2.30. The main features of the proposal are described as follows:

- (1) Adsorption of stearyl alcohol onto iron oxide occurs at an anion site ( $O^{2-}$ ) as a physical adsorption. The molecule adsorbs horizontally at low concentrations, but in the case of  $\alpha\text{-Fe}_2\text{O}_3$  and  $\gamma\text{-Fe}_2\text{O}_3$  vertical adsorptions occur at high concentrations. These two types of adsorption form different monolayers with different thicknesses.
- (2) Chemical adsorption of stearic acid onto iron oxide occurs on  $\text{Fe}^{3+}$  ions at tetragonal positions. However the  $\text{Fe}^{3+}$  ion at the octagonal position and the  $\text{Fe}^{2+}$  ion are not active for chemical adsorption.
- (3) The cleavage of dimer does not occur when stearic acid adsorbs physically on iron oxide.

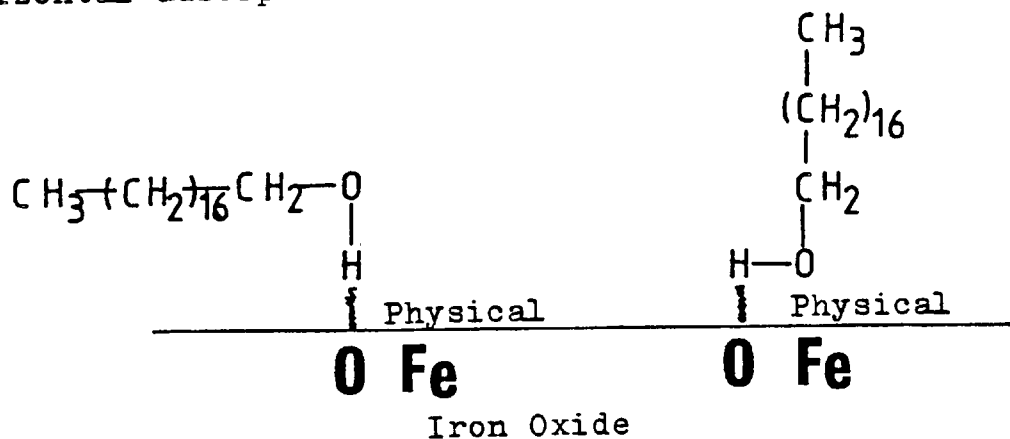
#### 2.45 Heat of Adsorption of DBDS

It is well known that sulphur-type EP additives such as DBDS produce sulphides and oxides on a lubricated surface of steel under high temperature and high pressure conditions in boundary or extreme pressure lubrication. However, this reaction must be a "supressed reaction" to control corrosion wear. It is desirable for sulphur-type EP additives not to have any chemical reaction with iron oxide at low temperature.

Stearyl Alcohol

Low Concentration  
horizontal adsorption

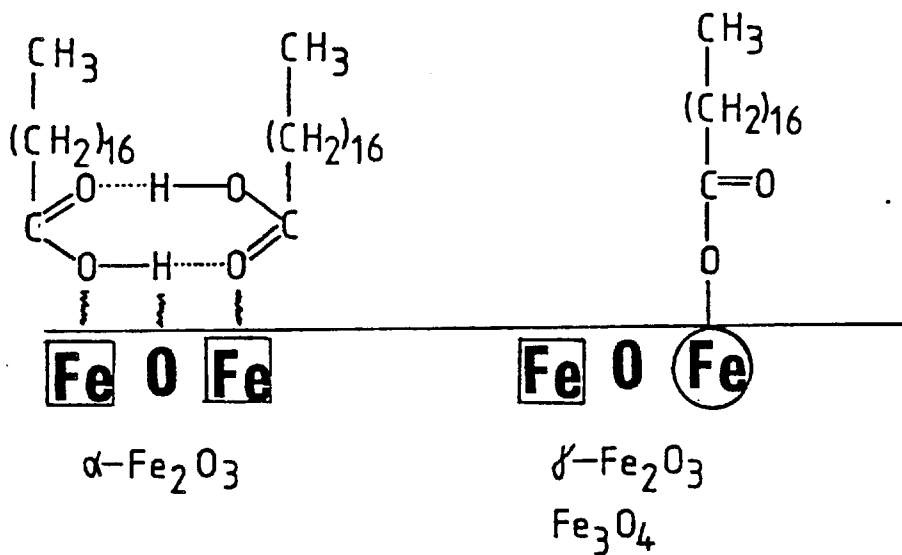
High Concentration  
vertical adsorption



Stearic Acid

Physical Adsorption

Chemical Adsorption



$\boxed{\text{Fe}}$  —  $\text{Fe}^{3+}$  ion at octagonal position  
 $\textcircled{\text{Fe}}$  —  $\text{Fe}^{3+}$  ion at tetragonal position

Fig.2-30, Mechanism of adsorption on iron oxides

The cumulative heat of adsorption of DBDS onto iron oxide ( $\alpha$ -Fe<sub>2</sub>O<sub>3</sub>,  $\gamma$ -Fe<sub>2</sub>O<sub>3</sub> and Fe<sub>3</sub>O<sub>4</sub>) were investigated, and the results were compared with those of oiliness reagents. The result onto  $\gamma$ -Fe<sub>2</sub>O<sub>3</sub> is illustrated in Figure 2.31. Saturation was achieved at 20m Mol/l and the amount of heat of adsorption after saturation is about 19mJ/m<sup>2</sup>, which is about half of that of methyl stearate. This adsorption was almost 100% reversible.

Although the measurement of heat of adsorption onto  $\alpha$ -Fe<sub>2</sub>O<sub>3</sub> and Fe<sub>3</sub>O<sub>4</sub> were tried, the heat release was so small that any reliable data was not obtained by the disturbance of heat of dilution, which was described in Section 2.23. It has become clear that the heat of adsorption of DBDS onto iron oxide is small in comparison with that of oiliness compounds and that there is no particular chemical interaction between DBDS and iron oxide at room temperature. The lack of room temperature chemical interaction is to be expected of an EP additive, since continuous reaction would produce unacceptable corrosive wear.

## 2.50 Conclusions

The following conclusions may be drawn from the results of heat of adsorption measurements of oiliness reagents onto iron oxides and iron (II) sulphide by a Filow Microcalorimeter.

- (1) Comparing the heats of adsorption of each oiliness reagent onto iron oxides and iron (II) sulphide at room temperature, the following order was obtained:



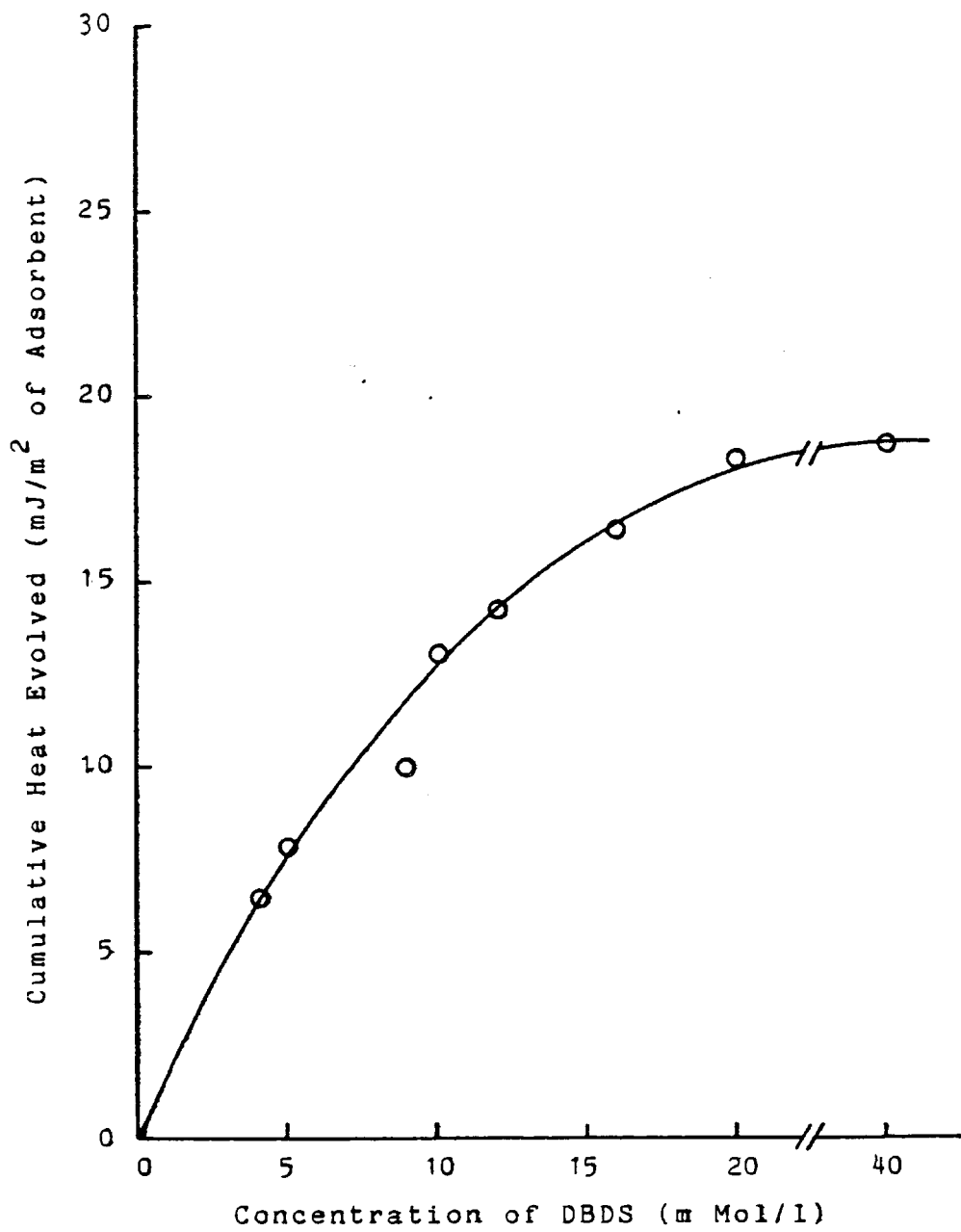


Fig.2-31, Cumulative heat of adsorption of DBDS onto  $\gamma$ -Fe<sub>2</sub>O<sub>3</sub> at 26.5°C

Stearic acid  $\gamma\text{-Fe}_2\text{O}_3 \gg \text{Fe}_3\text{O}_4 > \text{FeS} \sim \alpha\text{-Fe}_2\text{O}_3$   
Stearyl alcohol  $\alpha\text{-Fe}_2\text{O}_3 \sim \gamma\text{-Fe}_2\text{O}_3 \gg \text{Fe}_3\text{O}_4 > \text{FeS}$   
Methyl stearate  $\gamma\text{-Fe}_2\text{O}_3 > \alpha\text{-Fe}_2\text{O}_3 > \text{Fe}_3\text{O}_4 > \text{FeS}$

- (2) Heat of adsorption of oiliness reagents onto iron oxides and iron (II) sulphide is sensitive to temperature. This is especially observed at low temperature, where a large decrease in heat of adsorption is obtained for a small increase in temperature.
- (3) Solvent affects heat of adsorption onto  $\gamma\text{-Fe}_2\text{O}_3$ , but not onto  $\text{Fe}_3\text{O}_4$ .
- (4) Heat of adsorption of oiliness reagents onto iron (II) sulphide is significantly affected by the oxidation condition of the surface. Oxidation increases adsorption.
- (5) From (4) it is suggested that the interaction of oiliness reagents with iron sulphate is significantly stronger than with iron (II) sulphide.
- (6) A mechanism of adsorption of oiliness reagent onto iron oxides is proposed as follows:
- . Stearyl alcohol adsorbs on the anion site ( $\text{O}^{2-}$ ) and forms a physically adsorbed film.
  - . Stearyl alcohol adsorbs horizontally at low concentration and adsorbs vertically at high concentration. However this change does not occur in the adsorption onto  $\text{Fe}_3\text{O}_4$ .
  - . The chemical adsorption of stearic acid occurs on  $\text{Fe}^{3+}$  at tetragonal position in iron oxide. The other sites such as  $\text{Fe}^{3+}$  at octagonal and  $\text{Fe}^{3+}$  are not active for chemical adsorption of stearic acid.

CHAPTER THREE

ADSORPTION

3.10 Introduction

Chapter Two described the acquisition of heat of adsorption data using a Flow Microcalorimeter. In this chapter data on the degree of adsorption is obtained. By combining the two, it is possible to obtain further information about the phenomenon of adsorption and its relationship to lubrication. Because of its importance in boundary lubrication, the adsorption of polar compounds, e.g. fatty acids, alcohols, esters and amines on metals and metal oxides has been measured by many investigators.

Bowden (15) (70), Daniel (71) and Greenhill (84) (119) have studied the nature of adsorption of these polar compounds on metals and metal oxides and have discussed its relation to lubrication. They considered the formation of adsorption film by fatty acids, the effect of oxide film on adsorption and the reversibility of adsorption. Cook (68) (69) showed similar results for adsorption on metal, where the existence of a mixed film of polar compounds and solvent was found.

In all of the studies mentioned above, metals or metals covered by oxide film were used as adsorbents. Some authors obtained results of adsorption on iron and iron oxide. However, these results were not complete enough to elucidate the mechanism of the effect of oiliness compounds and sulphur-type EP additives on friction and wear, which is the main subject of this thesis. Sulphur-type EP additives

such as DBDS produce many products like  $\text{Fe}_3\text{O}_4$ ,  $\alpha\text{-Fe}_2\text{O}_3$ ,  $\text{FeS}$ ,  $\text{Fe}_{1-x}\text{S}_x$  and  $\text{FeSO}_4$  on the surface of steel (22) (37) (39) (41) (46).

The purpose of these adsorption experiments is to obtain adsorption isotherms of polar compounds on iron oxide and iron sulphide and to show the relation between adsorption isotherm and heat of adsorption. From both of these results, it is possible to comprehend the adsorption phenomena thermodynamically and to discuss the mechanism of oiliness reagents mentioned above.

Radioactive tracers are a useful method of obtaining adsorption data due to their high sensitivity. Many authors have used this method (68) (70) (72) (90). However, as the purpose of this experiment was to measure the amount of adsorption of polar compounds on powders with large surface areas, the change in concentration of adsorbates, as determined by IR spectrometry, gave enough information. The IR carbonyl peak was found to be very sensitive to concentration changes of stearic acid and methyl stearate, but the OH adsorption for stearyl alcohol was obscured by solvent peaks. Therefore, only adsorption isotherms for stearic acid and methyl stearate were obtained in these experiments.

### 3.20 Experimental

#### 3.21 Materials

The oiliness reagents, stearic acid and methyl stearate

were used as adsorbates, and n-heptane was used as the solvent in these experiments. The analytical data and purification methods of these compounds has been described in Section 2.21. The adsorbent powders,  $\alpha\text{-Fe}_2\text{O}_3$ ,  $\gamma\text{-Fe}_2\text{O}_3$ ,  $\text{Fe}_3\text{O}_4$  and FeS mentioned in Section 2.21 were used.

### 3.22 Procedure

5ml and 15ml sample bottles with plastic caps were used as adsorption cells. Prior to the measurement of adsorption, it was confirmed that this kind of sample bottle would prevent loss of n-heptane for several hours at room temperature. The rate of adsorption was investigated first. 15ml sample bottles were used as adsorption cells. About 0.5ml powders were weighed out to the nearest 0.1mg in a cell, and placed in an oil bath of temperature  $26.5 \pm 0.3^\circ\text{C}$ . Then, 8ml of solution containing 20.0m Mol/l adsorbate was poured into the cell. After 1, 2, 4 and 6 hours, about 1ml of the solution was withdrawn from the cell to measure concentration. During the adsorption reaction the cell was shaken occasionally to increase contact of adsorbate with adsorbent.

For the measurement of the adsorption isotherms, a 5ml sample bottle was used as an adsorption cell. 0.1-0.3ml powder was weighed and was poured into the cell. In a similar way to the experiment of adsorption rate, the cell was placed in the oil bath controlled at  $26.5 \pm 0.3^\circ\text{C}$ . Then, a specified volume of solution, which was measured with a pipet, was poured into the cell. After four hours

the top of the solution was decanted to another bottle with a close cap. The concentration of this solution was determined by IR spectrometry to obtain an adsorption isotherm.

### 3.23 Measurement of Concentration

As both stearic acid and methyl stearate have a carbonyl group, it was convenient to use IR spectrometry to measure the concentration directly by the use of liquid cells with NaCl windows, because there were no adsorption peaks by solvent (n-heptane) in the region of wavelength for carbonyl groups ( $\approx 1700\text{cm}^{-1}$ ). The IR spectrometer used was a Perkin Elmer Model 580B. The calibration curve is shown in Figure 3.1, in which a linear relationship for both reagents is obtained.

### 3.24 Calculation of Adsorption Value

Assuming that the change of concentration of solution in contact with powder depends on adsorption, the adsorption value can be calculated directly.

Example calculation: 2ml stearic acid of 20.0m Mol/l concentration was contacted with 100mg  $\gamma\text{-Fe}_2\text{O}_3$ . Absorbance of the solution by IR was 0.585.

- (i) From the calibration curve in Figure 3.1, concentration of stearic acid is 14.6m Mol/l.
- (ii) Depletion of stearic acid
$$= (20.0 - 14.6) \times 10^{-3} \times \frac{2}{1000} \text{ moles}$$
$$= 1.08 \times 10^{-5} \text{ moles}$$

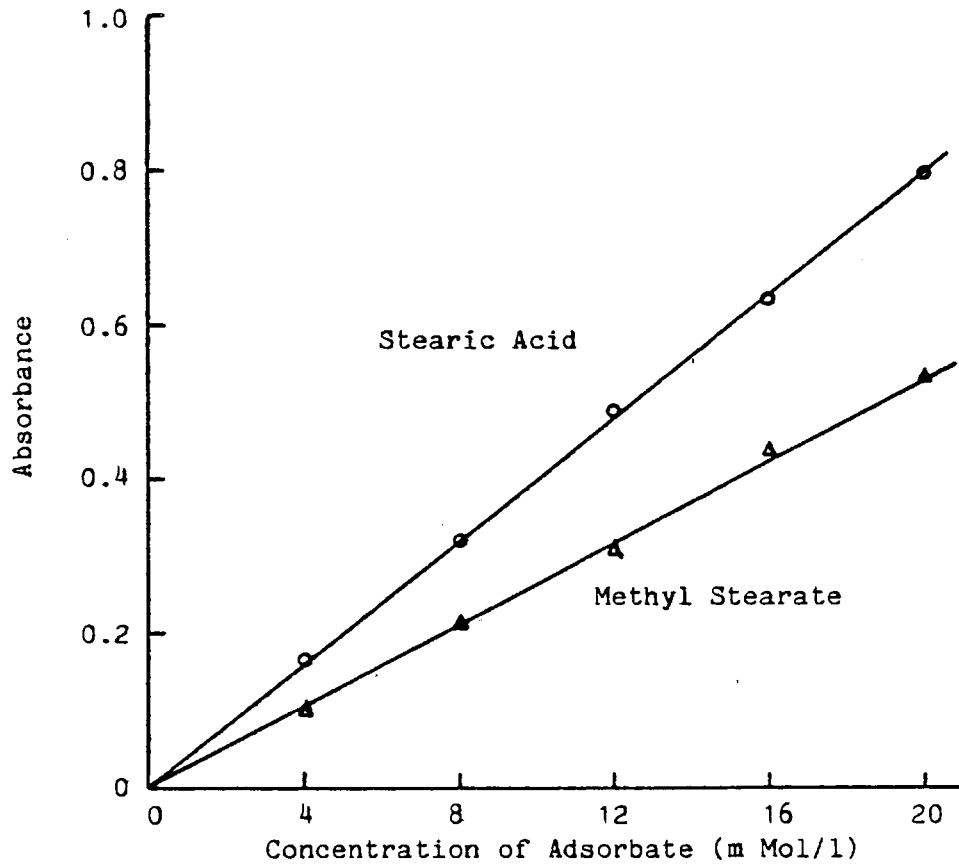


Fig.3-1, Absorbance of carbonyl absorption in IR vs. concentration of adsorbate

| Slope           |                             |
|-----------------|-----------------------------|
| Stearic Acid    | 25.0 (m Mol/l)/(Absorbance) |
| Methyl Stearate | 37.6 "                      |

$$\begin{aligned} \text{(iii) Adsorption per gram } \gamma\text{-Fe}_2\text{O}_3 & \\ &= \frac{1.08 \times 10^{-5}}{10^{-1}} \text{ moles/g} \\ &= 1.08 \times 10^{-4} \text{ moles/g} \end{aligned}$$

$$\begin{aligned} \text{(iv) Adsorption per m}^2 \text{ } \gamma\text{-Fe}_2\text{O}_3 & \\ &= 1.08 \times 10^{-4} \times \frac{1}{17} \text{ moles/m}^2 \\ &= 6.3 \times 10^{-6} \text{ moles/m}^2 \end{aligned}$$

Consequently, adsorption is  $6.3 \times 10^{-6}$  moles/m<sup>2</sup> at an equilibrium concentration of 14.6m Mol/l.

### 3.30 Results

#### 3.31 Rate of Adsorption

Rate studies of adsorption were undertaken to estimate the time to attain an equilibrium value. The adsorbates studied here were limited to stearic acid and methyl stearate. The results are illustrated in Figure 3.2, in which the time dependence of adsorption for initial six hours is shown.

As described in 3.22, the amounts of adsorption shown in Figure 3.2 was calculated from the concentration change of solution with an initial concentration 20.0m Mol/l in contact with adsorbent. Therefore, the concentration of adsorbate at each measurement point depended on the extent of adsorption. In the case of  $\gamma\text{-Fe}_2\text{O}_3$ , as this powder could adsorb much stearic acid, the concentration of stearic acid at each measurement was quite low, compared with other powders. Therefore, if the concentrations of adsorbate were controlled



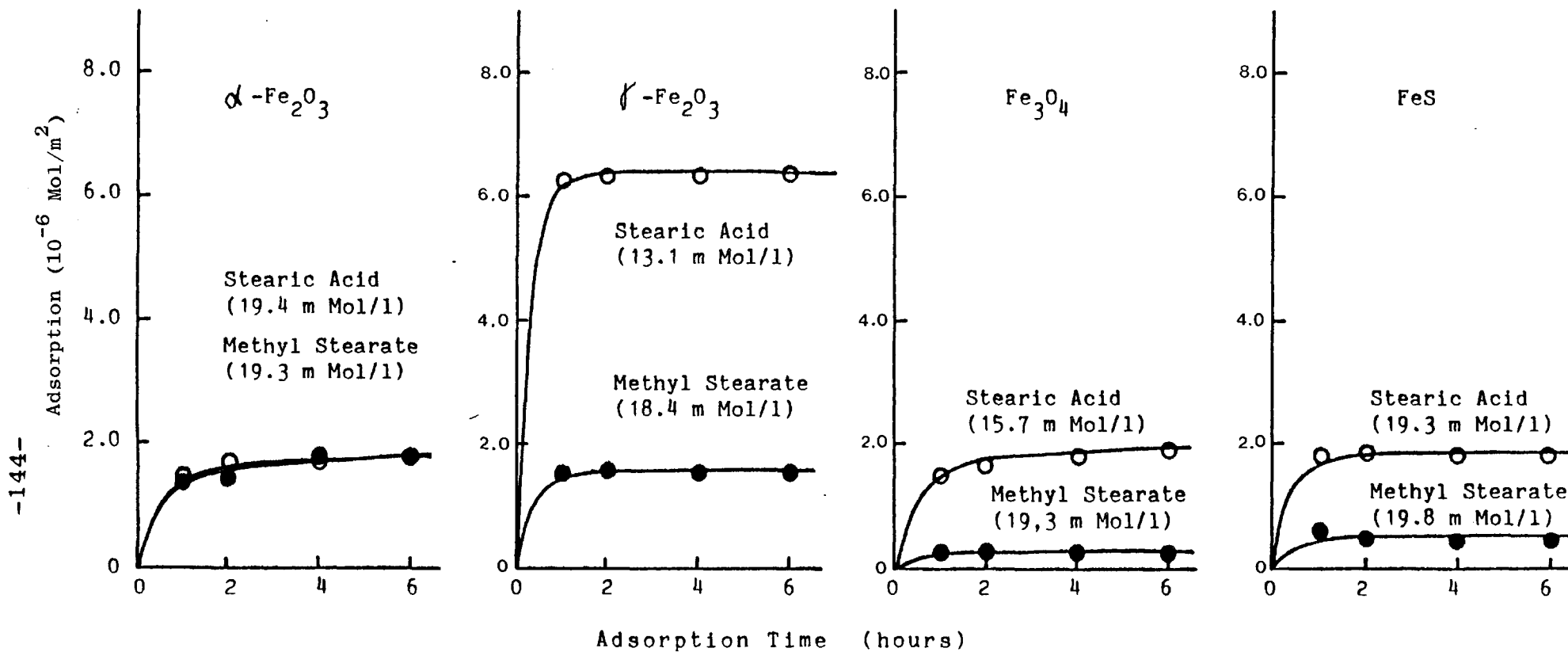


Fig.3-2, Adsorption rate at 26.5 °C

Figures in parentheses indicate the equilibrium concentration of adsorbate at the final stage

to the same level for all powders and adsorbates, possibly the different results from it shown in Figure 3.1 might be obtained.

The figures show the rapid achievement of equilibrium, except for the adsorption of stearic acid onto  $\text{Fe}_3\text{O}_4$  (Figure 3.1(c)). In most of the cases, equilibrium conditions were achieved within two hours. Four hours adsorption was enough for a complete adsorption isotherm.

The adsorption of stearic acid onto  $\text{Fe}_3\text{O}_4$  increased, however, gradually after a rapid initial process. Smith (77) and Cook (68) observed such increases in the case of adsorption of stearic acid onto iron oxide, and suggested the possibility of chemical reaction between the acid and the iron oxide. Considering the data obtained in this work, this reaction of stearic acid, can have occurred with  $\text{Fe}_3\text{O}_4$ , but not with other iron oxides like  $\alpha\text{-Fe}_2\text{O}_3$  and  $\gamma\text{-Fe}_2\text{O}_3$ .

The increasing speed of adsorption of stearic acid onto  $\text{Fe}_3\text{O}_4$  after a rapid initial process was not as high as the speed measured by Smith and Cook. As  $\text{Fe}_3\text{O}_4$  used in the present work was pure, it was expected there would be more reaction between the acid and  $\text{Fe}_3\text{O}_4$ .

However, Hirst (86) investigated the influence of water on the reaction between metal oxide and stearic acid and found a large effect of water on this reaction. It is therefore conceivable that the reason for the differences in results is due to a difference in water content of solution and powder.

### 3.32 Adsorption Isotherm

The adsorption isotherm of stearic acid and methyl stearate on iron oxide and iron sulphide at 26.5°C is illustrated in Figure 3.3, in which the isotherms are presented in Mol per m<sup>2</sup> of adsorbent. The characteristic features of each adsorption isotherm are described below.

α-Fe<sub>2</sub>O<sub>3</sub>: The curves for adsorption isotherms of stearic acid and methyl stearate are almost the same, only minor difference of isotherm levels revealed by Mol per m<sup>2</sup> was observed. There were no comprehensive differences in the isotherms presented by gram per m<sup>2</sup>. Therefore the difference of isotherm level in Figure 3.3(a) is dependent on the dimensions of each adsorbate molecule. Comparing the isotherms with the data on the heats of adsorption shown in Figure 2.9, the difference of heats of adsorption between stearic acid and methyl stearate is a little larger than the difference of degree of adsorption isotherm. This is due to stearic acid adsorbing on α-Fe<sub>2</sub>O<sub>3</sub> more strongly than methyl stearate.

γ-Fe<sub>2</sub>O<sub>3</sub>: The shape of the isotherm of stearic acid onto γ-Fe<sub>2</sub>O<sub>3</sub> is similar to that of the heat of adsorption. (Figure 3.3(b) and Figure 2.10). These two curves show an initial rapid increase with concentration at low concentrations and a secondary increase at high concentration near the solubility limit of stearic acid in n-heptane at 26.5°C. Also, the isotherm of methyl stearate is similar to that of methyl stearate onto α-Fe<sub>2</sub>O<sub>3</sub>. Therefore γ-Fe<sub>2</sub>O<sub>3</sub> powder has particularly active sites for stearic acid adsorption on the

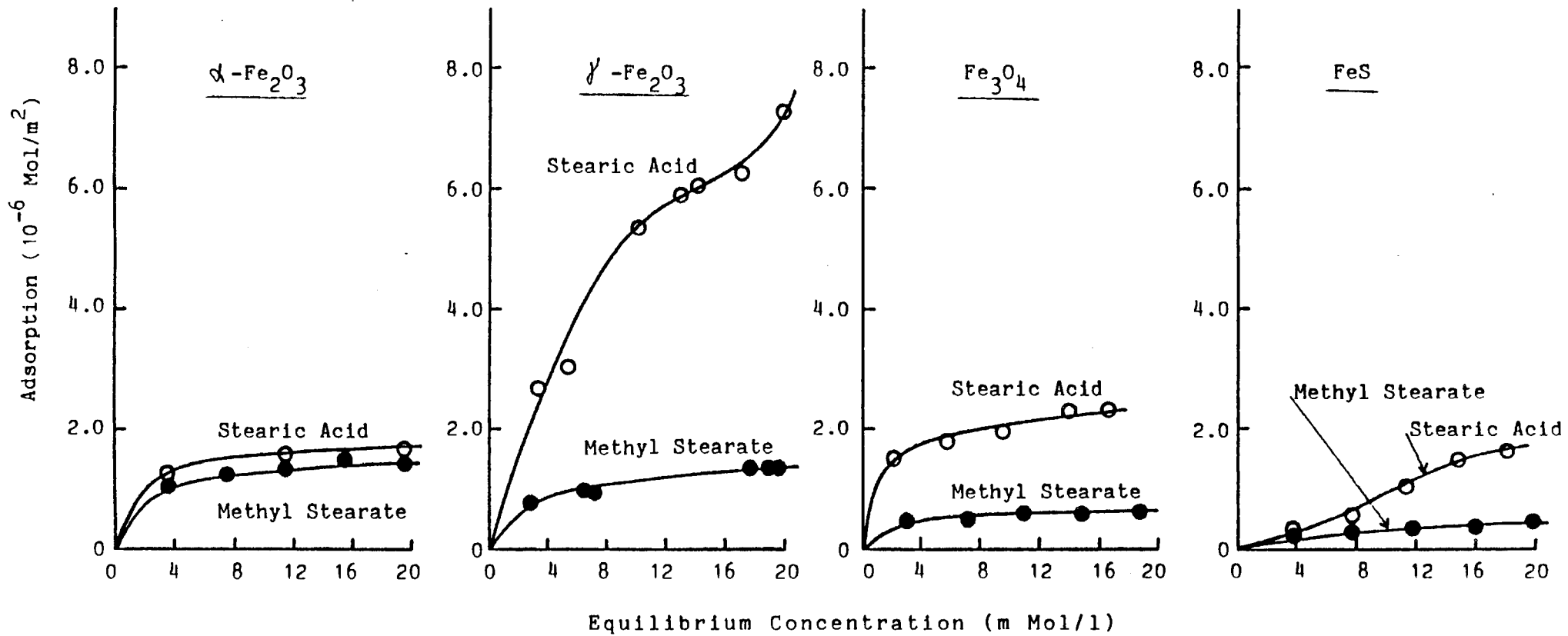


Fig.3-3, Adsorption isotherms at 26.5 °C

surface.

Fe<sub>3</sub>O<sub>4</sub>: The adsorption isotherms are illustrated in Figure 3.3(c). As shown in the previous section, the adsorption of stearic acid onto Fe<sub>3</sub>O<sub>4</sub> achieved equilibrium conditions slowly. However, as the increase of adsorption after the rapid initial process was relatively small, the adsorption isotherm in Figure 3.2(c) was obtained from the concentration change of solution in contact with Fe<sub>3</sub>O<sub>4</sub> powder after four hours. This was in accordance with the assumption of equilibrium condition after four hours adsorption. The amount of adsorption of stearic acid onto Fe<sub>3</sub>O<sub>4</sub> was not as large as onto γ-Fe<sub>2</sub>O<sub>3</sub> but was a little greater than onto α-Fe<sub>2</sub>O<sub>3</sub>. The adsorption isotherm of methyl stearate onto Fe<sub>3</sub>O<sub>4</sub> was small compared with that onto α-Fe<sub>2</sub>O<sub>3</sub> and γ-Fe<sub>2</sub>O<sub>3</sub>.

FeS: Although the surface of FeS powder used in this work was oxidized as shown in Table 2.6, it was nevertheless used to obtain adsorption isotherms of stearic acid and methyl stearate. The amount of adsorption of methyl stearate was similar to that onto iron oxide described above. The adsorption isotherm of stearic acid showed a different trend, however, i.e. it was quite small at low concentration but increased at high concentration.

Inspection of Figure 3.3(a) (b) and (c) revealed that the following order of level of adsorption isotherm for iron oxide is obtainable.

Stearic acid      γ-Fe<sub>2</sub>O<sub>3</sub> >> Fe<sub>3</sub>O<sub>4</sub> > α-Fe<sub>2</sub>O<sub>3</sub>

Methyl stearate   α-Fe<sub>2</sub>O<sub>3</sub> ≈ γ-Fe<sub>2</sub>O<sub>3</sub> > Fe<sub>3</sub>O<sub>4</sub>

The order of increasing adsorption of stearic acid is the

same as that of heats of adsorption, which is described in Section 2.31. On the other hand, the order for methyl stearate did not coincide with that of heats of adsorption, i.e. the heat of adsorption on  $\gamma\text{-Fe}_2\text{O}_3$  was bigger than that on  $\alpha\text{-Fe}_2\text{O}_3$ .

### 3.40 Discussions

#### 3.41 Heat of Adsorption per Mol

In this study, as both data of adsorption isotherms and heats of adsorption for stearic acid and methyl stearate were obtained, it was possible to calculate the heat of adsorption per Mol. As this parameter was, under the condition used, the enthalpy change of adsorption  $\Delta H_{\text{ads}}$ , further thermodynamic analysis is possible.

The results of calculating  $\Delta H_{\text{ads}}$  are listed in Table 3.1 and Figures 3.4 and 3.5, in which the values are presented in KJ/Mol for convenience of discussion. The enthalpy change of adsorption of stearic acid and methyl stearate onto  $\alpha\text{-Fe}_2\text{O}_3$  were about 25KJ/Mol and about 13KJ/Mol respectively. These enthalpy changes did not vary with the concentration of adsorbate. So there was little difference in the amounts of adsorption with concentration. If it is assumed that entropy change is not large, due to the low coverage density of adsorbate on the surface of  $\text{Fe}_3\text{O}_4$ , the free energy changes by adsorption  $\Delta G_{\text{ads}}$  are , for stearic acid:

$$\Delta G_{\text{ads}} \cong \Delta H_{\text{ads}} = 25\text{KJ/Mol}$$

TABLE 3.1

Heat of Adsorption per Mole (I)

a)  $\alpha\text{-Fe}_2\text{O}_3$

| Solution<br>(Mol/l)    | Adsorption<br>(Mol/m <sup>2</sup> ) | Cumulative<br>Heat of Adsorption. |          |
|------------------------|-------------------------------------|-----------------------------------|----------|
|                        |                                     | (mJ/m <sup>2</sup> )              | (KJ/Mol) |
| <u>Stearic Acid</u>    |                                     |                                   |          |
| 4 x 10 <sup>-3</sup>   | 1.35 x 10 <sup>-6</sup>             | 35                                | 26.0     |
| 8                      | 1.55                                | 40                                | 26.0     |
| 12                     | 1.60                                | 40                                | 24.7     |
| 16                     | 1.63                                | 40                                | 24.7     |
| 20                     | 1.66                                | 40                                | 23.9     |
| <u>Methyl Stearate</u> |                                     |                                   |          |
| 4 x 10 <sup>-3</sup>   | 1.10 x 10 <sup>-6</sup>             | 12                                | 10.9     |
| 8                      | 1.30                                | 16                                | 12.2     |
| 12                     | 1.33                                | 18                                | 13.8     |
| 16                     | 1.39                                | 20                                | 13.8     |
| 10                     | 1.40                                | 20                                | 13.8     |

b)  $\gamma\text{-Fe}_2\text{O}_3$

| Solution<br>(Mol/l)    | Adsorption<br>(Mol/m <sup>2</sup> ) | Cumulative<br>Heat of Adsorption |          |
|------------------------|-------------------------------------|----------------------------------|----------|
|                        |                                     | (mJ/m <sup>2</sup> )             | (KJ/Mol) |
| <u>Stearic Acid</u>    |                                     |                                  |          |
| 4 x 10 <sup>-3</sup>   | 3.00 x 10 <sup>-6</sup>             | 230                              | 76.7     |
| 8                      | 4.80                                | 355                              | 73.4     |
| 12                     | 5.70                                | 420                              | 73.7     |
| 16                     | 6.20                                | 485                              | 77.9     |
| 20                     | 7.30                                | 585                              | 79.6     |
| <u>Methyl Stearate</u> |                                     |                                  |          |
| 4 x 10 <sup>-3</sup>   | 0.83 x 10 <sup>-6</sup>             | 30                               | 34.8     |
| 8                      | 1.05                                | 100                              | 94.7     |
| 12                     | 1.15                                | 110                              | 96.0     |
| 16                     | 1.25                                | 115                              | 91.8     |
| 20                     | 1.35                                | 117                              | 86.7     |

TABLE 3.1

Heat of Adsorption per Mole (II)

c) Fe<sub>3</sub>O<sub>4</sub>

| Solution<br>(Mol/l)    | Adsorption<br>(Mol/m <sup>2</sup> ) | Cumulative<br>Heat of Adsorption<br>(mJ/m <sup>2</sup> ) (KJ/Mol) |      |
|------------------------|-------------------------------------|---|------|
| <u>Stearic Acid</u>    |                                     |   |      |
| 4 x 10 <sup>-3</sup>   | 1.70 x 10 <sup>-6</sup>             | 125   | 73.7 |
| 8                      | 1.90                                | 130   | 72.7 |
| 12                     | 2.05                                | 155   | 75.8 |
| 16                     | 2.25                                | 180   | 79.6 |
| 20                     | 2.45                                | 210   | 85.5 |
| <u>Methyl Stearate</u> |                                     |   |      |
| 4 x 10 <sup>-3</sup>   | 0.40 x 10 <sup>-6</sup>             | 8   | 20.1 |
| 8                      | 0.50                                | 10  | 20.1 |
| 12                     | 0.52                                | 12  | 23.0 |
| 16                     | 0.55                                | 12  | 21.8 |
| 20                     | 0.55                                | 12  | 21.8 |

d) FeS

| Solution<br>(Mol/l)    | Adsorption<br>(Mol/m <sup>2</sup> ) | Cumulative<br>Heat of Adsorption<br>(mJ/m <sup>2</sup> ) (KJ/Mol) |       |
|------------------------|-------------------------------------|---|-------|
| <u>Stearic Acid</u>    |                                     |   |       |
| 4 x 10 <sup>-3</sup>   | 0.40 x 10 <sup>-6</sup>             | 52  | 130.0 |
| 8                      | 0.60                                | 55  | 91.8  |
| 12                     | 1.10                                | 68  | 62.0  |
| 16                     | 1.50                                | 75  | 49.9  |
| 20                     | 1.70                                | 80  | 46.9  |
| <u>Methyl Stearate</u> |                                     |   |       |
| 4 x 10 <sup>-3</sup>   | 0.22 x 10 <sup>-6</sup>             | 5   | 23.0  |
| 8                      | 0.25                                | 6   | 23.9  |
| 12                     | 0.30                                | 7   | 23.0  |
| 16                     | 0.35                                | 8   | 23.0  |
| 20                     | 0.40                                | 8   | 20.0  |



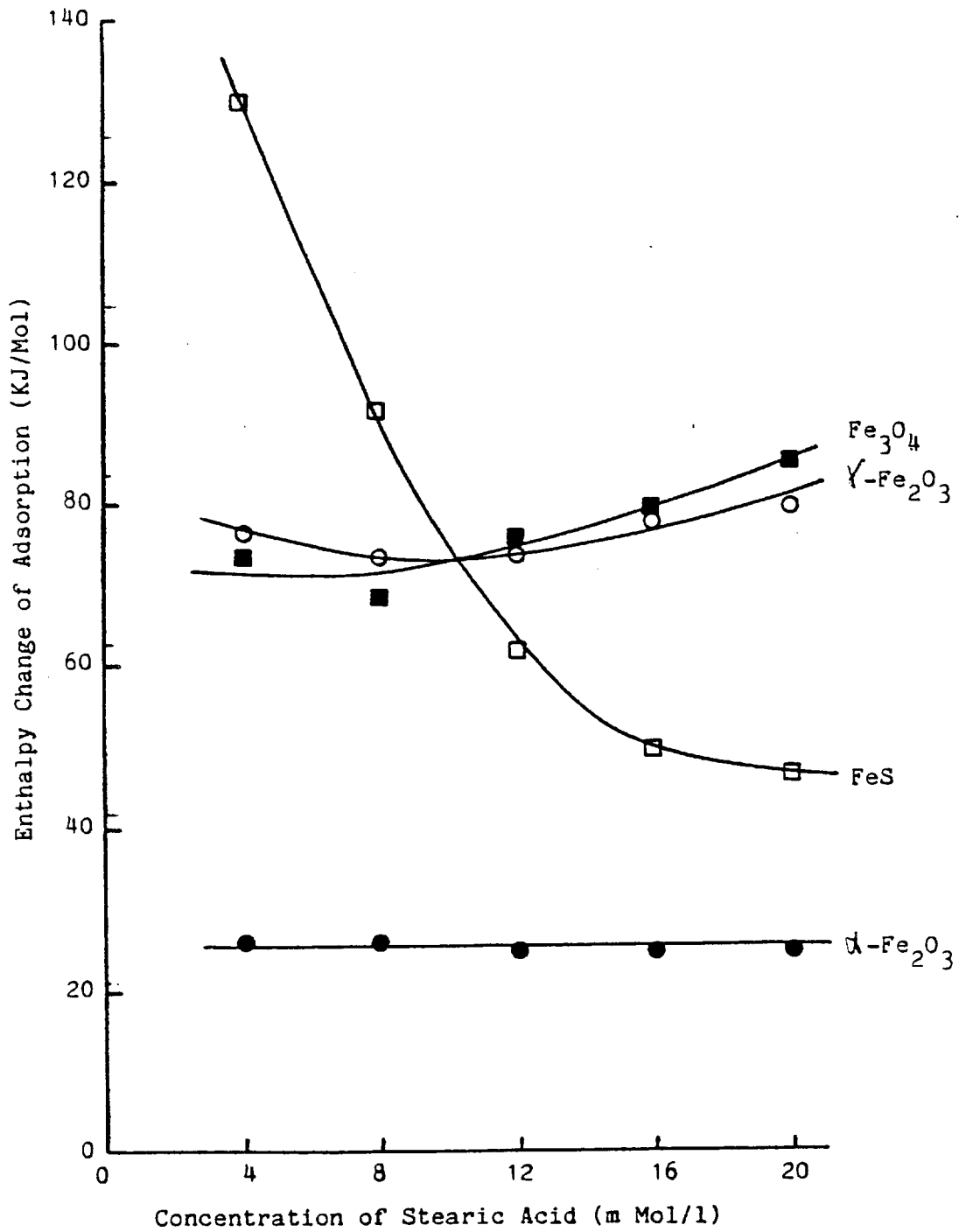


Fig.3-4, Enthalpy change of adsorption per mole for stearic acid

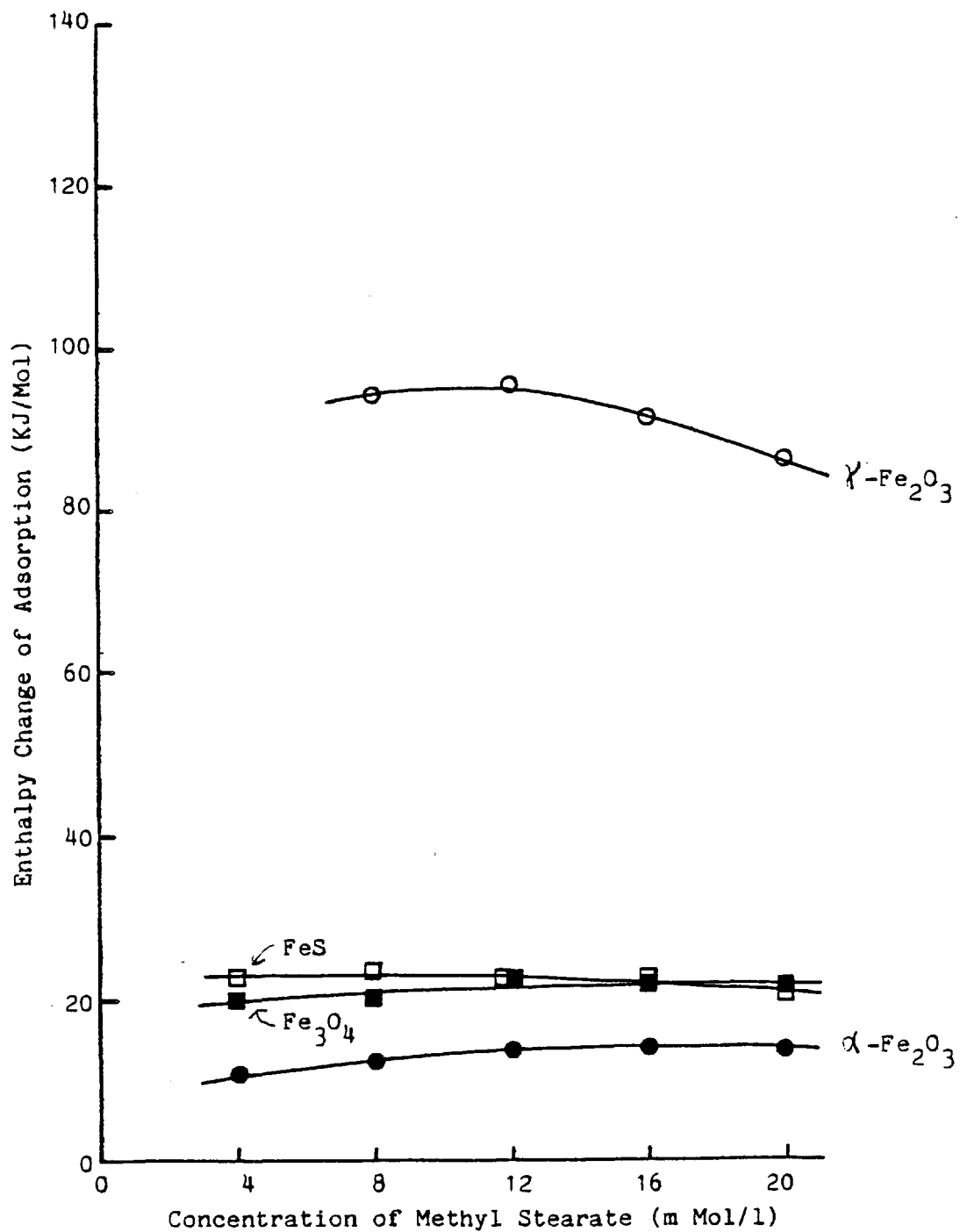


Fig.3-5, Enthalpy change of adsorption per mole for methyl stearate

for methyl stearate:

$$\Delta G_{\text{ads}} \cong \Delta H_{\text{ads}} = 13\text{KJ/Mol}$$

These values of free energy change by adsorption indicate physical adsorption. According to the reversibility results, which are shown in 2.43, the adsorption of stearic acid onto  $\alpha\text{-Fe}_2\text{O}_3$  was 100% reversible. These results suggest that only physical adsorption can occur on the surface of  $\alpha\text{-Fe}_2\text{O}_3$ .

Concerning  $\gamma\text{-Fe}_2\text{O}_3$ , enthalpy changes  $\Delta H_{\text{ads}}$  of stearic acid and methyl stearate adsorption are 73-80, 86-96KJ/Mol respectively. These levels are fairly high for physical adsorption. Spikes and Cameron (89) (90) reported similar high heats of adsorption and they explain their data using the equation provided by Salem, in which equation a high dispersion energy is caused by interactions between hydrocarbon chains as follows:

$$W_d = - 5.2 \times 10^{-2} (N_c/D^5) \text{ KJ/Mol} \quad (3.1)$$

where

$W_d$  : dispersion energy

$N_c$  : number of carbon atoms to interact

$D$  : distance (in nanometer) between two interacting chains

For a hexagonal adsorption assay, the energy due to lateral interaction is negligible for densities of packing below  $0.5\text{nm}^2/\text{molecule}$ , but increases to  $80\text{KJ/Mol}$  at  $0.3\text{nm}^2/\text{molecule}$ . In these experiments, n-heptane was used as a solvent. Therefore the lateral interactions between solvent and adsorbate are less than half of that for the adsorbate even if a

mixed adsorbed film of solvent and adsorbate exists. The high enthalpy change of stearic acid adsorption on  $\gamma\text{-Fe}_2\text{O}_3$  may be due to such lateral forces as high coverages. However no reason was found for the high enthalpy change for methyl stearate.

The enthalpy changes for adsorption of stearic acid onto  $\text{Fe}_3\text{O}_4$  are high, though the coverages are lower. Moreover, the enthalpy change rises with concentration of adsorbate. Inspection of reversibility of adsorption suggests that the adsorption of stearic acid onto  $\text{Fe}_3\text{O}_4$  includes both chemical and physical adsorption, and that the former is time dependent. It is possible that the increase of the enthalpy with concentration may be due to increasing chemical adsorption ratio at high concentration.

Adsorption of methyl stearate onto  $\text{Fe}_3\text{O}_4$  caused an enthalpy change of about 21KJ regardless of concentration of adsorbate. It has been found that chemical reactions between iron oxide and esters can occur at room temperature. As mentioned previously,  $\text{Fe}_3\text{O}_4$  is more reactive to oiliness compounds than to iron oxide  $\alpha\text{-Fe}_2\text{O}_3$ . Therefore, the enthalpy change of methyl stearate adsorption on  $\text{Fe}_3\text{O}_4$  is a little larger than on  $\alpha\text{-Fe}_2\text{O}_3$ .

A noteworthy trend is observed in the enthalpy change for adsorption of stearic acid onto FeS, i.e. the enthalpy change decreases rapidly with concentration. This trend is the opposite of that with  $\text{Fe}_3\text{O}_4$ . This result suggested the existence of a small amount of material highly reactive with stearic acid, on the surface. At low concentrations the majority of stearic acid adsorbed on this reactive

material, however this amount of such highly reactive material was not enough to adsorb much stearic acid at high concentration. It may be this reactive material that is rapidly oxidised, as described in Chapter 2, resulting in an observed marked drop in heat of adsorption.

As described above, it has been suggested that the variation of enthalpy change of adsorption with concentration depends on both the lateral interaction and the heterogeneity on surface of adsorbent. The differential enthalpy change of adsorption by concentration can take concrete form of this concept.

The results in Figures 3.4 and 3.5 were cumulative, so that heats of adsorption at higher coverages were averages of the heats of all the sites covered. Differential heats of adsorption give the heat of adsorption on each set of sites progressively occupied as adsorption proceeds. They can be calculated from the results of cumulative enthalpy change (Figures 3.4 and 3.5) and the adsorption isotherm (Figure 3.3). Because of errors arising in their computation, differential enthalpy changes are not accurate enough at low coverages of adsorbed films. An interesting result has been obtained in the differential enthalpy change of stearic acid (Figure 3.6). The figure shows the rapid increase of differential enthalpy change of stearic acid on  $\gamma\text{-Fe}_2\text{O}_3$  at the coverage 0.6~0.7 of a monolayer. This suggests the lateral interaction of adsorbed molecules at high coverages.

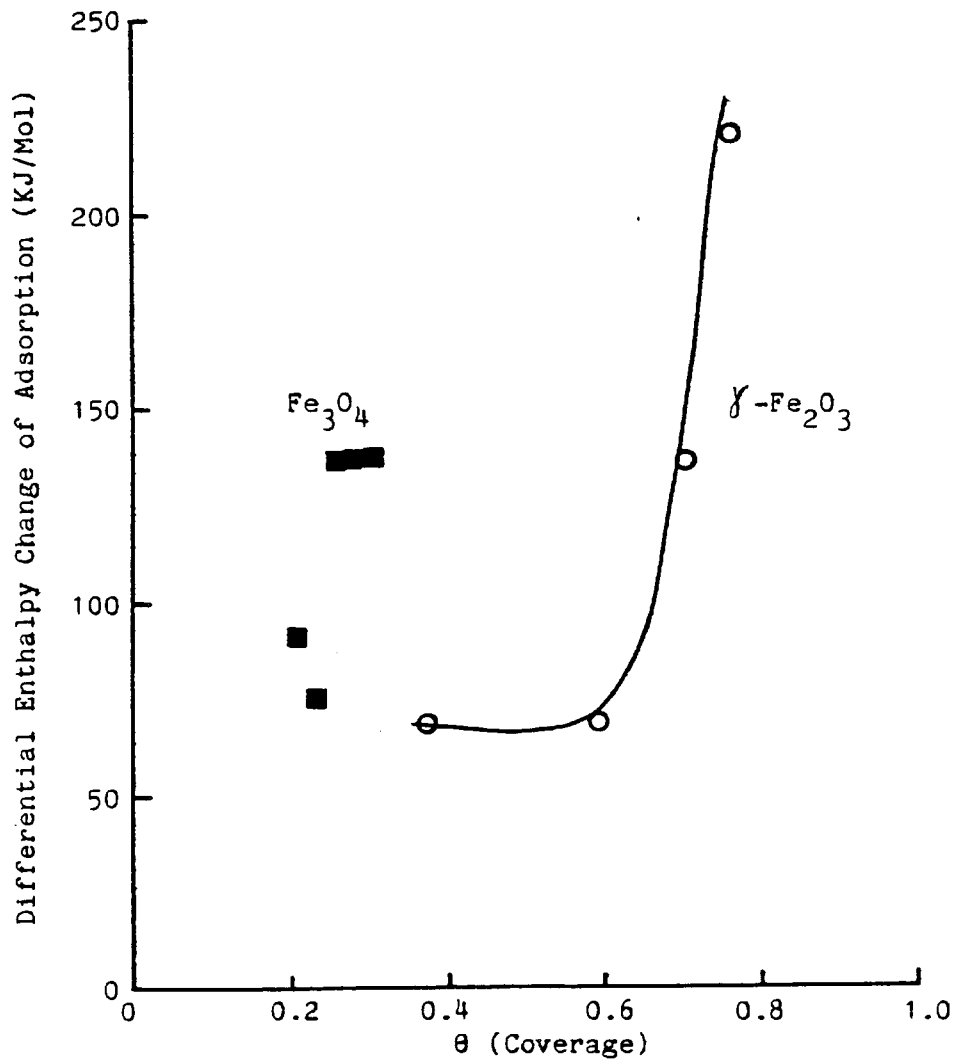


Fig.3-6, Differential enthalpy change of adsorption vs coverage of stearic acid

### 3.42 Thermodynamic Aspect of Adsorption

In the previous section, the enthalpy change of adsorption per molecule was estimated. This enthalpy change is considered to be a good parameter for expressing strength of adsorption of an adsorbate onto the solid surface. Therefore, this parameter can be used to discuss the stability of adsorbed layer under boundary lubrication. However, it is useful to investigate the other thermodynamic variables (free energy, entropy, etc) of adsorption also, in order to understand the relationships between the adsorption phenomena and boundary lubrication.

Frewing (87) obtained the enthalpy change of adsorption from the equation derived from a Van't Hoff equation and assumed that the transition from smooth sliding to stick-slip occurs when the surface concentration of the adsorbed and oriented film decreases to a definite value. Many authors have used this theory based on the Van't Hoff equation. He argued as follows: The original form of Van't Hoff equation is the the Gibbs-Helmholtz equation.

$$\left(\frac{\partial(\Delta G/T)}{\partial T}\right)_p = \frac{-\Delta H}{T^2} \quad (3.2)$$

As this equation assumes constant pressure, it is impossible to apply it to the equilibrium condition of the contact area where pressure changes. If the adsorption equilibrium of a surface in contact with bulk lubricant oil is considered, this equation can be applied precisely. In Equation (3.2), the concentration in the bulk phase is used. The Van't Hoff

isochore is derived from the Gibbs-Helmholtz equation by the assumption of constant pressure.

$$\frac{d \ln K}{dT} = - \frac{\Delta H}{RT^2} \quad (3.3)$$

where

$\Delta H$  : enthalpy change of adsorption

$K$  : equilibrium constant

Assuming that  $\Delta H$  is independent of  $T$ , the equation can be integrated

$$\ln K = \frac{\Delta H}{RT} + \text{constant} \quad (3.4)$$

Here, assuming the Langmuir type adsorption for equilibrium to be constant and that the coverage limit of adsorbed film for smooth sliding, (which is mentioned above), is  $\theta$  at  $T_t$

$$\ln \frac{\theta}{C(1 - \theta)} = \frac{\Delta H}{RT_t} + \text{const.} \quad (3.5)$$

whence

$$2.3 \log_{10} C = - \frac{\Delta H}{RT_t} + \text{const.} \quad (3.6)$$

where

$T_t$  : value of the transition temperature

$C$  : concentration

From the slope of a straight line obtained on plotting  $\log_{10} C$  against  $1/T_t$ , the enthalpy change of adsorption can be obtained. From this equation and the results of friction tests, the



following enthalpy changes of adsorption onto mild steel were obtained.

Stearic acid        54.5KJ/Mol

Methyl stearate    36.0KJ/Mol

As the test pieces used by Frewing were mild steel, the surfaces were covered by an oxide film. Therefore as the enthalpy change of adsorption is related to the interaction between iron oxide and adsorbate, it is possible to compare the enthalpy change here with heat of adsorption obtained in this study, which is shown in Table 3.1. These results are reasonable if the  $\alpha$ -Fe<sub>2</sub>O<sub>3</sub>,  $\gamma$ -Fe<sub>2</sub>O<sub>3</sub>, Fe<sub>3</sub>O<sub>4</sub> and other type of iron oxide cover the surface of the test piece.

On the other hand, Spikes and Cameron (89) (90) obtained enthalpy changes of adsorption of n-octadecylamine on stainless steel, using the data of adsorption isotherms. They used the following equation which used bulk concentration instead of the equilibrium constant in the Van't Hoff equation.

$$\left[ \frac{d(\ln c)}{d(1/T)} \right]_p = \frac{\Delta H}{R} \quad (3.7)$$

where

$\Gamma$  : adsorption density

They proposed three regions of adsorption which had enthalpy changes. (1) 21KJ/Mol at low temperature and low coverages, (2) a high value increasing to 100KJ/Mol at high coverage, and (3) 33 to 55KJ/Mol above 35°C. These results were interesting because the enthalpy change of adsorption is dependent on temperature and adsorption density. The dependence of enthalpy change of adsorption on adsorption density

was also observed here. Daniel (71) noted similar increases for octadecanoic acid adsorption on nickel. However, it is not easy to identify its cause, though Spikes and Cameron tried to explain it by lateral forces.

Similar values of enthalpy changes have been reported by other authors. Frewing (87) and Daniel (71) obtained enthalpy changes of adsorption of fatty acid. In this case, they considered the heat of dimerization because normally fatty acids exist in solution as dimers. They used 29KJ/Mol for heat of dimerization of stearic acid as a result of hydrogen bonding. Therefore a heat of dimerization of 29KJ/Mol must be borne in mind to compare results obtained in this study with their data directly. If adsorption of stearic acid were a chemical one and it made metal soap, it is natural to consider heat of dimerization because the adsorbed molecule exists as a salt of carbonic acid. However, in the case of physical adsorption, it is possible to adsorb on surface as a dimer, it is not necessary to discuss the effect of dissociation heat of dimer on enthalpy change of adsorption.

It is impossible to estimate the degree of dissociation of fatty acid dimer, even if such dissociation occurs. As discussed in Section 2.44, the adsorption of stearic acid on  $\alpha\text{-Fe}_2\text{O}_3$  should be considered physical owing to reversibility of the heat of adsorption. The heat of adsorption of stearic acid on  $\alpha\text{-Fe}_2\text{O}_3$  is about 25KJ/Mol as shown in Table 3.1. This value is too low to consider dissociation of dimer which has about 29KJ/Mol bonding energy. Therefore this result confirms that stearic acid can exist as a dimer

when physical adsorption occurs.

On the other hand, the adsorption of stearic acid on  $\gamma\text{-Fe}_2\text{O}_3$  and  $\text{Fe}_3\text{O}_4$  should be considered as a mixture of physical and chemical adsorption. Therefore the enthalpy change shown in Table 3.1 includes a significant part of the dissociation heat of dimer. The author estimates the degree of chemical adsorption of stearic acid on  $\gamma\text{-Fe}_2\text{O}_3$  and  $\text{Fe}_3\text{O}_4$  from the results reversibility, in which the ratio of chemical adsorption of  $\gamma\text{-Fe}_2\text{O}_3$  and  $\text{Fe}_3\text{O}_4$  were 25% and 88% respectively. Assuming that chemically adsorbed stearic acid is monomeric and that stearic acid is adsorbed physically as dimer, a correction of enthalpy change in Table 3.1 can be done by putting heat of dimerization as 29KJ/Mol. The corrected values for  $\gamma\text{-Fe}_2\text{O}_3$  and  $\text{Fe}_3\text{O}_4$  are 7 , 26 KJ/Mol respectively. Therefore the estimated value of enthalpy change for  $\gamma\text{-Fe}_2\text{O}_3$  is 80-87KJ/Mol and that for  $\text{Fe}_3\text{O}_4$  is 98-112KJ/Mol.

In this study, adsorption isotherms were obtained as shown in Figure 3.3. A method to derive free energy change from an adsorption isotherm was described by Spikes (90) and Daniel (71). According to a fundamental thermodynamic equation, free energy change  $\Delta G$  is

$$\Delta G = - RT \ln K \quad (3.8)$$

Therefore, as an exact value of equilibrium constant K is obtainable, free energy change of adsorption can be calculated. However, it is not easy to get an equilibrium constant of adsorption in solution, because the treatment of adsorption from solution involves a satisfactory treatment of the solution

itself as well as that of the interfacial phenomenon of adsorption.

Spikes (90) used a perfect adsorption system by Everett (120) to obtain a rough estimate of the free energy change of adsorption. In this model, a preferential adsorption of molecules from a perfect binary solution by a Langmuir-type adsorbing surface was assumed, i.e. the following phase exchange reaction was used.



As an ideal mixture is assumed here, it is possible to write the equilibrium constant as follows:

$$K = \frac{X_1^S X_2^L}{X_1^L X_2^S} \quad (3.10)$$

where

K : equilibrium constant of adsorption

$X_1^S$  : concentration of component 1 (solvent) in adsorbed phase (mole fraction)

$X_1^L$  : concentration of component (solvent) in solution (mole fraction)

$X_2^S$  : concentration of component 2 (adsorbate) in adsorbed phase (mole fraction)

$X_2^L$  : concentration of component 2 (adsorbate) in solution (mole fraction)

Everett obtained the following equation:

$$\frac{X_1^l \cdot X_2^l}{(\eta_o \Delta X_1^l / m)} = \frac{1}{n^S} \left( X_1^l + \frac{1}{K - 1} \right) \quad (3.11)$$

where

$n^S$  : the total adsorption of component 1 and 2  
per gram of solid

$\eta_o \Delta X_1^l / m$  : the apparent adsorption of component 1 per  
gram of solid

The precise derivation of this equation has been described elsewhere by Everett (120) and Spikes (90). Thus  $n^S$  and  $K_1$ , can be calculated from the slope and intercept of a linear plot. From the equilibrium constant  $K$ , the free energy changes of adsorption  $\Delta G$  can be calculated using Equation (3.8).

The application of the equilibrium equation is limited to a reversible process. Only adsorption isotherms of both stearic acid and methyl stearate onto  $\alpha\text{-Fe}_2\text{O}_3$  in this study were reversible. As other adsorption isotherms included some part of an irreversible process, it was therefore impossible to obtain the free energy change of these adsorptions. Equation (3.11) is applied in Figure 3.7 using three adsorption isotherms described above, which were taken from Figure 3.3. Figure 3.7 showed straight line plots almost to zero concentration, which indicated that assumptions for the model alone were correct and that adsorption isotherms used for this analysis were Langmuir-type isotherms. From Figure 3.7 and Equations (3.8) and (3.11) the free energy change  $\Delta G$  and equilibrium constant  $K$  were obtained as follows:

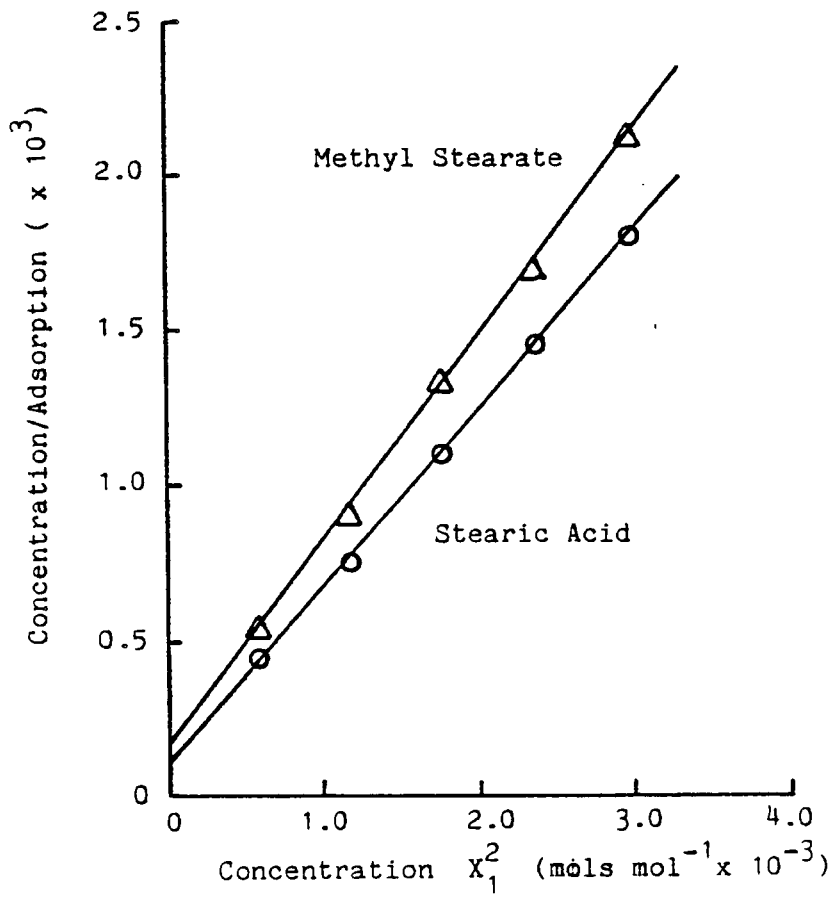


Fig.3-7, Concentration/Adsorption plotted against concentration  
Adsorbent  $\alpha$ -Fe<sub>2</sub>O<sub>3</sub>

| <u>Adsorption</u>                                | <u>Equilibrium Constant K</u> | <u>Free Energy Change <math>\Delta G</math> (KJ/Mol)</u> |
|--|-------------------------------|--|
| $\alpha\text{-Fe}_2\text{O}_3$ - Stearic Acid    | $5.7 \times 10^6$             | 39   |
| $\alpha\text{-Fe}_2\text{O}_3$ - Methyl Stearate | $3.9 \times 10^6$             | 38   |

The free energy changes obtained here were different from the free energy change of adsorbate and that of solvent n-heptane, according to the assumption of equilibrium constant in Equation (3.9). As n-heptane used here as a solvent can absorb physically on the adsorbent with a small free energy change, the absolute free energy changes of adsorption, which are measured in an inert solvent, are a little higher than the values estimated above. Normally it is said that physical adsorption has 8-40KJ/Mol free energy. Therefore, the values obtained here are very high if they are assumed physical adsorption.

In Section 3.41, the enthalpy changes of adsorption per one mole were calculated, they were shown in Table 3.1. Combining these results and the estimate of free energy change discussed above, it is possible to calculate entropy change of adsorption  $\Delta S$  from the following equation.

$$\Delta G = \Delta H - T\Delta S \quad (3.12)$$

$\Delta S$  for adsorption of stearic acid and methyl stearate onto  $\alpha\text{Fe}_2\text{O}_3$  is 42-48J.deg $^\circ\text{C.mol}^{-1}$ , 79-92J.deg $^\circ\text{C.mol}^{-1}$  respectively. Cameron (93) estimated  $\Delta S$  of adsorption of fatty acid 94-134J/mole deg C from results of friction tests. There are differences between both results. However, there is the effect of solvent on entropy change to be considered as

Cameron has reported in chain matching phenomena in lubrication. In order to compare both results, it is necessary to investigate the effect of solvent.

### 3.43 Structure of Adsorbed Film

It is not easy to investigate structure of adsorbed films in situ at a contact point under lubrication. However, many authors have reported studies of organic compounds in equilibrium conditions by X-ray diffraction, electron-diffraction (65) (73) (74) and contact angle measurement (121) (122). It has been stated that the structure of the film is dependent on the type of polar organic compound, equilibrium concentration of solution and temperature. In this study, adsorption isotherms and heats of adsorption of stearic acid, stearyl alcohol and methyl stearate onto iron oxide were obtained. From these results, the nature of adsorption of these long chain compounds is deduced.

It is well known that a long chain alcohol in benzene adsorbs on metal diagonally at low concentrations and adsorbs vertically at high concentration (71). In the results of heats of adsorption in this study, the increase of heat release which was considered to be in accordance with this result was seen in the adsorption of stearyl alcohol onto  $\alpha$ -Fe<sub>2</sub>O<sub>3</sub> and  $\gamma$ -Fe<sub>2</sub>O<sub>3</sub>, but was not onto Fe<sub>3</sub>O<sub>4</sub>. (Figures 2.9, 2.10 and 2.11). As discussed in Section 2.44, the author has proposed that the adsorption of stearyl alcohol occurs by an interaction between hydrogen atom of hydro radical and oxygen iron ( $O^{2-}$ ) of iron oxide. This interaction was



to be a physical adsorption and the surfaces of  $\alpha\text{-Fe}_2\text{O}_3$  and  $\gamma\text{-Fe}_2\text{O}_3$  were assumed to be homogeneous for adsorption of stearyl alcohol as this process was 100% reversible as described in Section 2.43. For an adsorption like this, it is therefore possible to ascribe the cause of secondary increase of heat of adsorption described above, as due to the change of angle of the adsorbed molecule.

Assuming  $20.5\text{\AA}^2$  as the cross-sectional area per adsorbed stearyl alcohol molecule and  $23.8\text{\AA}$  as the length of each molecule, the area occupied by a molecule adsorbed almost horizontally is about  $122\text{\AA}^2$ . This value is about six times as much as that of a vertically adsorbed molecule. In the results illustrated in Figures 2.9 and 2.10, comparing the height of plateau after primary increase with that after secondary increase, there is about six-fold difference. This value is near the ratio of the cross-sectional area of vertically adsorbed molecules and that of almost horizontally adsorbed molecules. This indicates that the stearyl alcohol molecule adsorbs on  $\alpha\text{-Fe}_2\text{O}_3$  or  $\gamma\text{-Fe}_2\text{O}_3$  surface almost horizontally at the condition of the plateau between primary and secondary increase of heat of adsorption. Assuming a monolayer at the condition of vertical adsorption, this plateau is at about one sixth monolayer.

The establishment of monolayer described above, is influenced by temperature, solvent and adsorbent. Inspection of Figures 2.13 and 2.15 show that the monolayer is attainable only at low temperatures below  $45^\circ\text{C}$  when n-heptane is used as a solvent. On the other hand, as seen in Figure 2.21, the monolayer is obtained at low concentrations of adsorbate when

a solvent of large molecules is used. This solvent effect may be related to the phenomena of chain matching discussed by many authors (92) (93) (123) (124) (125), although more data is necessary to state this concretely.

Summarising the structure of adsorbed layers of stearyl alcohol, the monolayer, which is the state of vertical adsorption, can be obtainable under limited conditions such as low temperature and high concentration of adsorbate. In most cases, stearyl alcohol adsorbs almost horizontally and the density of adsorbed molecule is about one sixth of that of the monolayer.

It is reported that stearic acid adsorbs on metal or metal oxide almost vertically at first adsorption. However, at more advanced adsorption, the molecule inclines slightly and forms a simple rhombic structure (73) (74). In this case the structure is not continuous but consists of islands of  $10^2-10^3 \text{ \AA}$ .

In this study, only  $\gamma\text{-Fe}_2\text{O}_3$  produced a high density adsorbed film as shown in Figure 3.2. Assuming  $20.5 \text{ \AA}^2$  for the cross-section of the adsorbed acid in the similar way to stearyl alcohol,  $8.1 \times 10^{-6}$  mole of stearic acid can adsorb on a solid of  $1 \text{ m}^2$  as a monolayer (72). On the basis of this calculation, even the adsorption onto  $\alpha\text{-Fe}_2\text{O}_3$  cannot achieve a monolayer. The adsorption isotherm of stearic acid onto  $\alpha\text{-Fe}_2\text{O}_3$  has a saturation at about  $1.5 \times 10^{-6} \text{ Mol/m}^2$ . This is about 0.2 of a monolayer. As for  $\text{Fe}_3\text{O}_4$ , that is 0.2 to 0.3 of a monolayer. Many authors have suggested the existence of mixed films of adsorbate and solvent molecules (25) (68) (69) (122). From an experiment of adsorption

of stearic acid in n-hexadecane, Cook (68) (69) reported that 0.2 to 0.3 of a monolayer of stearic acid was adsorbed within a few minutes after contact between adsorbent and solution. This confirms the results of adsorption onto  $\alpha\text{-Fe}_2\text{O}_3$  and  $\text{Fe}_3\text{O}_4$ .

The author suggests the existence of mixed film of stearic acid and n-heptane in the adsorption onto  $\alpha\text{-Fe}_2\text{O}_3$  and  $\text{Fe}_3\text{O}_4$ . However, the adsorption of stearic acid onto  $\text{Fe}_3\text{O}_4$  increases steadily as shown in Figure 3.2(c). This is due to chemical adsorption of stearic acid. After enough chemical adsorption the film is considered to approach a monolayer.

### 3.50 Conclusions

The following conclusions may be drawn from the results of the adsorption experiments.

(1) For adsorption of stearic acid and methyl stearate onto iron oxides and iron (II) sulphide. For all systems except stearic acid on  $\text{Fe}_3\text{O}_4$  equilibrium was reached within two hours.

(2) At room temperature the order of levels of adsorption at saturation are given by,

Stearic acid  $\gamma\text{-Fe}_2\text{O}_3 \gg \text{Fe}_3\text{O}_4 > \alpha\text{-Fe}_2\text{O}_3 \geq \text{FeS}$

Methyl stearate  $\alpha\text{-Fe}_2\text{O}_3 \sim \gamma\text{-Fe}_2\text{O}_3 > \text{Fe}_3\text{O}_4 > \text{FeS}$

(3) The coverage of stearic acid adsorbed film on  $\gamma\text{-Fe}_2\text{O}_3$  increases up to a complete monolayer at high concentration. However on  $\alpha\text{-Fe}_2\text{O}_3$ ,  $\text{Fe}_3\text{O}_4$  and FeS, only 0.2 to 0.3 of a monolayer is achieved even at high concentration.

(4) The coverage of adsorbed film of methyl stearate on all

adsorbent tested at room temperature is below 0.2 of a monolayer.

- (5) The values of cumulative enthalpy change were calculated. The values for stearic acid and methyl stearate on  $\alpha\text{-Fe}_2\text{O}_3$  are almost constant at low levels (below 25KJ/Mol). The values on  $\gamma\text{-Fe}_2\text{O}_3$  are higher (above 70KJ/Mol). For  $\text{Fe}_3\text{O}_4$ , the value of stearic acid is high (75-85KJ/Mol), whereas that of methyl stearate is low (about 20KJ/Mol). The cumulative enthalpy change of stearic acid onto FeS is very high and decreases with concentration of stearic acid.
- (6) The results of adsorption isotherms supports the mechanism of adsorption which is proposed in Chapter 2.

CHAPTER FOUR  
FRICITION AND WEAR

4.10 Introduction

In Chapters 2 and 3, extensive data on adsorption of oiliness reagents was obtained. This chapter describes friction and wear experiments using the same chemical systems as in Chapter 2 and 3 to investigate the relationship between adsorption and friction and wear. The main purpose of this work was to study the effects of interaction between oiliness agents and EP films.

Slow speed friction tests with a Bowden Leben machine were used. The merits of this slow speed test are (i) simplicity of the system and (ii) low frictional heating and thus minimal disturbance of the adsorption equilibrium on the surface of rubbing. An EN31 steel ball bearing and a mild steel flat were used as test pieces. For some specimens, the surface of the mild steel was covered with an EP film formed by reaction with DBDS in n-dodecane at 216°C.

These tests determined:

- (i) the coefficient of friction on each of ten successive traverse during running-in,
- (ii) the wear track width on a flat test piece after ten traverses.

## 4.20 Experimental

### 4.21 Materials

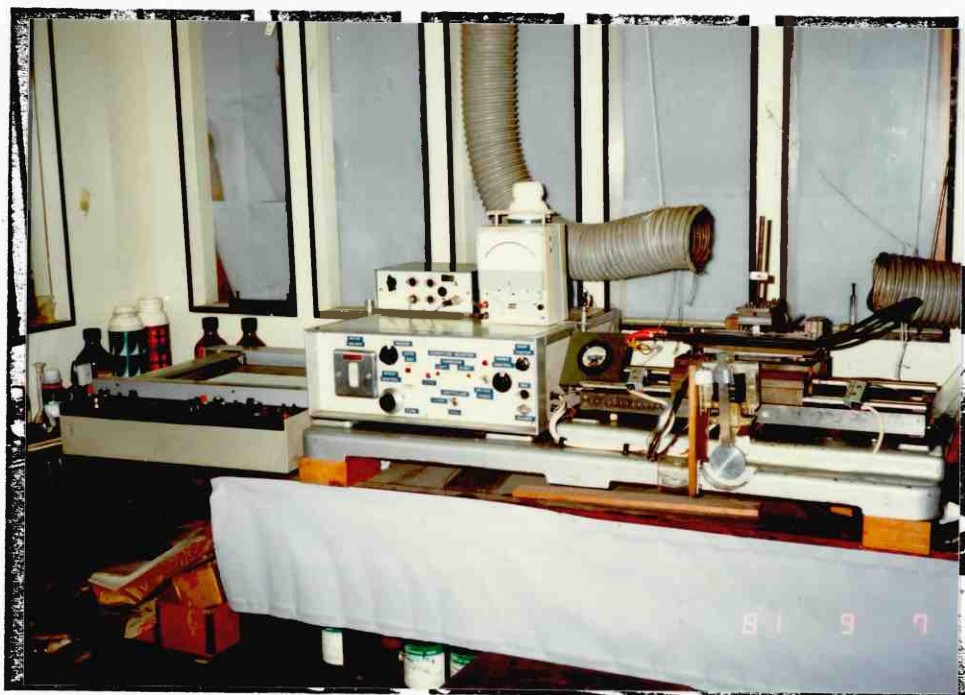
DBDS of purity described in Section 2.21 was used to form reaction films with iron on the mild steel test pieces (See Section 4.23). The oiliness reagents used in these experiments were stearic acid, stearyl alcohol and methyl stearate. The purification method and the analytical results of these additives were described in Section 2.31. n-Hexadecane purified, by the technique described in Section 2.21 was used as a base oil in these experiments.

### 4.22 Apparatus

In this experiment, a modified Bowden Leben machine was used to investigate the friction coefficient and wear during running-in. The details of this machine are in reference (126). A general view of the apparatus is shown in photograph 4.1. It consists of four basic parts;

- (1) Horizontal carriage and drive system,
- (2) Control system and heater,
- (3) Loading arm and lifting mechanism,
- (4) Recording unit.

(1) Carriage and drive system: The carriage is designed to move on two stainless steel rails by means of a lead screw connected to a special DC motor and a tachogenerator via a gearbox. The traverse speed of the carriage is variable between about  $10\text{mm}\cdot\text{s}^{-1}$  and  $0.025\text{mm}\cdot\text{s}^{-1}$ . In this



Photograph 4-1, View of a Bowden Leben Machine

experiment, all the measurements were carried out at a constant speed of  $0.87\text{mm}\cdot\text{s}^{-1}$ .

(2) Control system and heater: The direction of travel of the carriage is controlled by two heavy duty relays, which switch the motor and tachogenerator windings. These relays can also operate other circuits such as a variable resistor in the speed controller, which enables different speeds to be used for the two directions of travel. The relays can be triggered by micro-switches mounted on one of the rails which senses the position of the carriage.

In this experiment, the position of the micro-switches was adjusted to provide 40mm track length, and the traverse speed for traction direction and reverse direction were set to  $0.87\text{mm}\cdot\text{s}^{-1}$  and  $10\text{mm}\cdot\text{s}^{-1}$  respectively. In addition, a few seconds were needed to lift and lower the loading arm. Therefore the out-of-contact time in this experiment was 44-45 seconds.

A stainless steel trough is fixed onto the carriage described above. Around the trough a tubular electric heater is clamped. The input from the control unit enables a wide range of heating rates to be obtained. All of the experiments in this work were carried out at a constant temperature of  $25 \pm 0.5^\circ\text{C}$ , controlled manually, to measured on the surface of lower test piece by a copper/constantan thermocouple.

(3) Loading arm and lifting mechanism: Friction was measured by a set of strain gauges, mounted on the cantilever, which were wired as a Wheatstone bridge and connected to a purpose-built regulated power supply of about 6.2V.



This machine is equipped with a special arrangement for automatically lifting and gently lowering the arm, as described in reference (126). However, this action was considered to be too fierce for the mild steel specimen used, therefore the lifting and lowering of the arm was done by hand. Loading was controlled by weights on the loading arm, i.e. four loads, 0.63, 1.63, 2.63 and 4.63kg respectively.

(4) Recording unit: A X-Y recorder was used to record the friction force signal from the strain gauge. The X axis of the recorder was set to time.

#### 4.23 Preparation of Test Piece

EN31 steel ball bearings (1/4 inch) were used as an upper testpiece in all the experiments. These balls were already polished and required no further mechanical preparation.

The flat lower test pieces of length 55mm were cut from a commercially available mild steel bar. The upper and lower faces were then precision ground to a very fine finish resulting in specimens about 5mm thick. The upper surfaces of the specimens were further polished with emery paper in water. At first, a 350A paper was used and then the surface was polished in the direction of sliding with a 600 paper. Surface roughness of the test piece was not measured.

From the polished specimens, eight kinds of test piece were prepared by a reaction with DBDS at 216°C and

acid immersion into  $0.01\text{N-H}_2\text{SO}_4$ . The purpose of this process is the formation of EP film and then the removal of the sulphides from the film. The formation of EP films by a reaction with DBDS was carried out by refluxing a  $0.05\text{Mol/l}$  solution of DBDS in n-dodecane. This reaction condition was selected by consideration of reactivity of DBDS, i.e. this additive can produce EP film at the temperature over  $150^\circ\text{C}$  (6) but starts thermal decomposition at  $230^\circ\text{C}$  (12). Three reaction times, 1, 2 and 3 hours, were adopted to prepare test pieces with EP films of three different thicknesses.

Although the EP film produced by the reaction in this way is not always the same as that formed on lubricated surface by frictional heat, sulphides, oxides and sulphates are included in the film. The main purpose of this study is the investigation of the effect of interaction between EP film and oiliness reagents on friction and wear in boundary lubrication, in particular, the interaction between sulphides and oiliness reagents. Therefore the influence of removal of sulphide from the EP film was investigated. As sulphides are easily solved by a dilute acid,  $0.01\text{N-H}_2\text{SO}_4$  was used for this purpose, i.e. the selective removal of sulphides from the EP film produced by DBDS. The immersion time of test piece in the acid was fixed at 15 minutes. After 15 minutes of immersion, a dark brown thin film appeared on the surface. This film was removed by a tissue and then the test piece was washed with distilled water. Before use, a further washing in a soxhlett was carried out in the same way as the other test pieces. Consequently, the

following eight kinds of test piece were prepared.

| <u>Test Piece</u> | <u>Reaction with DBDS</u> | <u>Acid Immersion</u> |
|-------------------|---------------------------|-----------------------|
| A                 | 0 hours                   | 0 minutes             |
| B                 | 0 "                       | 15 "                  |
| C                 | 1 "                       | 0 "                   |
| D                 | 1 "                       | 15 "                  |
| E                 | 2 "                       | 0 "                   |
| F                 | 2 "                       | 15 "                  |
| G                 | 3 "                       | 0 "                   |
| H                 | 3 "                       | 15 "                  |

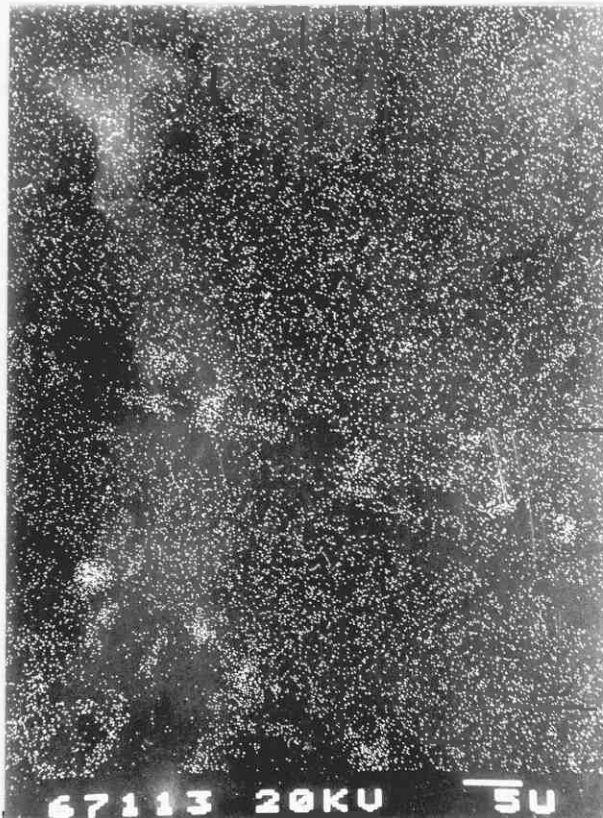
The sulphur concentration on the surfaces of those test pieces were measured by an energy dispersive X-ray fluorescence technique (EDXRF). The results are shown in Figure 4.1, in which the strength of sulphur X-ray ( $S_{K\alpha}$ :cps) from a circle area of 15mm $\phi$  of each specimen is shown. Inspections of the results show that the reaction with DBDS form sulphur compounds on the surface and the acid immersion process reduced the sulphur content in the EP film. In order to investigate the distribution of sulphur compounds on the surface, the image of sulphur X-ray are also measured (Photograph 4.2).

#### 4.24 Preparation of Test Lubricant

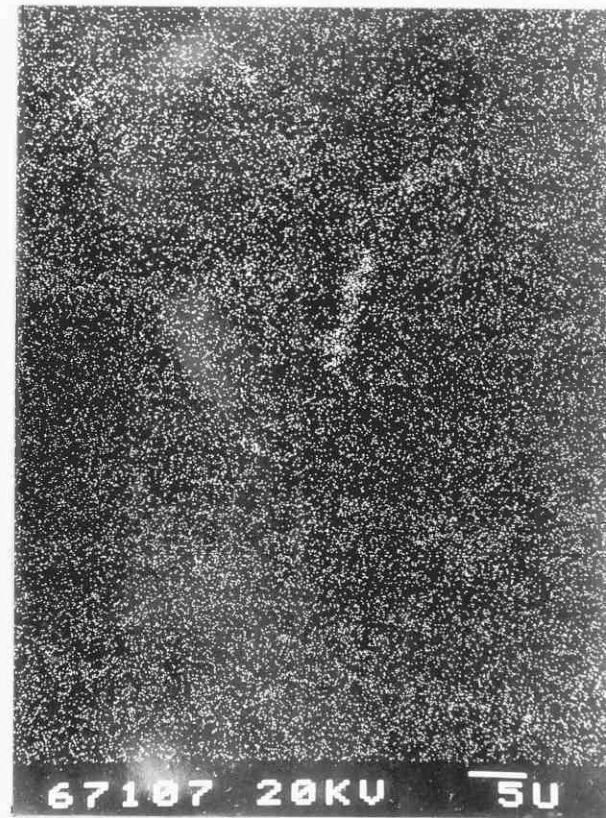
All of the experiments used n-hexadecane ( $C_{16}H_{34}$ ), which was purified by the method described in Section 2.21, as a base oil. From preliminary experiments, it was found that stearic acid was more effective in reducing friction and wear than stearyl alcohol and methyl



(a)  
Test Piece : 1 hr Reaction

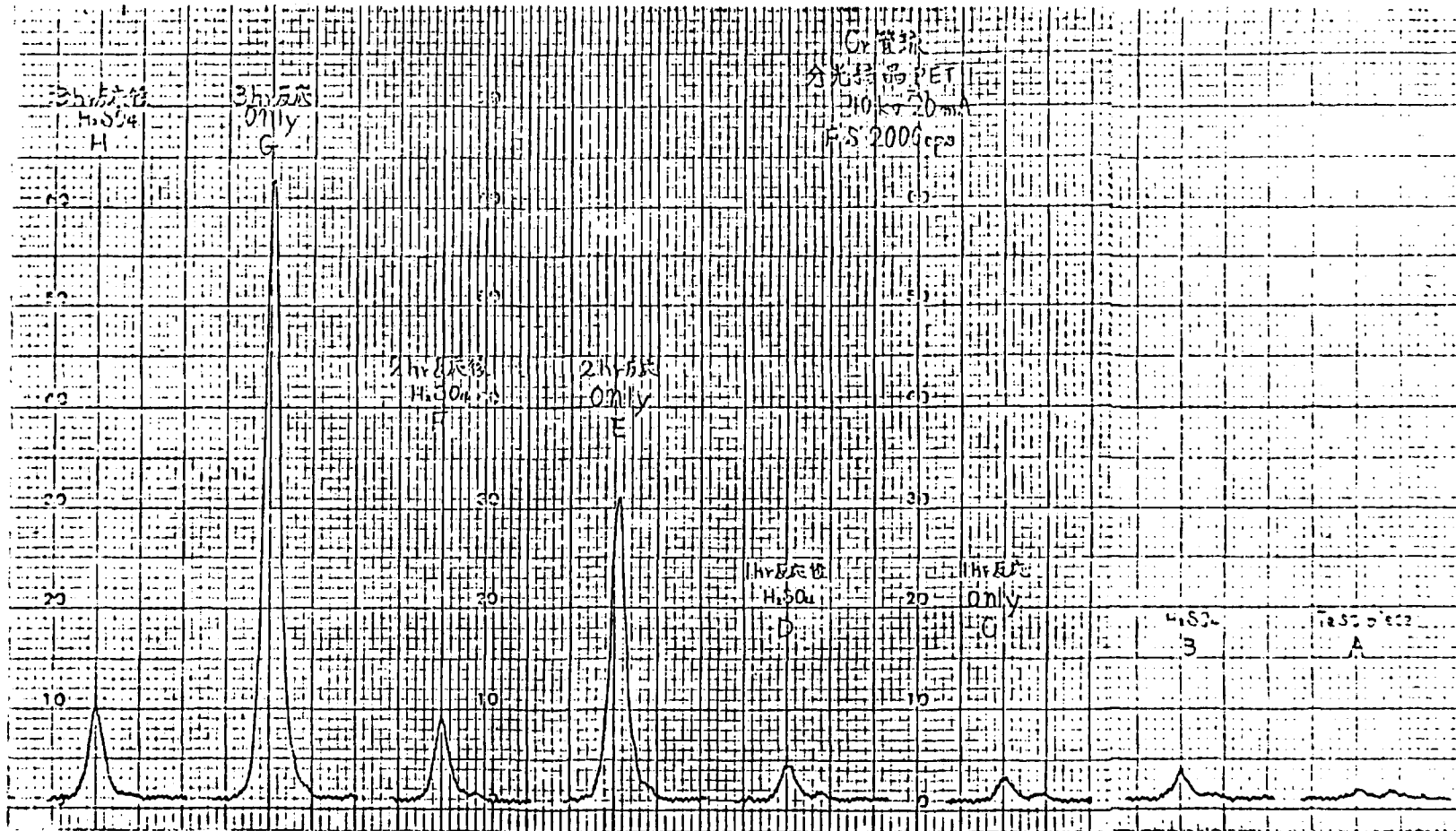


(b)  
Test Piece : 2 hrs Reaction



(c)  
Test Piece : 3 hrs Reaction

Photograph, 4-2, X-ray microanalysis of test pieces treated with DBDS reaction at 216 C



|   |     |      |     |     |    |    |    |     |
|---|-----|------|-----|-----|----|----|----|-----|
| Test Piece                              | H   | G    | F   | E   | D  | C  | B  | A   |
| (Reaction Time, hrs)                    | 3   | 3    | 2   | 2   | 1  | 1  | 0  | 0   |
| (Acid Immersion, min.)                  | 15  | 0    | 15  | 0   | 15 | 0  | 15 | 0   |
| Sulphur Content<br>( $S_{k\alpha}$ cps) | 200 | 1240 | 160 | 600 | 70 | 50 | 60 | nil |

Fig.4-1, Analytical results of sulphur content on the test pieces by EDXRF

stearate, and as the solubility limits of stearic acid in n-hexadecane solution at room temperature was lower than 20mMol/l, the concentrations of oiliness reagents in test lubricants was decided as follows:

| <u>Oiliness Reagent</u> | <u>Concentration (mMol/l)</u> |     |      |      |
|-------------------------|-------------------------------|-----|------|------|
| Stearic Acid            | 0.01                          | 0.1 | 1.0  | 10.0 |
| Stearyl Alcohol         | 1.0                           | 4.0 | 12.0 | 20.0 |
| Methyl Stearate         | 1.0                           | 4.0 | 12.0 | 20.0 |

#### 4.25 Procedure

(i) Cleaning of test piece: The upper and lower test pieces described in Section 4.23 were first washed with acetone in an ultrasonic bath. They were then cleaned by toluene in a soxhlett apparatus for four hours and allowed to dry. Nothing then touched these surfaces until the test pieces were set in the trough.

While washing of the trough, the stainless steel chuck and wedge, which were used to fix the upper and lower test pieces, was also important, as these were in contact with the test lubricant during the test run. First these were rubbed with silicon carbide paper to remove any visible dirt. Then the trough was washed with acetone, and the stainless steel chuck and wedge were cleaned in the same way as the test pieces.

Cleanliness is essential in boundary lubrication experiments as demonstrated by Spikes (96) and many others. It was particularly important to exclude polar impurities in this study, since such compounds could affect the

adsorption of oiliness reagent, which was being investigated.

(ii) Operation of a Bowden Leben Machine: The sliding speed and track length were set as described in Section 4.22. The operation of the Bowden Leben Machine was carried out in the following steps:

- (1) fitting the low flat test piece in the trough
- (2) fitting the upper ball test piece with a stainless steel chuck
- (3) fitting the trough on the carriage
- (4) pouring the test lubricant into the trough (11ml)
- (5) controlling the surface temperature of test piece within  $25 \pm 0.5^{\circ}\text{C}$
- (6) waiting adsorption equilibrium for at least one hour, and setting the zero point of recorder
- (7) putting into operation the friction test for ten traverses
- (8) setting up for the next experiment

As the position of the casrriage could not be adjusted in this machine, after 10th traverse operation, the carriage was moved to expose a new flat test piece surface for the next experiment. On the upper test piece ball a new surface was obtained by revolving the ball in the chuck. As each flat test piece had a width of 20mm, it was possible to carry out the severe friction tests under high load and in lubricants without oiliness reagent, these sliding distances of the carriage was kept long so as to minimise end effects in the rubbing motion. After all the friction tests, the flat test piece was washed with acetone to measure width of wear tracks on the surface.

(iii) Calibration of friction coefficient: The friction force obtained from the strain gauges were calibrated by applying a known force to the loading arm. while it was held free of the carriage. A fixed pulley, cord and several 200g weights were used for this purpose. The resulting calibration curve can be seen in Figure 4.2. There was no hysteresis in this friction force. The base line on the chart recorder, however, drifted during the warming-up of the machine. Therefore several observations of the zero point were necessary for the measurement of the small friction force. The loading force was measured with a weighing machine. The loading by weights were transferred precisely to the contact point.

(iv) Measurement of wear: The width of wear track was measured to investigate the effect of oiliness reagent on wear. A measuring microscope with an accuracy of 0.01mm, was used for this purpose. As the width of wear track was not constant throughout the test, the average value was obtained from the measurements at several points.

#### 4.30 Results

The friction and wear tests were carried out under boundary lubrication conditions using the eight kinds of test pieces with different EP films. It is well known that many parameters can affect on the friction and wear. In this study, the following parameters were kept constant,



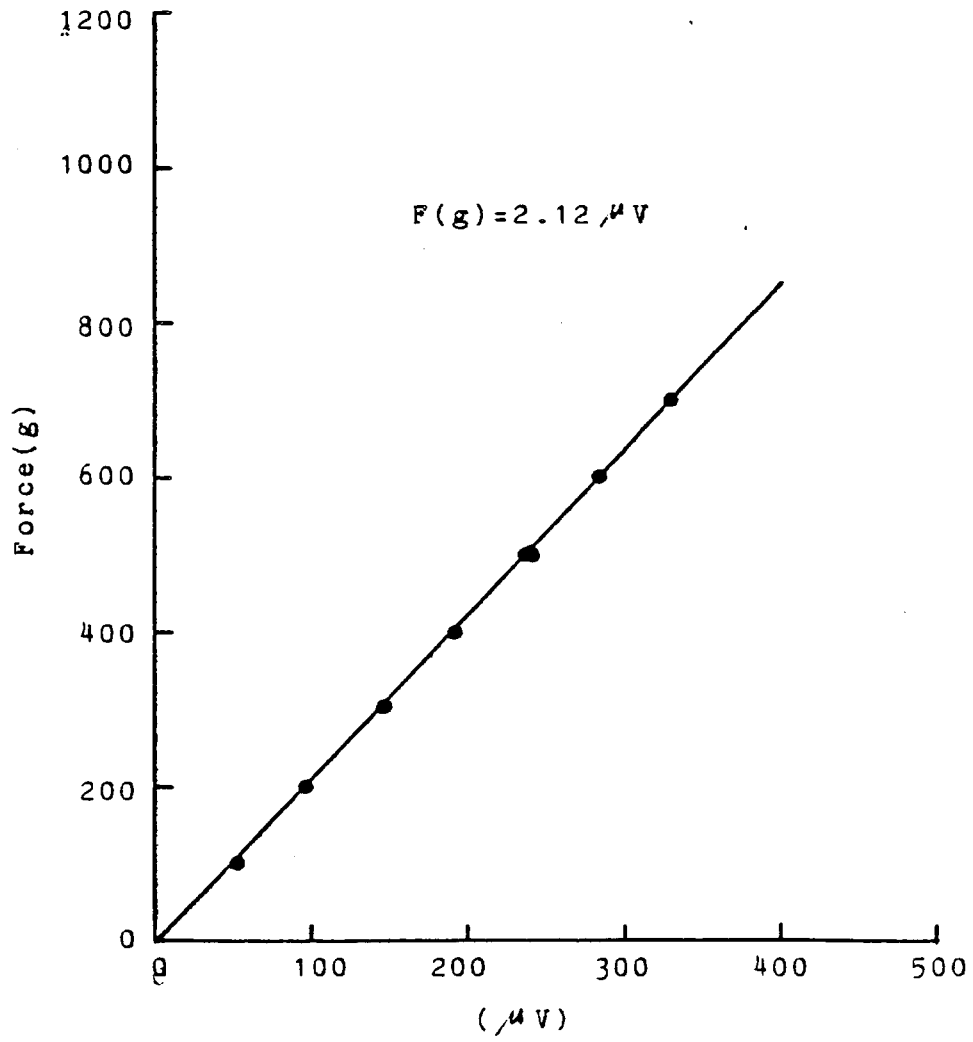


Fig.4-2, Calibration curve for fiction force

Temperature - 25°C  
Sliding speed - 0.87mm/sec  
Base oil - n-hexadecane  
Surface roughness  
.of test piece - same polishing  
Upper test piece - EN31 steel ball bearing (1/4 inch)  
Traverses - 10

The effects of the following variables were investigated,

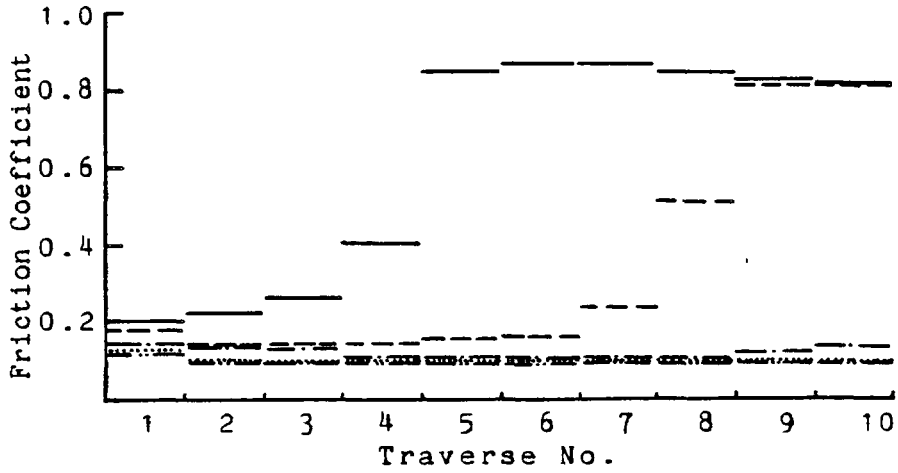
EP films - shown in Section 4.23  
Oiliness reagent - stearic acid  
                                  stearyl alcohol  
                                  methyl stearate  
Load - 0.63, 1.63, 2.63, 4.63kg

A typical result of changing friction coefficient with the number of traverses is illustrated in Figure 4.3. All other data are shown in Appendix B. In these figures, mean values of each traverse are shown. The fluctuation of results on the chart recorder was usually approximately 10%, though on rare occasions it rose to  $\pm 30\%$ .

#### 4.31 Effect of EP Film on Friction Coefficient

Friction coefficient results with n-hexadecane are shown in Figures 4.4 in which the results are first to fifth and tenth traverse are illustrated respectively. In these experiments, the test pieces were reacted with DBDS at 216°C for different times were used. Therefore, the surface of these test pieces is covered with an EP film containing iron sulphides and iron oxides, and the thickness

Test Piece : Original Mild Steel  
Load : 1.63kg



Test Piece : 1 hr Reaction with DBDS  
Load : 1.63kg

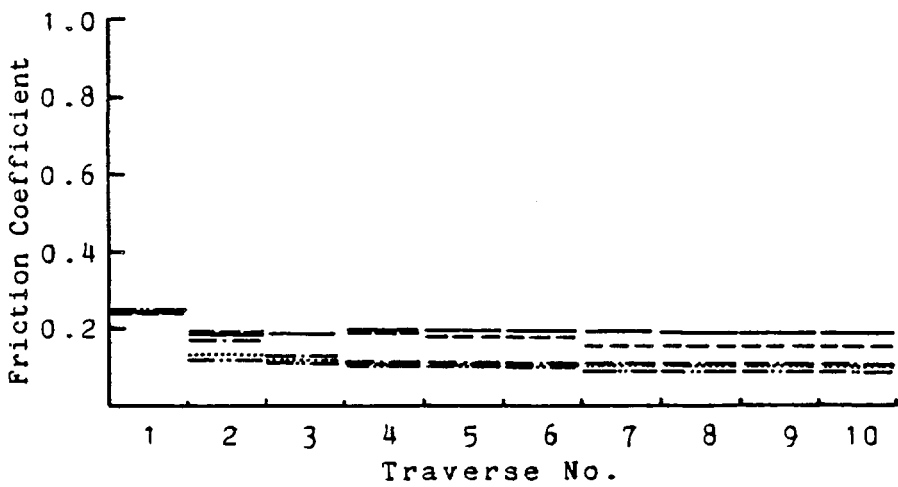


Fig.4-3, Typical change of friction coefficient with Traverse

Stearic Acid in n-Hexadecane  
( m Mol/l )

- 0
- - - 0.01
- · - · 0.1
- · · · 1.0
- · · · 10

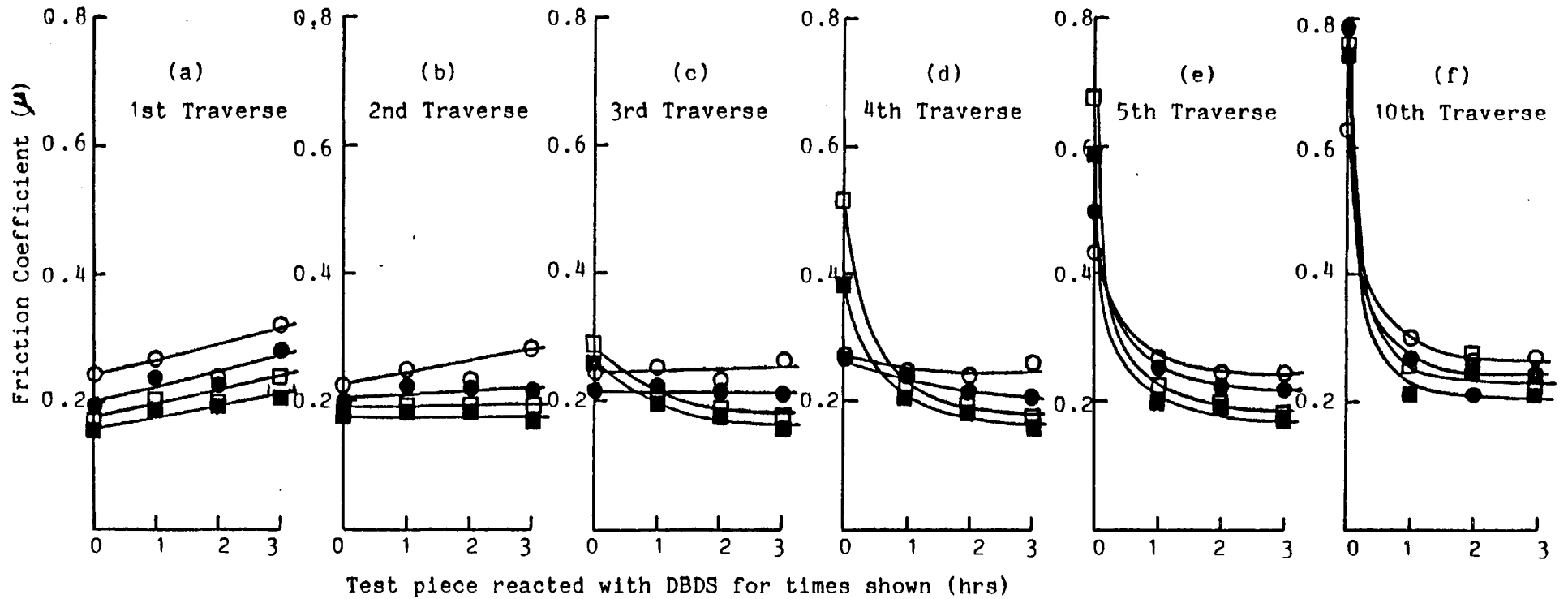


Fig.4-4, Influence of e.p. film formed by the reaction with DBDS on coefficient of friction during running-in  
Load      ○ : 0.63kg, ● : 1.63kg, □ : 2.63kg, ■ : 4.63kg

of the film depends on the reaction time. The experiment was carried out at four stages of loading, 0.63, 1.63, 2.63 and 4.63kg.

The results of the first traverse show that the friction coefficient increases slightly with the EP film and that the trend of this increase is not affected by load. In spite of this the load does have a minor effect on the level of friction coefficient. According to the boundary lubrication theory discussed in Section 1.21, the coefficient of friction in mixed lubrication is expressed as follows,

$$f_{BL} = \frac{F}{W} = \alpha_w \cdot \frac{S_{sol}}{P} + (1 - \alpha_w) \frac{S_{liq}}{P} + f_{plough} \quad (1.7)$$

If there were much contribution of ploughing by  $f_{plough}$  to the friction coefficient at the first traverse, much reduction of the friction coefficient after the second traverse should be recognised. However, as such a trend was not seen in this experiment, the trend of friction coefficient with EP films was not related to the ploughing effect. This trend had no relation to  $W$ , as this depended on loading. Consequently, this trend should be considered to be affected by the change of shear strength of solid surface covered by an EP film. The EP film produced by the reaction with DBDS may slightly increase the shear strength at which solid contact occurred.

The treatment of the test piece with DBDS did not influence the friction coefficient at the second traverse. This may be due to the disappearance of the material, which

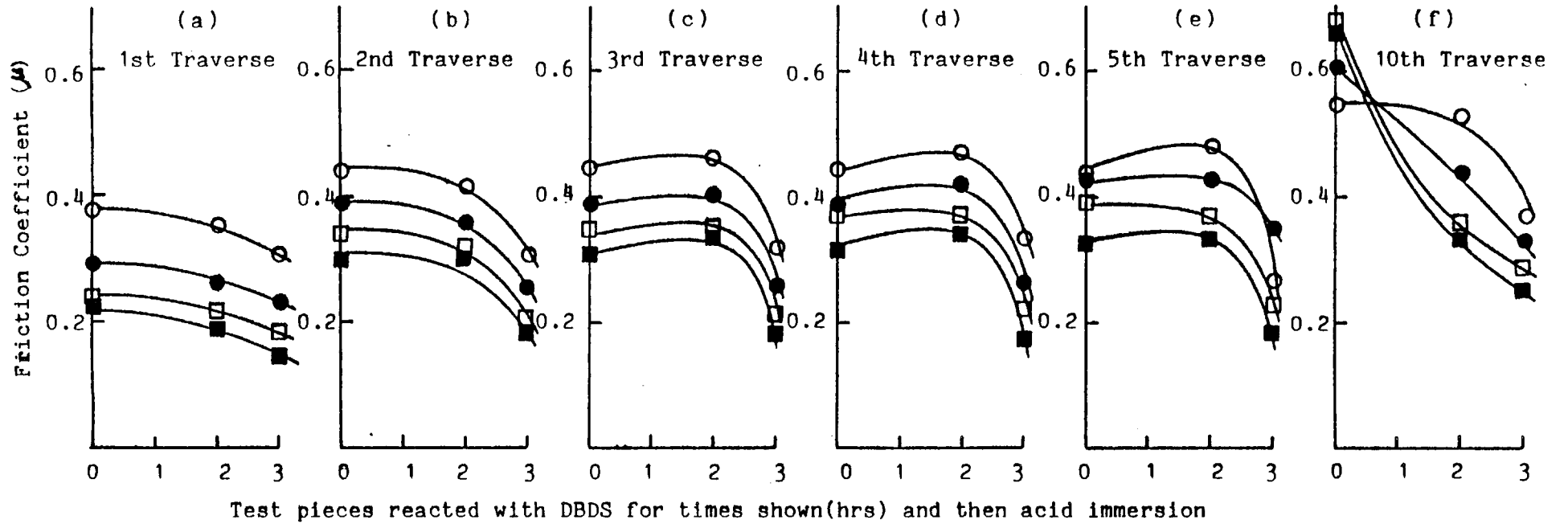


Fig.4-5, Influence of the film formed by the reaction with DBDS and acid immersion on coefficient of friction during running-in

Load      ○ : 0.63kg,   ● : 1.63kg,   □ : 2.63kg,   ■ : 4.63kg

increases the shear strength, by the first traverse. From the third traverse onward a noticeable effect of DBDS became evident. Specimens untreated with DBDS gave increasingly higher friction on the 3rd to 10th traverse, especially at high loads. Treatment with DBDS prevented this friction increase, and the bigger the treatment, the more effective in preventing friction increase. It is probable that untreated surfaces produce a thin oxide, hydrated oxide or other contaminant layer which maintains a low friction even without DBDS treatment for the first two traverses. Treatment with DBDS produces a film slightly less effective at reducing friction initially. However, this film appears capable of maintaining low friction beyond the first two traverses. Therefore it is suggested that the EP film derived from the reaction with DBDS has an effect on boundary lubrication during running-in even if there are no polar compounds such as oiliness reagents in the lubricating oil.

Lubricant tests were carried out on test pieces which were immersed in a dilute  $H_2SO_4$  solution after reaction with DBDS. This immersion into acid was in order to eliminate the sulphur compounds from the surface reacted with DBDS, but the iron oxide produced by the reaction with DBDS was thought to remain on the surface. The friction coefficient of these test pieces is illustrated in Figure 4.5. In this figure, the results from the test pieces after one hour reaction time were omitted owing to scatter of the data. The friction coefficient at the first traverse decreased with reaction time, in opposition to that in Figure 4.4(a), in which the friction coefficient of the test piece without acid

immersion were shown. Considering this result, the increase of friction coefficient with EP film, which was shown in Figure 4.4(a), is related to sulphur compounds in the EP film. The shear strength of sulphur compounds in the EP film may be slightly higher than that of iron oxide.

In the data from second to fifth traverse, the friction coefficients of zero and two hours reaction time test pieces increased gradually with traverse, while the friction coefficients of three hours reaction time test pieces remained at almost the same level. There was much increase of the friction coefficient of zero reaction time test piece at the tenth traverse.

#### 4.32 Friction Coefficient at First Traverse

The influence of oiliness reagents on friction coefficient at first traverse was shown in Figure 4.6 to 4.9. In Figure 4.6 the results from the non-reacted test pieces and acid immersion test pieces of non-reacted specimens are illustrated, in which stearic acid, stearyl alcohol, methyl stearate were investigated.

For non-reacted test pieces, all oiliness reagents of stearic acid, stearyl alcohol and methyl stearate had an effect on friction coefficient under loading condition from 0.63kg to 4.63kg. As stearic acid was investigated at a wide range of concentration, the graphs for it used logarithmic axes to clarify the characteristics at low concentration. Linear scales were used for the other two oiliness reagents. Comparing the results in Figure 4.6(a),



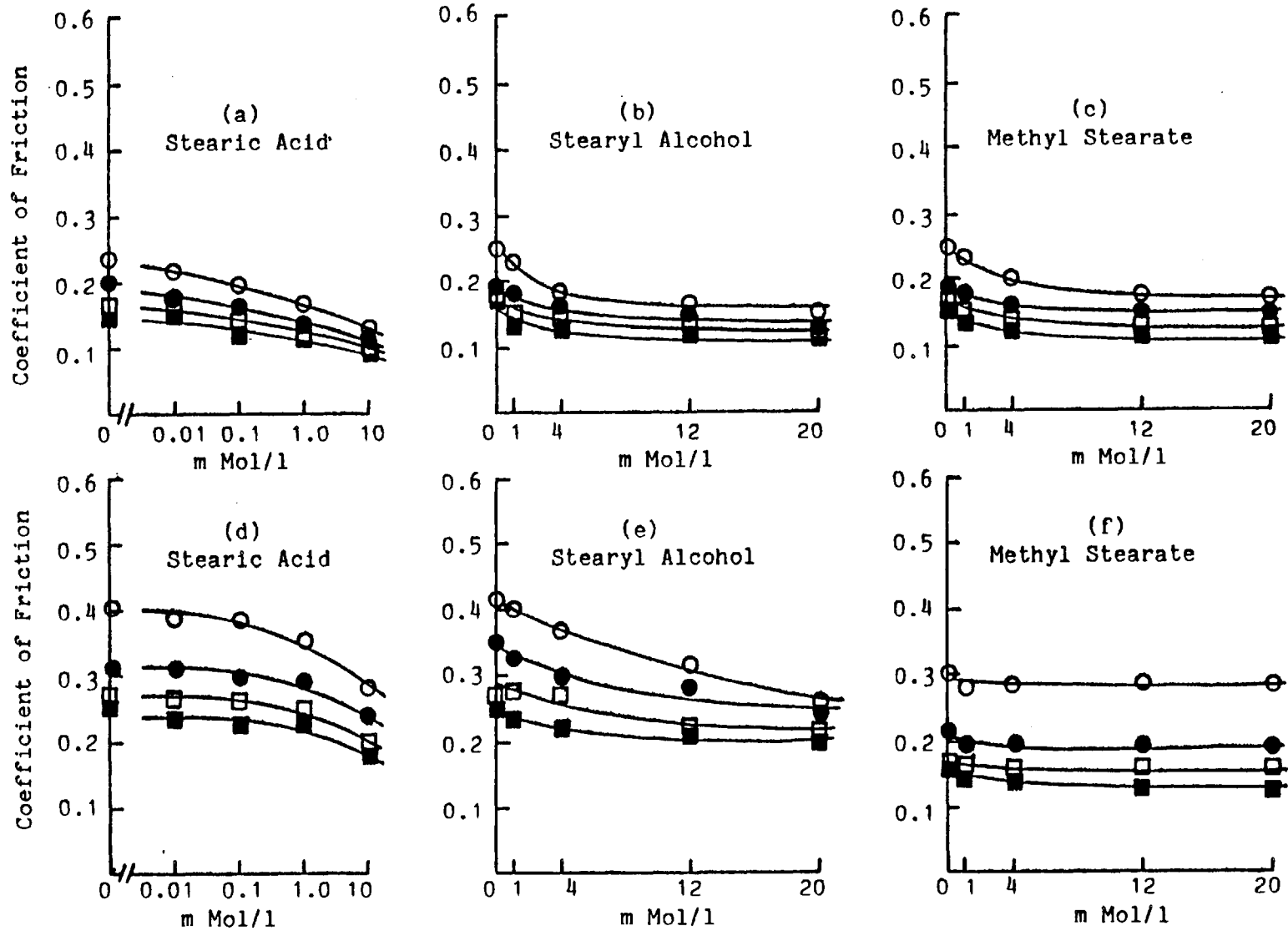


Fig.4-6, Influence of oiliness reagents on coefficient of friction at first traverse (I)

Test Piece (a)(b)(c)-Original mild steel, (d)(e)(f)-Acid immersion

Load ○;0.63kg, ●;1.63kg, □;2.63kg, ■;4.63kg

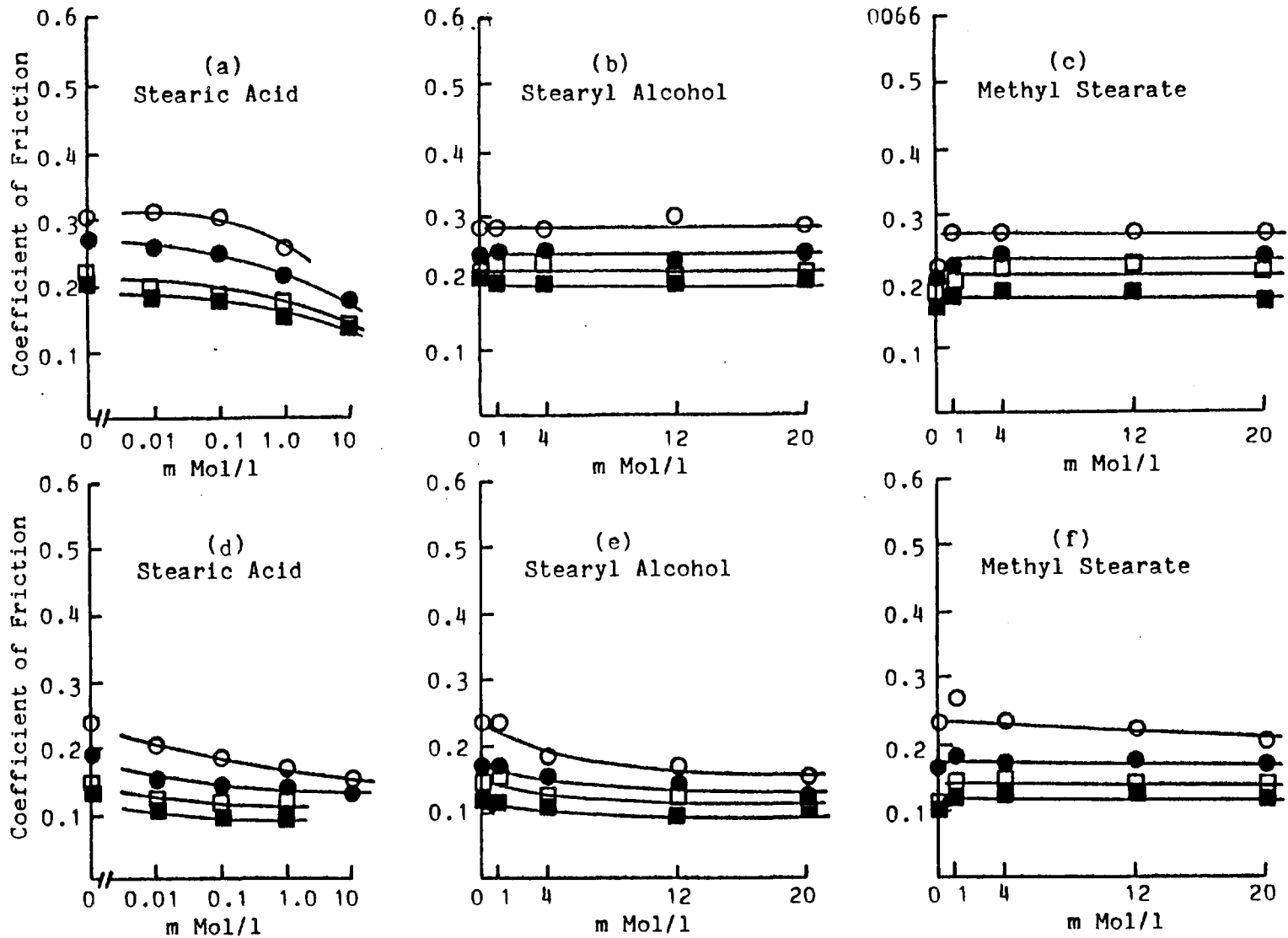


Fig. 4-7, Influence of oiliness reagents on coefficient of friction at first traverse (II)  
 Test Piece (a)(b)(c)-1 hr reaction, (d)(e)(f)-Acid immersion after 1 hr reaction  
 Load ○:0.63kg, ●:1.63kg, □:2.63kg, ■:4.63kg

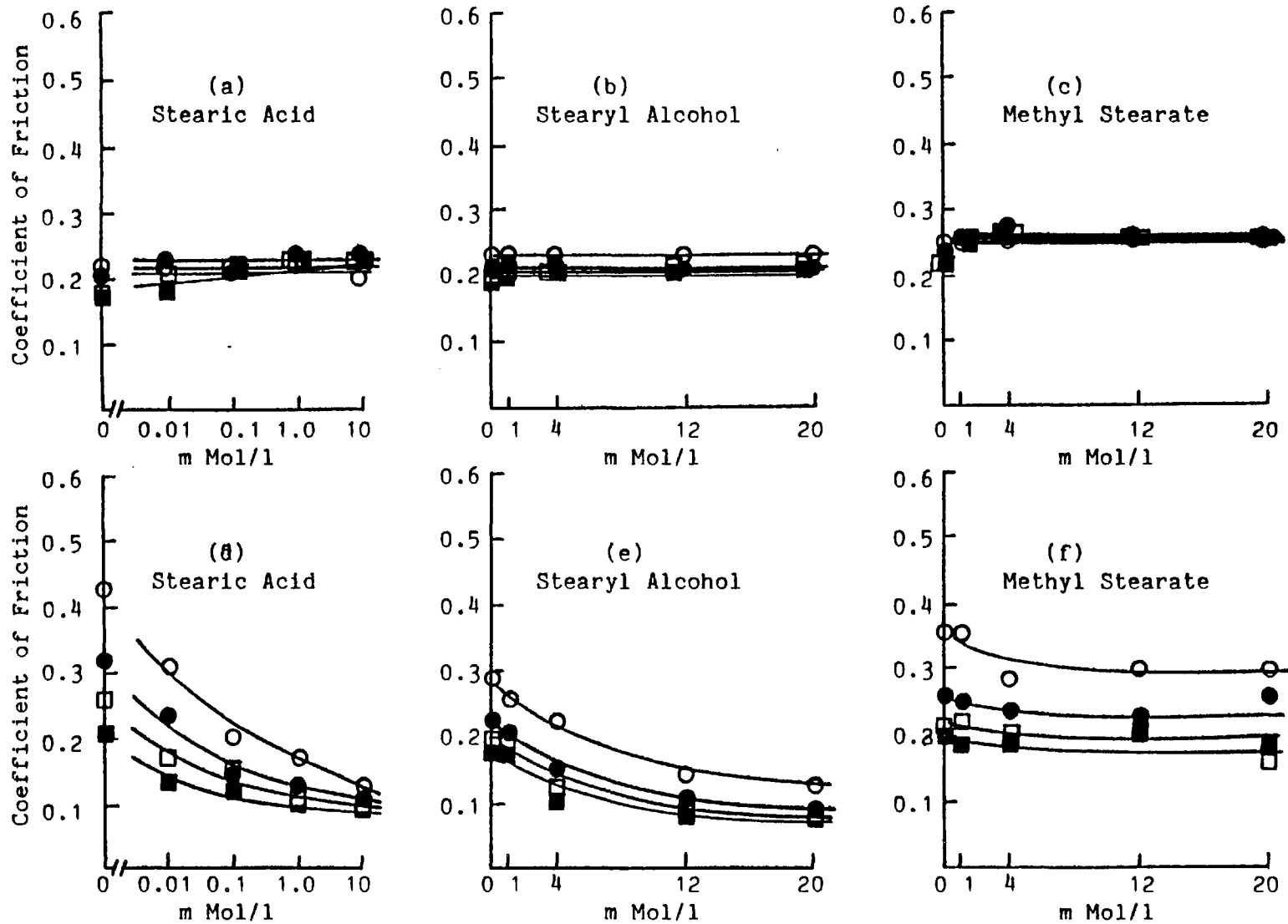


Fig.4-8, Influence of oiliness reagents on coefficient of friction at first traverse (III)  
Test Piece (a)(b)(c)-2 hrs reaction, (d)(e)(f)-Acid immersion after 2 hrs reaction  
Load ○ :0.63kg, ● :1.63kg, □ :2.63kg, ■ :4.63kg

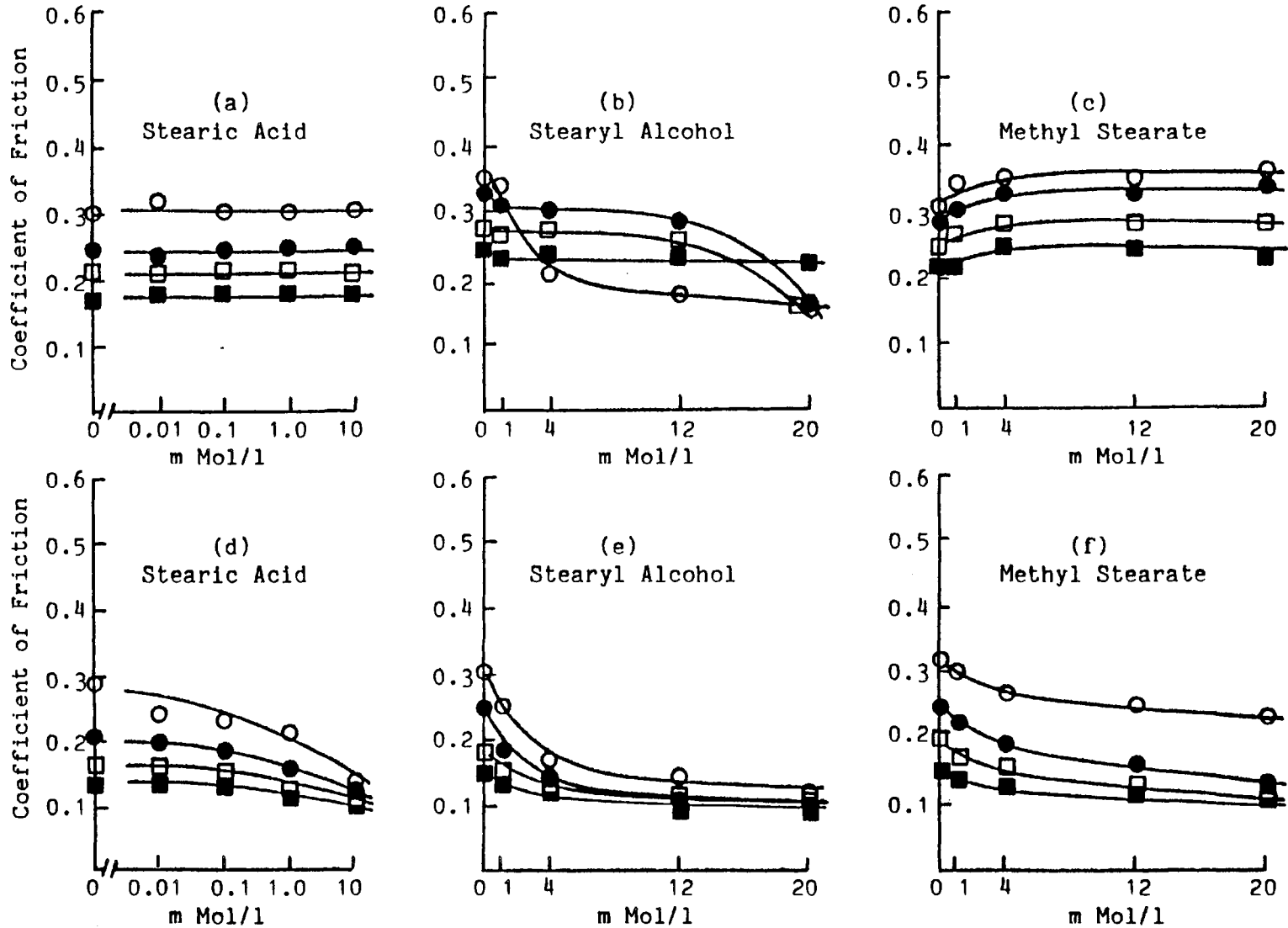


Fig.4-9, Influence of oiliness reagents on coefficient of friction at first traverse (IV)  
Test Piece (a)(b)(c)-3 hrs reaction, (d)(e)(f)-Acid immersion after 3hrs reaction  
Load ○ :0.63kg, ● :1.63kg, □ :2.63kg, ■ :4.63kg

(b) and (c), stearic acid was the most effective material as an oiliness reagent for reducing the friction coefficient. The effectiveness of stearyl alcohol and methyl stearate were almost the same. These materials were effective at low concentration below about 5mMol/l and no apparent decrease of friction coefficient could be seen at higher concentrations. The effectiveness of oiliness reagent was more vivid under lower loading conditions.

Results of unreacted test pieces treated by acid immersion are shown in Figures 4.6(d), (e) and (f). Stearic acid had an effect on friction coefficient at a higher concentration than 0.1mMol/l. Stearyl alcohol also had an influence on friction coefficient in the whole range of concentration. However, there was only a little effect at very low concentration in the case of methyl stearate.

The results from the test pieces which were reacted with DBDS for one hour and then immersed in acid are illustrated in Figure 4.7(a), (b) and (c) and Figure 4.7(d), (e) and (f) respectively. The friction coefficient of the test piece of one hour reaction was decreased by stearic acid of more than 0.01mMol/l, but were not influenced by either stearyl alcohol nor methyl stearate. On the other hand, in the case of test pieces immersed into acid after one hour reaction, stearic acid and stearyl alcohol had an effect on friction coefficient in the same manner, but there was no appreciable effect on methyl stearate.

Figure 4.8 shows the results for the test pieces of two hours reaction time and acid immersion after two hour reaction. As shown in Figure 4.8 (a), (b) and (c), there

were no appreciable influence of oiliness reagents in the friction coefficients of test pieces of two hours reaction time, and the effect of loading on the level of friction coefficient was negligible.

On the other hand, in the cases of test pieces of acid immersion after two hours reaction, there was some effect of oiliness reagents on friction coefficient, and the order of this was stearic acid, stearyl alcohol and methyl stearate.

The results of the test piece after three hours reaction and acid immersion after the reaction time are illustrated in Figures 4.9(a), (b) and (c) and Figures 4.9 (d), (e) and (f) respectively. Stearic acid did not affect the friction coefficient at all in the case of tests of three hours reaction time. However, stearyl alcohol and methyl stearate gave characteristic friction coefficient traces. In the case of stearyl alcohol, at low loads, there was a critical concentration which decreased the friction coefficient rapidly. Methyl stearate had an effect of increasing the friction coefficient at low concentrations. This phenomenon of increase of friction coefficient with concentration was observed only in the case of methyl stearate. In the case of the test pieces of acid immersion after three hours reaction, stearic acid, stearyl alcohol and methyl stearate influenced on friction coefficient in a similar way.

Comparing the friction coefficient of each oiliness reagent, the following descriptions are obtained:

Summary

Test piece without acid immersion,

Stearic acid: friction coefficients of test pieces after no reaction and one hour reaction decreased with stearic acid. However, there was no effect of stearic acid on friction coefficients of test piece of 2 hours and 3 hours reaction time.

Stearyl alcohol: stearyl alcohol decreased friction coefficient of no reacted test pieces. No influence of stearyl alcohol was seen in the friction coefficient of test pieces of one and two hours reaction. The test piece of the three hours reaction gave special results.

Methyl stearate: low concentration of methyl stearate decreased friction coefficient of no reacted test piece. On the other hand, test pieces reacted with DBDS increased friction coefficient slightly at the low concentrations.

Test piece with acid immersion,

Stearic acid: Friction coefficients decreased with stearic acid, and this was observed with all the test pieces. This trend had no relation to the reaction time with DBDS before acid immersion.

Stearyl alcohol: the trend for stearyl alcohol was similar to that for stearic acid. The reaction with DBDS before acid immersion did not induce

any appreciable change of interaction between stearyl alcohol and surface of test piece.

Methyl stearate: the test piece of non-reacted and one hour reacted before acid immersion gave slight changes of friction coefficient at low concentrations of methyl stearate. However, the test pieces of two and three hours reaction time gave a friction coefficient decrease with methyl stearate.

#### 4.33 Friction Coefficient at 10th Traverse

Friction coefficients at the 10th traverse are illustrated in Figure 4.10. The level of friction coefficient depended on the antiwear performance of the oiliness reagent and the nature of the surface of the test piece.

The friction coefficient of the non-reacted test pieces are shown in Figures 4.10(a), (b) and (c). Stearic acid had a large effect on this friction coefficient. A concentration of stearic acid 0.01mMol/l was enough to maintain good lubrication for 10 traverses, stearyl alcohol and methyl stearate were also effective on the friction coefficient. The order of effectiveness of these oiliness reagents were stearic acid > stearyl alcohol > methyl stearate. The limits of concentration for good lubrication by the inferior oiliness reagent, stearyl alcohol were clearly influenced by loaded. High concentrations were necessary under high loading. Friction coefficients in good lubrication



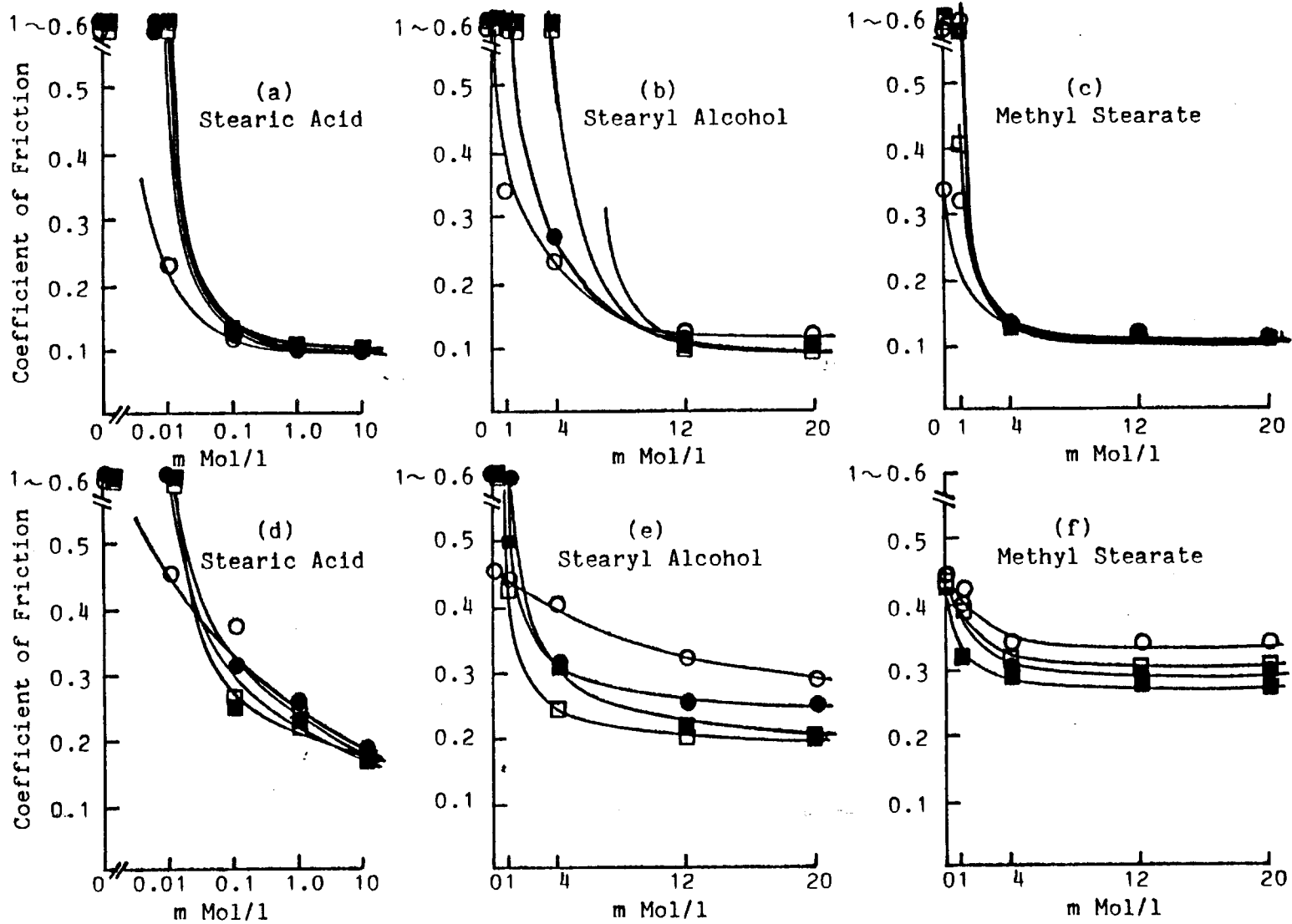


Fig.4-10, Influence of oiliness reagents on coefficient of friction at 10th traverse (I)  
Test Piece (a)(b)(c)-Original mild steel, (d)(e)(f)-Acid immersion  
Load ○ :0.63kg, ● :1.63kg, □ :2.63kg, ■ :4.63kg

were hardly influenced by loading, though the difference of friction coefficient were seen in the results at first traverse.

The results of friction coefficients on the tenth traverse test pieces after acid immersion but not-reacted with DBDS are illustrated in Figures 4.10(d), (e) and (f). In these results, the influence of oiliness reagents on friction coefficient is seen. Stearic acid less than 0.1mMol/l could not keep down the friction coefficient, while in the range greater than 0.1mMol/l the friction coefficient decreased proportionally with the concentration of stearic acid. Stearyl alcohol and methyl stearate also had an effect on friction coefficient at the low concentrations. Unlike the non-acid immersion tests [(a) to (c)], after acid immersion the same friction coefficient was not reached for all the three oiliness additives at high concentration. This may be due to differences of surface of the test piece after acid treatment.

The friction coefficient data at tenth traverse of test pieces of one to three hours reaction and test pieces of acid immersion after one to three hours reaction are illustrated in Figures 4.11 to 4.13.

The data in these figures is almost the same. Friction coefficient decreased with increase in concentration of oiliness reagent. There was not much difference of effectiveness between oiliness reagents. Furthermore, a distinct difference was not observed between the test pieces with and without acid immersion process.

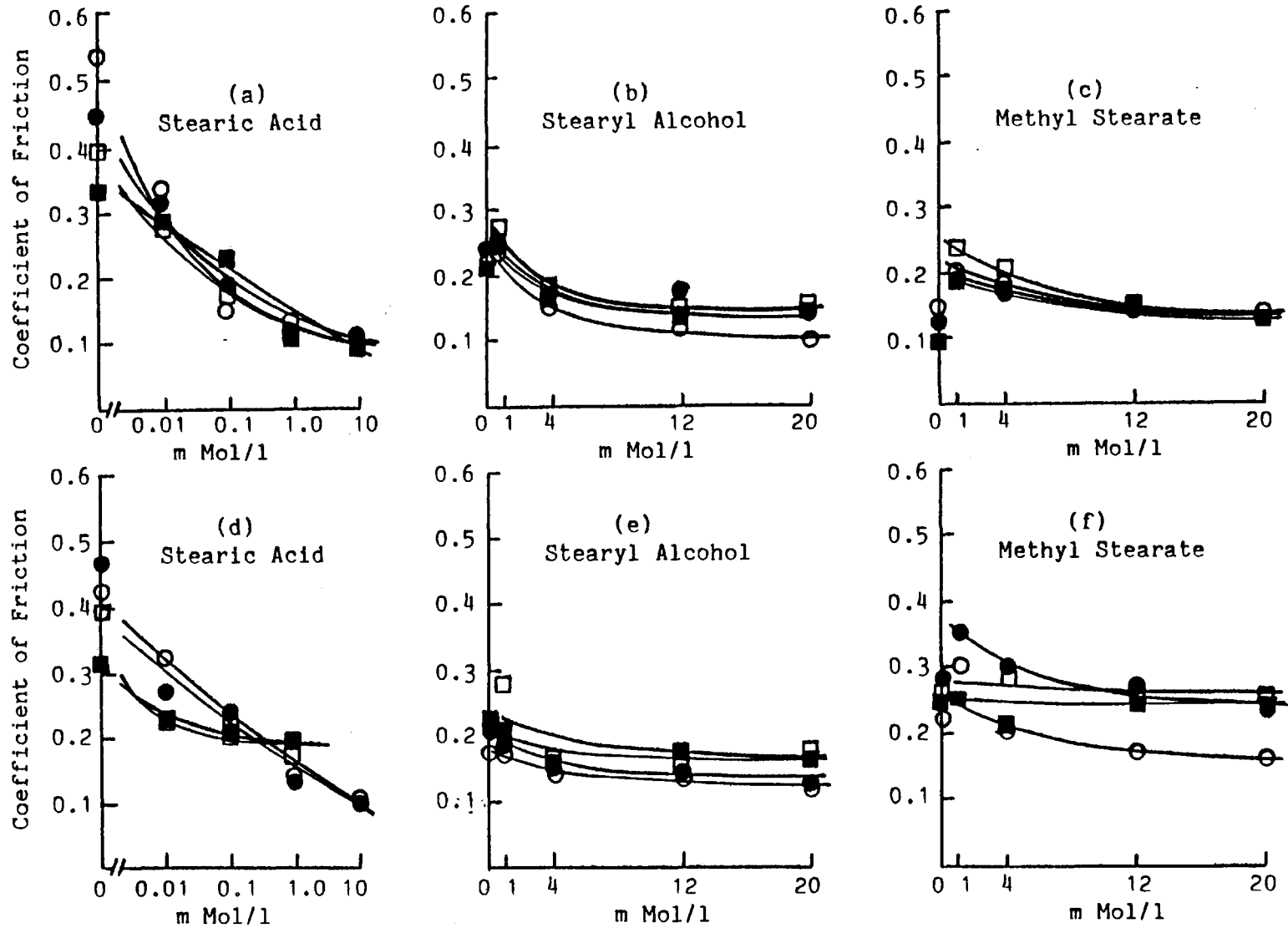


Fig.4-11, Influence of oiliness reagents on coefficient of friction at 10th traverse (II)  
Test Piece (a)(b)(c)-1 hr reaction, (d)(e)(f)-Acid immersion after 1 hr reaction  
Load ○ :0.63kg, ● :1.63kg, □ :2.63kg, ■ :4.63kg

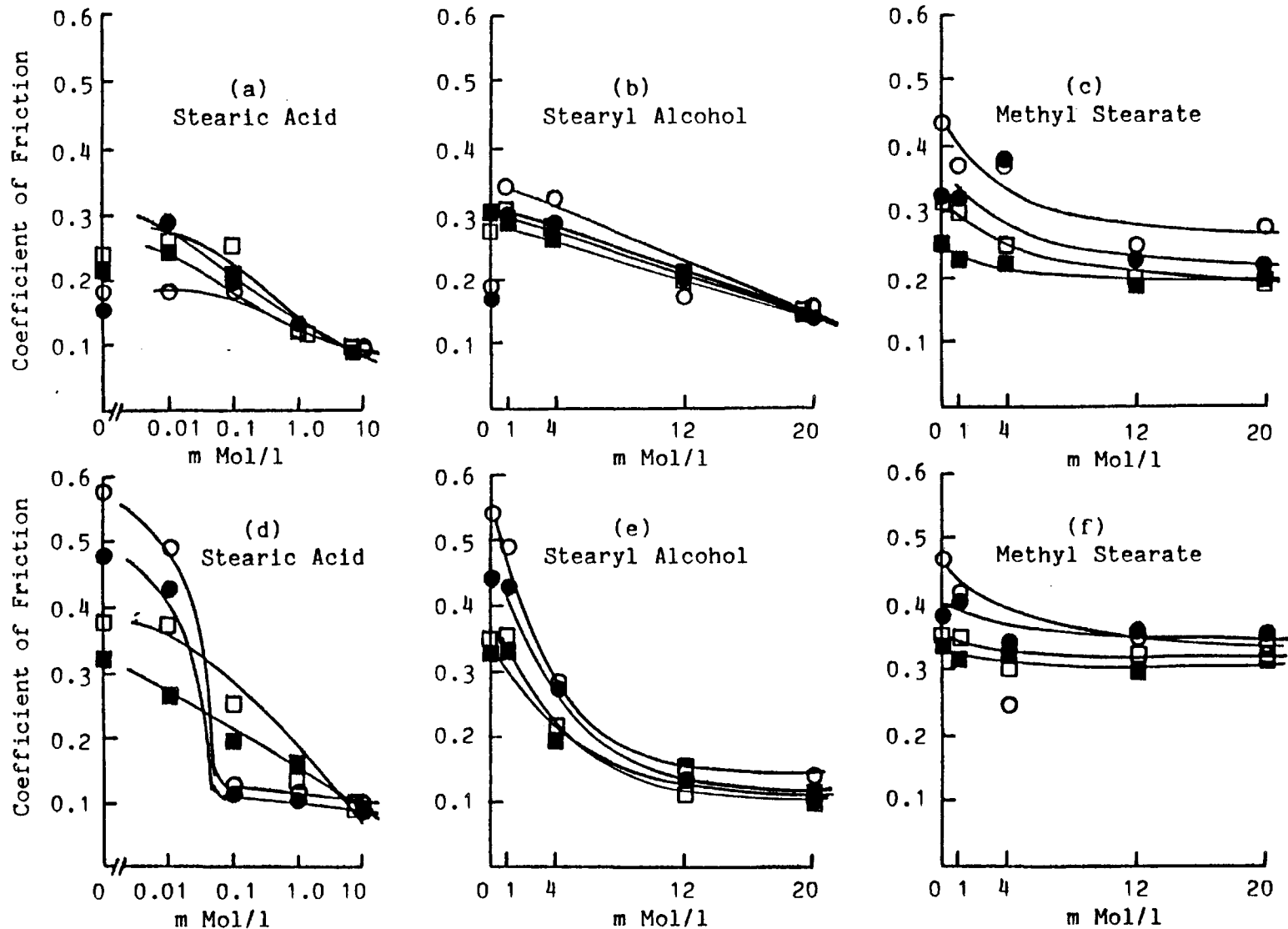


Fig.4-12, Influence of oiliness reagents on coefficient of friction at 10th traverse (III)  
Test Piece (a)(b)(c)-2 hrs reaction, (d)(e)(f)-Acid immersion after 2 hrs reaction  
Load ○ :0.63kg, ● :1.63kg, □ :2.63kg, ■ :4.63kg

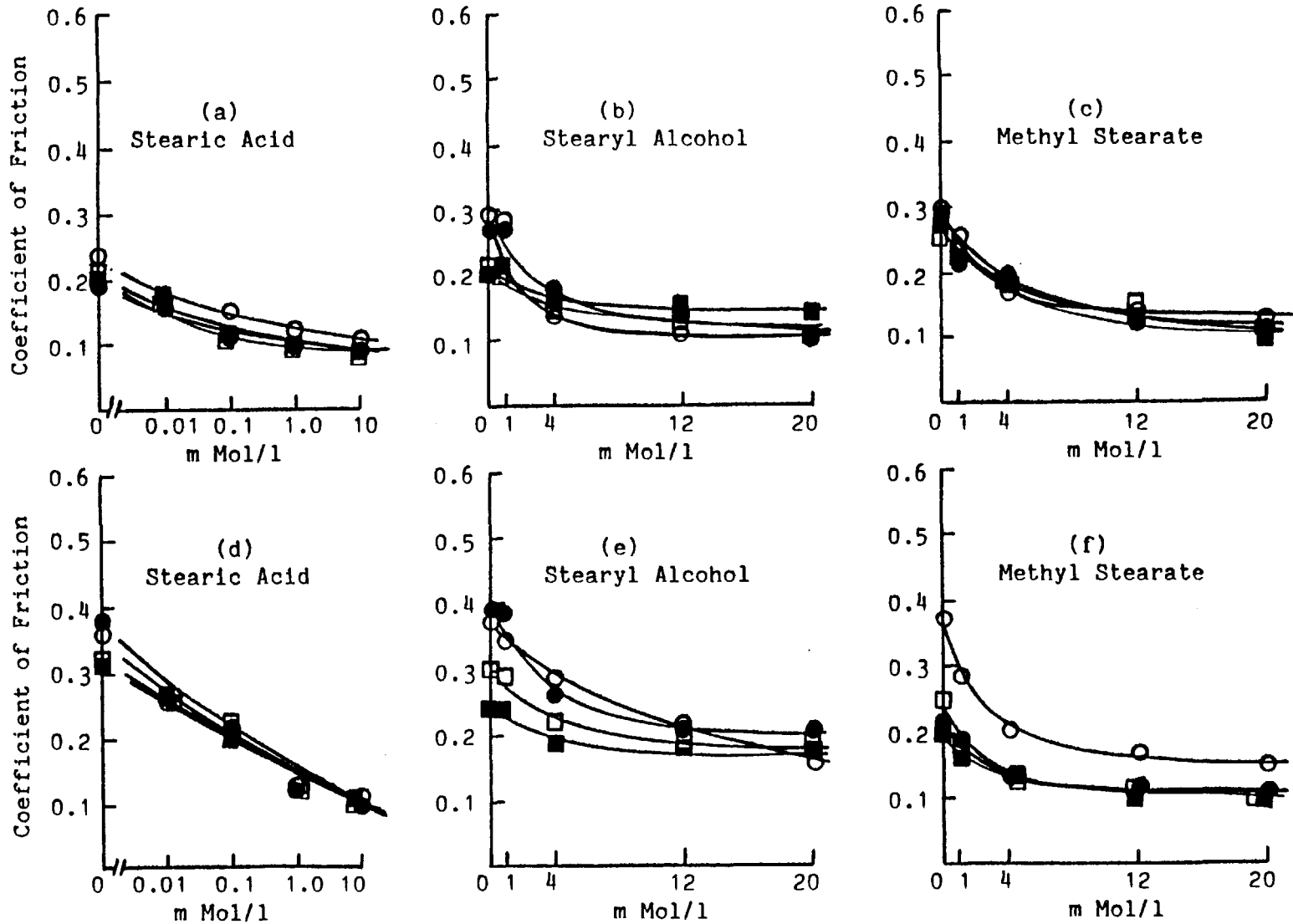


Fig.4-13, Influence of oiliness reagents on coefficient of friction at 10th traverse (IV)  
Test Piece (a)(b)(c)-3 hrs reaction, (d)(e)(f)-Acid immersion after 3 hrs reaction  
Load ○ :0.63kg, ● :1.63kg, □ :2.63kg, ■ :4.63kg

#### 4.34 Effect of EP Film and Oiliness Reagents on Wear

In order to investigate the effect of EP film and oiliness reagents on wear, the width of wear track on the surface of flat lower test pieces was measured after ten traverses. These results are shown in Figures 4.14 to 4.17. Some data has been omitted, since it showed extremely large scatter.

The wear, on an unreacted test piece, was influenced by oiliness reagents in a similar way to the friction coefficient at the tenth traverse. In this data, increase of wear track width was slower than the increase of the friction coefficient at the tenth traverse as shown in Figure 4.10(a), (b) and (c). However it was possible to determine the critical concentration for rapid increase of wear. The critical concentrations depended on oiliness reagent and loading. In Figures 4.14(a), (b) and (c), the critical concentrations are shown by broken lines. The critical concentration shifted to high concentrations with load. Comparing the critical concentrations for each oiliness reagent, the order of concentration was stearic acid > methyl stearate > stearyl alcohol. Therefore the order of effectiveness of oiliness reagent for wear by a test piece which was not reacted was:

stearic acid > methyl stearate > stearyl alcohol

In the case of the test piece of the acid immersion without DBDS reaction the results are illustrated in Figures 4.14(d),

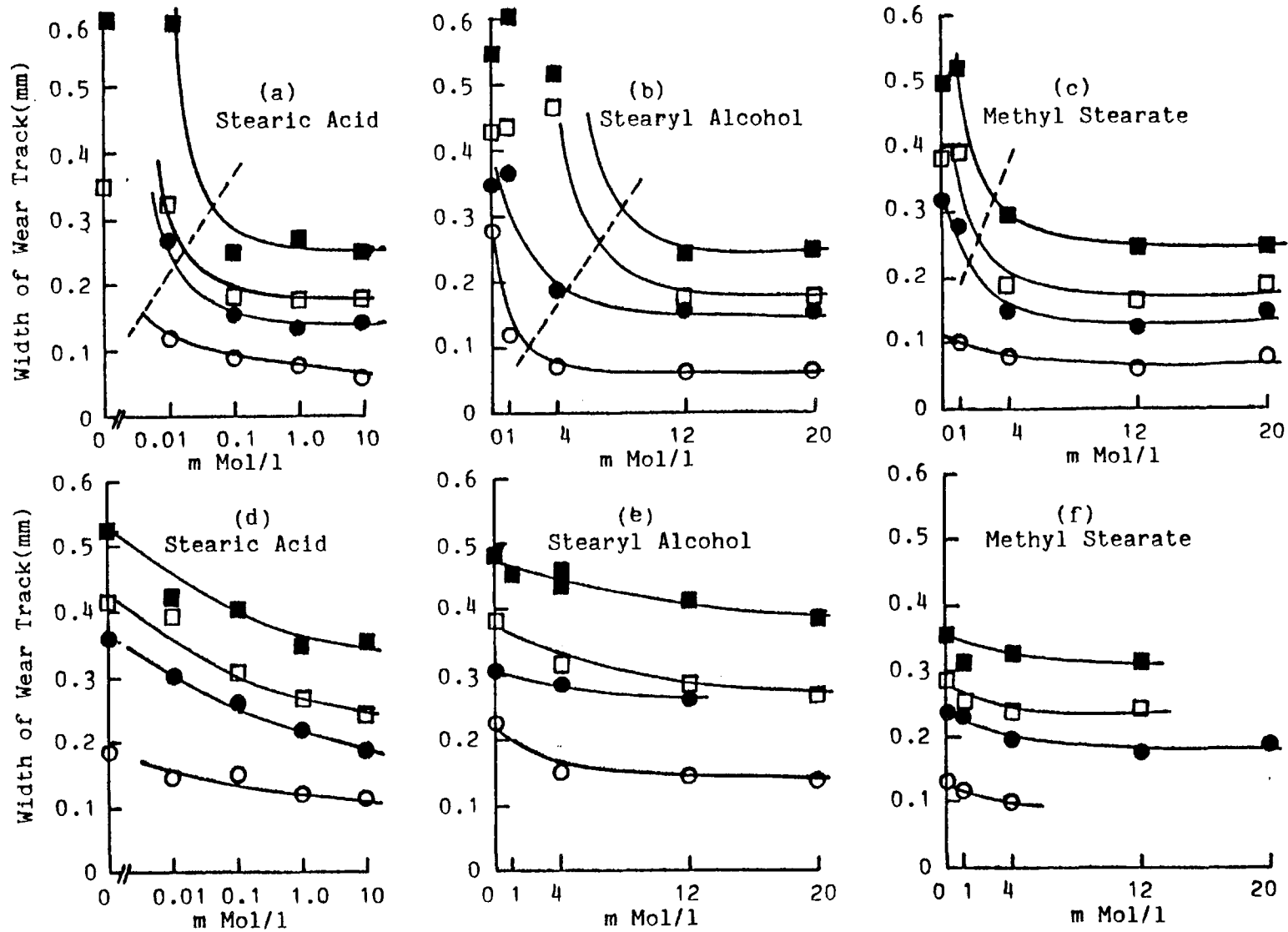


Fig.4-14, Influence of oiliness reagents on wear during running-in (I).  
 Test Piece (a)(b)(c)-Original mild steel, (d)(e)(f)-Acid immersion  
 Load ○ :0.63kg, ● :1.63kg, □ :2.63kg, ■ :4.63kg

(e) and (f). The phenomenon of rapid increase of wear was not seen in these figures, but the width of wear track decreased with the oiliness reagents. Comparing the oiliness reagents, stearic acid was a little more effective than other oiliness reagents. The wear data of the test piece after one hour's reaction time are shown in Figures 4.15(a), (b) and (c). In this case, stearic acid had an extremely small effect on wear. There was no appreciable influence on the wear results of stearyl alcohol and methyl stearate.

The results on the test piece of acid immersion after one hour reaction are illustrated in Figures 4.15 (d), (e) and (f). From this test piece the extremely small effect of oiliness reagent was observed in the results of stearic acid and stearyl alcohol.

The results of the test pieces of two and three hours reaction time are shown in Figures 4.16 and 4.17. In this data, there was no appreciable influence of oiliness reagents at any of the loads measured here. Without oiliness reagents, the EP films produced by the reaction with DBDS were enough to keep wear during running-in below a certain level.

The data from test pieces with acid immersion after two and three hours reaction time are also shown in Figures 4.16 and 4.17. The trend of a small decrease of wear with oiliness reagent is seen in this data.



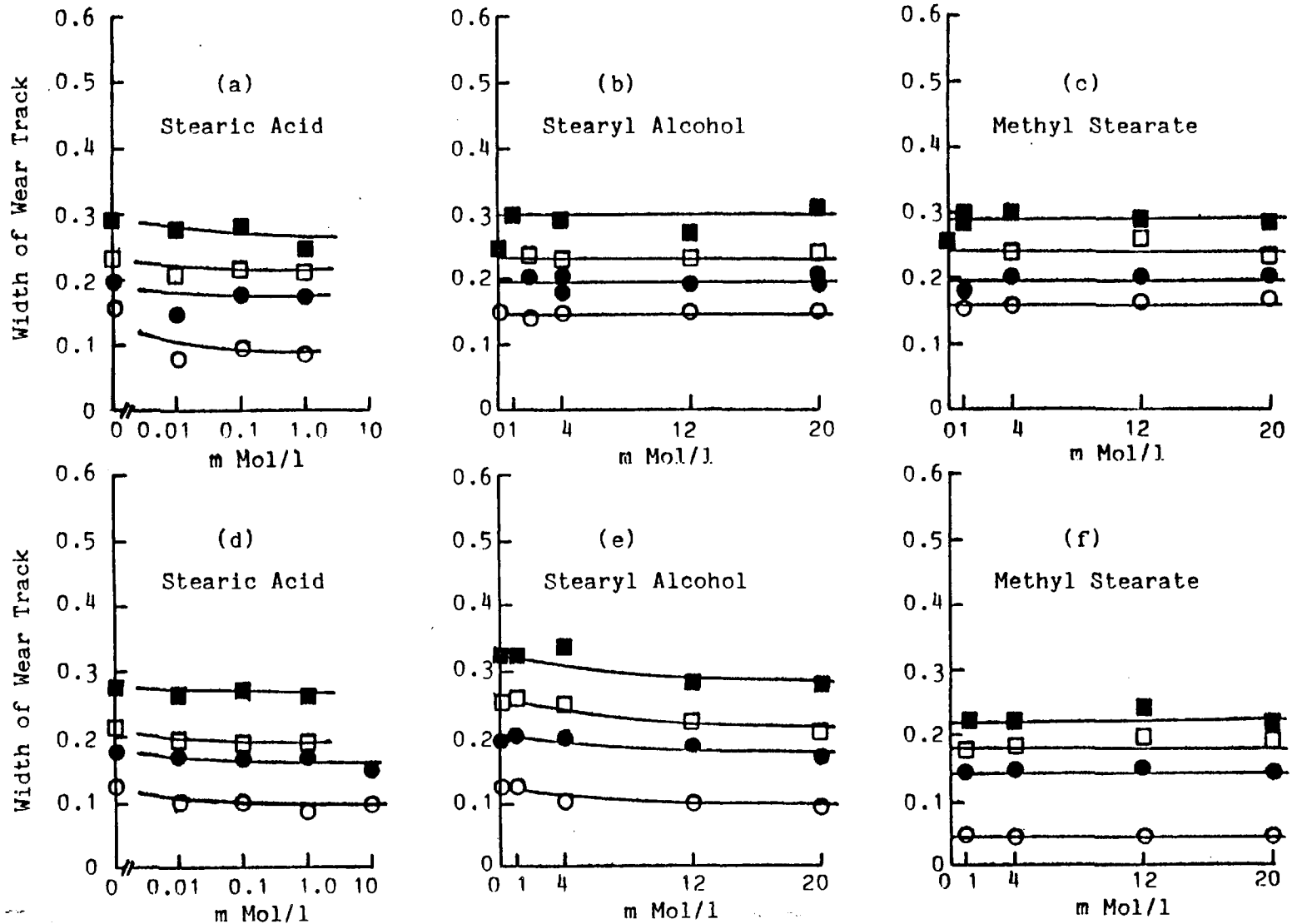


Fig.4-15, Influence of oiliness reagents on wear during running-in (II)  
Test Piece (a)(b)(c)-1 hr reaction, (d)(e)(f)-Acid immersion after 1 hr reaction  
Load ○:0.63kg, ●:1.63kg, □:2.63kg, ■:4.63kg

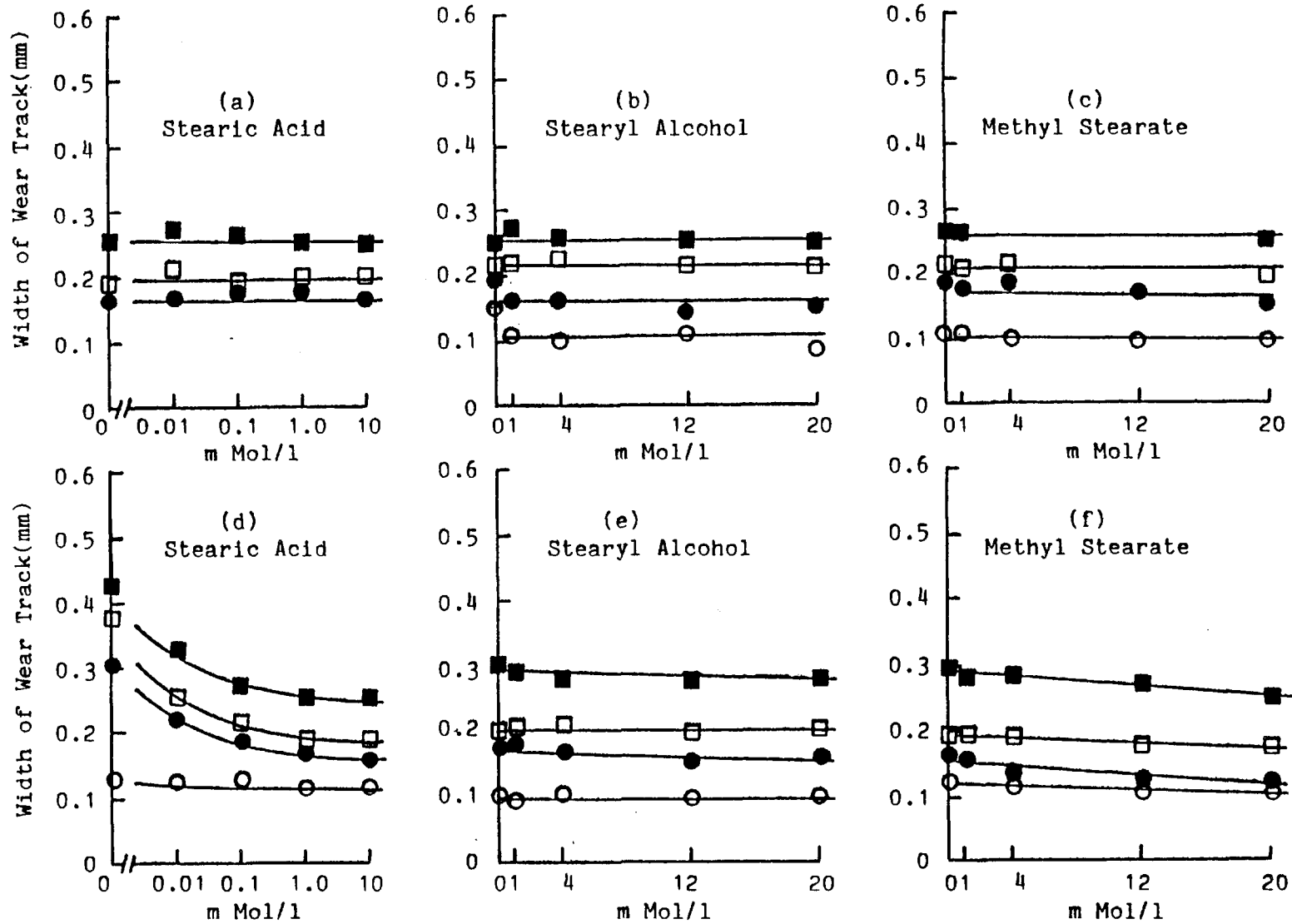


Fig.4-16, Influence of oiliness reagents on wear during running-in (III)  
 Test Piece (a)(b)(c)-2 hrs reaction, (d)(e)(f)-Acid immersion after 2 hrs reaction  
 Load ○ :0.63kg, ● :1.63kg, □ :2.63kg, ■ :4.63kg

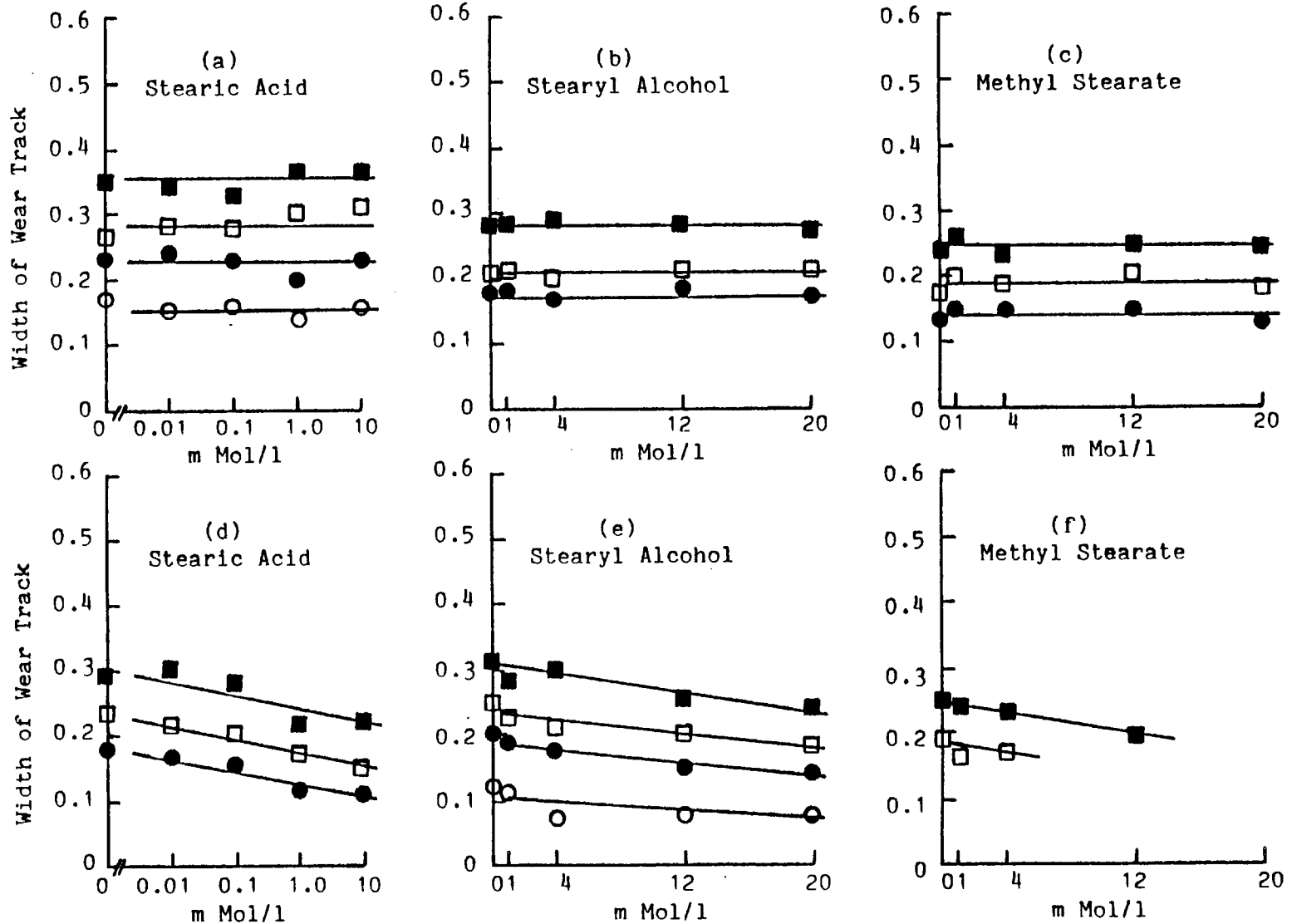


Fig.4-17, Influence of oiliness reagents on wear during running-in (IV)  
 Test Piece (a)(b)(c)-3 hrs reaction, (d)(e)(f)-Acid immersion after 3 hrs reaction  
 Load ○ :0.63kg, ● :1.63kg, □ :2.63kg, ■ :4.63kg

#### 4.40 Discussion

#### 4.41 Friction Coefficient

The friction coefficient in boundary lubrication can be expressed by Equation (1.7) shown in Section 1.21. Assuming the lubrication with a lubricant oil including oiliness reagent and EP additive, the equation consists of the terms of the fraction of metal, the fraction of base oil ( $\alpha_{liq}$ ), the fraction of adsorbed film of oiliness reagent ( $\alpha_{ads}$ ) and the fraction of EP film ( $\alpha_{EP}$ ) at the contact, i.e.

$$f_{BL} = (1 - \alpha_{liq} - \alpha_{ads} - \alpha_{EP}) \frac{S_{sol}}{\bar{p}} + \alpha_{liq} \frac{S_{liq}}{\bar{p}} + \alpha_{ads} \frac{S_{ads}}{\bar{p}} + \alpha_{EP} \frac{S_{EP}}{\bar{p}} \quad (4.1)$$

As  $S_{liq}$ ,  $S_{ads}$  and  $S_{EP}$  are small enough compared with  $S_{sol}$ , the total of  $\alpha_{liq}$ ,  $\alpha_{ads}$  and  $\alpha_{EP}$  at steady state decides the coefficient of friction. Temperature of the lubricated surface and the load vary the total value. According to the increase of load,  $\alpha_{liq}$  decreases with the transition from hydrodynamic lubrication to boundary lubrication.  $\alpha_{ads}$  decreases with the transition from the anti-wear region to the EP region in boundary lubrication, and  $\alpha_{EP}$  varies in the EP region. Similar variations occur with temperature.

The mechanisms described imply independent effect of each type of film. In practice, interactions between the

types may have a dominant influence on friction and wear. The interaction between base oil and oiliness reagents is very important. For example, the well known chain matching phenomenon is a result of this interaction. The interaction between oiliness reagent and EP film is the main subject of this thesis. These two interactions will be discussed in connection to the friction results obtained in the experiment.

(i) Interaction between base oil and oiliness reagent.

The results of friction coefficient measurement from the test pieces without EP film are shown in Figures 4.6(a), (b) and (c) for the data at the first traverse and Figures 4.10(a), (b) and (c) for the data at the tenth traverse. In these cases, as the experiments were carried out in normal atmosphere, the surface of the test pieces can be considered to be covered with an iron oxide film. The adsorption of oiliness reagent onto iron oxide occurs in this experiment.

The experimental results show that little effect of oiliness reagents on friction coefficient is observed at the first traverse, but a considerable influence of oiliness reagents is seen at the tenth traverse. These results are very similar to those for DBDS treatment on steel (Figure 4.4) and it can be seen that oiliness additives do not greatly improve friction on the first traverse, presumably because other contaminants are still playing their part in friction reduction. By the 10th traverse, however, such contaminants have been removed, but the oiliness additive is still able, when present, to keep the friction down.

The concentration of oiliness reagent required in such circumstances is low, i.e. about 0.1mMol/l for stearic acid, 4-12mMol/l for stearyl alcohol and 1-4mMol/l for methyl stearate.

The adsorption studies in Chapter 3 showed that oiliness reagents at the concentrations used give only 0.2-0.3 of a monolayer film. It is noteworthy that such sparse films can be so effective in keeping friction down under repeated rubbing. This may be due to the incorporation of base oil to form a mixed rigid film (25) (68) (69) (122). In other words, the existence of oiliness reagents not only increases  $\alpha_{ads}$  but also  $\alpha_{liq}$ , effectively increasing the residence time of base oil molecules on the surfaces.

(ii) Interaction between adsorption film and EP film.

There are two ways an EP film can affect the formation of oiliness film, i.e. (a) increase in the coverage  $\alpha_{ads}$  of oiliness reagent under particular condition, (b) increase of  $\Delta H_{ads}$  of the oiliness reagent under particular condition. As the friction coefficient measured in this experiment is limited to room temperature and several loading conditions, it does not provide sufficient data to discuss the latter. Only the former is discussed in this section.

The results of friction coefficients from the test pieces with EP films produced by DBDS are shown in Figures 4.7 to 4.9(a), (b) and (c) for the results at the first traverse and Figures 4.11 to 4.13(a), (b) and (c) for the results at the tenth traverse.

The results at the first traverse show that the effects of oiliness reagent are almost negligible and the coefficients of friction are increased slightly by the EP film. This means that the effect of EP film overwhelms any effect of interaction between oiliness reagent and EP film. Probably, these results depend on the change of hardness of the surface by formation of an EP film.

In the tenth traverse, the effects of oiliness reagents on friction coefficient are recognised. However, it is impossible to decide whether the effect is derived as a result of the particular interaction between oiliness reagent and EP film or not, since a similar effect occurs without DBDS treatment (Figure 4.10).

#### 4.42 Wear

It is very difficult to understand completely wear mechanisms owing to the many factors that affect wear and also transitions of the modes of wear, which are described in Section 1.22. At this moment, one of the least understood branches of tribology is wear and this is still in the classification stage (5).

A simple wear equation has been developed by Archard and further developments have been tried by several authors as described in Chapter One. Those equations can predict only the wear rate in steady state of a wear mode. It is therefore impossible to discuss the results of wear during running-in which are obtained in this study, using these theoretical equations. In this sense, the discussion in

this section is limited to qualitative descriptions.

The influence of oiliness reagents and EP film on wear after 10 traverses is shown in Figures 4.14 to 4.17. Where the surface of test piece is not covered with an EP film, including sulphur compounds (Figure 4.14(a), (b) and (c)), i.e. the original test piece. Wear decreases rapidly with oiliness reagent, so that a certain concentration of oiliness reagent is required to avoid a rapid wear. The concentration depends on load and oiliness reagent. The higher the load, the higher the concentration is required. The order of effectiveness of the oiliness reagent is stearic acid > methyl stearate > stearyl alcohol. This order is in agreement with that of wear tests performed on a Shell four-ball machine (10) (11). As the surface of the test piece is considered to be covered with iron oxide, these results are derived as a result of interaction between oiliness reagent and iron oxides.

However, this result of wear is not always coincidental with that of adsorption and heat of adsorption shown in Chapters Two and Three. The antiwear performance of methyl stearate is better than that of stearyl alcohol, though the adsorption and heat of adsorption of methyl stearate is not great compared with those of stearyl alcohol. In addition, the concentration of each oiliness reagents which are effective as an antiwear additive does not coincide to those which result in great amounts of adsorption and heat of adsorption onto iron oxide. The former is lower than the latter. It is difficult to make clear the causes of these differences.



It may be that adsorption of oiliness reagents onto materials other than  $\alpha\text{-Fe}_2\text{O}_3$ ,  $\gamma\text{-Fe}_2\text{O}_3$  and  $\text{Fe}_3\text{O}_4$  is important for anti-wear, because the solvent effect for the adsorption of these oiliness reagents is not so large as might be expected from the result in Section 2.33.

On the other hand, in the results from the test pieces in which the surface is covered with EP film produced by DBDS, no influence of oiliness reagents on anti-wear is observed, which does not support the possibility of interactions between the EP film and oiliness reagent. The EP film alone is sufficient to maintain a certain antiwear property. According to the consideration of values such as coefficient of friction in Equation (4.1), as  $\alpha_{\text{EP}}$  is too large, the effect of  $\alpha_{\text{ads}}$  and the interaction of oiliness reagents with EP film on antiwear may not be observed. More severe conditions or a longer time operation is desired to investigate this subject.

#### 4.50 Conclusions

The following conclusions may be drawn from the results of low speed friction and wear tests during running-in using a Bowden Leben Machine.

- (1) The coefficient of friction on mild steel test piece without EP film in pure n-hexadecane increases markedly during the first 10 traverses. However, the EP film formed by a reaction with DBDS prevents this increase.
- (2) Acid immersion, which reduced the sulphur content in

a DBDS EP film, decreases the effect of the EP film described in (1) above.

- (3) The influence of oiliness reagents on the coefficient of friction at the first traverse (i.e. coefficient of friction of a single pass test) is appreciable, when there is no EP film on the test piece. However, no further friction reduction occurs with oiliness reagents on test pieces with EP films.
- (4) Oiliness reagents reduce the coefficient of friction at the 10th traverse on test pieces without EP films. The order of the effect is given by,  
  
stearic acid > methyl stearate > stearyl alcohol
- (5) Oiliness reagents slightly reduce the coefficient of friction on the 10th traverse of test pieces with EP films. Judging from these results, the interaction of oiliness reagents with EP films is not effective in showing further improvement of friction coefficient during running-in.
- (6) Wear during running-in in boundary lubrication increases with load.
- (7) Wear of test pieces without EP films during running-in is affected by oiliness reagents as follows,

stearic acid > methyl stearate > stearyl alcohol

This order is in agreement with that of the coefficient of friction on the 10th traverse.

- (8) In the case of a test piece with EP films, there is little effect of oiliness reagents on wear during running-in.

CHAPTER FIVE

CONCLUSIONS AND SUGGESTIONS FOR FURTHER WORK

5.10 General Conclusions

The purpose of this work is to clarify the mechanism of adsorption of oiliness reagents onto EP films formed with sulphur-type EP additive, and to investigate the influence of this phenomenon on friction and wear in boundary lubrication. For this purpose, three kinds of experiments, heat of adsorption, adsorption and friction and wear tests, have been carried out. As the conclusions of each of the experimental sections are described in Chapters 2, 3 and 4 respectively, general conclusions are discussed in this chapter.

- (1) The existence of rigid films of polar compounds, which are effective in reducing friction and wear in boundary lubrication, on FeS formed by the EP reaction has been suggested by Cameron following work by Sakurai. These results for heat of adsorption did not support this suggestion. The heat of adsorption of oiliness reagents on FeS is not as large (at room temperature) as on iron oxides such as  $\alpha\text{-Fe}_2\text{O}_3$ ,  $\gamma\text{-Fe}_2\text{O}_3$  and  $\text{Fe}_3\text{O}_4$ . However, the adsorption of oiliness reagents on the oxidised FeS, oxidised in water and on which sulphates were detected by ESCA on the surface, released considerable heats of adsorption. The most probable material that forms rigid films of polar compounds, which are effective

in reducing friction and wear, is possibly iron sulphates. Since Barcroft (46) has detected  $\text{FeSO}_4$  on lubricated surface. The mechanism of adsorbed film lubrication suggested here should be limited to low temperature conditions.

- (2) For stearyl alcohol, experimental results of heat of adsorption support the mechanism of a horizontal adsorption at low concentration and a vertical adsorption at high concentration, which has been proposed by Daniel (71). In addition, the influence of temperature on the change from horizontal to vertical adsorption was also investigated. This change occurs only at low temperatures below  $45^\circ\text{C}$ . Moreover the vertical adsorption occurs only on  $\alpha\text{-Fe}_2\text{O}_3$  and  $\gamma\text{-Fe}_2\text{O}_3$  not on  $\text{Fe}_3\text{O}_4$ . The results of heat of adsorption are compared with results of friction and wear tests during running-in under boundary lubrication conditions at room temperature. It was found that the effective concentration of stearyl alcohol in reducing friction and wear on mild steel, the surface of which is considered to be covered by iron oxides, is around that of the change from horizontal to vertical adsorption. In this case, high concentration of stearyl alcohol was required at high load friction. This means that the most effective adsorbed film for friction reduction is a vertically adsorbed one. Horizontal adsorption only gives low friction and wear at low loads.

- (3) A mechanism of adsorption of stearic acid on iron oxides is proposed.  $\text{Fe}^{3+}$  at the tetragonal position in iron oxide is considered to be active for a chemical adsorption of stearic acid. Other cation sites such as  $\text{Fe}^{3+}$  at the octagonal position and  $\text{Fe}^{2+}$  sites are not active for chemical adsorption. Therefore, the formation of  $\text{Fe}_3\text{O}_4$  and  $\gamma\text{-Fe}_2\text{O}_3$ , which contains active sites of  $\text{Fe}^{3+}$  at the tetragonal position, on the lubricated surfaces reduces friction and wear in boundary lubrication by a chemically adsorbed film of stearic acid. On the other hand,  $\alpha\text{-Fe}_2\text{O}_3$  does not form an effective chemically adsorbed film for reducing friction and wear, since this oxide does not have active  $\text{Fe}^{3+}$  at the tetragonal position. This mechanism of adsorption explains the poor lubricity of  $\alpha\text{-Fe}_2\text{O}_3$ .
- (4) The combination of results of adsorption and heat of adsorption made the calculation of cumulative enthalpy changes of adsorption per mole possible. The values for the adsorption of stearic acid on  $\gamma\text{-Fe}_2\text{O}_3$  and  $\text{Fe}_3\text{O}_4$  are high enough to predict an occurrence of chemical adsorption (70-85KJ/Mol). On the other hand, the values of stearic acid and methyl stearate are within the range of physical adsorption (about 25KJ/Mol). The differential enthalpy change of adsorption was also calculated to investigate the influence of lateral interactions at high coverages of adsorbed molecules on the enthalpy change of adsorption, since the differential values

give the enthalpy change of adsorption on each set of sites progressively occupied as adsorption proceeds. The rapid increase of the differential enthalpy change of stearic acid on  $\gamma\text{-Fe}_2\text{O}_3$  at the coverage 0.6-0.7 of a monolayer shows the increase of lateral interaction.

- (5) In order to elucidate the relationship between the adsorption phenomena described above [conclusions (1)-(4)] and friction and wear in boundary lubrication, friction and wear tests were carried out using a Bowden Leben Machine. Oiliness reagents were useful in reducing friction and wear on mild steel. The concentrations of oiliness reagents which are effective in preventing an increase of friction coefficient during the first ten traverses are 0.01-0.1mMol/l for stearic acid, 4-12mMol/l for stearyl alcohol and 1-4mMol/l for methyl stearate. This order of effectiveness of oiliness reagent is not in agreement with the order of heat of adsorption on iron oxides, which were measured with a Flow Microcalorimeter. The results of wear after ten traverses (during running-in) is in agreement with the results of friction tests.

Methyl stearate is more effective in reducing friction and wear than stearyl alcohol, though the cumulative heat of adsorption of methyl stearate on iron oxides is smaller than that of stearyl alcohol. The reasons for this could not be explained by this work. However it is likely that the superior effectiveness of

stearic acid is due to the formation of a chemically adsorbed film on iron oxide.

- (6) EP films on a mild steel test pieces were prepared by reaction with DBDS at 216°C to investigate the interaction of it with oiliness reagents and the effect on friction and wear. The EP films are effective in preventing friction increases during repeated rubbing, and wear during running-in. However, the addition of oiliness reagents in pure n-hexadecane base oil does not improve the effectiveness of these films on friction and wear. This result does not support the view that the adsorption of polar compounds on FeS in EP films formed with a sulphur-type EP additive is very effective in reducing friction and wear. It is in agreement with the results described in conclusion (1).

#### 5.20 Suggestions for Further Work

- (1) It is well known that FeS is easily oxidised in air. Nevertheless, the measurement of heat of adsorption with a Flow Microcalorimeter was carried out using FeS powder kept in a desiccator for several months. Analytical results of the FeS powder by ESCA showed that the surface of the sample had already oxidised. The sample was not suitable to investigate the interaction between FeS and oiliness reagent. Although the results from this sample showed that cumulative heats of adsorption of oiliness reagents on FeS were



not great, further study is necessary to confirm this finding. In that case, it is hoped that the measurement should be carried out using freshly made FeS and in an atmosphere of inert gas such as N<sub>2</sub> or Ar to avoid oxidation.

- (2) It is found that the oxidation of FeS increases heat of adsorption of oiliness reagents. In this case, sulphates were detected on the surface of the oxidised FeS powder by ESCA analysis. As FeSO<sub>4</sub> can be an active material in forming a rigid absorbed film of polar compounds, future work should aim at further investigation of adsorption on FeSO<sub>4</sub> instead of FeS. This should lead to a more complete understanding of the action of sulphur EP additives.
- (3) It is suggested that oiliness reagents owe their effectiveness in reducing friction and wear to the formation of a mixed monolayer with the base oil. It would be interesting to investigate this idea of a mixed monolayer in view of the chain matching phenomena found in friction measurement by many authors. The use of base oils other than hexadecane, such as poly- $\alpha$ -olefin, is clearly indicated.
- (4) It has been shown that the combination of an adsorption isotherm and a direct measurement of heat of adsorption with a Flow Microcalorimeter produces useful information on such items as cumulative enthalpy change of adsorption per mole and differential enthalpy change of adsorption. The measurement of adsorption isotherms was limited to stearic acid and methyl

stearate owing to the difficulty of measurement of concentration of stearyl alcohol by IR spectrometry. It is hoped to extend the measurement of adsorption isotherms for stearyl alcohol by Gas Liquid Chromatography to obtain the cumulative enthalpy change of adsorption per mole and the differential enthalpy change. The precise measurement of adsorption isotherms for stearyl alcohol, could make possible the estimation of the degree of cohesive force, which is an important factor in forming a rigid adsorption film. The adsorption is considered to make a film of high density of vertically adsorbed molecules at high concentration.

APPENDIX A

HEAT OF ADSORPTION ON A DIFFERENT  $\alpha\text{-Fe}_2\text{O}_3$

As described in Section 2.42, there was a large difference of heat of adsorption onto  $\alpha\text{-Fe}_2\text{O}_3$  between Sakurai and co-workers' data and the results in this study. In order to investigate the causes of this difference, new  $\alpha\text{-Fe}_2\text{O}_3$  powder was purchased from the same company which supplied  $\alpha\text{-Fe}_2\text{O}_3$  powder used in Sakurai's work, references (10) (11) (106). Although this powder had the same specification which was 100-200 mesh and 99% purity, as that in these references, the surface area of this powder was unfortunately so small that reliable results were not obtained. Therefore as a reference, brief results with this powder are shown in this appendix.

The surface area measured by BET method is as follows:

| N <sub>2</sub> method |                       | Kr method             |
|-----------------------|-----------------------|-----------------------|
| 1st measurement       | 2nd measurement       |                       |
| 0.44m <sup>2</sup> /g | 0.33m <sup>2</sup> /g | 0.27m <sup>2</sup> /g |

Generally speaking, it is very difficult to obtain precise values for powders of small surface area by the BET method. Although there is much difference in the data shown above, in this appendix heats of adsorption were calculated using a value 0.27m<sup>2</sup>/g obtained by the Kr method, in accordance with the results in Chapter Two.

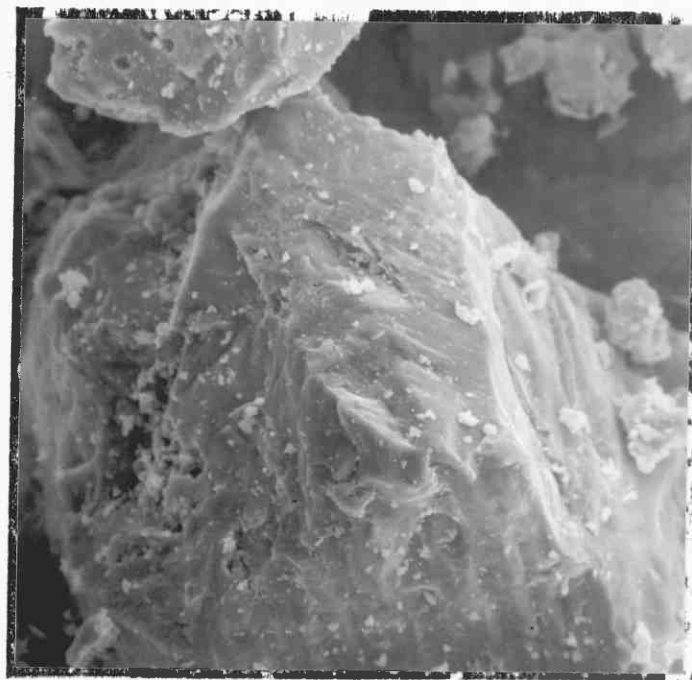
The secondary SEM image of this powder is shown in

Photograph A.1. Each powder exists as clusters of fine particles below  $5\mu$ , some having smooth surfaces. These observations are very different from the other  $\alpha\text{-Fe}_2\text{O}_3$  shown in Chapter Two. This difference may be due to the method of manufacture. Iron content determined by a chemical analysis was 68.36%, which is similar to that of the other  $\alpha\text{-Fe}_2\text{O}_3$  shown in Table 2.2. The results of X-ray diffraction analysis showed that this powder mostly consisted of hematite but this material included some magnetite and fayalite  $(\text{Fe}_x\text{Mg}_y)_2\text{O}\cdot\text{SiO}_2$  as impurity.

Heats of adsorption of this  $\alpha\text{-Fe}_2\text{O}_3$  powder were determined by the process described in Section 2.23. The results are shown in Figures A.1 to A.3. The heats of adsorption of stearic acid and stearyl alcohol, which are given in Figure A.3, are very large, compared with those shown in Figure 2.25(a). This may however be due to under-estimation of the surface area of the powder, as determined by the BET method.



— 50u



— 5u

Photo.A-1, The secondary images of scanning electron micrograph of  $\alpha$ -Fe<sub>2</sub>O<sub>3</sub>(new)

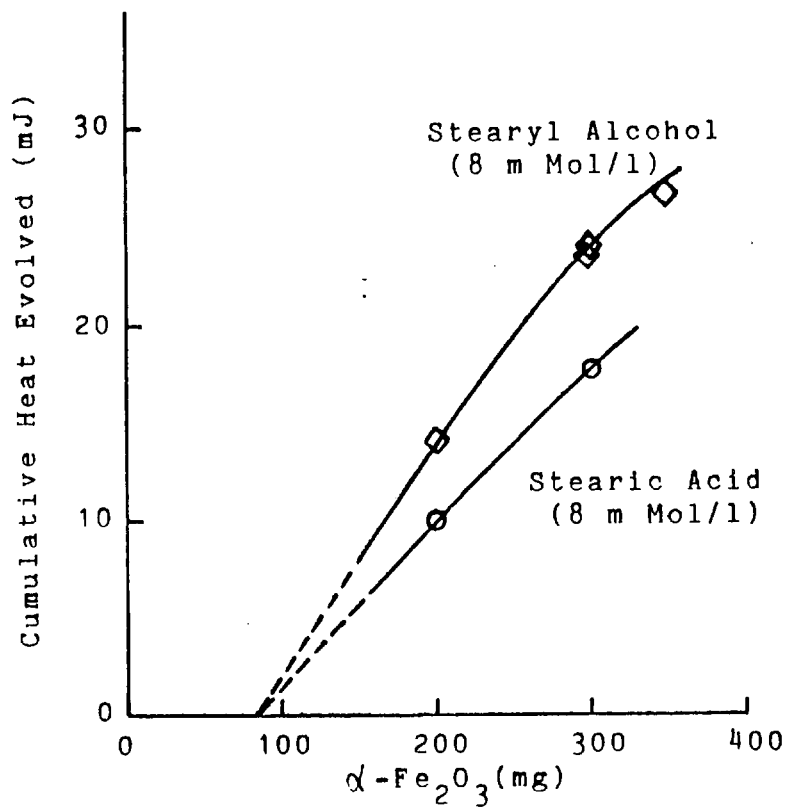


Fig.A-1, Cumulative heat evolved vs. amount of  $\alpha$ -Fe<sub>2</sub>O<sub>3</sub> powder(new)

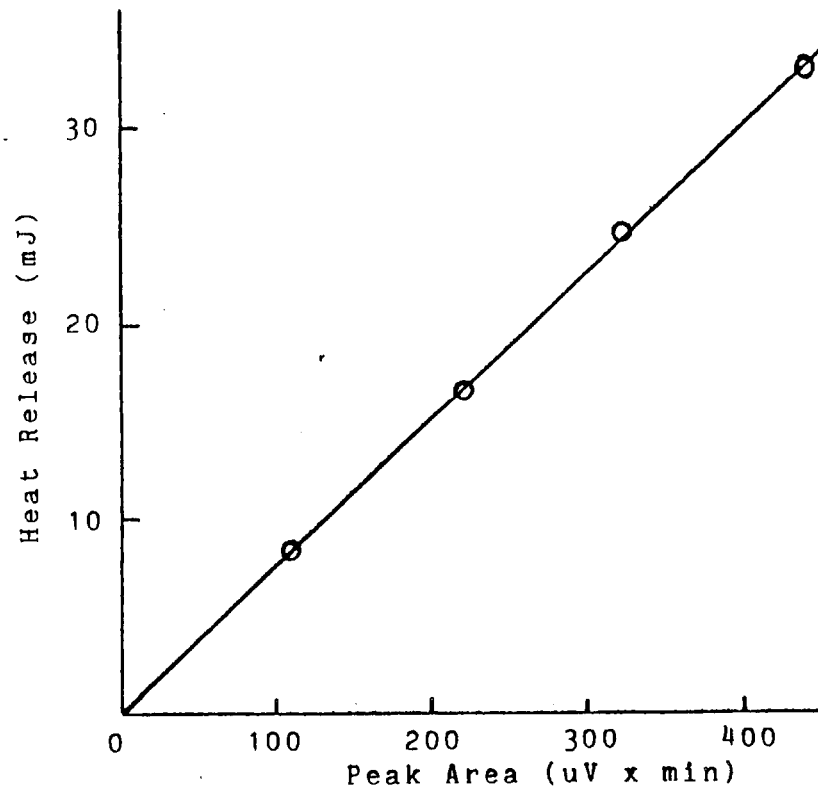


Fig.A-2, Calibration curve for new  $\alpha$ -Fe<sub>2</sub>O<sub>3</sub> powder

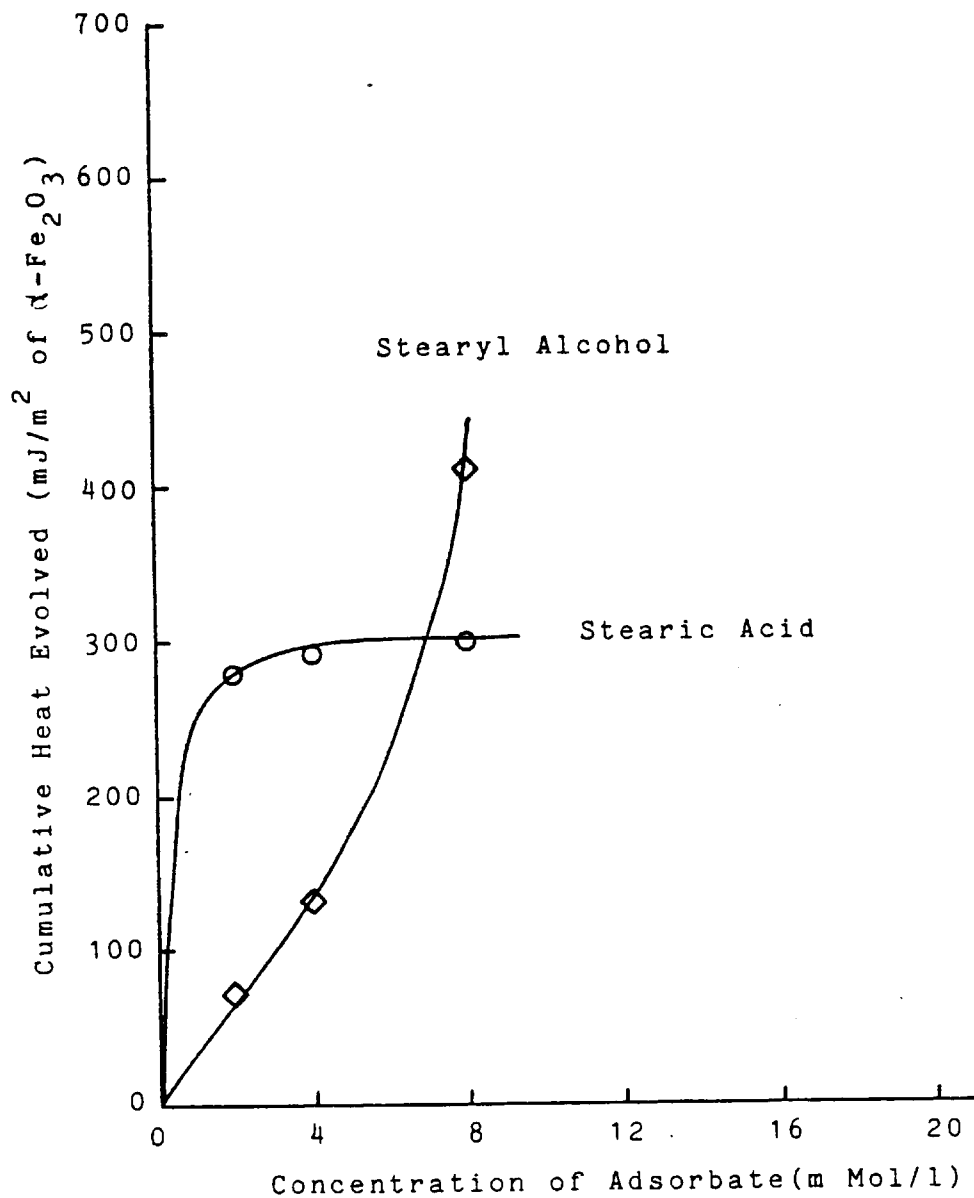


Fig.A-3, Cumulative heat of adsorption onto  $\alpha$ -Fe<sub>2</sub>O<sub>3</sub>(new) at 26.5 C

APPENDIX B

CHANGE OF FRICTION COEFFICIENT WITH TRAVERSE

The change of friction coefficient with traverses is shown in this appendix. All of the friction data in Chapter 4 were derived from this.

This friction test was performed with a Bowden Leben Machine in order to investigate the effect of the EP film and the oiliness reagent on friction. For this purpose, eight kinds of test pieces were prepared and oiliness reagents of stearic acid, stearyl alcohol and methyl stearate were used. The details of these were reported in Chapter 4. The original data of these are shown in Figures B.1 to B.24.



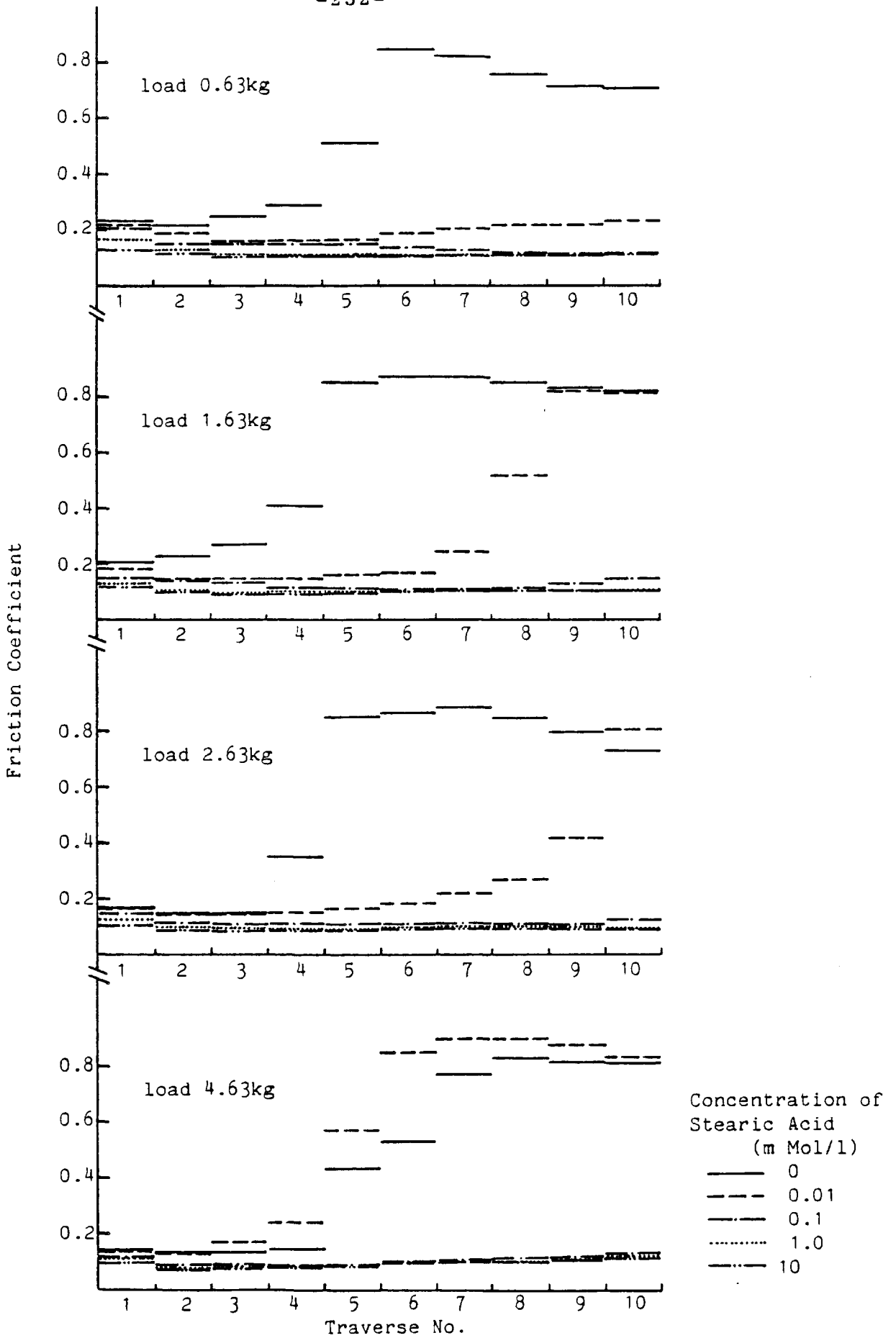


Fig.B-1, Influence of stearic acid on friction coefficient during running-in  
Test Piece : Original Mild Steel

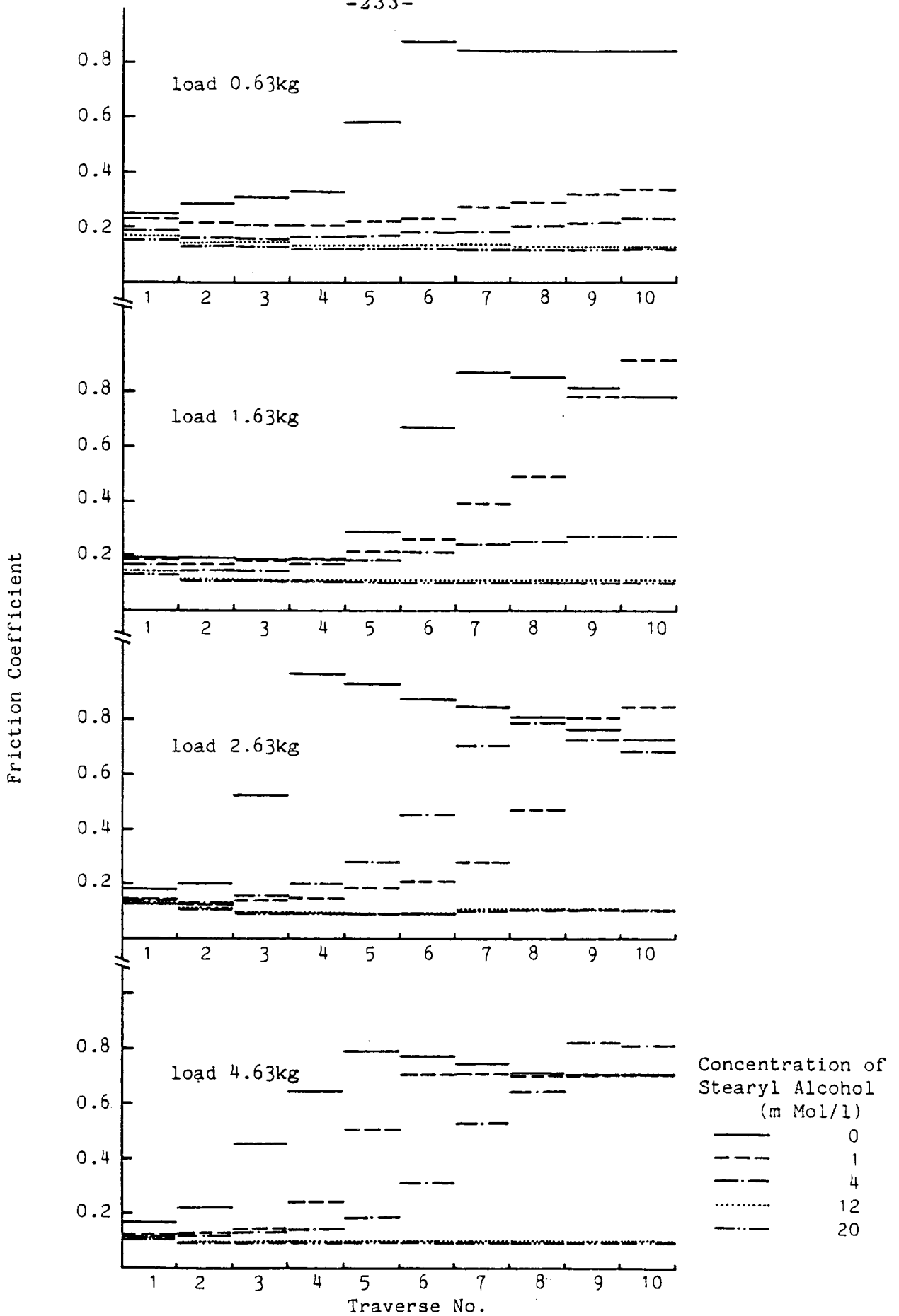


Fig.B-2, Influence of stearyl alcohol on friction coefficient during running-in  
Test Piece : Original Mild Steel

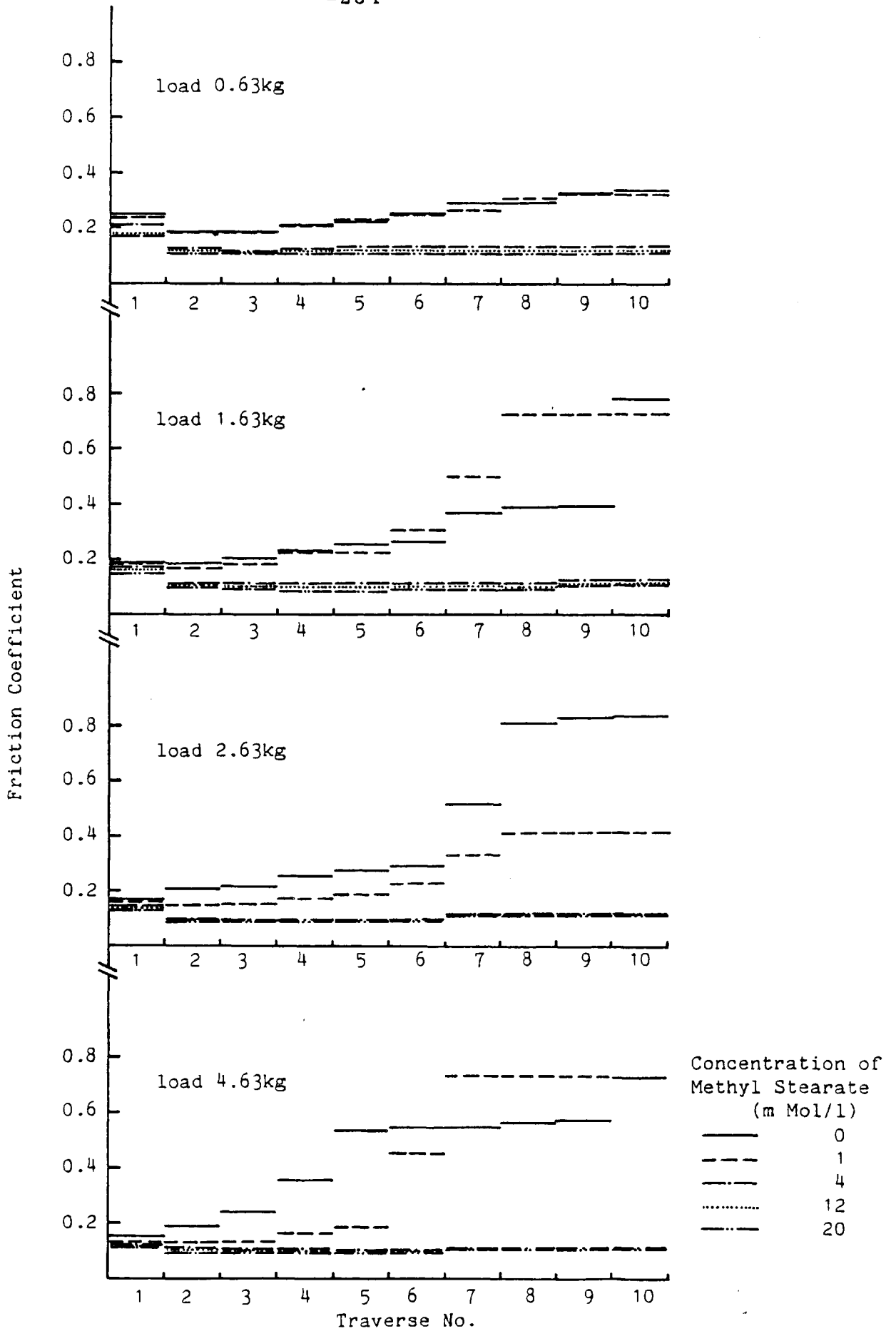


Fig.B-3, Influence of methyl stearate on friction coefficient during running-in  
Test Piece : Original Mild Steel

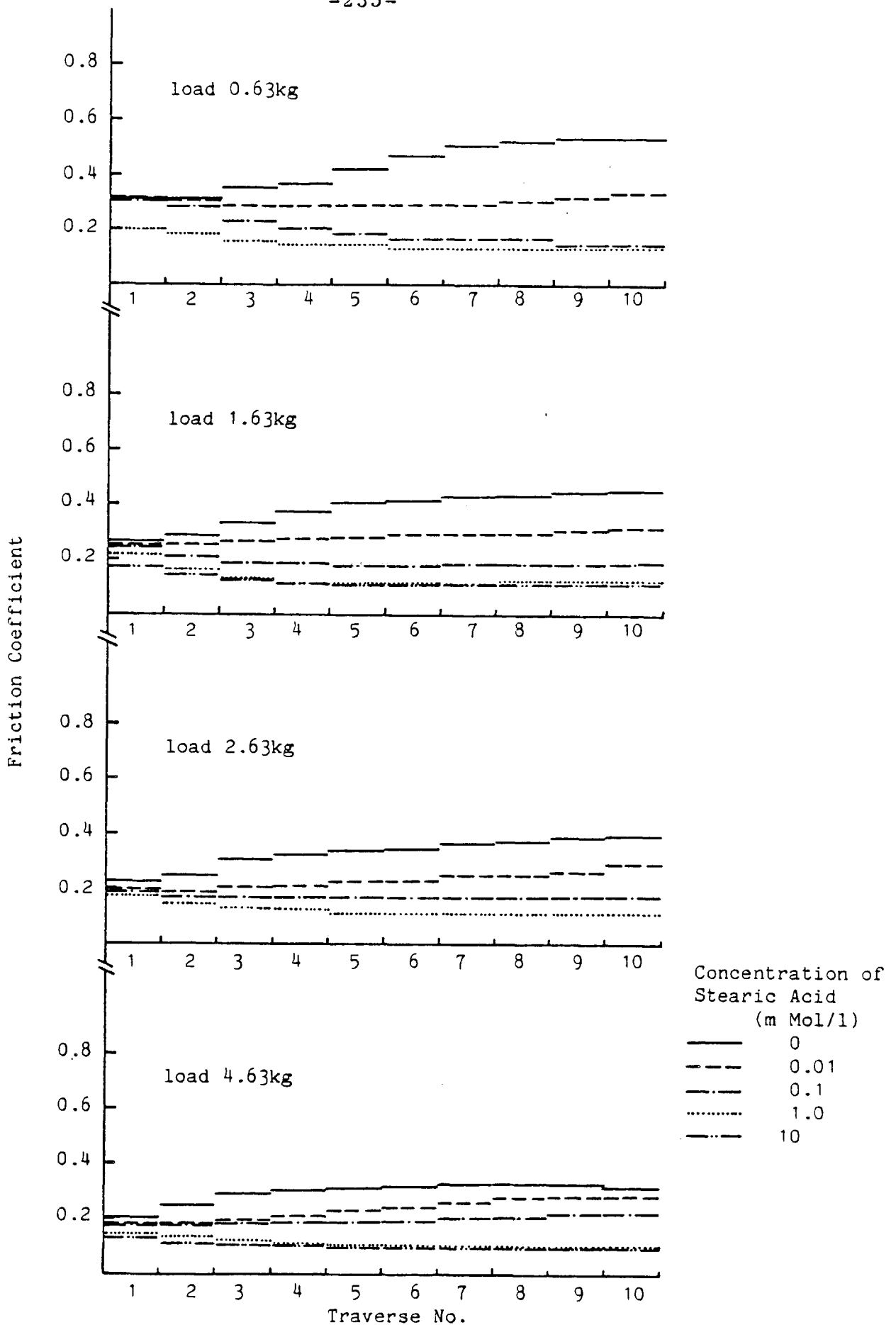


Fig.B-4, Influence of stearic acid on friction coefficient during running-in  
Test Piece : 1 hr Reaction with DBDS

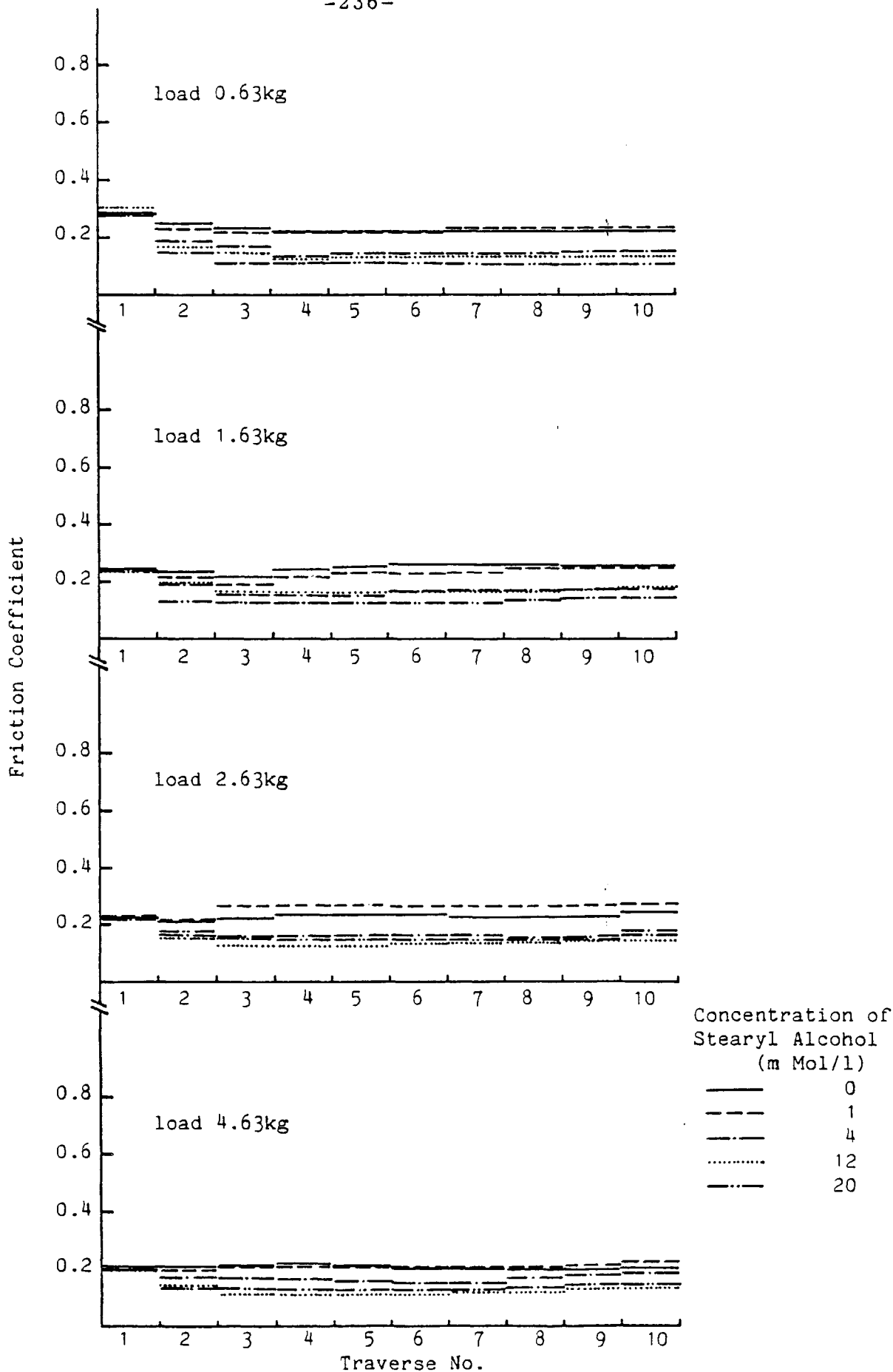


Fig.B-5, Influence of stearyl alcohol on friction coefficient during running-in  
Test Piece : 1hr Reaction with DBDS

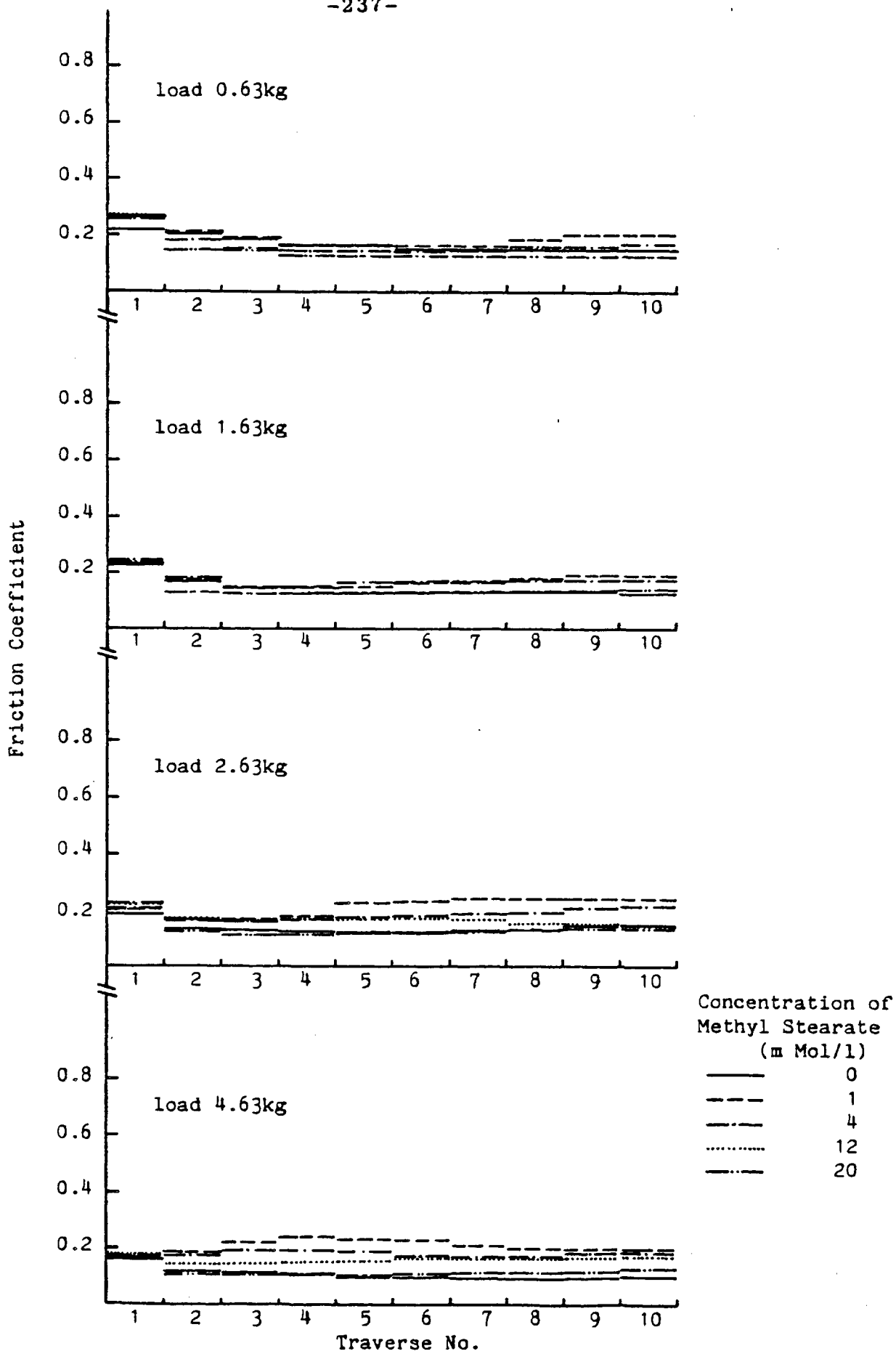


Fig.B-6, Influence of methyl stearate on friction coefficient during running-in  
Test Piece : 1 hr Reaction with DBDS

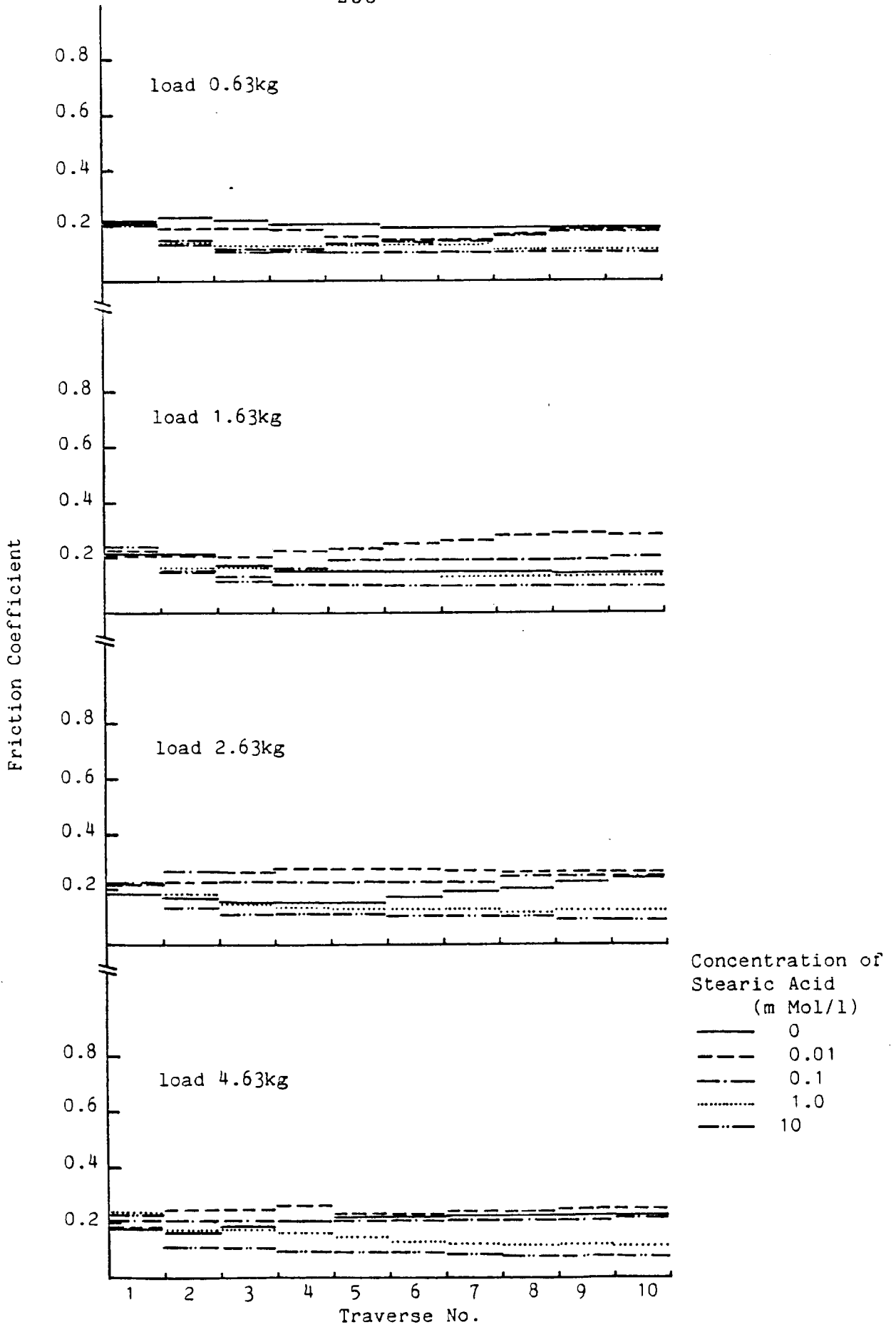


Fig.B-7, Influence of stearic acid on friction coefficient during running-in  
Test Piece : 2 hrs Reaction with DBDS

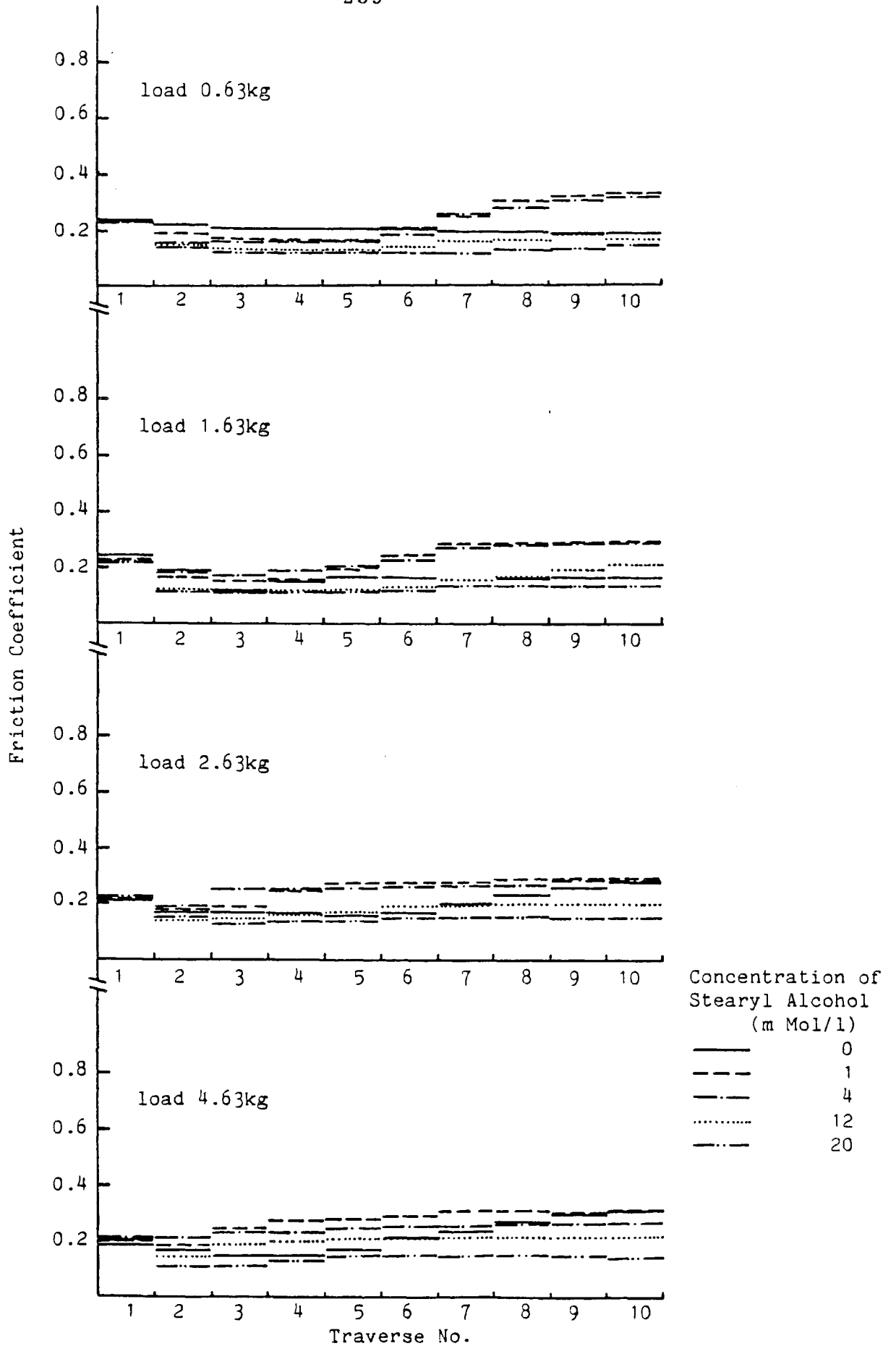


Fig.B-8, Influence of stearyl alcohol on friction coefficient during running-in  
Test Piece : 2 hrs Reaction with DBDS



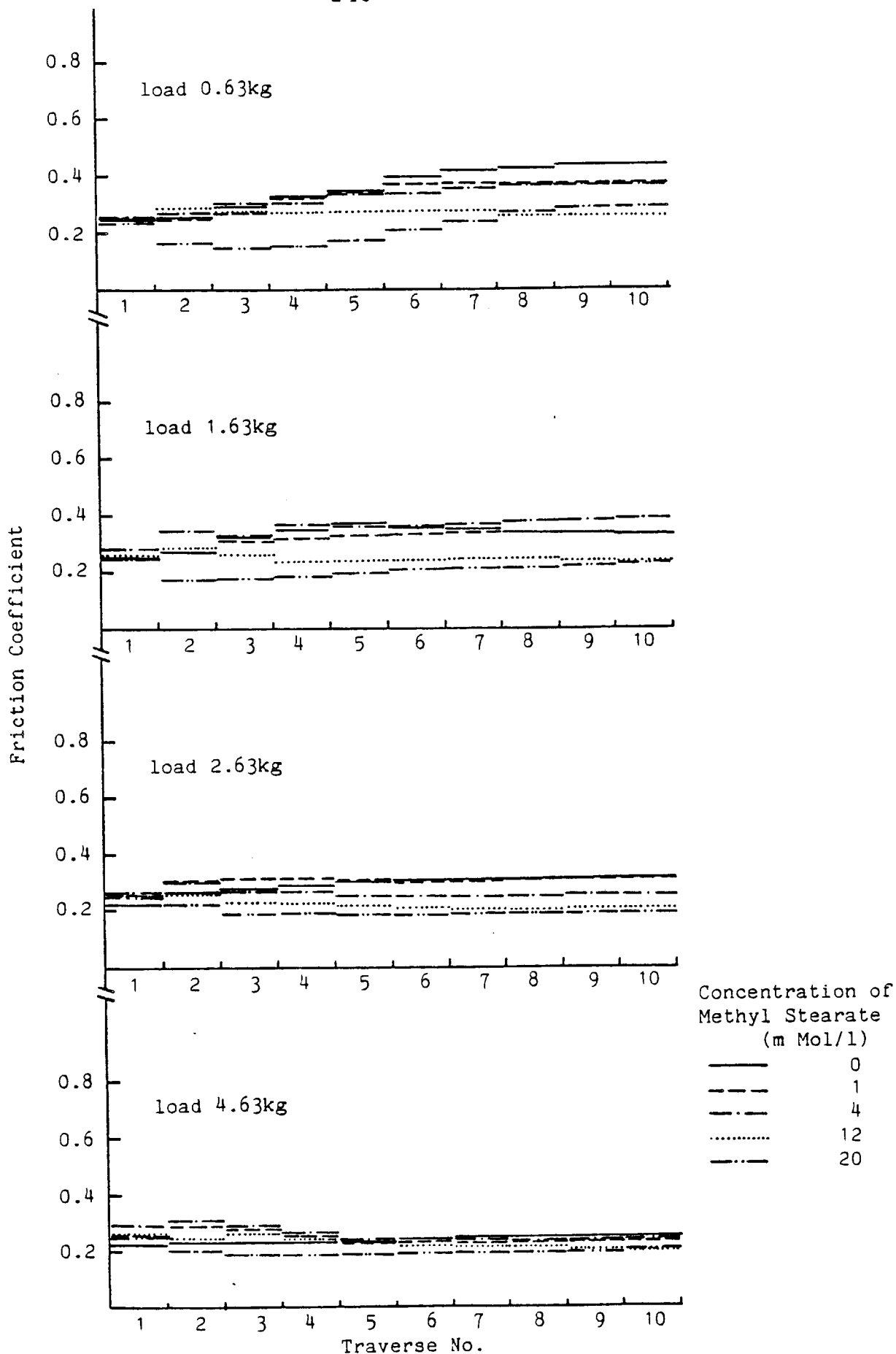


Fig.B-9, Influence of methyl stearate on friction coefficient during running-in  
Test Piece : 2 hrs Reaction with DBDS

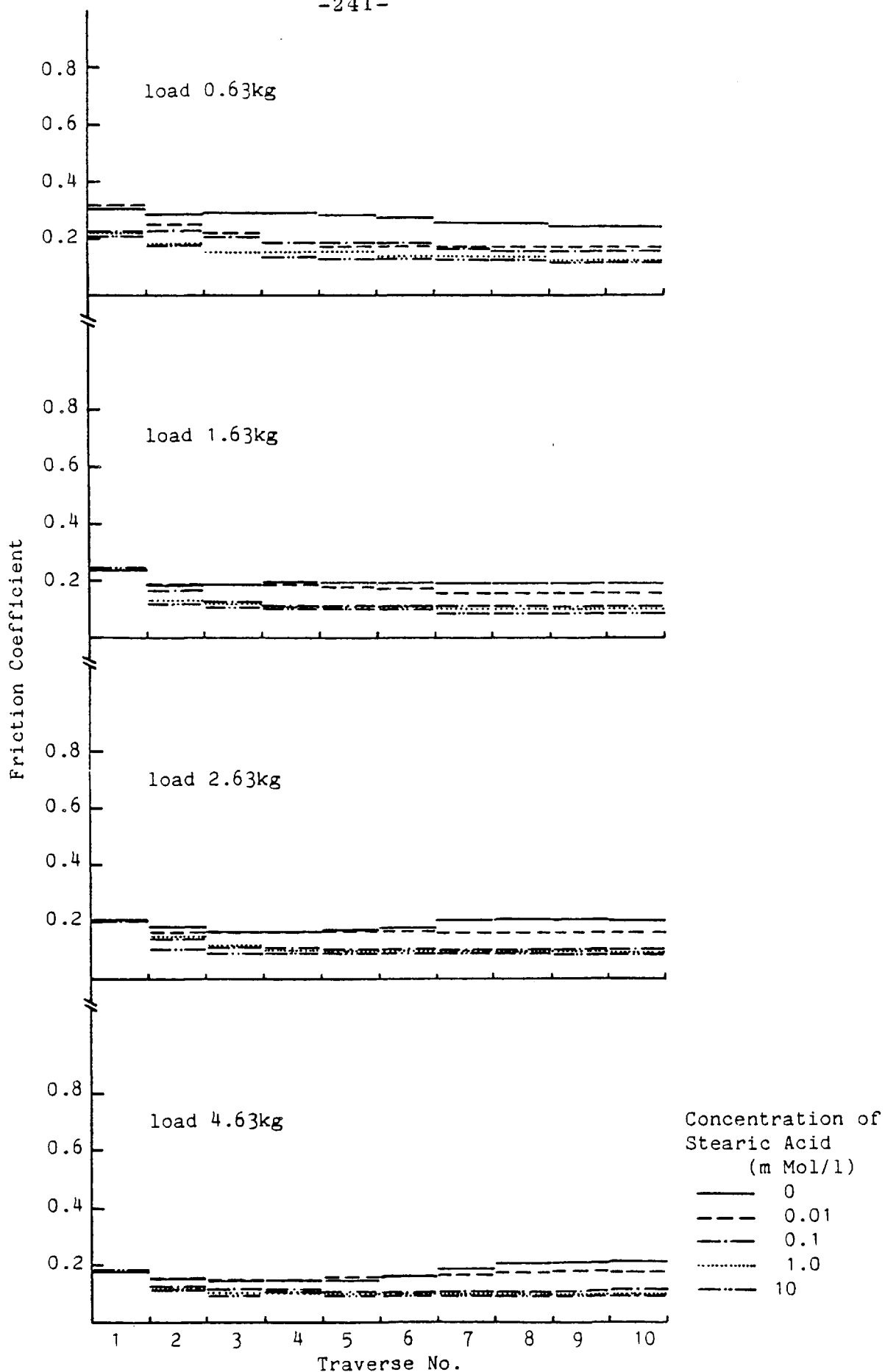


Fig.B-10, Influence of stearic acid on friction coefficient during running-in  
Test Piece : 3 hrs Reaction with DBDS

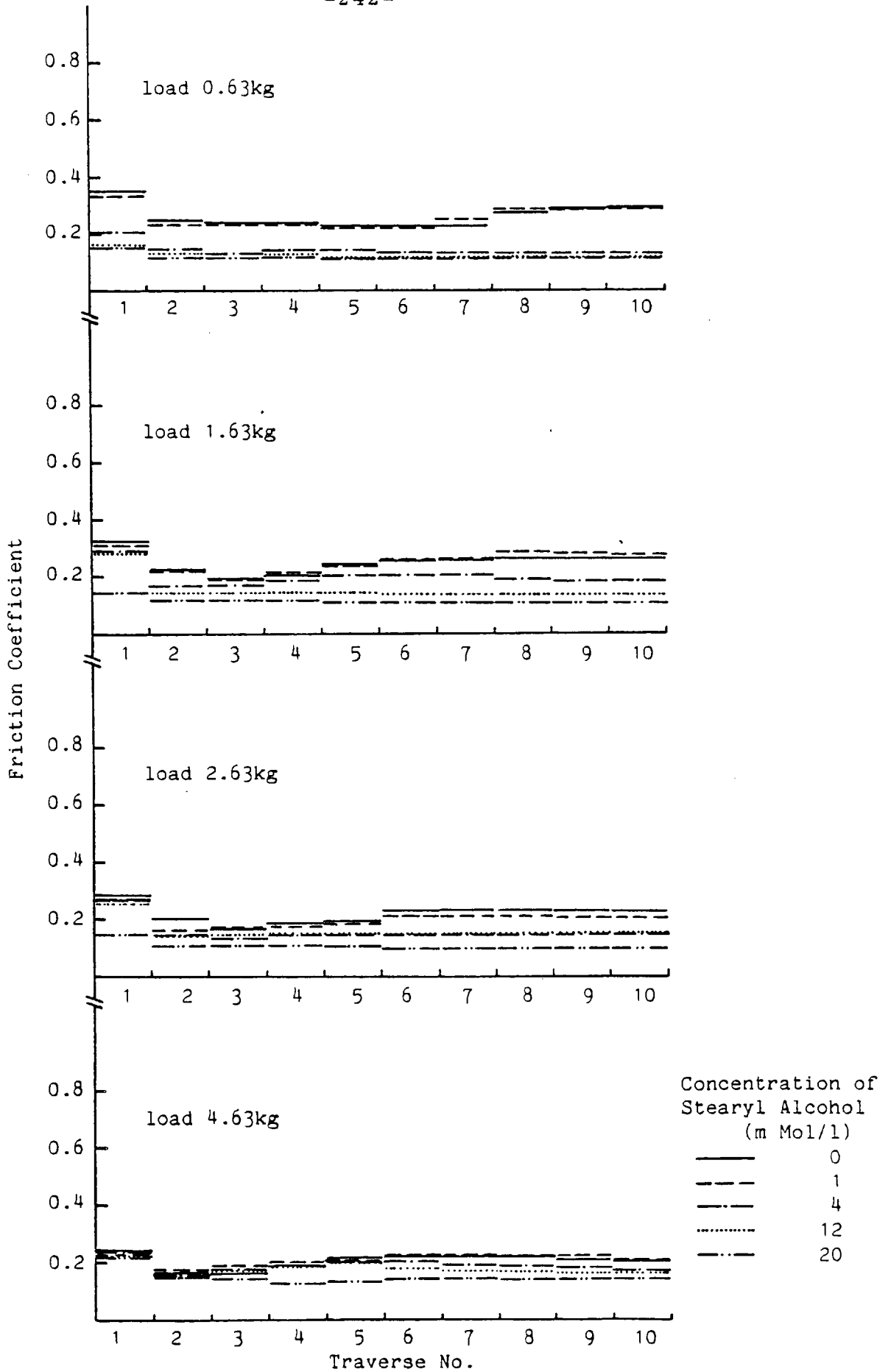


Fig.B-11, Influence of stearyl alcohol on friction coefficient during running-in  
Test Piece : 3 hrs Reaction with DBDS

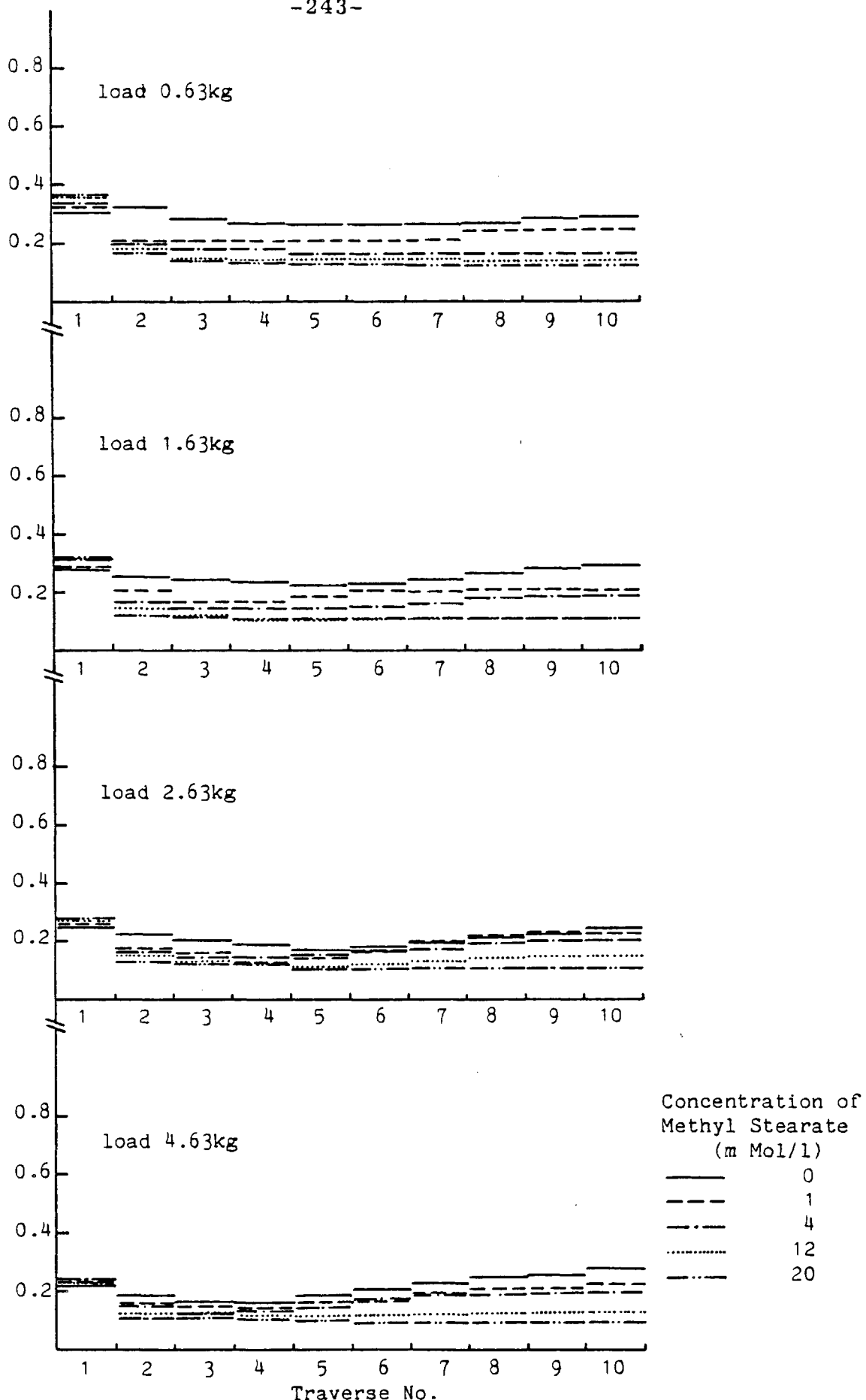


Fig.B-12, Influence of methyl stearate on friction coefficient during running-in  
Test Piece : 3 hrs Reaction with DBDS

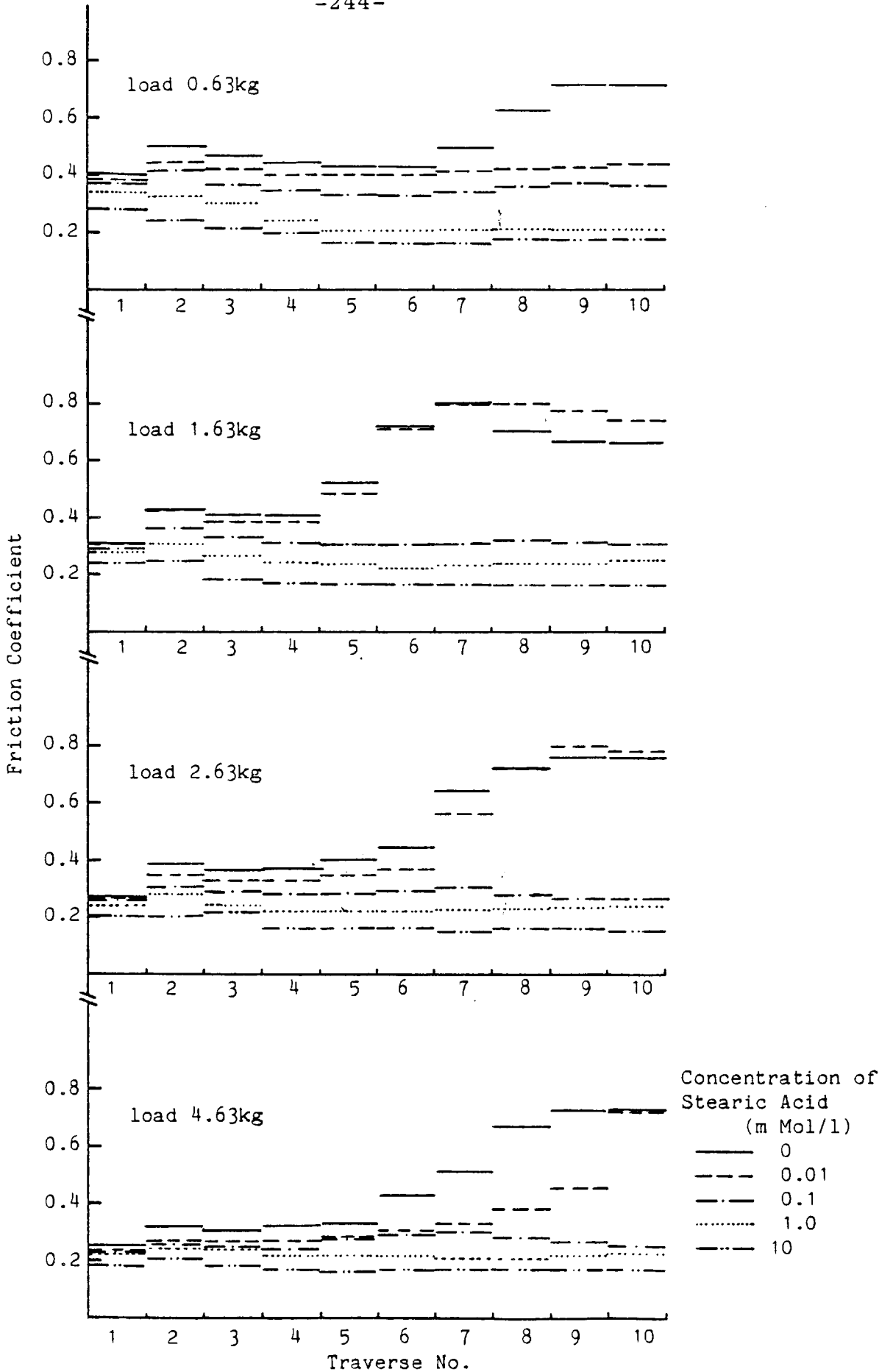


Fig.B-13, Influence of stearic acid on friction coefficient during running-in  
Test Piece : Acid immersion

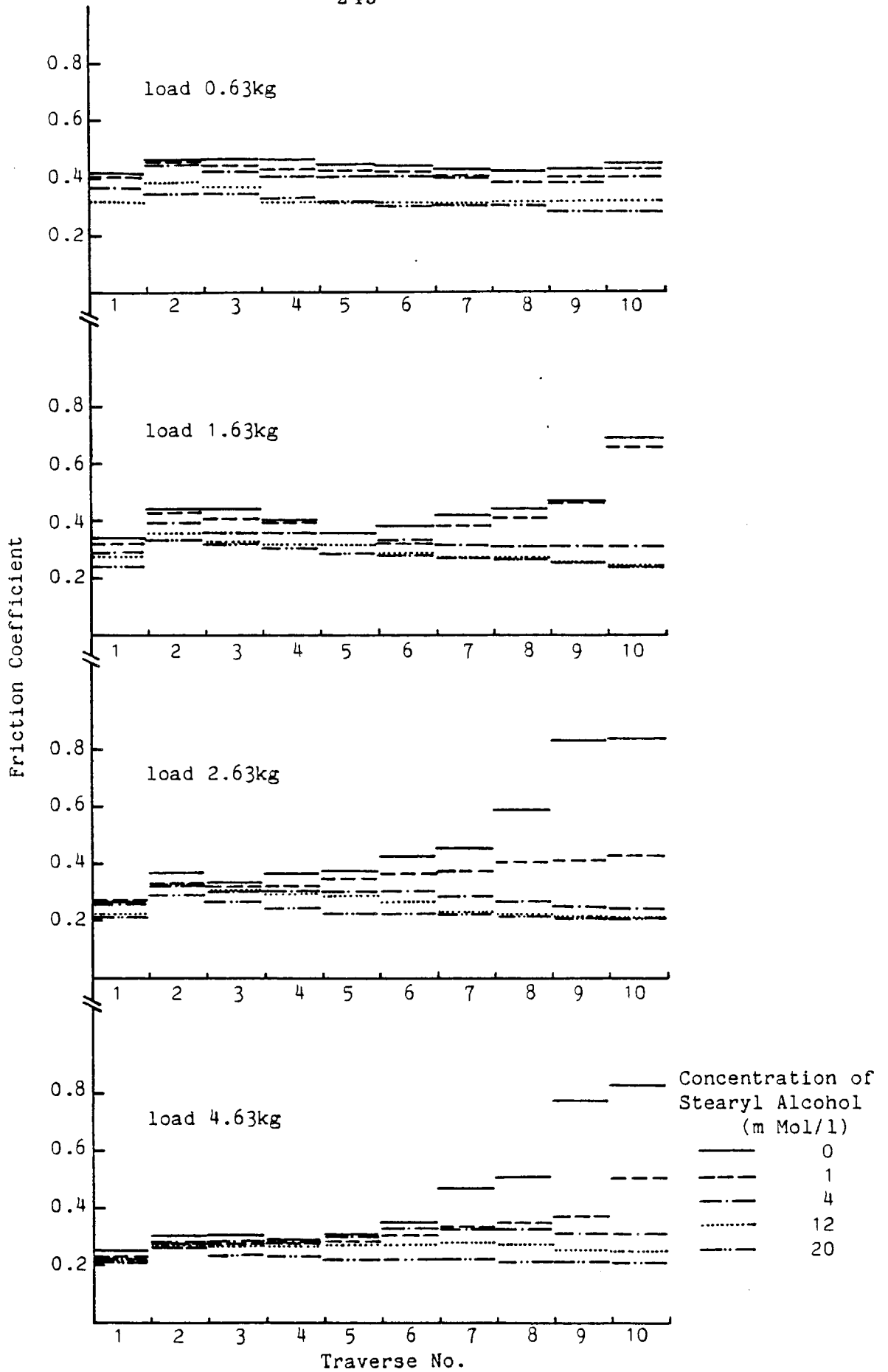


Fig.B-14, Influence of stearyl alcohol on friction coefficient during running-in  
Test Piece : Acid immersion

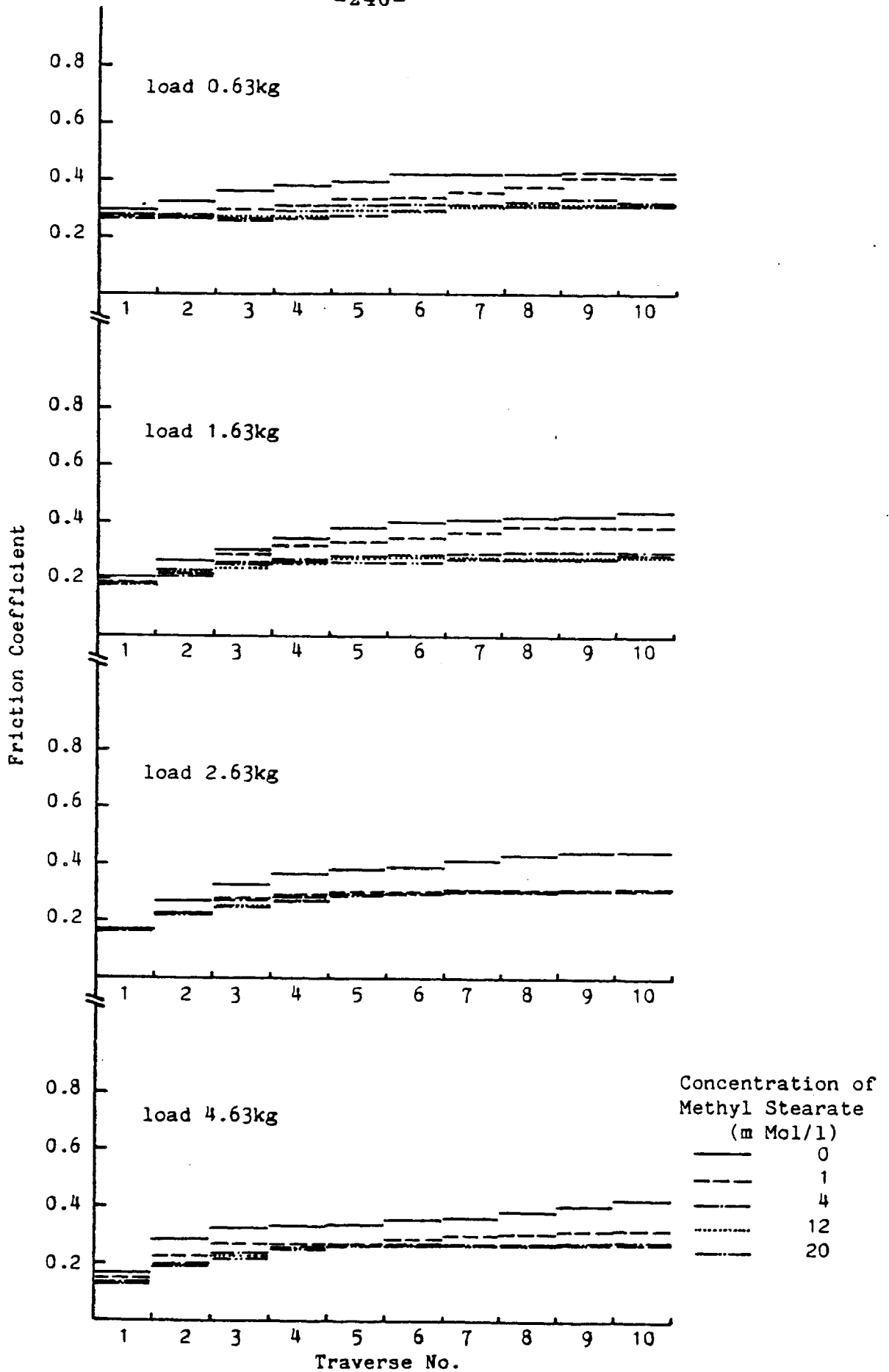


Fig.B-15, Influence of methyl stearate on friction coefficient during running-in  
Test Piece : Acid immersion

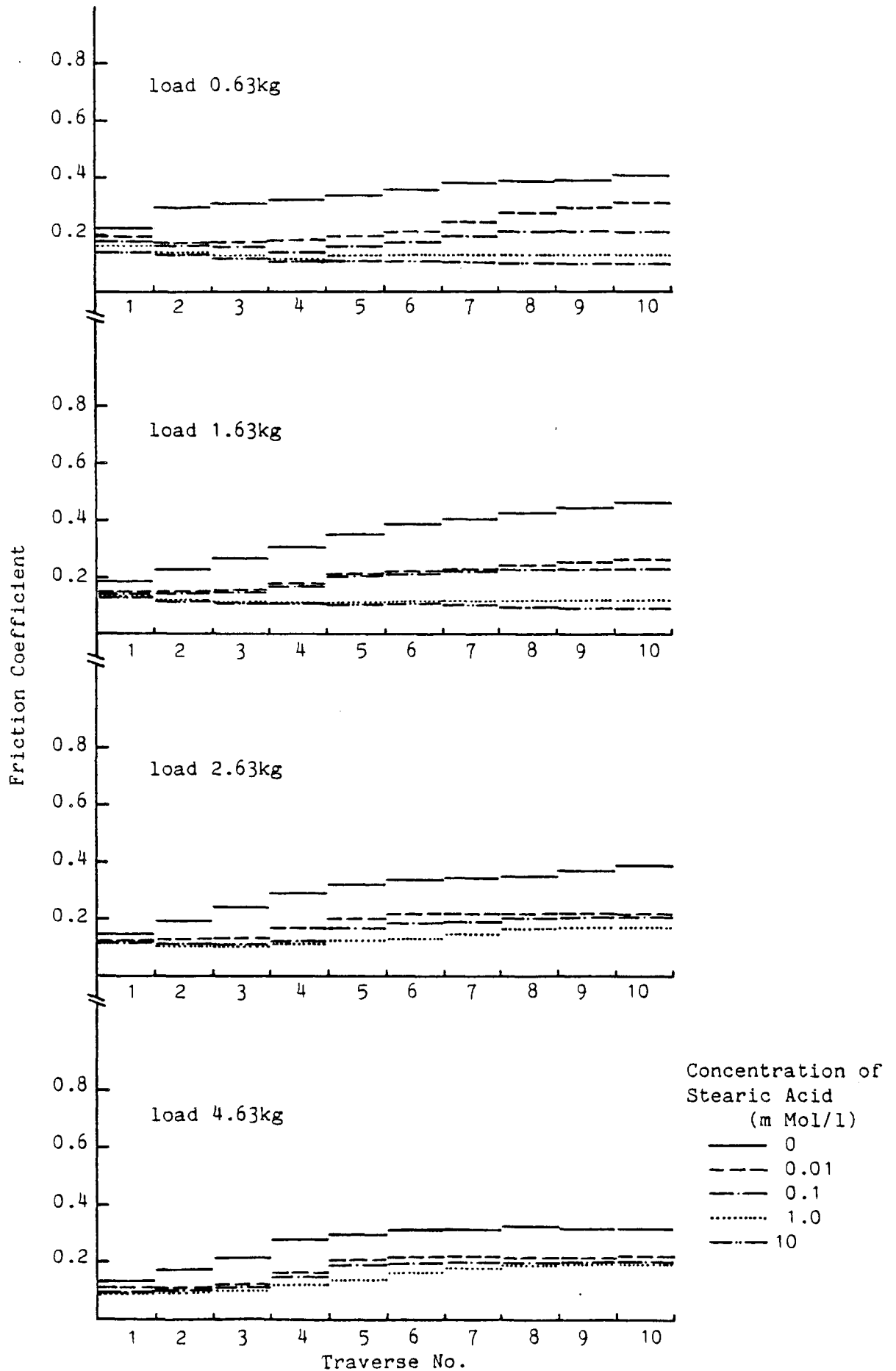


Fig.B-16, Influence of stearic acid on friction coefficient during running-in  
Test Piece : 1 hr Reaction with DBDS and then acid immersion



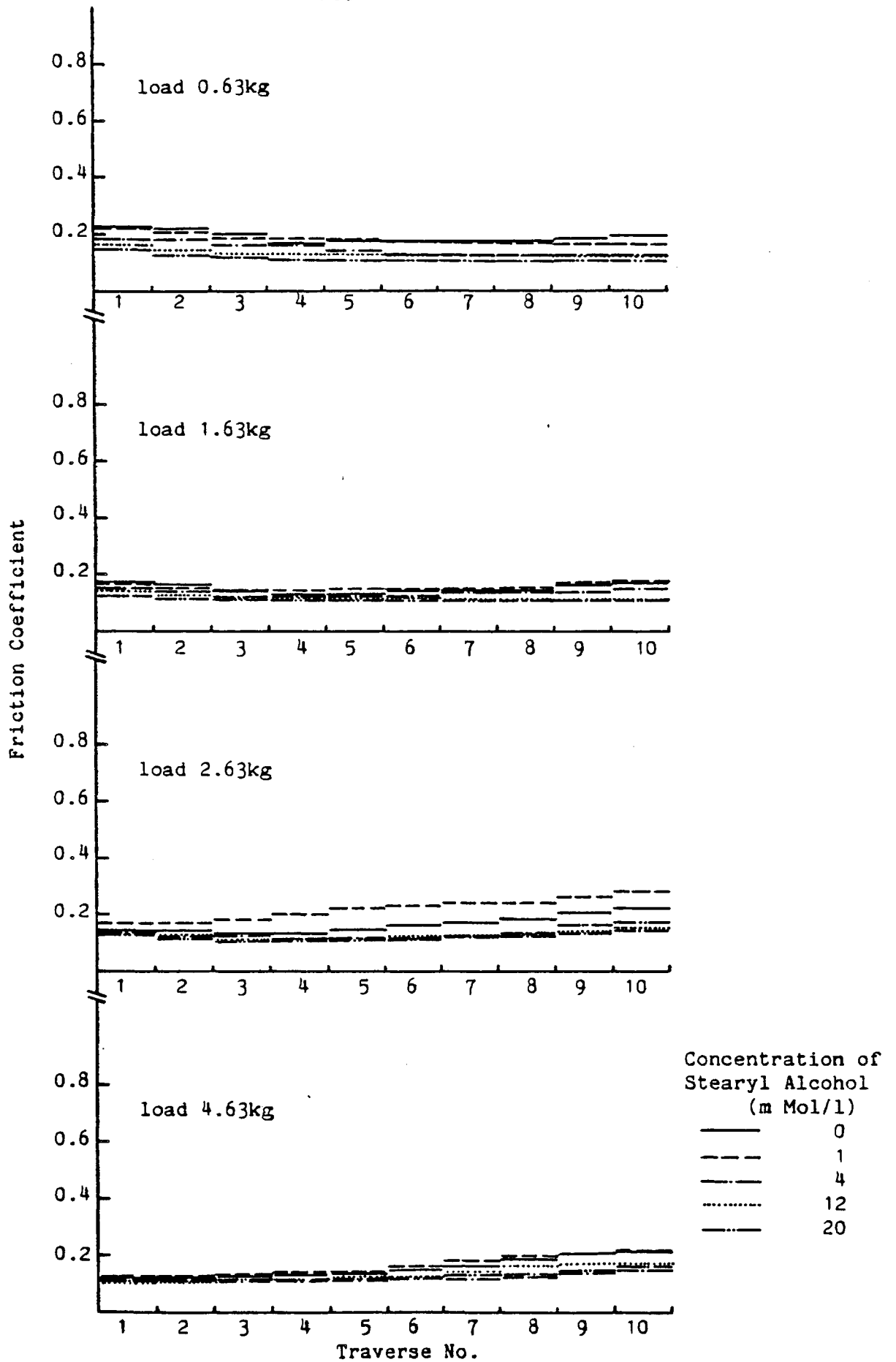


Fig.B-17, Influence of stearyl alcohol on friction coefficient during running-in  
Test Piece : 1 hr Reaction with DBDS and then acid immersion

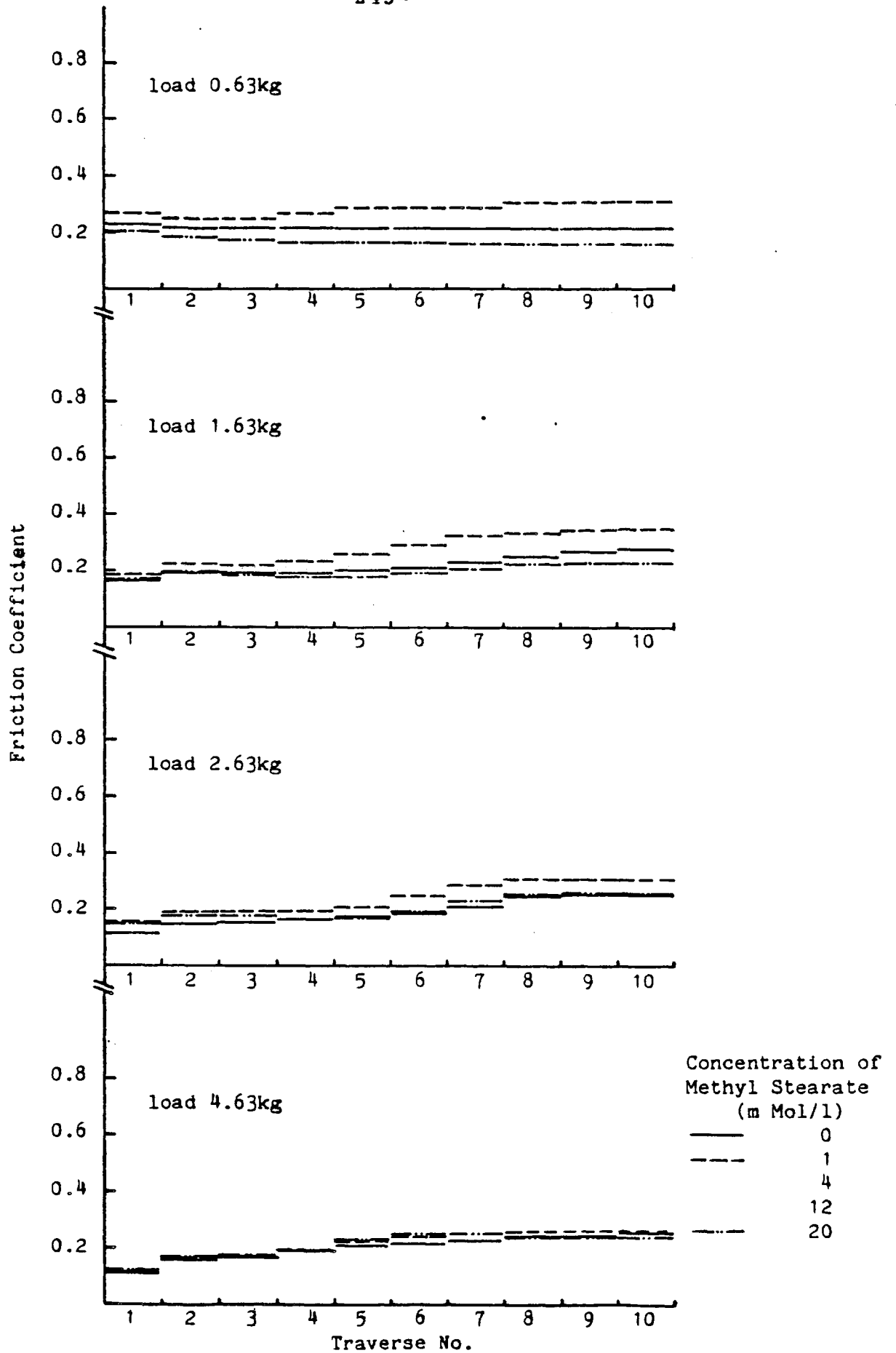


Fig.B-18, Influence of methyl stearate on friction coefficient during running-in  
Test Piece : 1 hr Reaction with DBDS and then acid immersion

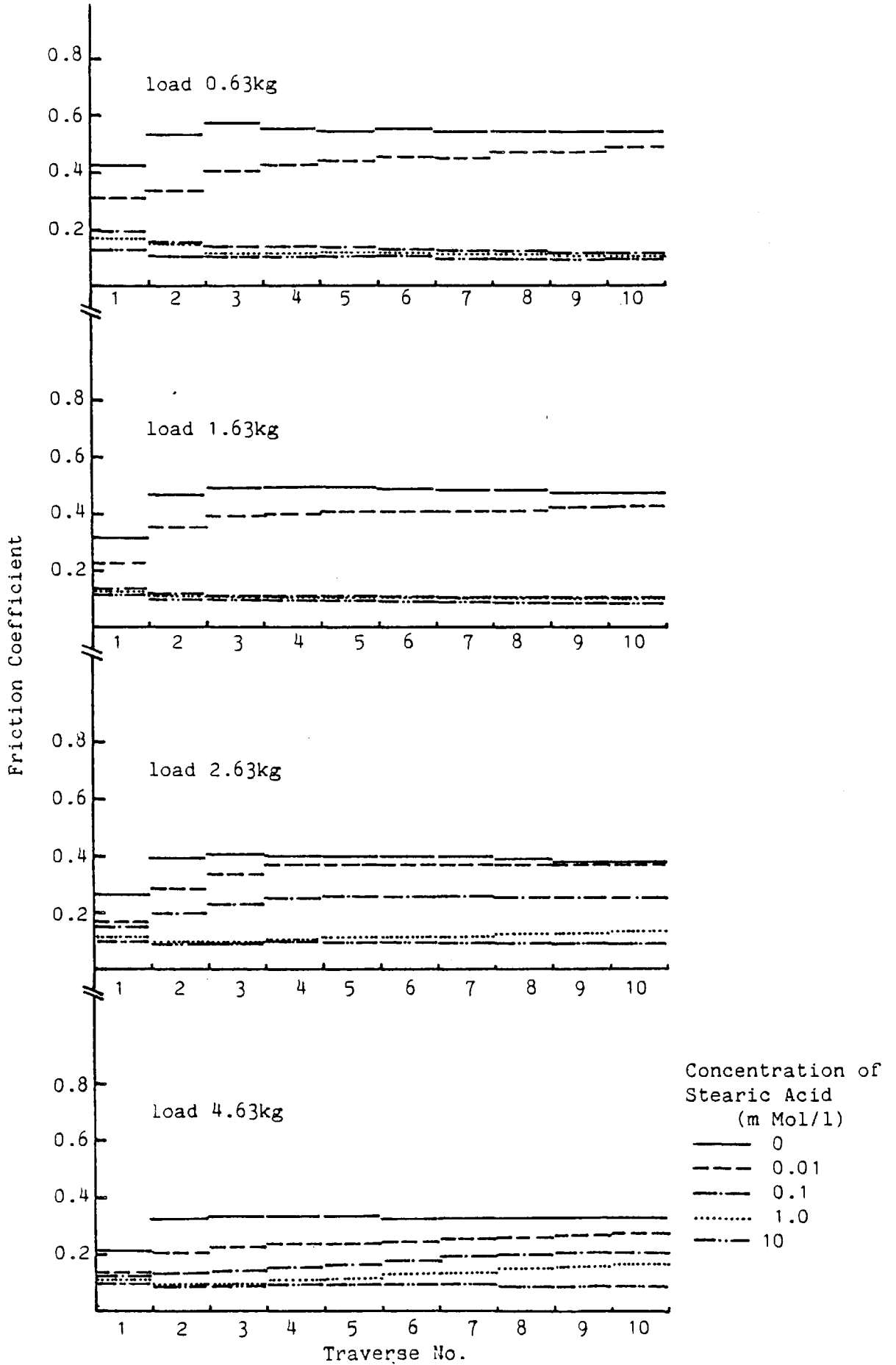


Fig.B-19, Influence of stearic acid on friction coefficient during running-in  
Test Piece : 2 hrs Reaction with DBDS and then acid immersion

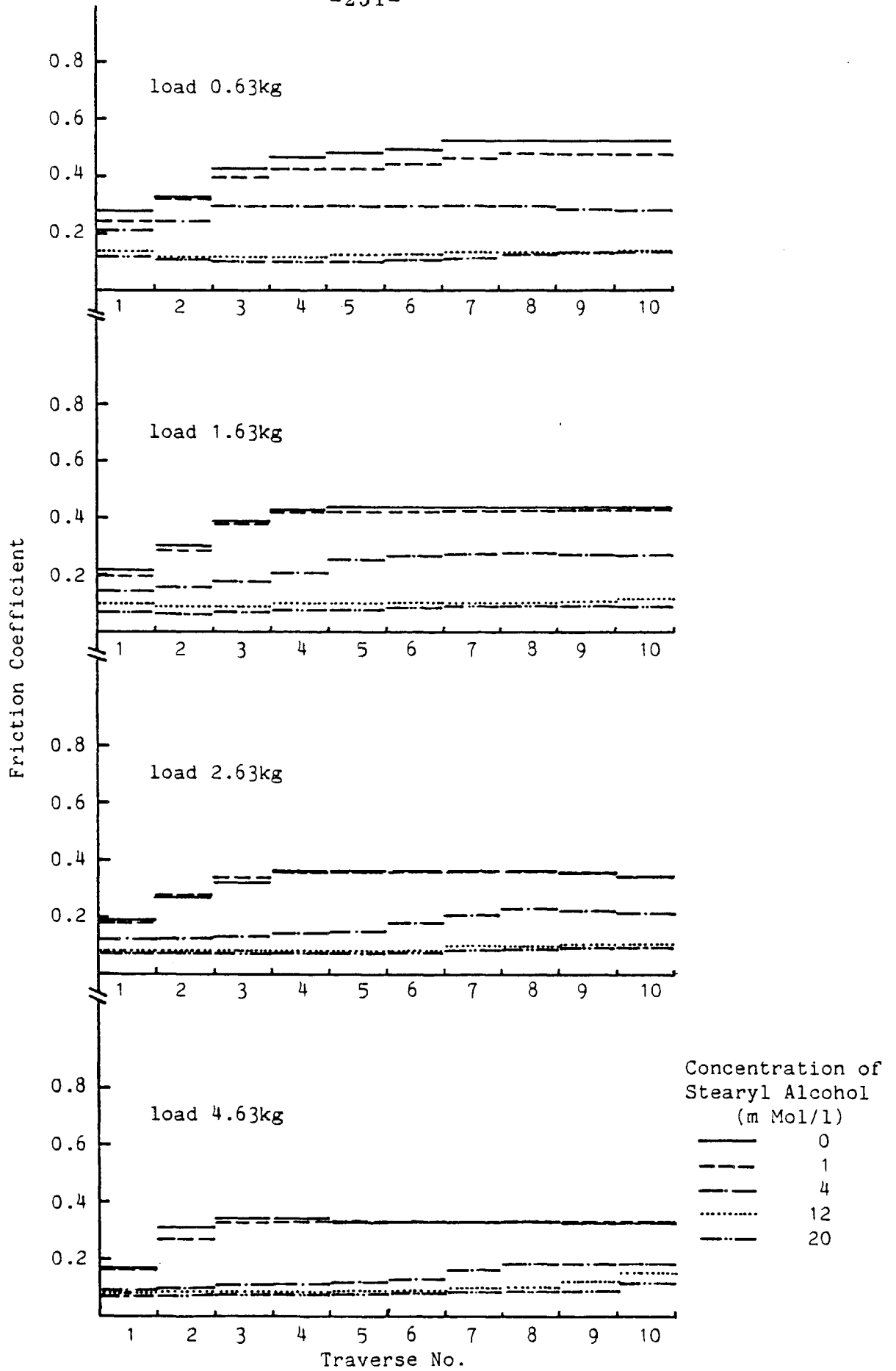


Fig.B-20, Influence of stearyl alcohol on friction coefficient during running-in  
Test Piece : 2 hrs Reaction with DBDS and then acid immersion

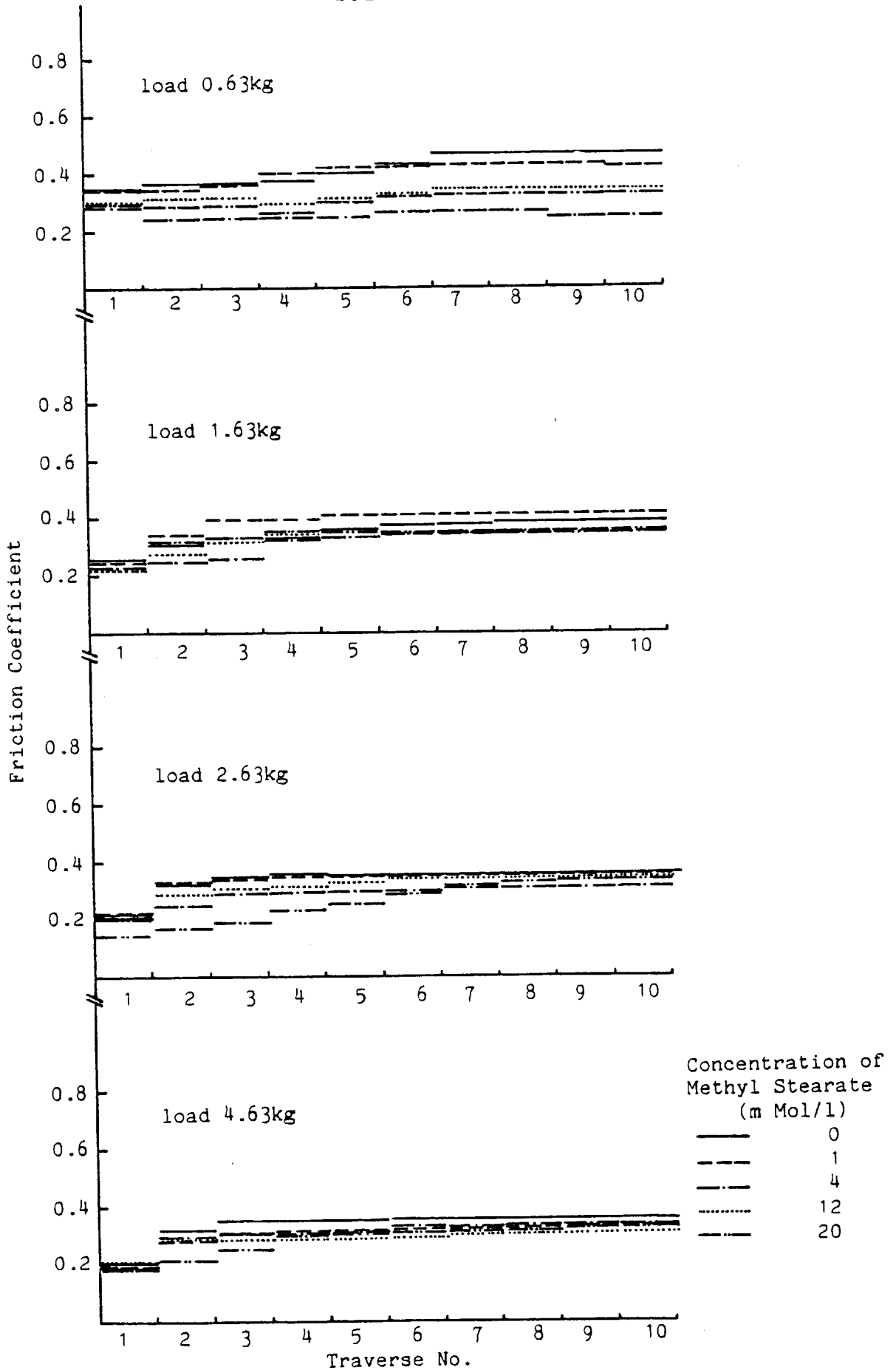


Fig.B-21, Influence of methyl stearate on friction coefficient during running-in  
Test Piece : 2 hrs Reaction with DBDS and then acid immersion

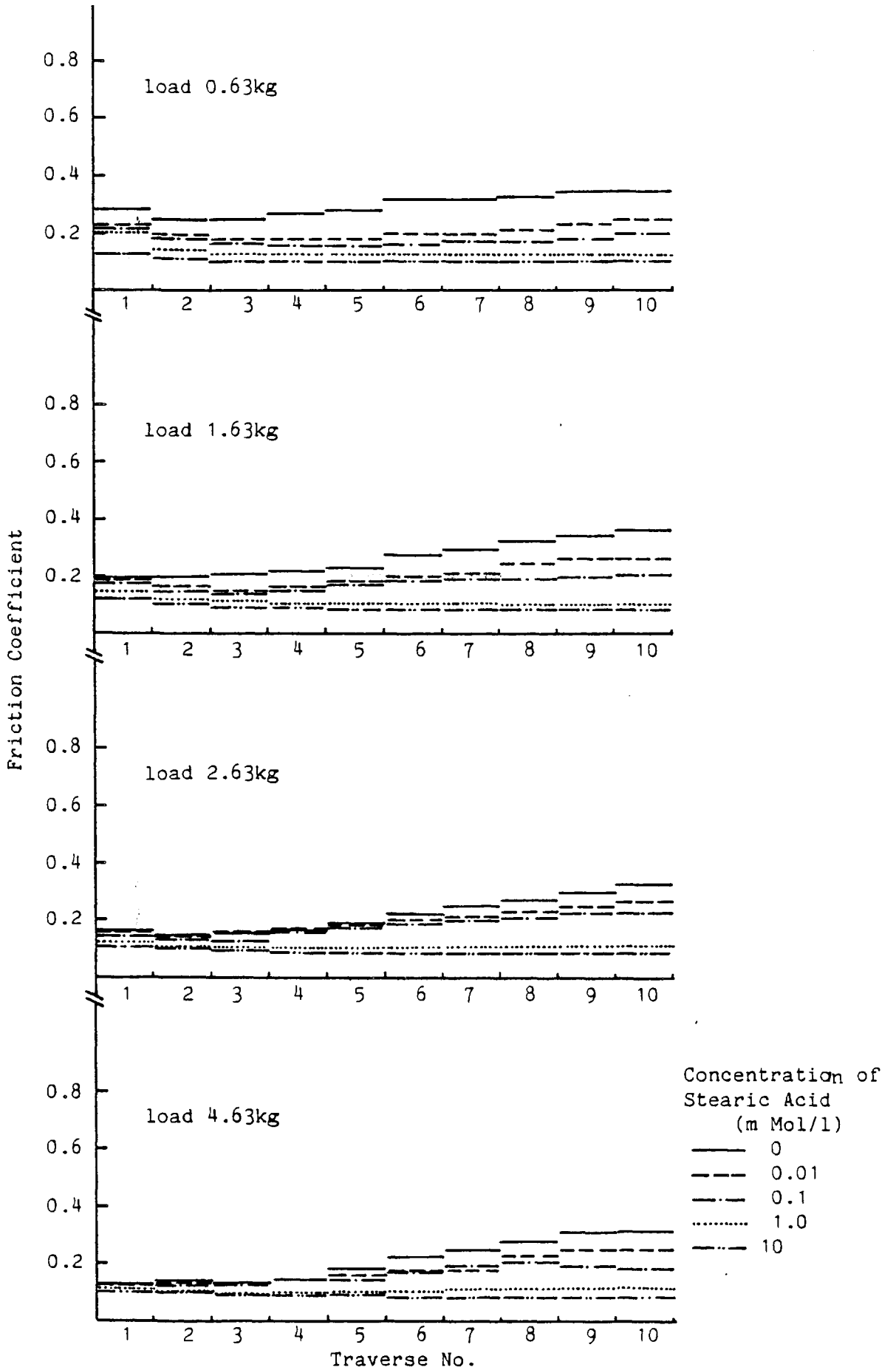


Fig.B-22, Influence of stearic acid on friction coefficient during running-in  
Test Piece : 3 hrs Reaction with DBDS and then acid immersion

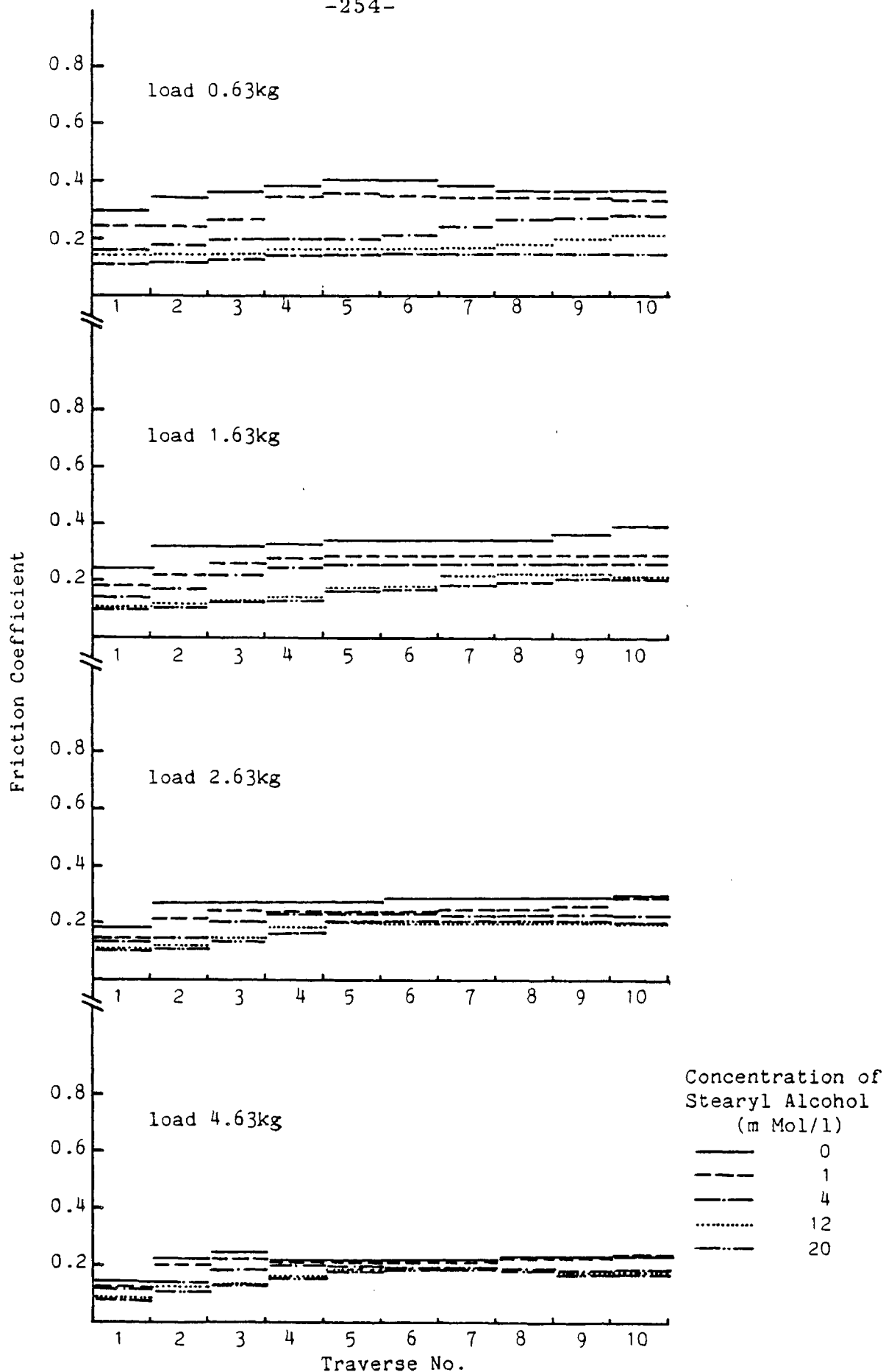


Fig.B-23, Influence of stearyl alcohol on friction coefficient during running-in  
Test Piece : 3 hrs Reaction with DBDS and then acid immersion

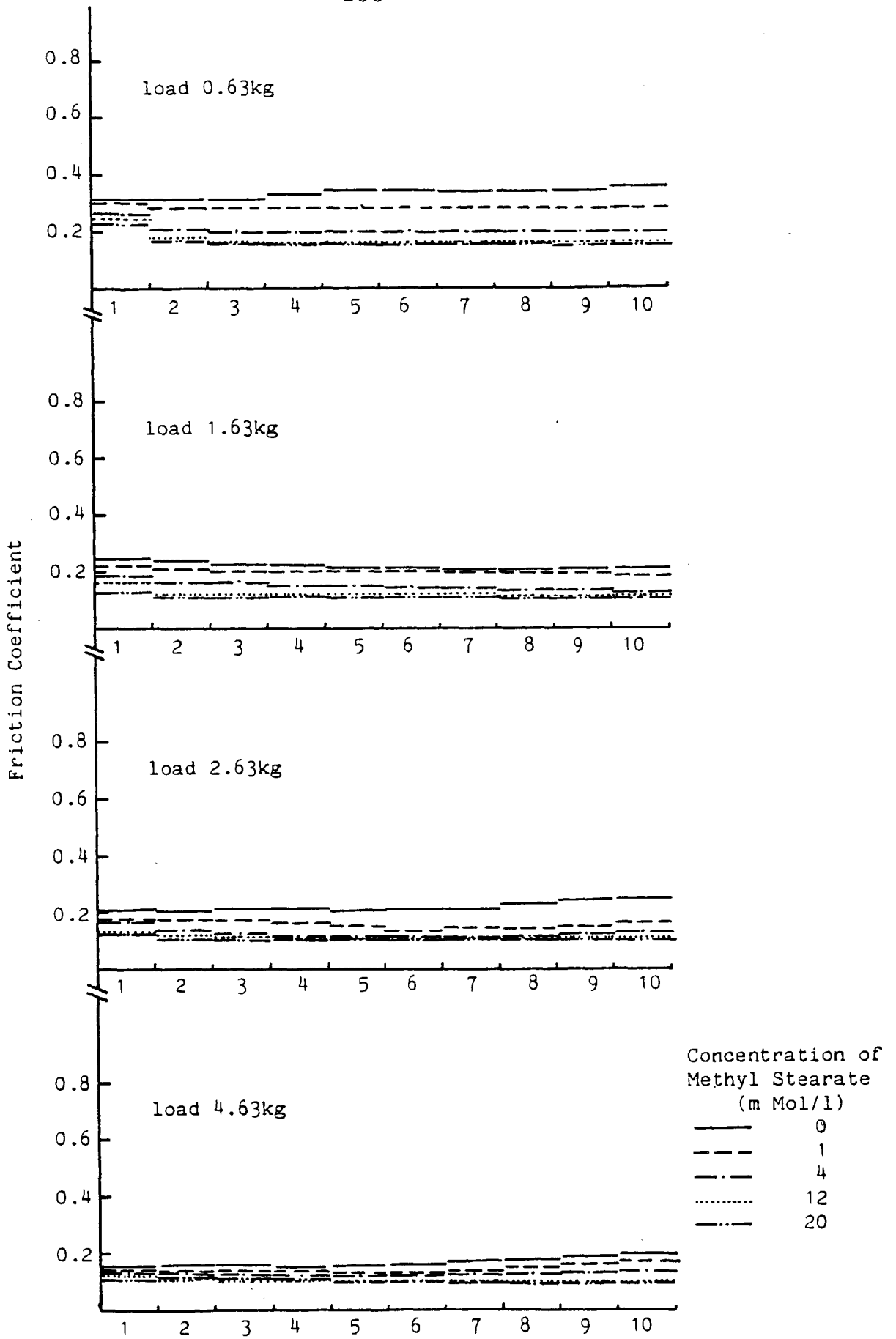


Fig.B-24, Influence of methyl stearate on friction coefficient during running-in  
Test Piece : 3 hrs Reaction with DBDS and then acid immersion



REFERENCES

- (1) A Cameron, "The Role of Surface Chemistry in Lubrication and Scuffing", ASLE Trans, 23, 388-392 (1979)
- (2) F P Bowden and D Tabor, "The Friction and Lubrication of Solids", Oxford University Press (1971)
- (3) H Czichos, "Tribology", Elsevier Scientific Publishing Company (1978)
- (4) A Cameron, "Basic Lubrication Theory", Longman Group Limited (1970)
- (5) A Cameron, "Basic Lubrication Theory, 3rd Edition", Ellis Horwood Limited (1981)
- (6) H A Spikes and A Cameron, "Additive Interference in Dibenzyl Disulphide Extreme Pressure Lubrication", ASLE Trans, 17, 283-289 (1974)
- (7) R W Hiley, "Polysulphide as Extreme Pressure Lubricant Additives", ASLE Preprint No 80-LC-7A-3 (1980)
- (8) T N Mills and A Cameron, "A New Lubricant Test Device", ASLE Preprint No 80-AM-40-1 (1980)
- (9) T Sakurai, S Ikeda and H Okabe, "The Mechanism of Reaction of Sulphur Compounds with Steel Surface During Boundary Lubrication Using S-35 as a Tracer", ASLE Trans, 5, 67-74 (1962)
- (10) S Hironaka, Y Yahagi and T Sakurai, "Heat of Adsorption and Anti-Wear Properties of Some Surface Active Substances", Bull Japan Petrol Inst, 17, 201-205 (1975)

- (11) S Hironaka, Y Yahagi and T Sakurai, "Effect of Adsorption of Some Surfactants on the Anti-Wear Properties", ASLE Trans, 21, 231-235 (1977)
- (12) M Kagami, M Yagi, S Hironaka and T Sakurai, "Wear Behaviour and Chemical Friction Modification in Binary-Additives System under Boundary Lubrication Conditions", ASLE Preprint, No 80-LC-8A-2 (1980)
- (13) D F Moore, "Principles and Applications of Tribology", Pergamon Press Limited (1975)
- (14) H Blok, "Fundamental Mechanical Aspects of Boundary Lubrication", SAE Trans, 46 (2) 54-68 (1940)
- (15) F P Bowden, J N Gregory and D Tabor, "Lubrication of Metal Surfaces by Fatty Acids", Nature, 156, (392), 97-101 (1945)
- (16) J T Burwell, Jr, "Survey of Possible Wear Mechanisms", Wear 1, 119-141 (1957/58)
- (17) W A Glaeser, "Friction of Boundary Films", Fundamentals of Tribology edited by N P Suh and N Saka, 381-384 (1978)
- (18) T F J Quinn, "The Classifications, Laws, Mechanisms and Theories of Wear", Fundamentals of Tribology edited by N P Suh and N Saka, 477-492 (1978)
- (19) S L Rice, "A Review of Wear Mechanism and Related Topics", Fundamentals of Tribology edited by N P Suh and N Saka, 469-476 (1978)
- (20) S Jahanmir, "On the Wear Mechanisms and the Wear Equations", Fundamentals of Tribology edited by N P Suh and N Saka, 455-468 (1978)

- (21) M B Peterson, "Boundary Lubrication", edited by F F Ling, ASME, 19 (1969)
- (22) M Tomaru, S Hironaka and T Sakurai, "Effects of Oxygen on the Load-Carrying Action of Some Additives", Wear, 41, 117-140 (1977)
- (23) T S Eyre, "The Mechanism of Wear", Tribology, 91-95 (1978)
- (24) K Nakayama, H Okabe and T Sakurai, "The Mechanism of Adhesive Wear of Copper Under Boundary Lubrication", ASLE Trans, 16, 91-96 (1973)
- (25) D Levine and W A Zisman, "Physical Properties of Monolayers Adsorbed at the Solid-Air Interface. II. Mechanical Durability of Aliphatic Polar Compounds and Effect of Halogenation", J Phys Chem, 61, 1188-1196 (1957)
- (26) K Nakayama and T Sakurai, "A Contribution to the Mechanism of Chemical Wear under Boundary Lubrication", Bull Japan Petrol Inst 15, 107-114 (1973)
- (27) T Sakurai, K Sato and Y Yamamoto, "Reaction Between Chlorine Extreme Pressure Additives and Metal Surfaces at High Temperatures", Bull Japan Petrol Inst 7, 17-24 (1965)
- (28) C F Prutton, D Turnbull and G Dlouhly, "Reaction Rate of Hydrogen Chloride and Sulphide with Steel", Ind Eng Chem, 37, (11), 1092-1097 (1945)
- (29) D H Buckley, "Friction Induced Surface Activity of Some Simple Organic Chloride and Hydrocarbons with Iron", ASLE Trans, 17, 36-43 (1974)

- (30) G L Simard, H W Russell and H R Nelson, "Extreme Pressure Lubricants: Film-Forming Action of Lead Naphthenate and Free Sulphur", Ind Eng Chem, 33, (11), 1352-1359 (1941)
- (31) O Beck, J W Givens and E C Williams, "On the Mechanism of Boundary Lubrication, II. Wear Prevention by Addition Agents", Proc Roy Soc (London) Ser A177, 103-118 (1940)
- (32) D Godfrey, "The Lubrication Mechanism of Tricresyl Phosphate on Steel", ASLE Trans, 8, 1-11 (1965)
- (33) D H Buckley, "Oxygen and Sulphur Interactions with a Clean Iron Surface and the Effect of Rubbing Contact on These Interactions", ASLE Trans, 17, 206-212 (1974)
- (34) A Sethuramiah, H Okabe and T Sakurai, "Effect of Surface Temperature in Extreme Pressure Lubrication", Bull Japan Petrol Inst, 14, 27-39 (1972)
- (35) T Sakurai, K Sato, H Hamaguchi and K Matsuo, "Effect of Internal Stress on the Wear Behaviour of Steel During Boundary Lubrication", ASLE Trans, 17, 213-223 (1974)
- (36) H Hamaguchi, K Sato and T Sakurai, "Effect of Internal Stress on the Wear Behaviour of Steel During Boundary Lubrication - Effects of Load and Argon Atmosphere", Proc JSLE/ASLE International Lubrication Conference, 386-394 (1975)
- (37) K G Allen and E S Forbes, "The Load-Carrying Mechanism of Organic Sulphur Compounds - Application of Electron Probe Microanalysis", ASLE Trans, 11, 162-175 (1968)

- (38) E S Forbes, "The Load-Carrying Action of Organo-Sulphur Compounds - A Review", *Wear*, 15, 87-96 (1970)
- (39) R C Coy and T F J Quinn, "The Use of Physical Methods of Analysis to Identify Surface Layers Formed by Organo-Sulphur Compounds in Wear Tests", *ASLE Trans*, 18, 163-174 (1975)
- (40) A Begelinger, A W J de Gee and G Salomon, "Failure of Thin Film Lubrication - Function - Oriented Characterisation of Additives and Steels", *ASLE Trans*, 23, 23-34 (1979)
- (41) D Godfrey, "Chemical Changes in Steel Surfaces During Extreme Pressure Lubrication", *ASLE Trans*, 5, 57-60 (1962)
- (42) T Sakurai, K Sato and K Ishida, "Reaction Between Sulphur Compounds and Metal Surfaces at High Temperatures", *Bull Japan Petrol Inst*, 6, 40-99 (1964)
- (43) T Sakurai, H Okabe and M Tomaru, "Effect of Stress-Induced Heterogeneity on Corrosion of Iron Surface of High Temperatures", *Bull Japan Petrol Inst*, 14, 161-168 (1972)
- (44) Y Mizutani, "On the Definition and Effect of Chemical Properties of Surfaces in Friction, Wear and Lubrication", *Fundamentals of Tribology* edited by N P Suh and N Saka 223-236 (1978)
- (45) W Davey and E D Edwards, "The Extreme Pressure Lubricating Properties of Some Sulphides and Disulphides, in Mineral Oil, as Assessed by the Four-Ball Machine", *Wear*, 1, 291-304 (1957/58)

- (46) F T Barcroft and S Daniel, Inst Mech Eng Lubrication and Wear Conference, Paper 17, London, May (1965)
- (47) E S Forbes, K G Allum, E L Neustadter and A J D Reid, "The Load-Carrying Properties of Diester Disulphides", Wear, 15, 341-352 (1970)
- (48) H Okabe, H Nishio and M Masuko, "Tribochemical Surface Reaction and Lubricating Oil Film", ASLE Trans, 22, 65-70 (1979)
- (49) T Sakurai, S Ikeda and H Okabe, "A Kinetic Study on the Reaction of Labelled Sulphur Compounds with Steel Surface during Boundary Lubrication", ASLE Trans, 8, 39-47 (1965)
- (50) T Sakurai, H Okabe and Y Takahashi, "A Kinetic Study of the Reaction of Labelled Sulphur Compounds in Binary Additive Systems during Boundary Lubrication", ASLE Trans, 10, 91-101 (1967)
- (51) A A Mantenffel, K P Yates, H T Bickford and G Wolfram, "Radiotracers Reveal Activity of Extreme-Pressure Additives in Lubrication", ASLE Trans, 7, 249-256 (1964)
- (52) F T Barcroft, "A Technique for Investigating Reaction Between EP Additives and Metal Surfaces at High Temperatures", Wear, 3, 440-453 (1960)
- (53) T Sakurai and K Sato, "Study of Corrosivity & Correlation Between Chemical Reactivity and Load-Carrying Capacity of Oils Containing Extreme Pressure Agents", ASLE Trans, 9, 77-87 (1960)
- (54) E S Forbes and A J D Reid, "Liquid Phase Adsorption/Reaction Studies of Organo-Sulphur Compounds and their Load-Carrying Mechanism", ASLE Trans, 16, 50-60 (1973)

- (55) K G Allum and E S Forbes, "The Load-Carrying Properties of Organic Sulphur Compounds. Part II. The Influence of Chemical Structure on the Anti-Wear Properties of Organic Disulphides", J Inst Petrol, 53, 173-185 (1967)
- (56) R W Mould, H B Silver and R J Syrett, "Investigation of the Activity of Cutting Oil Additives I. Organo-Sulphur Containing Compounds", Wear, 19, 67-80 (1971)
- (57) M Tomaru, S Hironaka and T Sakurai, "Effect of Some Classical Factors on Film Failure Under EP Conditions", Wear, 41, 141-155 (1977)
- (58) M Toyoguchi, Y Takai and M Kato, "Reaction Between Iron and Sulphur Compound with S-35 as a Tracer", Bull Japan Petrol Inst, 2, 50-56 (1960)
- (59) J Llopis, J M Gamboa, L Arizmendi and J A Gomez-Minana, "Surface Reactions of Iron with Hydrocarbon Solutions of Organic Sulphides", Corrosion Science, 4, 27-49 (1964)
- (60) J J Kipling, "Adsorption from Solutions of Non-Electrolytes", Academic Press Inc Ltd (1965)
- (61) V Ponec, Z Knoz and S Cerny, "Adsorption on Solids", Butterworth and Co (Publisher) Ltd., (1974)
- (62) A Block and B B Simons, "Desorption and Exchange of Adsorbed Octadecylamine and Stearic Acid on Steel and Glass", J Coll and Interface Sci, 25, 514-518 (1967)
- (63) C O Timmons, R L Patterson and L B Lockhart, Jr, "The Adsorption of C<sup>14</sup> - Labelled Stearic Acid on Iron", J Coll and Interface Sci, 26, 120-127 (1968)
- (64) R L Cottingham, E G Shafrin and W A Zisman, "Physical Properties of Monolayers at the Solid/Air Interface. III. Friction and Durability of Films on Stainless Steel", J Phys Chem, 62; 513-518 (1958)

- (65) W C Bigelow and L D Brockway, "Variation of Contact Angle and Structure with Molecular Length and Surface Density in Adsorbed Films of Fatty Acids", J Colloid Sci, 11, 60-68 (1956)
- (66) L E St Pierre, R S Owens and R V Klint, "Chemical Effects in the Boundary Lubrication of Aluminium", Wear, 9, 160-168 (1966)
- (67) J H Schulman, R B Waterhouse and J A Spink, "Adhesion of Amphipathic Molecules to Solid Surface", Kolloid Zeit, 146, 77, (1956)
- (68) H D Cook and H E Ries, Jr, "Adsorption of Radiostearic Acid and Radiostearyl Alcohol from n-Hexadecane onto Solid Surfaces", J Phys Chem, 63, 226-230 (1959)
- (69) E L Cook and N Hackerman, "Adsorption of Polar Organic Compounds on Steel", J Phys Chem, 55, 549-557 (1951)
- (70) F P Bowden and A C Moore, "Physical and Chemical Adsorption of Long Chain Compounds on Radioactive Metals", Trans Farad Soc, 60, 1803-1813 (1964)
- (71) S G Daniel, "The Adsorption on Metal Surfaces of Long Chain Polar Compounds from Hydrocarbon Solution", Trans Farad Soc, 47, 1345-1357 (1951)
- (72) H A Smith and K A Allen, "The Adsorption of n-Nonadecanoic Acid on Metal Surfaces", J Phys Chem, 68, 449-452 (1954)
- (73) J V Sanders and D Tabor, "Structure of Thin Films of Aliphatic Esters and Alcohols on Metals", Proc Roy Soc, 204A, 525-533 (1950)
- (74) J W Menter and D Tabor, "Orientation of Fatty Acid and Soap Films on Metal Surfaces", Proc Roy Soc, 204A, 514-524 (1950)



- (75) T Sakurai, T Baba and S Ohara, "Film Strength and Load Carrying Capacity of Lubricating Oils", Bull Japan Petrol Inst, 1, 23-32 (1959)
- (76) T Sakurai and T Baba, "Surface Chemical Behaviour of Polar Compounds in Nonaqueous Liquids. Dispersing Effect of the Soap Solution", Wear, 3, 286-296 (1960)
- (77) H A Smith and R M McGill, "The Adsorption of n-Nonadecanoic Acid on Mechanically Activated Metal Surfaces", J Phys Chem, 61, 1025-1036 (1957)
- (78) J A Russell, W E Campbell, R A Burton and P M Ku, "Boundary Lubrication Behaviour of Organic Films at Low Temperatures", ASLE Trans, 8, 48-58 (1965)
- (79) G W Rowe, "Vapour Lubrication and the Friction of Clean Surface", Inst Mech Eng Conf on Lubrication and Wear, 333-338 (1957)
- (80) T Kayaba and A Iwabuchi, "Effect of the Hardness of Hardened Steels and the Action of Oxides on Fretting Wear", Wear, 66, 27-41 (1981)
- (81) E E Klaus and H E Bieber, "Effect of Some Physical and Chemical Properties of Lubricants on Boundary Lubrication", ASLE Trans, 7, 1-10 (1964)
- (82) M Cooks, "The Role of Atmospheric Oxidation in High Speed Sliding Phenomena - II", ASLE Trans, 1, 101-107 (1958)
- (83) Y Nagai, H Miyazaki, H Ishida, Y Tamai, T Sakurai and M Toyoguchi, "On the Oiliness of Lubricating Oil Measured in Various Atmospheres", The 5th World Petroleum Congress, Section V, Paper 28 (1959)

- (84) E B Greenhill, "Adsorption of Long Chain Polar Compounds from Solution on Metal Surfaces", Trans Farad Soc, 45, 625-630 (1949)
- (85) D W Morecroft, "Reactions of Octadecane and Decoic Acid with Clean Iron", Wear, 18, 333-339 (1971)
- (86) W Hirst and J K Lancaster, "Effect of Water on the Interaction Between Stearic Acid and Fine Powders", Trans Farad Soc, 47, 315-322 (1951)
- (87) J J Frewing, "The Heat of Adsorption of Long-Chain Compounds and Their Effect on Boundary Lubrication", Proc Roy Soc, A182, 272-285 (1944)
- (88) W C Bigelow, D C Pickett and W A Zisman, "Oleophobic Monolayers. I. Films Adsorbed from Solution in Non-Polar Liquids", J Colloid Sci, 1, 513-538 (1946)
- (89) H A Spikes and A Cameron, "A Comparison of Adsorption and Boundary Lubricant Failure", Proc Roy Soc Lond, A336, 407-419 (1974)
- (90) H A Spikes, "Physical and Chemical Adsorption in Boundary Lubrication", PhD Thesis, University of London
- (91) H A Spikes and A Cameron, "Scuffing as a Desorption Process - An Explanation of the Borsoff Effect", ASLE Trans, 17, 92-96 (1974)
- (92) A Cameron, R S Day, J P Sharma and A J Smith, "Studies in Interaction of Additive and Base Stock", ASLE Preprint, No 75-AM-1A-2
- (93) J P Sharma and A Cameron, "Surface Roughness and Load in Boundary Lubrication", ASLE Trans, 16, 258-266, (1973)

- (94) T C Askwith, A Cameron and R F Crouch, "Chain Length of Additives in Relation to Lubricants in Thin Film and Boundary Lubrication", Proc Roy Soc Lond, A291, 500-519 (1966)
- (95) W J S Grew and A Cameron, "Thermodynamics of Boundary Lubrication and Scuffing", Proc Roy Soc Lond, A327, 47-59 (1972)
- (96) A J Groszek, "Selective Adsorption at Graphite/Hydrocarbon Interfaces", Proc Roy Soc Lond, A314, 473-498 (1970)
- (97) A J Groszek, "Heat of Preferential Adsorption of Surfactants on Porous Solids and its Relation to Wear of Sliding Steel Surfaces", ASLE Trans, 5, 105-114 (1962)
- (98) A J Groszek, "Preferential Adsorption of Compounds with Long Methylene Chains on Cast Iron, Graphite, Boron Nitride and Molybdenum Disulphide", ASLE Trans, 9, 67-76 (1966)
- (99) A J Groszek, "Heats of Preferential Adsorption of Boundary Additives at Iron Oxide/Liquid Hydrocarbon Interface", ASLE Trans, 13, 278-287 (1970)
- (100) A J Groszek, "Heat of Adsorption Measurements in Lubricating Oil Research", Chem and Ind, 482-489 (1965)
- (101) A J Groszek, "Methods, Apparatus and Technique", Chem and Ind, 1754-1756 (1966)
- (102) E S Forbes, A J Groszek and E L Neustadter, "Adsorption Studies on Lubricating Oil Additives", J Colloid and Interface Sci, 33, 629 (1970)

- (103) G I Andrews, A J Groszek and N Hairs, "Measurement of Surface Areas of Basal Plane and Polar Sites in Graphite and MoS<sub>2</sub> Powders", ASLE Trans, 15, 184-191 (1972)
- (104) A J Groszek, "Heats of Adsorption of Polycyclic Aromatic Hydrocarbons at Graphite/Cyclohexane Interfaces", Proc Int Conference, Chemical Thermodynamics, Baden, Austria, 67-74 (1973)
- (105) A J Groszek, "New Lubricating Oils by Graphite Treatments of Petroleum Distillates", ASLE Preprint No. 80-LC-8A-4
- (106) Y Yahagi, "Sulphur Lubricant Additives for Oils and Emulsions", PhD Thesis, University of London
- (107) E P Kingsbury, "Some Aspects of the Thermal Desorption of a Boundary Lubricant", J Applied Phys, 29, 888-891 (1958)
- (108) C N Rowe, "Some Aspects of the Heat of Adsorption in the Function of a Boundary Lubrication", ASLE Trans, 9, 100-111 (1966)
- (109) C N Rowe, "A Relation Between Adhesive Wear and Heat of Adsorption for the Vapour Lubrication of Graphite", ASLE Trans, 10, 10-18 (1967)
- (110) D Godfrey, "Review of Usefulness of New Surface Analysis Instruments in Understanding Boundary Lubrication", Fundamentals of Tribology edited by N P Suh and N Saka, 945-968 (1978)
- (111) W A Brainard and D H Buckley, "Adhesion and Friction of PTFE in Contact with Metals as Studied by Auger Spectroscopy, Field Ion and Scanning Electron Microscopy", Wear, 26, 75-93 (1973)

- (112) R J Bird and G D Galvin, "The Application of Photoelectron Spectroscopy to the Study of EP Films on Lubricated Surfaces", *Wear*, 37, 143-167 (1976)
- (113) K G Allum and J F Ford, "The Influence of Chemical Structure on the Load-Carrying Properties of Certain Organo-Sulphur Compounds", *J Inst Petrol*, 51, 145-161 (1965)
- (114) B A Baldwin, "Relationship Between Surface Composition and Wear: an X-ray Photoelectron Spectroscopic Study of Surface Tested with Organosulphur Compounds", *ASLE Trans*, 19, 335-344 (1976)
- (115) Y Tamai, "Role of Mechanochemical Activity in Boundary Lubrication", *Fundamentals of Tribology* edited by N P Suh and N Saka, 975-980 (1978)
- (116) A J Groszek, Private Communication
- (117) W G Robertson, "Studies of Wear and Load-Carrying Capacity in the Pin and Disk Machine", *ASLE Trans*, 8, 91-99 (1965)
- (118) A F Wells, "Structure Inorganic Chemistry, Third Edition", Oxford University Press
- (119) E B Greenhill, "The Lubrication of Metal Surfaces by Mono- and Multi- Molecular Layers", *Trans Farad Soc*, 45, 631-635 (1949)
- (120) D H Everett, "Thermodynamics of Adsorption from Solution, Part I - Perfect Systems", *Trans Farad Soc*, 60, 1803-1813 (1964)
- (121) G L Gaines, Jr, "Some Observations on Monolayers of Carbon-14 Labelled Stearic Acid", *J Colloid Sci*, 15, 321-339 (1960)

- (122) O Levine and W A Zisman, "Physical Properties of Mono-Layer Adsorbed at the Solid-Air Interface. I. Friction and Wettability of Aliphatic Polar Compounds and Effect of Halogenation", J Phys Chem, 61, 1068-1077 (1957)
- (123) T N Mills, "Boundary Lubricated Contacts at High Repetition Rates", PhD Thesis, University of London
- (124) H Okabe and T Kanno, "Behaviour of Polar Compounds in Lubricating Oil Films", ASLE Preprint No 80-LC-7A-4
- (125) H Okabe, M Masuko and H Oshino, "Effects of Viscosity and Contact Geometry on Tribochemical Surface Reaction", ASLE Preprint No 80-LC-8A-3 (1980)
- (126) A N Syrop, "Lubricant Activity in Slow Speed Friction Tests", PhD Thesis, University of London